Polarons: Part I

Yury Holubeu *

December 12, 2025

This draft is not aimed for distribution.

Contents

*https://yuriholubeu.github.io/, yuri.holubev@gmail.com

Preface to Part I

Amazing facts

(I'll reveal it later)

Puzzles for motivation

(I'll reveal it later)

Part I
Polarons in a Nutshell

0.1 Main Formulas and Ideas (?)

Part II
My Theory of Polarons

1 Physics Behind Polarons

1.0.1 Concept of Polarization for Polarons

(??? see note on ED, I'll write what is it??? how exactly it is introduced???)

1.0.2 When Electron-Phonon Coupling is Large

(??? this determines the model that can be used. but how to know, what is it from other experiments or from other theory?)

1.0.3 Requirement of Being Semiconductor to Have Polarons

(??? why exactly semiconductors are assumed???)

2 Main Models of Polarons

(see Alexandrov, Mott for now)

3 Numerical Simulation of Polarons

(there are references in Alexandrov, Mott, but it is a complicated topic...)

4 Experimental Consequences of Polarons

(see Alexandrov, Mott for now)

Part III
Examples and Solved Problems

Part IV
Well-known and Important Theories

5 Polarons and Bipolarons by Alexandrov, Mott

5.1 Introduction

(here, explanation is not clear, one needs to read original works to figure out what is meant here. It is a very very bad introduction.)

The concept of polarons was first introduced by Landau (1933). If an electron is placed into the conduction band of an ionic crystal the force on another electron at a distance r from it would be $e^2/\epsilon_0 r^2$. But if the ions did not move the force would be $e^2/\epsilon r^2$, where ϵ_0 and ϵ are the static and high-frequency dielectric constants, respectively.

(?????? some assumed properties of a dielectric constant are here. I don't understand it. (???))

Thus an electron is acted upon by a potential energy

$$-\frac{e^2\left(\epsilon^{-1}-\epsilon_0^{-1}\right)}{r} \tag{0.1}$$

Since this is a Coulomb potential, localised states must exist. The electron is 'trapped by digging its own hole'.

Mott and Gurney (1940) argued that the trapped electron must be mobile but heavy, and find it remarkable that no such entity had been observed. The concept was treated in much greater detail by Fröhlich (1954), Yamashita and Kurosawa (1958), Sewel (1958), Holstein (1959), Toyozawa (1961), Eagles (1963), Reik (1963), Friedman (1964), Holstein and Friedman (1968), Austin and Mott (1969), Emin and Holstein (1969), Emin (1970), the Russian school: Pekar (1951), Tjablikov (1952), Rashba (1957), Klinger (1961), Lang and Firsov (1962) and later by many others.

In Holstein's treatment an electron is trapped by the self induced deformation of two-atomic molecules. (???)

A Franck-Condon model is used to calculate their quasistatic displacement and the frequency with which the polaron can move to a neighboring molecule. (what are quasistatic displacement and the frequency?)

This (in the so-called adiabatic approximation) involves the excitation of both the occupied and empty molecules to the same energy, so that the electron can tunnel backwards and forwards between them. (why???)

This excitation involves an activation energy $E_p/2$, and the excitation can occur through the action of temperature or zeropoint motion. (how does it involve an activation energy?)

In the former case the polaron moves by thermally activated hopping, with a diffusion coefficient

$$\omega a^2 \exp\left(-\frac{E_p}{2k_B T}\right) \tag{0.2}$$

where a is the distance between molecules.

In the latter case, for $k_B T < \hbar\omega/2$ the motion is coherent, the polaron behaves like a heavy particle with the mass

$$m^* \sim \exp\left(\frac{E_p}{\hbar\omega}\right) \tag{0.3}$$

and with a mean free path determined by the phonon and impurity scattering. (what is a coherent motion???)

Here ω is the characteristic phonon frequency (how to find out what is it?).

For ionic crystals we may write

$$E_p = \frac{e^2\left(\epsilon^{-1} - \epsilon_0^{-1}\right)}{r_p} \tag{0.4}$$

where r_p is the radius of the volume within the wave function trapped by the lattice deformation (polaron radius). (mean radius?) This can be greater than or comparable with the lattice constant a.

It is of course possible that the process described only leads to a small phase shift in the wave function at each hop if $E_p \ll \hbar^2/ma^2$, where m is a rigid band mass. (he just wrote that there is diffusion and hopping, so why there could be only phase shifts???)

The polaron is than called 'large', and can be described as a free particle moving in an elastic continuum.

The most sophisticated treatment of the large or 'continuum' polaron is due to Feynman and co-workers (1962) (they calculated some impedance, I don't understand what is it?) following that given by Pekar (1951) and Fröhlich (1954) (??? I'll read these papers later).

This treatment leads to a mass enhancement, but not to a hopping conduction (?? why not to it?? read that articles??) or to a narrow polaron band (how could it be?).

It is in this sense that we use the term 'large polaron'. Some authors used the term 'large' to describe only situations where $(\epsilon^{-1} - \epsilon_0^{-1})$ is considerably less than unity (why?).

But even this is by no means the case of large polarons if the bare electron band is sufficiently narrow (why???).

For non-ionic materials (elements) (which?), large polarons in our sense do not exist.

If we take the Holstein model with the phonon coordinate x (molecular deformation) which lowers the electron energy by $x\omega\sqrt{2ME_p}$ (why???), then the deformation region of the size r_p with one localised electron in it costs the energy

(??? I have no idea what happens here, I'll better read original articles)

$$E\left(u, r_p\right) \simeq \frac{\hbar^2}{2mr_p^2} - x\omega\sqrt{2ME_p} + \frac{M\omega^2 x^2}{2}\left(\frac{r_p}{a}\right)^3. \tag{0.5}$$

Minimising it with respect to the displacement one obtains

$$x_0 = \sqrt{\frac{2E_p}{M\omega^2}}\left(\frac{a}{r_p}\right)^3 \tag{0.6}$$

and the minimum

$$E\left(x_0, r_p\right) = \frac{\hbar^2}{2mr_p^2} - E_p\left(\frac{a}{r_p}\right)^3 \tag{0.7}$$

The energy has a minimum for $r_p = 0$; therefore the electron collapses into a point at any value of the polaron binding energy E_p. In fact r_p is restricted from below by the lattice constant a. Therefore there is a critical value of the coupling constant $\lambda = E_p/\frac{\hbar^2}{2ma^2}$

$$\lambda_c = 1 \tag{0.8}$$

No polarons are formed in the weak coupling region $\lambda < \lambda_c\,(r_p = \infty)$, and only small polarons ($r_p = a$) exist in the strong-coupling regime $\lambda > \lambda_c$.

The concept of a small polaron was first applied to an electron or hole in a nonmetal (e.g. in alkali halides). For the new superconductors our model is of course that of a degenerate gas of small polarons or bipolarons which are also degenerate below T_c and nondegenerate above. The bound state of two large polarons on an elastic polarisable continuum (large bipolaron) was introduced by Vinetskii and Giterman (1957) using a variational approach. Vinetskii and Pashitskii (1983) also discussed low-dimensional large bipolarons with disklike morphology and the possibility of their Bose-Einstein condensation. In ionic crystals the polarization wells and wave functions of macroscopic (large) bipolarons with the radius $r_B \gg a$, where a is the lattice constant, overlap strongly and this should result in their dissociation if the
carrier density is sufficiently high $n > 10^{20}$ cm^{-3}. However at low density (less than 10^{18} cm^{-3}) a gas of large bipolarons can be condensed below some critical temperature T_c without any overlapping of the polarization wells. Eagles (1969) examined a possibility of explaining the superconductivity of $SrTiO_3$ through such particles.

The concept of a small on-site localised bipolaron was introduced by Anderson (1975) and by Street and Mott (1975). It was applied to glassy semiconductors (chalcogenide glasses) to explain their magnetic and electric properties. Small bipolarons different from those were identified by Lakkis et al (1976) in Ti_4O_7 and $Ti_{4-x}V_xO_7$. These are inter-site small bipolarons, which are bound states of two Ti^{+3} ions stabilised by a large lattice distortion. At low temperatures they form a charged ordered state and are immobile. Chakraverty (1981) discussed bipolarons in connection with superconductivity, but considered that bipolarons would be immobile and therefore inactive as superconducting carriers.

The introduction of small mobile bipolarons and small polarons into the theory of superconductivity dated from the work of Alexandrov and Ranninger (1981a,b) and Alexandrov (1983), respectively. Many authors applied the BCS approach to describe the behavior of materials with strong interaction, so that the electron-phonon coupling constant λ increases (for review see Scalapino (1969)). The new point is that $\lambda \simeq 1$ is the condition for polaron formation, and it is shown that for a value of λ in the neighborhood of unity there is a fairly sharp transition to a situation in which all the carriers form small polarons. The electron band collapses into a narrow smallpolaron band (half bandwidth $w < \omega$) so that the gap extends across the whole Fermi distribution. The discovery of the new superconductors by Bednorz and Müller in 1986 lead to renewed interest in the bipolaronic superconductivity. We consider bipolarons as a key element for the understanding of the high- T_c phenomenon. Most of the experimental work has been in copper oxides, for which there is convincing evidence that the carriers are small polarons and bipolarons (Alexandrov and Mott (1994)).

In this book single-particle and cooperative properties of selflocalised carriers on a lattice are discussed at a fairly basic level with an emphasis on developments of the strong-coupling theory of superconductivity. Polaron and bipolaron formation provides a number of new physical phenomena both in the normal and superconducting ntates. Highly non-adiabatic motion of selftrapped carriers results in fundamental difference of low mobility conductors compared with simple metals and BCS superconductors.

The book starts with a single polaron problem. Both large and small polarons are discussed in Chapter 1. In the second Chapter the bipolaron formation is considered in ionic and atomic solids. The canonical theory of the electron-phonon interaction in metals is discussed in Chapter 3. In Chapter 4 we introduce the multi-polaron problem. Polar doped M O 11 milto described in Chapter 5. In chapter are We pay perconductivity and CDW in the strong coupling regime. far special attention to a charged Bose gas (CBG) in Chapter 7 as a simple but I_{C} maching model

explaining many thermodynamic and kinetic properties of highthe the textreonductors. A discriminating selection of clear-cut experiments confirming correstence of mobile small polarons and bipolarons is presented in Chapter 8. In conclusion we suggest an overview of the high- T_c problem.

5.2 1 Large and small polaron

5.2.1 How to know, which type of polaron is present?

(????????????? I have no idea, I haven't seen a discussion of it here)

5.2.2 1.1 Strong-coupling large polaron

Theory

This book is about cooperative properties of self-trapped carriers in solids with strong electron-lattice interaction. To approach the many polaron problem we first discuss a single electron interacting with the lattice deformation.

The simplest case studied by Pekar (1946) is a free electron interacting with the dielectric polarisable continuum, described by the static ϵ_0 and the optical (high frequency) dielectric constant ϵ.

This is the case for carriers interacting with optical phonons in ionic crystals under the condition that the size of the self-trapped state is large compared with the lattice constant so the lattice discreteness is irrelevant.

Describing the ionic crystal as a polarisable dielectric continuum one should keep in mind that only the ionic part of the total polarisation contribute to the polaron state. (how it could be otherwise??)

The interaction of a carrier with valence electrons responsible for the optical properties is taken into account with the Hartree-Fock periodic potential and included in the band mass m, Chapter 3 (? I'll think later, how it is done?).

Therefore only ion displacements contribute to the self-trapping.

Following Pekar we minimise the sum $E(\psi)$ of the electron kinetic energy and the potential energy due to the self-induced polarisation field

$$E(\psi) = \int d\mathbf{r} \left[\psi^*(\mathbf{r}) \left(-\frac{\nabla^2}{2m} \right) \psi(\mathbf{r}) - \mathbf{P}(\mathbf{r}) \cdot \mathbf{D}(\mathbf{r}) \right] \tag{1.1}$$

where

$$\mathbf{D}(\mathbf{r}) = e\nabla \int d\mathbf{r}' \frac{|\psi(\mathbf{r}')|^2}{|\mathbf{r} - \mathbf{r}'|} \tag{1.2}$$

in the electric field of an electron in the state with the wave function $\psi(\mathbf{r})$ and $\mathbf{P}$ is the ionic part of the lattice polarisation.

(???? !!! write better, which idea is assumed here???)

Here and further we set $\hbar = c = k_B = 1$ unless specified otherwise.

Minimising $E(\psi)$ with respect to $\psi^*(\mathbf{r})$ at fixed $\mathbf{P}$ and $\int d\mathbf{r}|\psi(\mathbf{r})|^2 = 1$ one arrives at the equation of motion

$$\left(-\frac{\nabla^2}{2m} - e \int d\mathbf{r}' \mathbf{P}(\mathbf{r}') \cdot \nabla' \frac{1}{|\mathbf{r}' - \mathbf{r}|} \right) \psi(\mathbf{r}) = E_0 \psi(\mathbf{r}) \tag{1.3}$$

where E_0 is the electron part of the ground state energy.

(I'll check the transformation later, maybe it is not that hard)

The ionic part of the total polarisation is given by the definition of the susceptibilities χ_0 and χ

$$\mathbf{P} = (\chi_0 - \chi)\,\mathbf{D}. \tag{1.4}$$

(why???)

The dielectric susceptibilities χ_0 and χ are expressed through the static and high frequency dielectric constants, respectively $(\chi_0 = (\epsilon_0 - 1)/4\pi\epsilon_0, \chi = (\epsilon - 1)/4\pi\epsilon)$ to obtain

$$\mathbf{P} = \frac{\mathbf{D}}{4\pi\kappa} \tag{1.5}$$

with $\kappa^{-1} = \epsilon^{-1} - \epsilon_0^{-1}$.

(I need to revise electrodynamics)

Then the equation of motion is

$$\left(-\frac{\nabla^2}{2m} - \frac{e^2}{4\pi\kappa}\int d\mathbf{r}' \int d\mathbf{r}''\,|\psi(\mathbf{r}')|^2\,\nabla'\frac{1}{|\mathbf{r}' - \mathbf{r}''|}\cdot\nabla'\frac{1}{|\mathbf{r}' - \mathbf{r}|}\right)\psi(\mathbf{r}) = E_0\psi(\mathbf{r}) \tag{1.6}$$

Differentiating by parts with the use of the equation $\nabla^2\frac{1}{r} = -4\pi\delta(\mathrm{r})$, we obtain

$$\left(-\frac{\nabla^2}{2m} - \frac{e^2}{\kappa}\int d\mathbf{r}'\frac{|\psi(\mathbf{r}')|^2}{|\mathbf{r}' - \mathbf{r}|}\right)\psi(\mathbf{r}) = E_0\psi(\mathbf{r}) \tag{1.8}$$

(I'll check the transformation later, maybe it is not that hard)

(write here the idea better!!! why do we introduce a functional???? what this method is???)

The solution of this nonlinear integral-differential equation can be obtained with the help of a variational minimisation of the functional

$$J(\psi) = \frac{1}{2m}\int d\mathbf{r}|\nabla\psi(\mathbf{r})|^2 - \frac{1}{2ma_B}\int d\mathbf{r}d\mathbf{r}'\frac{|\psi(\mathbf{r})|^2\,|\psi(\mathbf{r}')|^2}{|\mathbf{r}' - \mathbf{r}|} \tag{1.9}$$

where $a_B = \kappa/me^2$ is the effective Bohr radius.

The simplest choice of the normalised trial function is

$$\psi(\mathbf{r}) = Ae^{-r/r_p}, \tag{1.10}$$

with

$$A = \frac{1}{\sqrt{\pi r_p^3}} \tag{1.11}$$

Here we take the volume of the crystal $\Omega = 1$. Substitution of Eq.(1.10) into Eq.(1.9) yields

$$J(\psi) = T + \frac{1}{2}U \tag{1.12}$$

where the kinetic energy is

$$T = \frac{1}{2mr_p^2} \tag{1.13}$$

(I'll check all what is below later, it is a technical part)

To calculate the potential energy U we first integrate in Eq.(1.9) over the angle θ between $\mathbf{r}$ and $\mathbf{r}'$

$$\int_{-\pi}^{\pi}\frac{\sin\theta d\theta}{|\mathbf{r} - \mathbf{r}'|} = \frac{2\Theta(r - r')}{r} + \frac{2\Theta(r' - r)}{r'} \tag{1.14}$$

to obtain

$$U = -\frac{32\pi^2}{ma_B}\int_0^\infty drr^2\psi^2(r)\int_r^\infty dr'r'\psi^2(r') \tag{1.15}$$

Here $\Theta(x) = 1$ for $x > 0$ and zero otherwise. With Eq.(1.10) we find

$$U = -\frac{5}{8ma_Br_p}$$

and the function to be minimised with respect to r_p is

$$J(\psi) = \frac{1}{2mr_p^2} - \frac{5}{16ma_Br_p} \tag{1.17}$$

As a result, for the polaron radius we obtain

$$r_p = \frac{16a_B}{5} \tag{1.18}$$

and the ground state energy $E_0 = T + U$ is

$$E_0 = -0.146\frac{1}{ma_B^2} \tag{1.19}$$

this is the first important result of this model

This can be compared with the ground state energy of the hydrogen atom $-0.5m_ee^4$, where m_e is the free electron mass. Their ratio is $0.3m/m_e\kappa^2$. In polar solids $4 < \kappa \simeq 20$. Then the large polaron binding energy is below 0.25 eV if $m \simeq m_e$. The potential energy in the ground state is

$$U = -4T = \frac{4}{3}E_0 \tag{1.20}$$

The lowest photon energy $\nu_{\min}$ to excite a polaron into the electron band is

$$\nu_{\min} = |E_0|\,. \tag{1.21}$$

The ion configuration is not changed during the photoexcitation of a polaron. A lower activation energy W_T is necessary, however, if the self-trapped state disappears together with the polarisation well due to a thermal fluctuation

$$W_T = |E_0| - U_d, \tag{1.22}$$

where U_d is the deformation energy. In ionic crystals

$$U_d = \frac{1}{2}\int d\mathbf{r}\mathbf{P}(\mathbf{r})\cdot\mathbf{D}(\mathbf{r}) \tag{1.23}$$

which for the ground state is

$$U_d = \frac{2}{3}|E_0|\,. \tag{1.24}$$

Therefore the thermal activation energy is

$$W_T = \frac{1}{3}|E_0|\,. \tag{1.25}$$

The ratio of four characteristic energies for the large strong-coupling polaron is given by

$$W_T : U_d : \nu_{\min} : |U| = 1 : 2 : 3 : 4. \tag{1.26}$$

Different trial functions yield practically the same ground state energy with numerically different polaron radius. In particular, with Pekar's choice

$$\psi(r) = A\left(1 + r/r_p + \beta r^2\right) e^{-r/r_p} \tag{1.27}$$

one obtains $A = 0.12/r_p^{3/2}, \beta = 0.45/r_p^2$ and the polaron radius

$$r_p = 1.51 a_B \tag{1.28}$$

The ground state energy is

$$E_0 = -0.164 \frac{1}{m a_B^2} \tag{1.29}$$

How exactly the strong-coupling large polaron is related to other models?

(??)

5.2.3 1.2 Effective mass of large strong-coupling polaron

Theory

(somehow another model appears... why???)

Any polaron in a perfect crystal can move because of the translational symmetry. However, the dynamical lattice deformation does not follow perfectly well the polaron motion. The retardation is responsible for the polaron mass enhancement. Within the continuum harmonic approximation the evolution of the lattice polarisation $\mathbf{P}(\mathbf{r}, t)$ is described by the harmonic oscillator subjected to an external force $\sim \mathbf{D}/\kappa$:

$$\omega^{-2} \frac{\partial^2 \mathbf{P}(\mathbf{r}, t)}{\partial t^2} + \mathbf{P}(\mathbf{r}, t) = \frac{\mathbf{D}(\mathbf{r}, t)}{4\pi\kappa}, \tag{1.30}$$

where ω is the optical phonon frequency. If during the characteristic time of the lattice relaxation $\simeq \omega^{-1}$ the polaron moves a distance much less than the polaron radius, the polarisation practically follows the polaron motion. Therefore for a slow motion with the velocity

$$v \ll \omega a_B \tag{1.31}$$

the first term in Eq.(1.30), responsible for the retardation is a small perturbation. Then

$$\mathbf{P}(\mathbf{r}, t) \simeq \frac{1}{4\pi\kappa} \left(\mathbf{D}(\mathbf{r}, t) - \omega^{-2} \frac{\partial^2 \mathbf{D}(\mathbf{r}, t)}{\partial t^2} \right) \tag{1.32}$$

The total energy of the crystal with an extra electron

$$E = E(\psi) + 2\pi\kappa \int d\mathbf{r} \left[\mathbf{P}^2(\mathbf{r}, t) + \omega^{-2} \left(\frac{\partial \mathbf{P}(\mathbf{r}, t)}{\partial t} \right)^2 \right] \tag{1.33}$$

is determined in such a way that it gives Eq.(1.30) if minimised with respect to $\mathbf{P}$. We note that the first term of the lattice contribution is the deformation energy U_d, discussed in the previous section. As follows from Eq.(1.32) the lattice part of the total energy depends on the polaron velocity and contributes to the effective mass. Replacing the static wave function $\psi(\mathbf{r})$

in all expressions for $\psi(\mathbf{r}-\mathbf{v}t)$ and neglecting a contribution to the total energy of higher order than v^2 one obtains

$$E = E_0 + U_d + \frac{m^* v^2}{2}, \tag{1.34}$$

where

$$m^* = -\frac{1}{12\pi\omega^2\kappa}\int d\mathbf{r}\mathbf{D}(\mathbf{r})\cdot\nabla^2\mathbf{D}(\mathbf{r}) \tag{1.35}$$

is the polaron mass. The use of the equation

$$\nabla^2\mathbf{D} = -4\pi e\nabla|\psi(\mathbf{r})|^2 \tag{1.36}$$

and

$$\nabla\cdot\mathbf{D} = -4\pi e|\psi(\mathbf{r})|^2 \tag{1.37}$$

yields

$$m^* = \frac{4\pi e^2}{3\omega^2\kappa}\int d\mathbf{r}|\psi(\mathbf{r})|^4 \tag{1.38}$$

Calculating the integral in Eq.(1.38) with the trial function Eq.(1.10) one obtains

$$m^* \simeq 0.02\alpha^4 m \tag{1.39}$$

where α is the dimensionless constant, defined by Fröhlich as

$$\alpha = \frac{e^2}{\kappa}\sqrt{\frac{m}{2\omega}}. \tag{1.40}$$

To conclude our discussion of the strong-coupling large polaron let us determine the condition of its existence. The polaron radius should be large compared with the lattice constant, $r_p \gg a$ to justify the continuum effective mass approximation for the electron. Then the value of α should not be very large,

$$\alpha \ll \sqrt{\frac{D}{z\omega}}, \tag{1.41}$$

where $D \simeq z/2ma^2$ is half of the bare electron bandwidth, z is the lattice nearest neighbor number. On the other hand the continuum (classical) approximation for the lattice polarisation is justified if the number of phonons taking part in the polaron formation is large. This number is of order U_d/ω. The total energy of the immobile polaron and deformed lattice, Eq.(1.34) is expressed as

$$E = -0.109\alpha^2\omega \tag{1.42}$$

and $U_d = 0.218\alpha^2\omega$. Then α is bounded below by the condition $U_d/\omega \gg 1$, which yields

$$\alpha^2 \gg 5. \tag{1.43}$$

The adiabatic ratio D/ω is of order 10 to 100. In fact in many transition metal oxides with narrow bands and a high optical phonon frequency this ratio is below 10, which makes Eq.(1.41) and Eq.(1.43) incompatible. Therefore the large strong coupling polaron is difficult to realise in practice, and we do not know of any solid in which it has been observed.

5.2.4 1.3 Fröhlich large polaron

Theory

Fröhlich (1950), Fröhlich et al (1950) and other workers applied the second quantisation form of the electron-lattice interaction to describe a week-coupling large polaron when $\alpha \leq 1$, so the quantum nature of the lattice polarisation becomes important. The electron potential energy in a crystal field distorted by phonons is

$$V(\mathbf{r}) = \sum_1 v\left(\mathbf{r} - \mathbf{R}_1\right), \tag{1.44}$$

where the interaction of an electron with a single ion is described by the potential $v(\mathbf{r})$. The distance of ions $\mathbf{u}_1 = \mathbf{R}_1 - 1$ from the equilibrium positions 1 is small compared with a lattice constant a, which allows us to expand $v\left(\mathbf{r} - \mathbf{R_1}\right)$ near equilibrium:

$$v\left(\mathbf{r} - \mathbf{R}_1\right) \simeq v(\mathbf{r} - 1) - \mathbf{u}_1 \cdot \nabla v(\mathbf{r} - 1).$$

The lattice part of the Hamiltonian can be diagonalised with harmonic phonons (see Chapter 3) such, that the ion displacement is a linear combination of their annihilation $d_{\mathbf{q}}$ and creation $d^{\dagger}_{\mathbf{q}}$ bosonic operators:

$$\mathbf{u_l} = \sum_{\mathbf{q}} \frac{\mathbf{e_q}}{\sqrt{2NM\omega_{\mathbf{q}}}} d_{\mathbf{q}} e^{i\mathbf{q}\cdot\mathbf{l}} + \text{ h.c.} \tag{1.46}$$

where q is the phonon momenta in the first Brillouin zone, ω_q the phonon frequency, M ionic mass, $\mathrm{e_q}$ is a unit polarisation vector, and N is the number of ions (sites) in a crystal. With the help of the Fourier expansion

$$v(\mathbf{r}) = \sum_{\mathbf{k}} v_{\mathbf{k}} e^{i\mathbf{k}\cdot\mathbf{r}} \tag{1.47}$$

the electron-phonon interaction in the second quantization is written as:

$$H_{e-ph} = \frac{1}{\sqrt{2N}} \sum_{\mathbf{q}} \gamma(\mathbf{q}) \omega_{\mathbf{q}} d_{\mathbf{q}} e^{i\mathbf{q}\cdot\mathbf{r}} + h.c. \tag{1.48}$$

where the dimensionless matrix element is

$$\gamma(\mathbf{q}) = -i \frac{N \mathbf{e_q} \cdot \mathbf{q}}{\sqrt{M\omega^3_{\mathbf{q}}}} v_{\mathbf{q}} \tag{1.49}$$

In ionic crystals the interaction $v(\mathbf{r})$ is the Coulomb one with the Fourier component $v_{\mathrm{q}} \simeq 4\pi/\Omega\kappa q^2$ (Ω is the crystal volume). Then the coupling with longitudinal ($\mathbf{e_q} \| \mathbf{q}$) ionic plasmons is

$$\frac{\gamma(\mathbf{q})\omega}{2N} \equiv V_{\mathbf{q}} = -\frac{i\omega}{q} \left(\frac{4\pi\alpha}{\Omega\sqrt{2m\omega}} \right)^{1/2} \tag{1.50}$$

where α is the Fröhlich constant and $\omega = \sqrt{4\pi N e^2 / M\Omega\kappa}$ is the ionic plasma frequency. The complete Hamiltonian including the quantised deformation energy has the form

$$H = -\frac{\nabla^2}{2m} + \sum_{\mathbf{q}} \left(V_{\mathbf{q}} d_{\mathbf{q}} e^{i\mathbf{q}\cdot\mathbf{r}} + h.c. \right) + \sum_{\mathbf{q}} \omega_{\mathbf{q}} \left(d^{\dagger}_{\mathbf{q}} d_{\mathbf{q}} + 1/2 \right) \tag{1.51}$$

The quantum states of the noninteracting electron and phonons are classified with the electron momentum $\mathbf{k}$ and with the phonon occupation numbers $\left\langle d^{\dagger}_{\mathbf{q}} d_{\mathbf{q}} \right\rangle \equiv n_{\mathbf{q}} = 0, 1, 2, \ldots \infty$.

For zero temperature the unperturbed state is the vacuum $|0\rangle$ of phonons and the electron plane wave

$$|\mathbf{k}, 0\rangle = \frac{1}{\sqrt{\Omega}} e^{i\mathbf{k}\cdot\mathbf{r}} |0\rangle \tag{1.52}$$

While the coupling is weak one can apply perturbation theory. The interaction couples the state Eq.(1.52) with the energy $k^2/2m$ and states of a single phonon of momentum q and the electron of momentum k − q with the energy $(\mathrm{k} - \mathrm{q})^2/2m + \omega$

$$|\mathbf{k} - \mathbf{q}, 1_{\mathbf{q}}\rangle = \frac{1}{\sqrt{\Omega}} e^{i(\mathbf{k}-\mathbf{q})\cdot\mathbf{r}} \, |1_{\mathbf{q}}\rangle \tag{1.53}$$

The corresponding matrix element is

$$\langle \mathbf{k} - \mathbf{q}, 1_{\mathbf{q}}| \, H_{e-ph} |\mathbf{k}, 0\rangle = V_{\mathbf{q}}^* \tag{1.54}$$

There are no diagonal matrix elements of H_{e-ph}. Then the renormalised energy $\tilde{E}_{\mathbf{k}}$ in the lowest second order is

$$\tilde{E}_{\mathbf{k}} = \frac{k^2}{2m} - \sum_{\mathbf{q}} \frac{|V_{\mathbf{q}}|^2}{(\mathbf{k} - \mathbf{q})^2/2m + \omega - k^2/2m} \tag{1.55}$$

As in section 1.2 we consider a slow electron, such as

$$k < q_p \tag{1.56}$$

where

$$q_p = \min(m\omega/q + q/2) = \sqrt{2m\omega} \tag{1.57}$$

In this case there is no imaginary part of $\tilde{E}_{\mathrm{k}}$, which means that the momentum is conserved. On substituting the expression for $V_{\mathbf{q}}$, Eq.(1.50), changing the sum over q to integrals, and taking the upper limit infinity for q one obtains

$$\tilde{E}_{\mathbf{k}} = \frac{k^2}{2m} - \frac{\alpha\omega}{\pi} \int_{-1}^{1} dx \int_0^{\infty} \frac{dy}{y^2 - 2yxk/q_p + 1} \tag{1.58}$$

The integral over q converges because the coupling constant ($\sim 1/q$) decreases with q. Therefore long wave optical phonons contribute mainly to the polaron self-energy. That is not the case for molecular or acoustical phonons when all states of the Brillouin zone contribute. Evaluating the integrals one arrives at

$$\tilde{E}_{\mathrm{k}} = \frac{k^2}{2m} - \frac{\alpha\omega q_p}{k} \arcsin\left(\frac{k}{q_p}\right) \tag{1.59}$$

which for a very slow motion $k \ll q_p$ yields

$$\tilde{E}_{\mathbf{k}} \simeq -\alpha\omega + \frac{k^2}{2m^*} \tag{1.60}$$

Here the first term is the polaron binding energy. The effective mass of the polaron is enhanced

$$m^* = \frac{m}{1 - \alpha/6} \simeq m\left(1 + \frac{\alpha}{6}\right) \tag{1.61}$$

This is due to a phonon cloud accompanying a slow polaron. The number of virtual phonons N_{ph} in the cloud is given by taking the expectation value of the phonon number operator

$$N_{ph} = \left\langle \sum_{\mathbf{q}} d^{\dagger}_{\mathbf{q}} d_{\mathbf{q}} \right\rangle \tag{1.62}$$

where bra and ket refer to the perturbed state

$$\rangle = |0\rangle + \sum_{\mathbf{q}'} \frac{V^{*}_{\mathbf{q}'}}{k^2/2m - (\mathbf{k}-\mathbf{q}')^2/2m - \omega} |1_{\mathbf{q}'}\rangle \tag{1.63}$$

For a polaron at rest ($\mathbf{k} = 0$) one obtains

$$N_{ph} = \sum_{\mathbf{q}} \frac{|V_{\mathbf{q}}|^2}{(\omega + q^2/2m)^2} \tag{1.64}$$

The value of the integral in Eq.(1.64) is

$$N_{ph} = \frac{\alpha}{2} \tag{1.65}$$

Therefore the Fröhlich coupling constant measures directly the cloud 'thickness'. One can also calculate the lattice-charge density induced by the electron. The electrostatic potential $e\phi(\mathbf{r})$ is given by the average of the interaction term of the Hamiltonian

$$e\phi(\mathbf{r}) = \left\langle \sum_{\mathbf{q}} V_{\mathbf{q}} e^{i\mathbf{q}\cdot\mathbf{r}} d_{\mathbf{q}} + h.c. \right\rangle \tag{1.66}$$

and the charge density $\rho(\mathbf{r})$ is related to the electrostatic potential by Poisson's equation

$$\nabla\phi = -4\pi\rho \tag{1.67}$$

As a result

$$\rho(\mathbf{r}) = -\frac{1}{2\pi e} \sum_{\mathbf{q}} \frac{q^2 |V_{\mathbf{q}}|^2 \cos[\mathbf{q}\cdot\mathbf{r}]}{\omega + q^2/2m} \tag{1.68}$$

By integration over q one obtains

$$\rho(\mathbf{r}) = -\frac{eq_p^3}{4\pi\kappa} \frac{e^{-q_p r}}{q_p r} \tag{1.69}$$

The mean extension of the phonon cloud which can be taken as the radius of a weak coupling polaron is

$$r_p = q_p^{-1} \tag{1.70}$$

The total induced charge is

$$Q = \int d\mathbf{r}\rho(\mathbf{r}) = -\frac{e}{\kappa} \tag{1.71}$$

5.2.5 1.4 Intermediate-coupling large polaron

Theory

Many polar materials are in the intermediate regime $1 < \alpha < 10$. (why??)

One can approach this regime applying the Lee-Low-Pines (LLP, 1953) canonical transformation, removing the electron coordinate followed by the displacement transformation (Tjablikov (1952), Lee and Pines (1952), Gurari (1953)). (why??)

The latter serves to account for that part of the lattice polarisation which follows the electron instantaneously.

The remaining part of the polarisation field turns out to be small if the coupling constant is not extremely large.

(check these statements!)

In the opposite extreme limit, which is Pekar's strong-coupling regime already discussed one can construct the perturbation theory by an expansion in descending powers of α (Bogoliubov (1950)). (read this article, maybe it is a good one!)

Alternatively one can apply Feynman's path-integral formulation (1955) of quantum mechanics to remove the phonon field at the expense of a non-instantaneous interaction of electron with itself. (do it!! a good exercise)

Here we consider the canonical transformation approach referring the reader to the papers by Allcock (1962) and Bogoliubov Jr.(1994) for the strong-coupling large polaron theory and by Schultz (1962) for Feynman's path integral method, which is also discussed in section 2.3. (I am not sure how useful is path integral here, so I'll read it later)

A canonical transformation can be written as

$$|\tilde{N}\rangle = \exp(S)|N\rangle \tag{1.72}$$

where in our case $|N\rangle$ is a single-electron multi-phonon wave function, $|\tilde{N}\rangle$ is a transformed one, satisfying the Schrödinger equation :

$$\tilde{H}|\tilde{N}>= E|\tilde{N}> \tag{1.73}$$

with the transformed Hamiltonian

$$\tilde{H} = \exp(S)H\exp(-S) \tag{1.74}$$

If all operators are transformed according to Eq.(1.74) the physical averages, in particular the energy remain unchanged. LLP transformation eliminating the electron coordinate from the Hamiltonian is defined as

$$S_{LLP} = i\sum_{\mathbf{q}}(\mathbf{q}\cdot\mathbf{r})d^{\dagger}_{\mathbf{q}}d_{\mathbf{q}} \tag{1.75}$$

In the new representation the phonon operator is

$$\tilde{d}_{\mathbf{q}} = e^{S_{LLP}}d_{\mathbf{q}}e^{-S_{LLP}} = d_{\mathbf{q}}e^{-i\mathbf{q}\cdot\mathbf{r}} \tag{1.76}$$

and the electron momentum operator is

$$-i\tilde{\nabla} = -ie^{S_{LLP}}\nabla e^{-S_{LLP}} = -i\nabla - \sum_{\mathbf{q}}\mathbf{q}d^{\dagger}_{\mathbf{q}}d_{\mathbf{q}} \tag{1.77}$$

To derive Eq.(1.76) and Eq.(1.77) one can apply transformed operators to the eigenstates of the phonon-number operator and to the plane waves, respectively. The transformed Hamiltonian is therefore

$$\tilde{H} = \frac{1}{2m}\left(-i\nabla - \sum_{\mathbf{q}} \mathbf{q} d^{\dagger}_{\mathbf{q}} d_{\mathbf{q}}\right)^2 + \sum_{\mathbf{q}} \left(V_{\mathbf{q}} d_{\mathbf{q}} + h.c.\right) + \omega \sum_{\mathbf{q}} \left(d^{\dagger}_{\mathbf{q}} d_{\mathbf{q}} + 1/2\right) \tag{1.78}$$

The electron coordinate is absent from $\tilde{H}$. Hence the eigenstates $|\tilde{N}\rangle$ are classified with the momentum $\mathbf{K}$, which is the conserving total momentum of the system

$$|\tilde{N}\rangle = \frac{1}{\sqrt{\Omega}} e^{i\mathbf{K}\cdot\mathbf{r}} \left|\tilde{N}_{ph}\right\rangle \tag{1.79}$$

where the phonon part of the wave function $\left|\tilde{N}_{ph}\right\rangle$ satisfies to the Schrödinger equation with the phonon Hamiltonian

$$\tilde{H} = \frac{1}{2m}\left(\mathbf{K} - \sum_{\mathbf{q}} \mathbf{q} d^{\dagger}_{\mathbf{q}} d_{\mathbf{q}}\right)^2 + \sum_{\mathbf{q}} \left(V_{\mathbf{q}} d_{\mathbf{q}} + h.c.\right) + \omega \sum_{\mathbf{q}} \left(d^{\dagger}_{\mathbf{q}} d_{\mathbf{q}} + 1/2\right) \tag{1.80}$$

As follows from the Fröhlich perturbation analysis the number of virtual phonons is not small in the intermediate coupling regime. Therefore one cannot apply the perturbation theory to $\tilde{H}$. However, one can remove the essential part of the interaction term from the Hamiltonian by the displacement canonical transformation

$$S = \sum_{\mathbf{q}} f(\mathbf{q}) d_{\mathbf{q}} - h.c. \tag{1.81}$$

where the c-number $f(\mathbf{q})$ is to be determined by minimisation of the ground state energy

$$- \quad \frac{\partial E_0}{\partial f^*(\mathbf{q})} = 0 \tag{1.82}$$

The transformed phonon operator is

$$\tilde{d}_{\mathbf{q}} = e^S d_{\mathbf{q}} e^{-S} = d_{\mathbf{q}} - f^*(\mathbf{q}) \tag{1.83}$$

which is obtained with the help of the expansion

$$e^S d_{\mathbf{q}} e^{-S} = d_{\mathbf{q}} + [d_{\mathbf{q}}, S] + \frac{1}{2}\left[[d_{\mathbf{q}} S], S\right] + \ldots \tag{1.84}$$

Because $[d_{\mathbf{q}}, S] = -f^*(\mathbf{q})$ is a c-number all terms after the second vanish. From Eq.(1.83) it follows that $\exp S$ displaces ions to new equilibrium positions. Assuming that the transformed ground state is a phonon vacuum

$$\left|\tilde{\tilde{N}}_{ph}\right\rangle = e^S \left|\tilde{N}_{ph}\right\rangle = |0\rangle \tag{1.85}$$

one finds for the energy $\tilde{E}_{\mathrm{K}} \equiv \langle 0|\tilde{\tilde{H}}|0\rangle$

$$\tilde{E}_{\mathbf{K}} = \frac{K^2}{2m} - \sum_{\mathbf{q}} \left(V_{\mathbf{q}} f^*(\mathbf{q}) + h.c.\right) + \sum_{\mathbf{q}} |f(\mathbf{q})|^2 \left(\omega - \frac{\mathbf{K}\cdot\mathbf{q}}{m} + \frac{q^2}{2m}\right)$$
$$+\frac{1}{2m} \sum_{\mathbf{q}} \sum_{\mathbf{q}'} \Bigg| f\left(\mathbf{q} f\left(\mathbf{q}'\right)|^2 \mathbf{q}\cdot\mathbf{q}'\right. \tag{1.86}$$

Taking the functional derivative of Eq.(1.86) to be zero one arrives at

$$f(\mathbf{q})\left[\left(\omega-\frac{\mathbf{K}\cdot\mathbf{q}}{m}+\frac{q^2}{2m}\right)+\frac{1}{m}\sum_{\mathbf{q}'}\left|f\left(\mathbf{q}'\right)\right|^2\mathbf{q}\cdot\mathbf{q}'\right]=V_{\mathbf{q}} \tag{1.87}$$

It is essential in eliminating a large part of the Fröhlich interaction that the linear term with respect to the phonon operators vanishes from $\tilde{\tilde{H}}$ if $f(\mathbf{q})$ satisfies to Eq.(1.87). Introducing a constant η determined as

$$\sum_{\mathbf{q}'}\left|f\left(\mathbf{q}'\right)\right|^2\mathbf{q}'=\eta\mathbf{K} \tag{1.88}$$

one finds a formal solution to Eq.(1.87)

$$f(\mathbf{q})=\frac{V_{\mathbf{q}}}{\omega+q^2/2m-(1-\eta)\mathbf{q}\cdot\mathbf{K}/m} \tag{1.89}$$

and with Eq.(1.86)

$$\tilde{E}_{\mathbf{K}}=\frac{\left(1-\eta^2\right)K^2}{2m}-\sum_{\mathbf{q}}\frac{\left|V_{\mathbf{q}}\right|^2}{\omega+q^2/2m-(1-\eta)\mathbf{q}\cdot\mathbf{K}/m} \tag{1.90}$$

The last equation is the same as Eq.(1.55) if $\eta=0$. However, $\eta=0$ is not a solution of the self-consistent equation for η which is obtained by substituting Eq.(1.89) into Eq.(1.88)

$$\eta\mathbf{K}=\sum_{\mathbf{q}}\frac{\left|V_{\mathbf{q}}\right|^2\mathbf{q}}{\left(\omega+q^2/2m-(1-\eta)\mathbf{q}\cdot\mathbf{K}/m\right)^2} \tag{1.91}$$

Integrating gives

$$\tilde{E}_{\mathbf{K}}=\frac{\left(1-\eta^2\right)K^2}{2m}-\frac{\alpha\omega q_p}{K(1-\eta)}\arcsin\left(\frac{K(1-\eta)}{q_p}\right) \tag{1.92}$$

with

$$\eta(1-\eta)^2=\frac{\alpha q_p^3}{2K^3}\left(\frac{(1-\eta)K}{\sqrt{q_p^2-(1-\eta)^2K^2}}-\arcsin\frac{(1-\eta)K}{q_p}\right) \tag{1.93}$$

For a slow polaron with $K\ll q_p$ only the term independent of K needs to be retained in η

$$\eta=\frac{\alpha/6}{1+\alpha/6} \tag{1.94}$$

Then the energy up to order K^2 is

$$\tilde{E}_{\mathbf{K}}=-\alpha\omega+\frac{K^2}{2m^*} \tag{1.95}$$

where the polaron mass is now

$$m^*=m(1+\alpha/6) \tag{1.96}$$

This result shows that the perturbation theory, Eq.(1.61) can be extended even to $\alpha>1$. Lee, Low and Pines evaluated also the corrections due to the off-diagonal part of the transformed Hamiltonian $\tilde{\tilde{H}}$ and found that they are below 0.02α for the polaron shift in Eq.(1.95) and below $-0.02\alpha^2/(1+\alpha/6)$ for the effective mass. A lower value of the ground state energy (approximately by 10%) and heavier effective mass was obtained by Feynman using the path

integral. The difficulty with the path integral is that the effective action is not quadratic with respect to the electron coordinate. Therefore to determine an upper bound to the ground state energy the action was approximated by an effective quadratic action with two variational parameters. The general conclusion is that for a wide range of α the Feynman estimate of the ground state energy is lower than that obtained by the canonical transformation. Both the Feynman variational path integral approach and the LLP transformation are inaccurate for the strong coupling large polaron, $\alpha > 10$.

5.2.6 1.5 Small polaron: two-site Holstein model

Theory

When the coupling with phonons increases the polaron radius decreases and becomes of the order of the lattice constant. Then all momenta of the Brillouin zone contribute to the polaron wave function and the effective mass approximation cannot be applied. This regime occurs if the characteristic potential energy E_p due to the local lattice deformation is comparable or larger than the half bandwidth D. The strong coupling regime with the dimensionless coupling constant

$$\lambda \equiv \frac{E_p}{D} \geq 1 \tag{1.97}$$

is called a small polaron. In general, E_p is estimated using the perturbation theory, Eq.(1.55)

$$E_p = \frac{1}{2N} \sum_{\mathbf{q}} |\gamma(\mathbf{q})|^2 \omega_{\mathbf{q}} \tag{1.98}$$

for any type of phonons involved in the polaron cloud. For the Fröhlich interaction with optical phonons one estimates

$$E_p \simeq \frac{q_D e^2}{\pi \kappa} \tag{1.99}$$

where $q_d = (6\pi^2/\Omega)^{1/3}$ is the Debye momentum. With parameters appropriate for high T_c copper oxides $\epsilon_0 \gg \epsilon_\infty \simeq 5$ and $q_D \simeq 0.7\text{Å}^{-1}$, one obtains $E_p \simeq 0.6\text{eV}$. The exact value of λ_c when the large polaron collapses into a small one depends on the lattice structure and phonon frequency dispersion. The transition occurs around $\lambda_c \simeq 0.5$ in the Holstein model (see Section 1.8). Small polarons are expected to be the carriers in high- T_c oxides, which are strongly polarisible doped semiconductors with rather narrow electron bands (Chapter 8). The band structure and kinetic properties are drastically different in the small polaron regime compared with the large polaron as was discussed by Tjablikov (1952), Yamashita and Kurosava (1958), Sewell (1958), Holstein (1959), and by the Russian school: Rashba (1957), Klinger (1962), Firsov and co-workers(1962) and others.

The main features of the small polaron are revealed in the simplest Holstein model consisting of only two vibrating molecular sites and one electron between them. Neglecting the intermolecular coupling the vibration (molecular) part of the Hamiltonian is written as

$$H_{ph} = -\frac{1}{2M} \sum_{i=1,2} \left(\frac{\partial^2}{\partial x_i^2} + \frac{M\omega^2 x_i^2}{2} \right) \tag{1.100}$$

where $x_{1,2}$ is the intramolecular coordinate, which is the change of the distance between two ions of a diatomic molecule on site 1 and 2 , respectively, and M is the relative mass. The interaction of an electron with two rigid molecules is described by the 'electronic' part of the Hamiltonian

$$H_e = -\frac{\nabla^2}{2m} + V\left(\mathbf{r} - \mathbf{l}_1\right) + V\left(\mathbf{r} - \mathbf{l}_2\right), \tag{1.101}$$

where $l_{1,2}$ are site coordinates, and the interaction term is

$$V(\mathbf{r} - 1) = v(\mathbf{r} - 1 - \mathbf{a}/2) - v(\mathbf{r} - 1 + \mathbf{a}/2) \tag{1.102}$$

in case of the molecules consisting of two ions with the opposite charge and the equilibrium distance a between them, Fig.1.1.

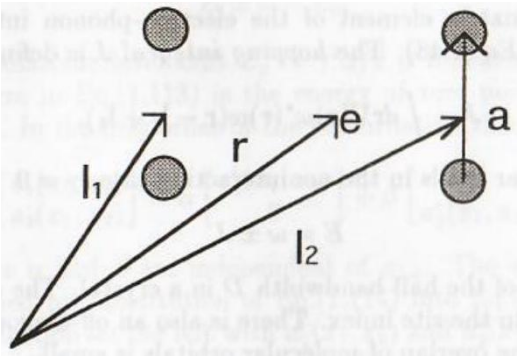

Fig.1.1. Two-site one-electron Holstein model.

And finally, the electron-phonon interaction with a stretching molecular mode is a linear function of the displacements

$$H_{e-ph} = -\sum_{i=1,2} \frac{x_i}{2} \frac{\partial}{\partial x} \left[v\left(\mathbf{r} - \mathbf{l}_i - \mathbf{a}/2\right) + v\left(\mathbf{r} - \mathbf{l}_i + \mathbf{a}/2\right)\right]. \tag{1.103}$$

The state of the system is expressed as a linear superposition

$$|\mathbf{r}, x_1, x_2\rangle = \sum_{i=1,2} a_i\left(x_1, x_2\right) w\left(\mathbf{r} - \mathbf{l}_i\right) \tag{1.104}$$

of electron wave functions, $w(\mathrm{r} - 1)$ each localised about particular molecular site 1 and assumed to be normalised and orthogonal. If the molecules are separated by a large distance these Wannier (site) wave functions are molecular orbitals satisfying the Schrödinger equation for an isolated molecule

$$\left(-\frac{\nabla^2}{2m} + V(\mathbf{r})\right) w(\mathbf{r}) = 0 \tag{1.105}$$

where the electron energy of a rigid molecule is taken to be zero. Equations for the $a_i\left(x_1, x_2\right)$ are obtained by substitution of Eq.(1.104) into the Schrödinger equation of the system with the complete Hamiltonian $H_e + H_{e-ph} + H_{ph}$ followed by multiplication on the left with $w^*\left(\mathrm{r} - \mathrm{l}_i\right)$ and integration over the electron coordinate, r. This procedure gives

$$\left[E + \frac{1}{2M}\left(\frac{\partial^2}{\partial x_1^2} + \frac{\partial^2}{\partial x_2^2}\right) - \frac{M\omega^2\left(x_1^2 + x_2^2\right)}{2} - \gamma\omega\sqrt{M\omega}x_1\right] a_1\left(x_1, x_2\right) = -J a_2\left(x_1, x_2\right), \tag{1.106}$$

and

$$\left[E + \frac{1}{2M}\left(\frac{\partial^2}{\partial x_1^2} + \frac{\partial^2}{\partial x_2^2}\right) - \frac{M\omega^2\left(x_1^2 + x_2^2\right)}{2} - \gamma\omega\sqrt{M\omega}x_2\right] a_2\left(x_1, x_2\right) = -J a_1\left(x_1, x_2\right), \tag{1.107}$$

where

$$\gamma = -\frac{1}{2\omega\sqrt{M\omega}} \int d\mathbf{r}|w(\mathbf{r})|^2 \frac{\partial}{\partial x}[v(\mathbf{r}-\mathbf{a}/2)+v(\mathbf{r}+\mathbf{a}/2)] \tag{1.108}$$

is the dimensionless matrix element of the electron-phonon interaction as in the Fröhlich Hamiltonian, Eq.(1.48). The hopping integral J is defined as

$$J = \int d\mathbf{r} V(\mathbf{r}) w^*(\mathbf{r}) w\left(\mathbf{r} - \mathrm{l}_2 + \mathrm{l}_1\right) \tag{1.109}$$

There are two molecular levels in the noninteracting case, $\gamma = 0$

$$E \quad E = \omega \pm J$$

with $2J$ playing a role of the half bandwidth D in a crystal. The matrix element γ is diagonal with respect to the site index. There is also an off-diagonal matrix element, which is negligible if the overlap of molecular orbitals is small.

The strong coupling condition $\lambda > 1$ corresponds to $\gamma^2 > 4J/\omega$. Two limiting methods are available for the treatment of the system of two coupled differential equations (1.106, 107) in this strong-coupling regime; the perturbation and the adiabatic approaches, valid in the case of large or small adiabatic parameter ω/J, respectively.

5.2.7 1.6 Nonadiabatic small polaron

Theory

In the perturbation nonadiabatic approach the lattice moves fast and the electron slow. Then one can take $J = 0$ in zero approximation with two degenerate eigenstates $a^{l,r}$, corresponding to the polaron 'sitting' on the 'left' a^l and on the 'right' a^r molecule, Fig.1.2

$$a_1^l(x_1, x_2) = \exp\left[-\frac{M\omega}{2}\left(\left(x_1 + \frac{\gamma}{\sqrt{M\omega}}\right)^2 + x_2^2\right)\right]; a_2^l(x_1, x_2) = 0 \tag{1.111}$$

and

$$a_1^r(x_1, x_2) = 0; a_2^r(x_1, x_2) = \exp\left[-\frac{M\omega}{2}\left(\left(x_2 + \frac{\gamma}{\sqrt{M\omega}}\right)^2 + x_1^2\right)\right] \tag{1.112}$$

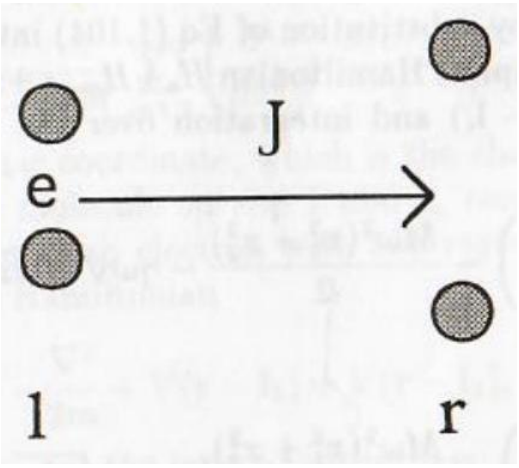

Fig.1.2. Zero-order deformation of the molecules.

The electron-phonon interaction leads to the shrinking of the molecular size by the value $\gamma/\sqrt{M\omega}$ and to the lowering of the molecular level by the polaronic level shift

$$E \simeq \omega - E_p. \tag{1.113}$$

We note that the polaronic level shift $E_p = \gamma^2\omega/2$ is independent of the molecular mass. The first term in Eq.(1.113) is the energy of zero point fluctuations of two vibrating molecules. In the first order of the perturbation theory

$$\begin{bmatrix} a_1(x_1,x_2) \\ a_2(x_1,x_2) \end{bmatrix} = \alpha \begin{bmatrix} a_1^l(x_1,x_2) \\ 0 \end{bmatrix} + \beta \begin{bmatrix} 0 \\ a_2^r(x_1,x_2) \end{bmatrix}. \tag{1.114}$$

Here the coefficients α and β are independent of $x_{1,2}$. The standard secular equation for E is obtained by substitution of Eq.(1.114) into Eq.(1.106) and Eq.(1.107) followed by multiplication on the left with $a_1^l(x_1,x_2)$ and $a_2^r(x_1,x_2)$, respectively and integration over the vibration coordinates, $x_{1,2}$. The result is

$$\det \begin{vmatrix} E-\omega+E_p & \tilde{J} \\ \tilde{J} & E-\omega+E_p \end{vmatrix} = 0 \tag{1.115}$$

with the renormalised hopping integral

$$\tilde{J} = J\frac{\int dx_1 \int dx_2 a_1^l(x_1,x_2)\, a_2^r(x_1,x_2)}{\int dx_1 \int dx_2 \left|a_1^l(x_1,x_2)\right|^2}. \tag{1.116}$$

The corresponding eigenvalues, $E_\pm$are

$$E_\pm = \omega - E_p \pm \tilde{J} \tag{1.117}$$

The hopping integral splits the molecular level. The effective 'bandwidth' is significantly reduced compared with the bare one

$$\tilde{J} = Je^{-g^2} \tag{1.118}$$

where $g = \gamma/\sqrt{2}$. The origin of the polaron band narrowing e^{-g^2} lies in a small overlap integral, Eq.(1.116) of two displaced oscillator wave functions a_1^l and a_2^r. This effect is beyond the large-polaron approximation.

5.2.8 1.7 Adiabatic small polaron

Theory

In the adiabatic approach when $J \gg \omega$, one assumes a wave function of the form

$$\begin{pmatrix} a_1(x_1,x_2) \\ a_2(x_1,x_2) \end{pmatrix} = \chi(x_1,x_2) \begin{pmatrix} \psi(x_1,x_2) \\ \phi(x_1,x_2) \end{pmatrix} \tag{1.119}$$

where ψ and ϕ are solutions of the 'electronic' hopping Hamiltonian with a frozen molecular deformation $x_{1,2}$

$$\begin{pmatrix} E(x_1,x_2) - \gamma\omega\sqrt{M\omega}x_1 & J \\ J & E(x_1,x_2) - \gamma\omega\sqrt{M\omega}x_2 \end{pmatrix} \begin{pmatrix} \psi(x_1,x_2) \\ \phi(x_1,x_2) \end{pmatrix} = 0. \tag{1.120}$$

The lowest eigenvalue of Eq.(1.120) is of interest in the adiabatic approximation

$$E(x_1, x_2) = \frac{\gamma\omega\sqrt{M\omega}\,(x_1 + x_2)}{2} - \left[\frac{\gamma^2 M\omega^3 (x_1 - x_2)^2}{4} + J^2\right]^{1/2} \tag{1.121}$$

As is known, $E(x_1, x_2)$ plays the role of a potential energy term in the equation for the 'vibration' wave function, $\chi(x_1, x_2)$, which reads

$$\left[E + \frac{1}{2M}\left(\frac{\partial^2}{\partial x_1^2} + \frac{\partial^2}{\partial x_2^2}\right) - \frac{M\omega^2 (x_1^2 + x_2^2)}{2} - E(x_1, x_2)\right]\chi(x_1, x_2) = 0. \tag{1.122}$$

Terms with the first and second derivatives of the 'electronic' functions ψ and ϕ are small compared with the corresponding terms with the derivatives of χ for the case in hand. The transformation

$$X = \frac{x_1 + x_2}{2}, x = x_2 - x_1 \tag{1.123}$$

leads to a product solution of the form $\chi(x_1, x_2) = F(X)\chi(x)$, where $F(X)$ is the ground state of a harmonic oscillator in the presence of a constant force $\gamma\omega\sqrt{M\omega}$ with the ground state energy $(\omega - E_p)/2$. The equation for $\chi(x)$ is

$$\left[E + \frac{E_p}{2} - \frac{\omega}{2} + \frac{1}{2\mu}\frac{\partial^2}{\partial x^2} - U(x)\right]\chi(x) = 0 \tag{1.124}$$

where $\mu = M/2$ and

$$U(x) = \frac{\mu\omega^2 x^2}{2} - \left[E_p\mu\omega^2 x^2 + J^2\right]^{1/2} \tag{1.125}$$

The potential energy of the problem $U(x)$ consists of two symmetrical potential wells, separated by a barrier, Fig.1.3.

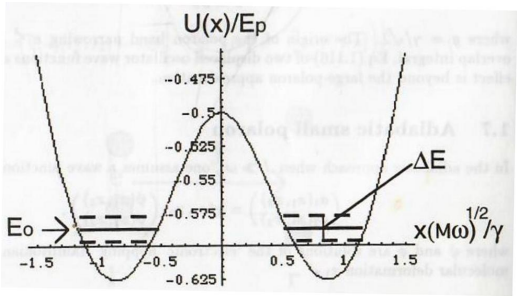

Fig.1.3. Double well potential of the adiabatic Holstein model for $\lambda = 1$.

Minima are located at

$$x_{\min} = \pm\sqrt{\frac{E_p}{\mu\omega^2}\left(1 - \frac{1}{4\lambda^2}\right)} \tag{1.126}$$

and have the common value

$$U_{\min} = -\frac{E_p}{2}\left(1 + \frac{1}{4\lambda^2}\right). \tag{1.127}$$

The barrier height is $-(J + U_{\min})$. If the barrier were impenetrable, there would be the ground state energy level E_0, the same for both wells. To determine its position one can expand the potential near the minimum as

$$U(x) \simeq U_{\min} + \frac{\mu\tilde{\omega}^2 \left(x - x_{\min}\right)^2}{2} \tag{1.128}$$

where

$$\tilde{\omega} = \omega\sqrt{1 - \frac{1}{4\lambda^2}}. \tag{1.129}$$

Then the system is a harmonic oscillator with the renormalised frequency $\tilde{\omega}$ and the ground state energy

$$E_0 - U_{\min} = \frac{\tilde{\omega}}{2} \tag{1.130}$$

The tunneling through the barrier results in the splitting of this level into two, corresponding to states in which electron moves simultaneously in both wells. This is a well known double well potential problem, which can be solved by the quasi-classical technique, if the condition

$$\left|\frac{d}{dx}\frac{1}{p(x)}\right| \ll 1 \tag{1.131}$$

is satisfied. Here $p(x) = \sqrt{2\mu\left[E_0 - U(x)\right]}$ is the classical momentum. Because $\omega \ll J < E_p$ the quasiclassical condition is satisfied practically for all x. The splitting is given by the textbook expression (Landau and Lifshitz (1977))

$$\Delta E = \frac{\tilde{\omega}}{\pi}\exp\left[-2\int_0^a |p(x)|dx\right] \tag{1.132}$$

where $a \simeq x_{\min} - 1/\sqrt{\mu\tilde{\omega}}$ is the classical turning point corresponding to the energy E_0. Fig.1.3. In the extreme strong coupling limit $\lambda \gg 1$ the integral in Eq.(1.132) is

$$\int_0^a |p(x)|dx \simeq \frac{E_p}{2\omega} + \frac{1}{4}\ln\frac{E_p}{\omega} + O(1) \tag{1.133}$$

Omitting a multiplier of the order of unity, one finds

$$\Delta E \sim \sqrt{E_p\omega}e^{-g^2}. \tag{1.134}$$

Holstein found corrections to this expression up to terms of the order of $1/\lambda^2$

$$\Delta E \simeq \sqrt{\frac{4E_p\omega}{\pi}}e^{-\tilde{g}^2} \tag{1.135}$$

where

$$\tilde{g}^2 = g^2\left[1 - \frac{1}{4\lambda^2}\ln(4\lambda) - \frac{1}{8\lambda^2}\right] \tag{1.136}$$

In the strong-coupling limit $\lambda \gg 1$ the exponent in the renormalised bandwidth Eq.(1.135) is the same, as for the nonadiabatic regime, Eq.(1.118) $\tilde{g} = g$. However, the term in front of the exponent differs from $2J$ for any value of λ. There is also an essential exponential difference between Eq.(1.135) and twice of Eq.(1.118) in the intermediate coupling region, where $\tilde{g}$ differs from g. As a result the adiabatic small polaron has much lower effective mass for the intermediate coupling compared with that estimated with the nonadiabatic expression (1.118). It is thus apparent that the perturbation nonadiabatic approach covers only part of the total small polaron region $\lambda \geq 1$. The upper limit of applicability of perturbation theory is given by $J < \sqrt{E_p\omega}$. For the remainder of this region, the adiabatic Eq.(1.135), rather than

the perturbation approach is to be employed. Finally, using the expression for the minima position $x_{\min}$ of the double well potential, Eq.(1.126) one can determine the critical value of λ at which the transition to small adiabatic polaron is expected. The double well disappears when $x_{\min} = 0$ and $\lambda = \lambda_c = 0.5$. At this coupling the renormalised phonon frequency $\tilde{\omega}$ is zero as one can see from Eq.(1.129).

5.2.9 1.8 From large to small polaron: numerical calculations

Theory

Two analytical approaches discussed above are based on the $1/\lambda$ or ω/J expansions.

A priori it is difficult to say to what extent they are reliable in the intermediate coupling region, $\lambda \simeq 1$, when the size of a polaron shrinks and for the intermediate value of the adiabatic parameter $\omega/J \simeq 1$.

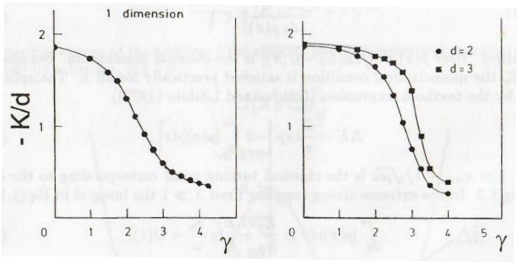

Fig.1.4. The 'Monte-Carlo' polaron collapse of the kinetic energy (K/J) of one-dimensional, two, $d = 2$, and three-dimensional, $d = 3$ fermions interacting with molecular phonons with the interaction constant γ for $\omega/J = 1$ (de Raedt and Lagendijk (1983)).

The ground state energy is not so sensitive to the parameters being about $-E_p$ for the small nonadiabatic and small adiabatic polarons. However, the effective mass and the bandwidth depends strongly on the polaron size and the adiabatic ratio. Several attempts to describe the intermediate region of the coupling $\lambda \simeq 1$ with and
without electron-electron correlations are known in the literature. These are based on the variational approach, the Monte-Carlo calculations and on the exact (numerical) solution of a several-site Holstein model. The transition from a wide band electron (or large polaron) to a narrow band small polaron is extremely sharp as seen in the Monte-Carlo simulations, Fig.1.4. The general conclusion is that there is a continuous but rather sharp evolution from a wide band electron to a narrow band small polaron in the intermediate region of the coupling $\lambda \simeq 1$.

The most reliable results for the intermediate region are obtained with the exact numerical diagonalisation of vibrating clusters (Kongeter and Wagner (1990), Ranninger and Thibblin (1992), Alexandrov et al. (1994a), Marsiglio (1995)). Numerical solution for several vibrating molecules coupled with one electron in the adiabatic $\omega/J < 1$ as well as in the nonadiabatic $\omega/J > 1$ regimes using numerical diagonalisation with 50 phonons shows that the adiabatic and the perturbation approximations are in excellent agreement with the exact solution in adiabatic and nonadiabatic regimes respectively for all values of the coupling constant.

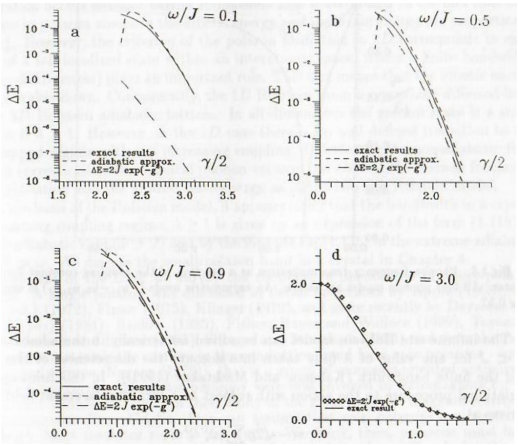

Fig.1.5. Band width (in units of J) of the two-molecular model (Alexandrov et al (1994a)).

To illustrate this we compare in Fig.1.5 the exact splitting of levels for two site cluster with the expression (1.118) for nonadiabatic case and with the Holstein quaniclassical formula Eq.(1.135) in the adiabatic case, generalised for the finite value of λ as

$$\Delta E = \sqrt{\frac{4E_p\omega}{\pi}}\beta^{5/2}\lambda^{1-\beta}[2(1+\beta)]^{-\beta}e^{-\tilde{g}^2} \tag{1.137}$$

where now $\tilde{g}^2 = g^2\{\beta - [\ln(2\lambda(1+\beta))]/4\lambda^2\}$. This generalisation takes into account the frequency renormalisation $\beta \equiv \tilde{\omega}/\omega = \sqrt{1-1/4\lambda^2}$ and the anharmonic corrections of the order of $1/\lambda^2$ to the turning point a in Eq.(1.132). A much lower effective mass of the adiabatic small polaron in the intermediate coupling region compared with that estimated from the perturbation theory expression (1.118) is revealed in Fig.1.5a. In the intermediate coupling region, the effective bandwidth of a smal adiabatic polaron ($\omega \ll J$) can be only one order of magnitude smaller than the bare band width. However, perturbation theory is reliable already for $\omega > 0.5J$ as one can see in Fig.1.5c,d for all values of the coupling. The renormalised phonon frequency has a minimum at the transition from large to small polaron. At large λ the frequencies remain unchanged, Fig.1.6 as predicted with the adiabatic formula Eq.(1.129).

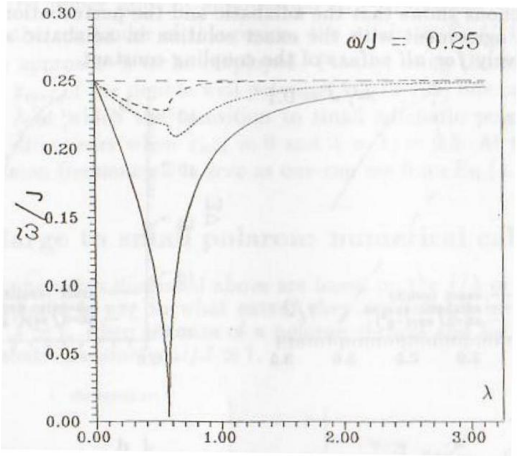

Fig.1.6. Phonon frequency renormalisation as a function of the coupling constant for a 4 -site cluster. All four phonon modes are shown. An asymmetric mode ($-u_{1},-u_{2}, u_{2}, u_{1}$) is unstable at $\lambda \simeq 0.57$.

The infinite-site Holstein model can be solved numerically in the adiabatic limit $\omega \ll J$ for

any value of λ fully taken into account the discreteness of the lattice and the finite bandwidth (Kabanov and Mashtakov (1993)). In this limit applying variational procedure to the action with respect to a local displacement field ϕ_i one arrives at

$$\phi_i = -\sqrt{2}g \sum_r \left|\psi_i^{(r)}\right|^2 n_r, \tag{1.138}$$

and

$$J \sum_{j\neq 0} \psi_{i+j}^{(r)} + \sqrt{2}g\omega\psi_i^{(r)}\phi_i = \epsilon_r \psi_i^{(r)} \tag{1.139}$$

These equations are written by the use of the extreme adiabatic approximation $\frac{\partial\phi}{\partial\tau} = 0$ with ψ_i describing an electron localised on a site i. They do not contain spatial derivatives because "bare" phonons are supposed to be dispersionless. n_r means the occupation number in the eigenstate r.

In the weak-coupling regime $\lambda \ll 1$ one can replace the discrete set for a continuous equation with the following exact solution in $1D$ (Rashba (1957)) :

$$\psi(x) \sim 1/\cosh\left(\frac{\lambda x}{a}\right) \tag{1.140}$$

The numerical analysis of the discrete set of the adiabatic equations leads to the conclusion that there is a smooth transition at $\lambda \simeq 1$ from large to small polaron, and the self-localization occurs without barrier formation in the $1D$ case.

In $2D$ case the situation changes qualitatively. The formation of a self-localized state in $2D$ case is accompanied by the formation of an energy barrier that separates the self-localized and delocalised state. The formation of the barrier is associated with a finite width $\sim J$ of the bare electronic band, while the numerical study of Eqs. (1.138, 139) in the continuous (effective mass) approximation shows that the selflocalization occurs without barrier formation. This is attributed to the fact that on a decrease in polaron size both the kinetic energy and the strain energy are proportional to $1/r_p^2$. However, the criterion of the polaron formation in $2D$ corresponds to existence of a self-localized state within an interatomic space, where a finite bandwidth (lattice discreteness) plays an important role. This fact means that the kinetic energy scaling brakes down. Consequently, the $1D$ Holstein chain is essentially different from $2D$ or $3D$ Holstein adiabatic lattices. In all dimensions the ground state is a small polaron if $\lambda \geq 1$. However, in the $1D$ case there is no well defined transition to the self-trapped regime with the increasing coupling. Calculating the nonadiabatic flucfuation corrections to the classical phonon vacuum one obtains the phonon frequency renormalisation and the ground state energy as in the two-site Holstein model.

On the basis of the Holstein model, it appears likely that the bandwidth in a crystal in the strong coupling regime, $\lambda \geq 1$ is given by an expression of the form (1.118) in the nonadiabatic case ($\omega > J$) and by the formula Eq.(1.135) in the extreme adiabatic case, $J \gg \omega$. We discuss the small-polaron band in a crystal in Chapter 4.

In the rest of the book we survey the cooperative phenomena in many-polaron nystems. A single polaron was discussed in detail in reviews by Appel (1968), Devresse(ed.) (1972), Firsov (1975), Klinger (1979), and more recently by Devreese and Peeters (eds) (1984), Rashba (1985), Fisher, Hayes and Wallace (1989), Toyozawa 1990), Gerlach and Lowen (1991), Shluger and Stoneham (1993) and several others. in magnetic materials the carriers in the conduction band form spin polarons - somemos called ferrons (Nagaev (1979)); that is a group of moments oriented antiparallel to that of the carrier. Magnetic polarons were first invoked in ferromagnets by von Molnar and Methfessel (1967) in their study of the giant negative magneto-resistance

in ferromagnetic $Eu_{1-x}Gd_xSe$. One can assume that spin polarons are carriers in Clie simple Mott insulator such as La_2CuO_4. We think, then, polarons must be of complex hybrid type. In the highly dielectric materials they will dies. Both spin and lattice will contribute to the mass enhant diin polarons are equivalent to the lattice ass enhancement. To some extent liy the hole is similar to the lattice one. and this fact makes some properties one. However, magnons are not perfect bosons, firent from those of lattice polaries of spin polarons (e.g. effective mass) quite dimily the linearised collective excitat. Nevertheless even in this case the idea that mil the constructive and the proble (magnons) of the spin system matter turns. Then be treated with them can be carrier strongly coupled with the spin powerful polaron formalism. We believe that (lie cooperative properties of spin and lattice bipolarons are those of charged bosons and can be described within the same formalism. Under certain conditions strongly correlated electrons can be described by a single-band $t-J$ model, in which the hole, constrained to a projected Hilbert space without double occupancy of sites, interacts with the spin density. The formation of small polarons in the Holstein $t-J$ model is examined in Chapter 5. It turns out that the correlations between electrons significantly reduce the critical value of the coupling constant λ helping to form small polarons.

5.3 3 Electrons and phonons

5.3.1 3.1 Electrons, phonons and the Fröhlich interaction

Theory

In this Chapter, we discuss electrons, phonons and their interaction starting from first principles. Physics and chemistry of solids, liquids and gases are described with the Hamiltonian

$$H = -\sum_i \frac{\nabla_i^2}{2m_e} + \frac{e^2}{2}\sum_{i\neq i'} \frac{1}{|\mathbf{r}_i - \mathbf{r}_{i'}|} - Ze^2 \sum_{ij} \frac{1}{|\mathbf{r}_i - \mathbf{R}_j|} + \frac{Z^2e^2}{2}\sum_{j\neq j'} \frac{1}{|\mathbf{R}_j - \mathbf{R}_{j'}|} - \sum_j \frac{\nabla_j^2}{2M} \tag{3.1}$$

where $\mathbf{r}_i, \mathbf{R}_j$ are coordinates of electrons and nuclei, $i = 1, \dots N_e; j = 1, \dots N; N_e = ZN$, $\nabla_i = \frac{\partial}{\partial \mathbf{r}_i}, \nabla_j = \frac{\partial}{\partial \mathbf{R}_j}$, Z is the number of protons in a nucleus, m_e, M are the electron and nuclear mass, respectively, and e is the elementary charge.

There is no possibility at present to solve the corresponding Schrödinger equation perturbatively because the Coulomb interaction is strong, the ratio of the characteristic interaction energy to the kinetic energy $r_s = m_e e^2/(4\pi n/3)^{1/3} \simeq 1$, or numerically for a condensed matter with the density $n = ZN/\Omega \sim 10^{23}$ cm^{-3}.

Here the normalised volume is taken $\Omega = 1$ unless specified otherwise. (can it play an important role??)

However, one can take advantage of the small value of the adiabatic ratio $m_e/M < 10^{-3}$. Because nuclei are heavy the amplitude $\langle|\mathrm{u}|\rangle \simeq \sqrt{1/M\omega_D}$ (derive this formula btw) of their vibrations near the equilibrium $\mathbf{R}_0 \equiv \mathbf{l}$ in a crystal is much smaller than the lattice constant $a = N^{-1/3}$

$$\frac{\langle|\mathrm{u}|\rangle}{a} \simeq (m_e/Mr_s)^{1/4} \ll 1. \tag{3.2}$$

To obtain this estimate we take into account that the characteristic vibration frequency ω_D is of the order of the ionic plasma frequency $\sqrt{4\pi NZ^2e^2/M}$. (check that it is so)

Using the smallness of the vibration amplitude we can expand the Hamiltonian in powers of $|\mathbf{u}|$ up to quadratic terms, responsible for the quasi-elastic forces returning ions to their equilibrium positions. (it is very not clear, how to do it, because there is no $|\mathbf{u}|$ in the Hamiltonian...)

Further progress requires a simplifying physical idea which is to approach the ground state of the many-electron system via a one-electron picture.

This is called a local density approximation (LDA) introducing an effective one-body potential $\mathcal{V}(\mathbf{r})$

$$\mathcal{V}(\mathbf{r}) = -Ze^2 \sum_j \frac{1}{|\mathbf{r} - \mathbf{R}_j|} + e^2 \int d\mathbf{r}' \frac{n(\mathbf{r}')}{|\mathbf{r} - \mathbf{r}'|} + \mu_{xc}(\mathbf{r}) \tag{3.3}$$

where $\mu_{xc}(\mathbf{r})$ is the exchange interaction, usually expressed by

$$\mu_{xc}(\mathbf{r}) = -\beta[n(\mathbf{r})]^{1/3} \tag{3.4}$$

with constant β. (write more, why is it so??)

Hohenberg and Kohn (1964) proved that $\mathcal{V}(\mathbf{r})$ is a unique functional of the electron density $n(\mathbf{r}) = \langle \psi^\dagger(\mathbf{r})\psi(\mathbf{r}) \rangle$. (check their paper???)

As a result the Hamiltonian in the second quantisation for electrons takes the form

$$H = H_e + H_{ph} + H_{e-ph} + H_{e-e}, \tag{3.5}$$

where

$$H_e = \int d\mathbf{r} \psi^\dagger(\mathbf{r}) \left(\frac{\nabla^2}{2m_e} + V(\mathbf{r}) \right) \psi(\mathbf{r}) \tag{3.6}$$

is the electron energy in a periodic crystal field $V(\mathbf{r}) = \sum_1 v(\mathbf{r} - 1)$, which is $\mathcal{V}(\mathbf{r})$ calculated with $\mathbf{R}_j = 1$ and with the periodic density $n^0(\mathbf{r} + 1) = n^0(\mathbf{r})$,

$$H_{ph} = \sum_{\mathbf{l}} \left(-\frac{\nabla^2_{\mathbf{u}}}{2M} + \mathbf{u}_{\mathbf{l}} \cdot \frac{\partial}{\partial \mathbf{l}} \int d\mathbf{r} n^0(\mathbf{r}) V(\mathbf{r}) \right) + \frac{1}{2} \sum_{\mathbf{l},\mathbf{l}',\alpha,\beta} u^\alpha_{\mathbf{l}} u^\beta_{\mathbf{l}'} D_{\alpha,\beta}(\mathbf{l} - \mathbf{l}') \tag{3.7}$$

is the vibration energy with $\alpha, \beta = x, y, z$ and

$$D_{\alpha,\beta}(\mathbf{l} - \mathbf{l}') = \frac{\partial^2}{\partial l^\alpha \partial l'^\beta} \left(\frac{Z^2 e^2}{2} \sum_{\mathbf{l}'' \neq \mathbf{l}'''} \frac{1}{|\mathbf{l}'' - \mathbf{l}'''|} + \int d\mathbf{r} n^0(\mathbf{r}) V(\mathbf{r}) \right) \tag{3.8}$$

(derive it!!!)

$$\begin{aligned} H_{e-ph} = & \sum_{\mathbf{l}} \mathbf{u}_{\mathbf{l}} \cdot \frac{\partial}{\partial \mathbf{l}} \int d\mathbf{r} \left(\psi^\dagger(\mathbf{r})\psi^\dagger(\mathbf{r}) - n^0(\mathbf{r}) \right) V(\mathbf{r}) \\ & + \frac{1}{2} \sum_{\mathbf{l},\mathbf{l}',\alpha,\beta} u^\alpha_{\mathbf{l}} u^\beta_{\mathbf{l}'} \frac{\partial^2}{\partial l^\alpha \partial l'^\beta} \int d\mathbf{r} \left(\psi^\dagger(\mathbf{r})\psi(\mathbf{r}) - n^0(\mathbf{r}) \right) V(\mathbf{r}) \end{aligned} \tag{3.9}$$

is the electron-lattice vibration interaction, and

$$\begin{aligned} H_{e-e} = & \int d\mathbf{r} d\mathbf{r}' \left(\frac{e^2}{2|\mathbf{r} - \mathbf{r}'|} \left[\psi^\dagger(\mathbf{r}') \psi(\mathbf{r}') - n^0(\mathbf{r}') \right] - \mu_{xc}(\mathbf{r}) \delta(\mathbf{r} - \mathbf{r}') \right) \psi^\dagger(\mathbf{r})\psi(\mathbf{r}) \\ & + \frac{Z^2 e^2}{2} \sum_{\mathbf{l} \neq \mathbf{l}'} \frac{1}{|\mathbf{l} - \mathbf{l}'|} - \frac{e^2}{2} \int d\mathbf{r} d\mathbf{r}' \frac{n^0(\mathbf{r}')}{|\mathbf{r} - \mathbf{r}'|} \psi^\dagger(\mathbf{r})\psi(\mathbf{r}) \end{aligned} \tag{3.10}$$

describes electron-electron correlations.

(derive it!!!)

We include the electrostatic repulsive energy of nuclei in H_{e-e}, so the average of H_{e-e} is zero in a Hartree-Fock approximation. (what is meant by Hartree-Fock a.????)

All integrals above include also summation of spin coordinates. If the magnetic interaction is important the spin-polarised LDA can be applied (for a review see Staunton (1994)). (???)

The vibration Hamiltonian H_{ph} is a quadratic form and therefore can be diagonalised with a linear canonical transformation for the displacement operators

$$\mathbf{u_l} = \sum_{\mathbf{q}} \frac{\mathbf{e}_{\mathbf{q},\nu}}{\sqrt{2NM\omega_{\mathbf{q},\nu}}} d_{\mathbf{q},\nu} \exp(i\mathbf{q}\cdot\mathbf{l}) + h.c., \tag{3.11}$$

$$\frac{\partial}{\partial \mathbf{u_l}} = \sum_{\mathbf{q}} \mathbf{e}_{\mathbf{q},\nu} \sqrt{\frac{M\omega_{\mathbf{q},\nu}}{2N}} d_{\mathbf{q},\nu} \exp(i\mathbf{q}\cdot\mathbf{l}) - h.c., \tag{3.12}$$

(at which point creation, annihilation operators appear? we had just a wave function)

where $\mathbf{q}$ is a phonon momentum, $d_{\mathbf{q},\nu}$ is a phonon (Bose) annihilation operator, $\mathbf{e}_{\mathbf{q},\nu}$ being a unit vector, and ω_{q} a phonon frequency.

Substitution of the last two equations into H_{ph} yields

(check it!!! and the coefficients)

$$H_{ph} = \sum_{\mathbf{q},\nu} \omega_{\mathbf{q},\nu} \left(d^{\dagger}_{\mathbf{q},\nu} d_{\mathbf{q},\nu} + 1/2 \right) \tag{3.13}$$

if eigenfrequencies $\omega_{\mathbf{q},\nu}$ and eigenstates $\mathbf{e}_{\mathbf{q},\nu}$ satisfy

$$M\omega^2_{\mathbf{q},\nu} e^{\alpha}_{\mathbf{q},\nu} = \sum_{\beta} D^{\alpha,\beta}_{\mathbf{q}} e^{\beta}_{\mathbf{q},\nu} \tag{3.14}$$

and

$$\sum_{\mathbf{q}} e^{*\alpha}_{\mathbf{q},\nu} e^{\beta}_{\mathbf{q},\nu} = N\delta_{\alpha,\beta} \tag{3.15}$$

The last equation and the bosonic commutation rules $d_{\mathbf{q},\nu} d^{\dagger}_{\mathbf{q}',\nu'} - d^{\dagger}_{\mathbf{q}',\nu'} d_{\mathbf{q},\nu} = \delta_{\mathbf{q},\mathbf{q}'}\delta_{\nu,\nu'}$ follow from $\frac{\partial}{\partial u^{\alpha}_1} u^{\beta}_1 - u^{\beta}_1 \frac{\partial}{\partial u^{\alpha}_1} = \delta_{\alpha,\beta}$. Here

$$D^{\alpha,\beta}_{\mathbf{q}} = \sum_{\mathbf{m}} \exp(i\mathbf{q}\cdot\mathbf{m}) D_{\alpha,\beta}(\mathbf{m}) \tag{3.16}$$

is the Fourier component of the second derivative of the ion potential energy, Eq.(3.8).

The first derivative in Eq.(3.7) is zero in the presence of a symmetry center. The different solutions of Eq.(3.14) are classified with the mode index ν, which is $1, 2, 3$ for a simple lattice, and $1, \ldots 3k$ for a lattice with k ions per unit cell.

The electron (periodic) part of the Hamiltonian is diagonal in the Bloch representation

(revise Bloch's theory)

$$\psi(\mathbf{r}) = \sum_{\mathbf{k},n,s} \phi_{\mathbf{k},n,s}(\mathbf{r}) c_{\mathbf{k},n,s} \tag{3.17}$$

where $c_{\mathrm{k},n,s}$ is a fermionic annihilation operator. The Bloch function obeys the Schrödinger equation

$$\left(-\frac{\nabla^2}{2m_e}+V(\mathbf{r})\right)\phi_{\mathbf{k},n,s}(\mathbf{r})=E_{\mathbf{k},n,s}\phi_{\mathbf{k},n,s}(\mathbf{r}) \tag{3.18}$$

One-particle states are classified with the momentum $\mathbf{k}$ in the Brillouin zone, band index n (how does it appear??)and spin s.

The solution of this equation is used to obtain the density $n^0(\mathbf{r})$, which determines the crystal field potential $V(\mathbf{r})$. (this is odd... how would we plug V in the equation then, if we need to get if from solution of the eq.?)

The LDA can explain the shape of the Fermi surface of wide band metals and gaps in narrow gap semiconductors. (why??)

The spin polarised version of LDA can explain a variety of properties of many magnetic materials. (why??)This is in contrast to narrow d and f band metals as well as to oxides and other ionic lattices with strong electron-phonon interaction and Coulomb correlations which display much less dispersion and wider gaps than the first-principles band structure methodology can predict.

Substituting Eq.(3.17) into the Hamiltonian one finally obtains

$$H=H_0+H_{e-ph}+H_{e-e}, \tag{3.19}$$

where

$$H_0=\sum_{\mathbf{k},n,s}\xi_{\mathbf{k},n,s}c^\dagger_{\mathbf{k},n,s}c_{\mathbf{k},n,s}+\sum_{\mathbf{q},\nu}\omega_{\mathbf{q},\nu}\left(d^\dagger_{\mathbf{q},\nu}d_{\mathbf{q},\nu}+1/2\right) \tag{3.20}$$

describes independent electron Bloch bands and phonons, $\xi_{\mathbf{k},n,s}=E_{\mathbf{k},n,s}-\mu$ is the band energy spectrum.

Because the electron-phonon interaction leads to the pairing of electrons it is convenient to consider an open system with a fixed chemical potential μ rather than to fix N_e to avoid some artificial difference between odd and even N_e. (don't understand how will it help to avoid and what is the problem?)

The ground state of an open system has the minimum expectation value of $H-\mu N_e$. That is why the electron energy is related to μ.

The part of the electron-phonon interaction, which is linear in phonon operators can be written as

(derive!!! where the bands at all come into the game??)

$$H_{e-ph}=\frac{1}{\sqrt{2N}}\sum_{\mathbf{k},\mathbf{q},n,n',\nu,s}\gamma_{n,n'}(\mathbf{q},\mathbf{k},\nu)\omega_{\mathbf{q},\nu}c^\dagger_{\mathbf{k},n,s}c_{\mathbf{k}-\mathbf{q},n',s}d_{\mathbf{q},\nu}+h.c. \tag{3.21}$$

with a dimensionless matrix element

$$\gamma_{n,n'}(\mathbf{q},\mathbf{k},\nu)=-\frac{N}{\sqrt{M\omega^3_{\mathbf{q},\nu}}}\int d\mathbf{r}\left(\mathbf{e}_{\mathbf{q},\nu}\cdot\nabla v(\mathbf{r})\right)\phi^*_{\mathbf{k},n,s}(\mathbf{r})\phi_{\mathbf{k}-\mathbf{q},n',s}(\mathbf{r}) \tag{3.22}$$

Low energy physics is often described within a single band approximation with the matrix element γ depending only on the momentum transfer q. If

$$\gamma_{n,n'}(\mathbf{q},\mathbf{k},\nu)=\gamma(\mathbf{q}) \tag{3.23}$$

we call the interaction the Fröhlich one. Terms of H_{e-ph} quadratic and higher order in phonon operators are small. They play a role only for those phonons which are not coupled with electrons by the linear interaction, Eq.(3.21) ($\gamma=0$). The correlation energy of a homogeneous electron system is written as

$$H_{e-e} = \frac{1}{2}\sum_{\mathbf{q}} V_c(\mathbf{q})\rho^{\dagger}_{\mathbf{q}}\rho_{\mathbf{q}} \tag{3.24}$$

where $V_c(\mathbf{q})$ is a matrix element of the Coulomb interaction, which is zero for $\mathbf{q} = 0$ because of electroneutrality (why??)and

$$\rho^{\dagger}_{\mathbf{q}} = \sum_{\mathbf{k},s} c^{\dagger}_{\mathbf{k},s} c_{\mathbf{k}+\mathbf{q},s} \tag{3.25}$$

is the density fluctuation operator. For doped semiconductors and amorphous metals a random potential should be included in H_0. (there are some exotic models about it, maybe I'll learn them later)

The harmonic approximation is sufficient for low temperature kinetics and thermodynamics of solids. Further corrections in $|u|$, especially those of third and fourth order, are known as anharmonic terms, and are of importance for the thermal expansion and lattice thermal conductivity. (I'll maybe meet them in another theory, here they are just not used)

5.3.2 3.2 Bare phonons and sound in a metal

Theory

(in this section, it is not clear, what problem is solved by this formalism, it is just a revision of well-known electron-phonon formalism with some unusual features. Basically, the main conclusion is that phonons are renormalized.)

In wide-band metals such as Na or K the correlation energy is relatively small ($r_s \leq 1$) and carriers are almost free. Core electrons together with nuclei form compact ions with an effective Z. The carrier wave function outside the core can be represented by a plane wave
(why??)

$$\phi_{\mathbf{k},n,s} \simeq e^{i\mathbf{k}\cdot\mathbf{r}} \tag{3.26}$$

and the carrier density $n^0(\mathbf{r})$ is constant. Therefore the only relevant interaction in the dynamical matrix is the Coulomb repulsion between ions, which yields
(check that it is the same formula as before, but simplified)

$$D_{\alpha,\beta}\left(\mathbf{l}-\mathbf{l}'\right) = \frac{Z^2e^2}{2}\frac{\partial^2}{\partial l^{\alpha}\partial l'^{\beta}}\sum_{\mathbf{l}''\neq\mathbf{l}'''}\frac{1}{|\mathbf{l}''-\mathbf{l}'''|} \tag{3.27}$$

The electron-phonon coupling constant is determined with the Coulomb electron-ion attraction $v(\mathbf{r}) = -Ze^2/r$ and with the plane waves in Eq.(3.22).
(hard task to do: find this coupling constant for some different types of material. maybe I'll do it in another note)

(here, there is some idea, why do we do such transformations as below??? I don't yet understand it)
The potential $1/r$ may be expanded in a Fourier series as

$$\frac{1}{r} = 4\pi\lim_{\kappa\to 0}\sum_{\mathbf{q}}\frac{1}{q^2+\kappa^2}e^{i\mathbf{q}\cdot r} \tag{3.28}$$

Substituting this expansion into Eq.(3.27) and Eq.(3.22) we find

$$D_{\alpha,\beta}(\mathbf{m}) = 4\pi \lim_{\kappa\to 0} \sum_{\mathbf{q}} \frac{q_\alpha q_\beta}{q^2+\kappa^2} \cos(\mathbf{q}\cdot\mathbf{m}) \tag{3.29}$$

and

$$\gamma(\mathbf{q}) = i\frac{4\pi NZe^2}{\sqrt{M\omega_{\mathbf{q}}^3}} \lim_{\kappa\to 0} \frac{\mathrm{e}_{\mathbf{q},\nu}\cdot\mathbf{q}}{q^2+\kappa^2} \tag{3.30}$$

Calculating the Fourier component of Eq.(3.29) one obtains for eigenfrequences and three eigenvectors

(how to do it????)

$$\omega_{\mathbf{q},\nu}^2 \mathbf{e}_{\mathbf{q},\nu} = \omega_i^2 \mathbf{q} \frac{\mathbf{e}_{\mathbf{q},\nu}\cdot\mathbf{q}}{q^2} \tag{3.31}$$

where $\omega_i = \sqrt{4\pi NZ^2e^2/M}$ is the ionic plasma frequency. A longitudinal mode with e $\|$q is an ionic plasmon

$$\omega_{\mathrm{q}} = \omega_i \tag{3.32}$$

and two shear (transverse) modes with $\mathbf{e} \perp \mathbf{q}$ have zero frequency, which is due to [a] hard core approximation. (why??)

In fact, the core electrons undergo a polarisation when ions are displaced from their equilibrium positions which yields a finite shear mode frequency.

According to Eq.(3.30) carriers interact with the longitudinal phonons. The interaction is strong, giving rise to a significant renormalisation of the bare phonon frequency, Eq.(3.32).

To calculate the renormalised phonon frequency one can apply following Migdal (1958) the Green's function (GF) formalism. The one-particle Green's function (GF) is determined as:

(never saw that GF has both Shr. and Heis. operators. is it ok?)

$$G(\mathbf{k},t) = -i\left\langle T_t c_{\mathbf{k}}(t) c_{\mathbf{k}}^\dagger \right\rangle \tag{3.33}$$

with $c_{\mathbf{k}}(t) = \exp(iHt)c_{\mathbf{k}}\exp(-iHt)$ and $T_t A(t)B = \Theta(t)A(t)B - \Theta(-t)BA(t)$ for any fermionic operators A, B and with the opposite sign of the second term for any bosonic operators, $\Theta(x) = 1$ for $x > 0$ and zero otherwise. The Fourier component of the free-electron GF ($H = H_0$) is given by

$$G^{(0)}(\mathbf{k},\omega) = \frac{\Theta(\xi_{\mathbf{k}})}{\omega - \xi_{\mathbf{k}} + i0^+} + \frac{\Theta(-\xi_{\mathbf{k}})}{\omega - \xi_{\mathbf{k}} - i0^+}, \tag{3.34}$$

with $\xi_{\mathbf{k}} = k^2/2m_e - \mu$ which is obtained by the direct integration of Eq.(3.33):

$$G^{(0)}(\mathbf{k},\omega) = \frac{1}{2\pi}\int_{-\infty}^{\infty} dt G^0(\mathbf{k},t) e^{i\omega t} \tag{3.35}$$

(check this. it should be straightforward)

For interacting electrons the electron self-energy is introduced asы

$$\Sigma(\mathbf{k},\omega) = \left(G^{(0)}(\mathbf{k},\omega)\right)^{-1} - (G(\mathbf{k},\omega))^{-1} \tag{3.36}$$

so

$$G(\mathbf{k},\omega) = \frac{1}{\omega - \xi_{\mathbf{k}} - \Sigma(\mathbf{k},\omega)} \tag{3.37}$$

It is a well-known formalism.

The phonon GF can be determined as

$$D(\mathbf{q},t) = -i\frac{\omega_{\mathbf{q}}}{2}\left\langle T_t\left(d_{\mathbf{q}}(t)d^{\dagger}_{\mathbf{q}} + d^{\dagger}_{\mathbf{q}}(t)d_{\mathbf{q}}\right)\right\rangle. \tag{3.38}$$

(check that such defs are in other books...)

Thus the Fourier component of the free phonon GF ($H = H_0$) is the dimensionless even function of frequency

$$D^{(0)}(\mathbf{q},\omega) = \frac{\omega^2_{\mathbf{q}}}{\omega^2 - \omega^2_{\mathbf{q}} + i0^+} \tag{3.39}$$

and the phonon self-energy

$$\Pi(\mathbf{q},\omega) = \left(D^{(0)}(\mathbf{q},\omega)\right)^{-1} - \left(D(\mathbf{q},\omega)\right)^{-1}. \tag{3.40}$$

(nothing is explained below, so one needs to know all this formalism in order to understand it)

The Feynman diagram technique is convenient, Fig.3.1.

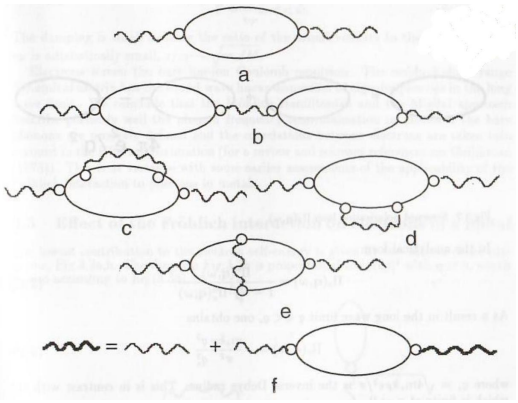

Fig.3.1. Second (a) and fourth order (b,c,d,e) corrections to the phonon GF. The phonon GF in the Migdal approximation, (f).

Thin straight and wavy lines correspond to $G^{(0)}$ and $D^{(0)}$ respectively, a vertex (circle) corresponds to the interaction matrix element $\gamma(\mathbf{q})\sqrt{\omega_{\mathbf{q}}/N}$ and bold lines represent G and D.

The Fröhlich interaction is a sum of two operators describing the emission and absorption of a phonon. Both events are taken into account by the definition of D. Therefore wavy lines have no direction. There are no first or higher odd-order corrections to D because the Fröhlich interaction is off-diagonal with respect to phonon occupation numbers. The second order term of D, Fig.3a includes a so-called polarisation loop Π^0_e, which is a convolution of two $G^{(0)}$. Among different fourth order diagrams the diagram Fig.3.1b with two polarisation loops is the most 'dangerous'. Different from others it is proportional to $1/q^2$, which is large for small q. On the other hand the singularity of internal vertices is integrated out in the diagrams Fig.3.1c,d,e. The sum of all 'dangerous' diagrams is given in Fig.3f, or in the analytical form

$$\Pi(\mathbf{q},\omega) = \frac{|\gamma(\mathbf{q})|^2\omega_{\mathbf{q}}}{N}\Pi_e(\mathbf{q},\omega) \tag{3.41}$$

where

$$\Pi_e(\mathbf{q},\omega) = \Pi^0_e(\mathbf{q},\omega) \tag{3.42}$$

with

$$\Pi^0_e(\mathbf{q},\omega) = -\frac{2i}{(2\pi)^4}\int d\mathbf{k}d\epsilon G^{(0)}(\mathbf{k}+\mathbf{q},\epsilon+\omega)G^{(0)}(\mathbf{k},\epsilon) \tag{3.43}$$

The additional 2 in the phonon self-energy is due to the contribution to the polarisation loop from two electron spins. It is convenient first to integrate over frequency in Eq.(3.43) with the following result:

$$\Pi_e^0(\mathbf{q},\omega) = \frac{1}{4\pi^3}\int d\mathbf{k}\frac{\Theta\left(\xi_{\mathbf{k}}\right) - \Theta\left(\xi_{\mathbf{k+q}}\right)}{\omega + \xi_{\mathbf{k}} - \xi_{\mathbf{k+q}} + i0^+\,\mathrm{sgn}\left(\xi_{\mathbf{k+q}}\right)} \tag{3.44}$$

Because of adiabaticity ω is small, $\omega \ll \mu$. Thus one can take $\omega = 0$ in $\Re\Pi_e^0$ and the first order term in ω in $\Im\Pi_e^0$ to obtain

$$\Re\Pi_e^0(\mathbf{q},\omega) = -\frac{m_e k_F}{2\pi^2} h\left(\frac{q}{2k_F}\right) \tag{3.45}$$

$$\Im\Pi_e^0(\mathbf{q},\omega) = -\frac{m_e^2}{2\pi q}|\omega|\Theta\left(2k_F - q\right) \tag{3.46}$$

with $h(x) = 1 + \frac{1-x^2}{2x}\ln\left|\frac{1+x}{1-x}\right|$ and the Fermi momentum $k_F = \sqrt{2m_e\mu} = \left(3\pi^2 n\right)^{1/3}$.
One should also take into account the Coulomb correlations because the corresponding vertex is singular in the long wave limit, $V_c(q) = 4\pi e^2/q^2$. This leads to a drastic renormalisation of the long wave behavior of Π_e. In the 'loop' or random phase (RPA) approximation we obtain Fig.3.2 as in the case of the electron-plasmon interaction, Fig.3.1f, but with the Coulomb (dashed) line instead of the wavy phonon line.

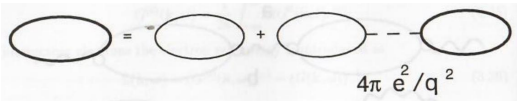

Fig.3.2. Screened polarisation loop $\Pi_{e}(\mathbf{q}, \omega)$.

In the analytical form

$$\Pi_e(\mathbf{q},\omega) = \frac{\Pi_e^0(\mathbf{q},\omega)}{1 - \frac{4\pi e^2}{q^2}\Pi_e^0(\mathbf{q},\omega)} \tag{3.47}$$

As a result in the long wave limit $q \ll q_s$ one obtains

$$\Pi_e(\mathbf{q},\omega) = -\frac{m_e k_F}{\pi^2}\frac{q^2}{q_s^2} \tag{3.48}$$

where $q_s = \sqrt{4m_e k_F e^2/\pi}$ is the inverse Debye radius. This is in contrast with Π_e^0, which is finite at $q \to 0$.
(this is a bad theory, because before it was written that $\Pi_e(\mathbf{q},\omega) = \Pi_e^0(\mathbf{q},\omega)$. Maybe it is meant $\Pi(\mathbf{q},\omega)$)

With the RPA expression, Eq.(3.41) and $\gamma(\mathbf{q})$ determined in Eq.(3.30) with $\omega_{\mathbf{q},\nu}\omega_i$ the phonon Green's function is

$$D(\mathbf{q},\omega) = \frac{\omega_i^2}{\omega^2 - \tilde{\omega}_{\mathbf{q}}^2} \tag{3.49}$$

A pole of D determines a new phonon dispersion and a damping Γ due to the interaction with electrons

$$\tilde{\omega}_{\mathbf{q}} = \frac{\omega_i}{\sqrt{\epsilon\left(\mathbf{q}, \tilde{\omega}_{\mathbf{q}}\right)}} \tag{3.50}$$

where

$$\epsilon(\mathbf{q}, \omega) = 1 - \frac{4\pi e^2}{q^2}\Pi_e^0(\mathbf{q}, \omega) \tag{3.51}$$

is the electron dielectric function.

(some formalism is assumed here. write it better! why polarization operator is connected to the dielectric function?)

In the long wave limit

$$\epsilon(\mathbf{q}, 0) = 1 + \frac{q_s^2}{q^2} \tag{3.52}$$

so one obtains a sound wave as the real part of $\tilde{\omega}$

$$\tilde{\omega}_{\mathbf{q}} = sq \tag{3.53}$$

with the sound velocity $s = Zk_F/\sqrt{3Mm_e}$, and a small damping as the imaginary part

$$\Gamma \sim \frac{s}{v_F}\tilde{\omega} \ll \tilde{\omega} \tag{3.54}$$

The damping is small because the ratio of the sound velocity to the Fermi velocity v_F is adiabatically small, $s/v_F \sim \sqrt{m_e/M}$.

Electrons screen the bare ion-ion Coulomb repulsion. The residual short range dynamical matrix has the sound wave linear dispersion of eigenfrequencies in the long wave limit. We conclude that the Fröhlich Hamiltonian and the Migdal approach describe perfectly well the phonon frequency renormalisation in metals if the bare phonons are properly defined and the correlations between electrons are taken into account in the RPA approximation (for a review and relevant references see Geilikman (1975)). This is at variance with some earlier assessments of the applicability of the Fröhlich interaction to phonons in metals.

5.3.3 3.3 Effect of the Fröhlich interaction on electrons in a metal

Theory

The lowest contribution to the electron self-energy is given by two second order diagrams, Fig.3.3a,b. The diagram Fig.3.3b is proportional to $|\gamma(\mathbf{q})|^2$ with $\mathbf{q} \equiv 0$, which is zero according to Eq.(3.30).

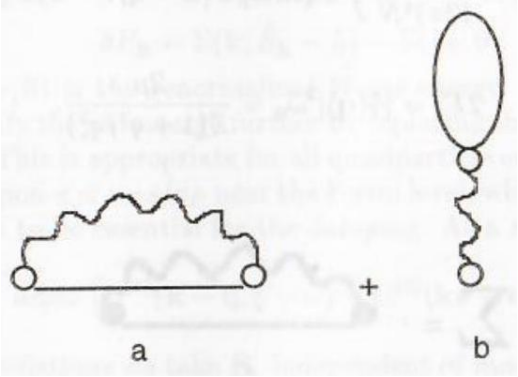

Fig.3.3. Second-order electron self-energy.

Higher order RPA diagrams are taken into account through the replacement of the bare ionic plasmon GF for the renormalised one, Eq.(3.49) and the bare electron-phonon interaction constant γ for a screened one, γ_{sc} as shown in Fig.3.4. In the analytical form the diagram Fig. 3.4 corresponds to

$$\gamma_{sc}(\mathbf{q},\omega) = \gamma(\mathbf{q}) + \frac{4\pi e^2}{q^2}\Pi_e^0(\mathbf{q},\omega)\gamma_{sc}(\mathbf{q},\omega) \tag{3.55}$$

or

$$\gamma_{sc}(\mathbf{q},\omega) = \frac{\gamma(\mathbf{q})}{\epsilon(\mathbf{q},\omega)} \tag{3.56}$$

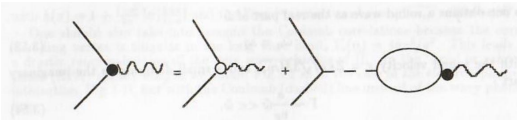

Fig.3.4.Screened electron-phonon interaction (dark circle).

For low-energy excitations $\omega \ll \mu$ the static approximation of the dielectric function, Eq.(3.52) is appropriate. Instead of D and γ_{sc} given in Eq.(3.49) and Eq.(3.56) one can introduce the acoustic phonon GF

$$\tilde{D}(\mathbf{q},\omega) = \frac{\tilde{\omega}_{\mathbf{q}}^2}{\omega^2 - \tilde{\omega}_{\mathbf{q}}^2} \tag{3.57}$$

and the electron-acoustic phonon vertex $\tilde{\gamma}(\mathbf{q})\sqrt{\frac{\bar{\omega}_{\mathbf{q}}}{N}}$ with

$$\tilde{\gamma}(\mathbf{q}) = \frac{\gamma(\mathbf{q})}{\epsilon(\mathbf{q},0)}\left(\frac{\omega_i}{\tilde{\omega}_{\mathbf{q}}}\right)^{3/2} \tag{3.58}$$

Finally one obtains the diagram, Fig.3.5 for the electron self-energy as a result of the summation of the 'most divergent' RPA diagrams (????)

$$\Sigma(\mathbf{k},\epsilon) = \frac{2i}{(2\pi)^4 N}\int d\mathbf{q}d\omega E_p G(\mathbf{k}-\mathbf{q},\epsilon-\omega)\tilde{D}(\mathbf{q},\omega) \tag{3.59}$$

with

$$2E_p = |\tilde{\gamma}(\mathbf{q})|^2\tilde{\omega}_{\mathbf{q}} = \frac{2\mu}{Z\,(1+q^2/q_s^2)} \tag{3.60}$$

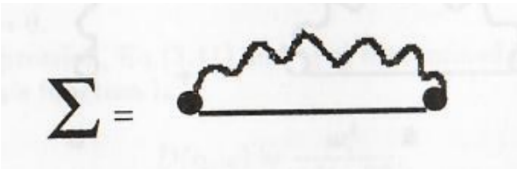

Fig.3.5. Electron self-energy in the Migdal approximation.

Because Z is of order of unity the electron-acoustic phonon interaction E_p is generally not small being of the order of the Fermi-energy in a metal. (??)

Therefore one has to consider fourth and higher order diagrams with the crossing phonon lines as in Fig.3.6, which are absent from Fig.3.5. (??)

Fortunately, as shown by Migdal their contribution is adiabatically small ($\sim s/v_F$) compared with Eq.(3.59). Moreover, the main contribution to the integral in Eq.(3.59) for Σ comes from the region $q \sim k_F \gg q_s$. In this region the dimensionless coupling constant

$$\lambda = 2E_p N(0) \tag{3.61}$$

is small

$$\lambda \simeq r_s \ll 1 \tag{3.62}$$

so the second order is sufficient for Σ. Here

$$N(0) = \frac{1}{N}\sum_{\mathbf{k}} \delta\left(\xi_{\mathbf{k}} - \mu\right) \tag{3.63}$$

is the density of states (DOS) per cell at the Fermi level.

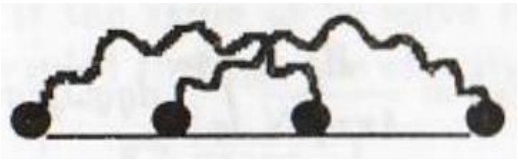

Fig.3.6. Adiabatically small corrections to the electron self-energy.

A new quasiparticle spectrum renormalised by the interaction is determined as a pole of the electron GF :

$$\tilde{E}_{\mathbf{k}} = \tilde{\mu} + v_F\left(k - k_F\right) + \delta E_{\mathbf{k}} \tag{3.64}$$

where

$$\delta E_{\mathbf{k}} = \Sigma\left(\mathbf{k}, \tilde{E}_{\mathbf{k}} - \tilde{\mu}\right) - \Sigma\left(k_F, 0\right) \tag{3.65}$$

and $\tilde{\mu} = \mu + \Sigma\left(k_F, 0\right)$ is the renormalised Fermi energy. The adiabatic condition allows one to simplify the self-energy further by replacing the exact GF in the integral Eq. (3.59) by $G^{(0)}$. This is appropriate for all quasiparticle energies with the exception of a very narrow region $\ll \omega_D s/v_F$ near the Fermi level, where the difference between G and $G^{(0)}$ appears to be essential for the damping. As a result one obtains

$$\delta E_{\mathbf{k}} = \frac{2iE_p}{(2\pi)^4}\int d\mathbf{q}d\omega\left(G^{(0)}(\mathbf{k}-\mathbf{q}, \tilde{\xi} - \omega) - G^{(0)}\left(\mathbf{k}_F - \mathbf{q}, -\omega\right)\right)\tilde{D}(\mathbf{q}, \omega) \tag{3.66}$$

To simplify the calculations we take E_p independent of momentum, apply the Debye approximation for acoustic phonons $\tilde{\omega}_{\mathrm{q}} = sq$ for $q < q_D$ where $q_D \simeq \pi/a$ is the Debye momentum, and consider a half-filled band, $k_F \simeq \pi/2a$ with the energy independent DOS near the Fermi level $N(0) = m_e a^2/4\pi$.

The main contribution to the integral Eq.(3.66) comes from the momentum region close to the Fermi-surface:

$$|\mathrm{k} - \mathrm{q}| \simeq k_F \tag{3.67}$$

This makes it convenient to introduce a new variable $k' = |\mathbf{k} - \mathbf{q}|$ instead of the angle Θ lietween k and q and extend the integration to $\pm\infty$ with the variable $\xi = v_F\,(k' - k_F)$. Thus the angular integration in Eq.(3.66) becomes:

$$\int d\Theta \sin\Theta(\ldots) \sim \int_{\infty}^{\infty} d\xi \frac{\tilde{\xi}}{\left[\tilde{\xi} - \omega - \xi + i0^+\,\mathrm{sgn}(\xi)\right]\left[\omega + \xi - i0^+\,\mathrm{sgn}(\xi)\right]} \tag{3.68}$$

This integral is non-zero only if $\tilde{\xi} > \omega > 0$ or $\tilde{\xi} < \omega < 0$. It is $-2\pi i$ in the first region and $2\pi i$ in the second one. Taking into account that $\tilde{D}$ is an even function of ω one obtains

$$\delta E_{\mathrm{k}} = \frac{2E_p}{(2\pi)^2 v_F N} \int_0^{q_D} dqq \int_0^{|\bar{\xi}|} d\omega\,\mathrm{sgn}(\tilde{\xi}) \frac{\tilde{\omega}_q^2}{\omega^2 - \tilde{\omega}_q^2 + i0^+} \tag{3.69}$$

The real and imaginary parts of Eq.(3.69) determine respectively the renormalised spectrum and the life time of quasiparticles

$$\Re\left(\delta E_{\mathbf{k}}\right) = \frac{E_p}{4\pi^2 v_F N} \int_0^{q_D} dqq\tilde{\omega}_q \ln\left|\frac{\tilde{\omega}_q - \tilde{\xi}}{\tilde{\omega}_q + \tilde{\xi}}\right| \tag{3.70}$$

$$\Im\left(\delta E_{\mathbf{k}}\right) = \frac{E_p}{4\pi v_F N} \int_0^{q_m} dqq\tilde{\omega}_q\,\mathrm{sgn}(\tilde{\xi}) \tag{3.71}$$

with $q_m = |\tilde{\xi}|/s$ if $|\tilde{\xi}| < \omega_D$ and $q_m = q_D$ if $|\tilde{\xi}| > \omega_D$. For the excitations far away from the Fermi surface with $|\tilde{\xi}| \gg \omega_D$ we find

$$\Re\left(\delta E_{\mathbf{k}}\right) = -\lambda\frac{\omega_D^2}{2\tilde{\xi}} \tag{3.72}$$

Here $\omega_D = sq_D$ is the Debye frequency. For low-energy excitations with $|\tilde{\xi}| \ll \omega_D$

$$\Re\left(\delta E_{\mathbf{k}}\right) = -\lambda\tilde{\xi} \tag{3.73}$$

which means an increase of the effective mass of the excitation due to the electron-phonon interaction

$$\tilde{\xi} = \frac{k_F}{m^*}\,(k - k_F) \tag{3.74}$$

The renormalised effective mass is

$$m^* = (1 + \lambda)m_e. \tag{3.75}$$

Thus the excitation spectrum of a metal has two different regions with two different values of the effective mass. The thermodynamic properties of a metal at low temperature $T \ll \omega_D$ involve m^*, but the optical properties in a frequency range $\nu \gg \omega_D$ are determined by the high-energy excitations, where according to Eq.(3.72) corrections are small and the mass is equal to the band mass m_e.

The damping has just the opposite behavior. The integral Eq.(3.71) yields

$$\Im\left(\delta E_{\mathbf{k}}\right) = \frac{\mathrm{sgn}(\tilde{\xi})\pi\lambda\omega_D}{3} \tag{3.76}$$

if $|\tilde{\xi}| > \omega_D$, and

$$\Im\left(\delta E_{\mathbf{k}}\right) = \frac{\mathrm{sgn}(\tilde{\xi})\pi\lambda|\tilde{\xi}|^3}{3\omega_D^2} \tag{3.77}$$

for $|\tilde{\xi}| \ll \omega_D$.
These expressions describe the rate of decay of the quasiparticles due to emission of phonons. In the immediate neighborhood of the Fermi surface $|\tilde{\xi}| \ll \omega_D$ the
decay is small compared with the quasiparticle energy $|\tilde{\xi}|$ even for a relatively strong coupling $\lambda \sim 1$, so that the concept of well-defined quasiparticles has a definite meaning. Hence, within the Migdal approximation the electron-phonon interaction does not destroy the Fermi-liquid behavior of electrons. The Pauli exclusion principle is responsible for the stability of the Fermi liquid. In the intermediate-energy region $|\tilde{\xi}| \sim \omega_D$, however, the decay is comparable with the energy and the quasiparticle spectrum looses its meaning. In the high-energy region $|\tilde{\xi}| \gg \omega_D$ the decay remains the same in absolute value but again becomes small in comparison with $|\xi|$ and the quasiparticle concept recovers its meaning.

To go beyond Migdal's approximation one has to consider adiabatically small higher order diagrams which is the same as to solve the Hamiltonian of free electrons and acoustic phonons coupled through the effective Fröhlich interaction

$$H_{e-ph} = \frac{1}{\sqrt{2N}} \sum_{\mathbf{k},\mathbf{q},s} \tilde{\gamma}(\mathbf{q})\tilde{\omega}_{\mathbf{q}} c^{\dagger}_{\mathbf{k},s} c_{\mathbf{k}-\mathbf{q},s} \tilde{d}_{\mathbf{q}} + h.c. \tag{3.78}$$

with $\tilde{d}_{\mathrm{q}}$ the acoustic phonon operator. From our consideration it follows that applying this Hamiltonian to electrons one should not consider the acoustic phonon self-energy. Acoustic phonons in a metal appear as the result of the electron-plasmon coupling and the Coulomb screening, so their frequency includes already the self-energy effect as discussed in section 3.2.

5.3.4 3.4 Broken gauge symmetry and the BCS ground state

(summary of BCS model)
(where is Broken gauge symmetry?)

Theory

The Migdal approach is justified if the ground state is stable versus a phase transition. Frohlich (1950) realised that the electron-phonon interaction, Eq.(1.48) leads to an attraction between two electrons and Cooper (1957) discovered that any attraction between degenerate electrons leads to their pairing; it does not matter how weak it in. Pairs are bosons, which undergo a Bose-Einstein condensation at some critical temperature T_c. The condensed state is described by the classical field, which is an average of the product of two annihilation field operators $F \sim \langle\psi\psi\rangle$ or two creation operators $F^{+} \sim \left\langle\psi^{\dagger}\psi^{\dagger}\right\rangle$. This average is macroscopically large below T_c in an open system. The appearance of the 'anomalous' averages brakes the gauge symmetry of the bare Hamiltonian, Eq.(3.19) and cannot be described perturbatively. Following Hardeen, Cooper and Schrieffer (1957) one has to go beyond the Migdal approximaNon, Fig. 3.5 including the anomalous averages in the ground state. This can be done milfonsistenly using the same self-energy diagram Fig. 3.5 as for the normal state but with the matrix electron GF (Eliashberg (1960)). At finite temperature the diagram in himique can be formulated for the 'temperature' GF defined by Matsubara(1955)

$$g(\mathrm{k},\tau) = -\left\langle\left\langle T_{\tau} c_{\mathrm{k}}(\tau) c^{\dagger}_{\mathrm{k}}\right\rangle\right\rangle, \tag{3.79}$$

will $c_k(\tau) = \exp(H\tau)c_{\mathbf{k}}\exp(-H\tau)$ and $0 < \tau < 1/T$ a 'thermodynamic' time. The imidie angular brackets correspond to the quantum as well as a statistical average willi the Cibbs distribution:

$$\langle\langle \ldots \rangle\rangle = \sum_{\nu} e^{\frac{\Omega - E_\nu}{T}} \langle\nu| \ldots |\nu\rangle \tag{3.80}$$

where Ω is the thermodynamic potential and $|\nu\rangle$ the eigenstates of $H - \mu N$ with the eigenvalues E_ν. Because the thermodynamic time is restricted by $1/T$ the temperature GF is expanded in the Fourier series:

$$g(\mathbf{k}, \tau) = T \sum_{\omega_n} e^{-i\omega_n \tau} g\left(\mathbf{k}, \omega_n\right) \tag{3.81}$$

with the discrete Matsubara frequencies $\omega_n = \pi T(2n+1), n = 0, \pm 1, \pm 2, \ldots$. For free electrons one obtains

$$g^{(0)}\left(\mathbf{k}, \omega_n\right) = \frac{1}{i\omega_n - \xi_{\mathbf{k}}} \tag{3.82}$$

and for phonons

$$\tilde{d}^{(0)}\left(\mathbf{q}, \omega_n - \omega_{n'}\right) = -\frac{\tilde{\omega}_{\mathbf{q}}^2}{\left[\omega_n - \omega_{n'}\right]^2 + \tilde{\omega}_{\mathbf{q}}^2}. \tag{3.83}$$

To take into account the Cooper pairing of two electrons with the opposite momentum and spin one can introduce, following Gor'kov (1958) and Nambu (1960) the matrix GF:

$$\hat{g}(\mathbf{k}, \tau) = -\begin{pmatrix} \left\langle\left\langle T_\tau c_{\mathbf{k},\uparrow}(\tau) c^\dagger_{\mathbf{k},\uparrow} \right\rangle\right\rangle & \langle\langle T_\tau c_{\mathbf{k},\uparrow}(\tau) c_{-\mathbf{k},\downarrow} \rangle\rangle \\ \left\langle\left\langle T_\tau c^\dagger_{-\mathbf{k},\downarrow}(\tau) c^\dagger_{\mathbf{k},\uparrow} \right\rangle\right\rangle & \left\langle\left\langle T_\tau c^\dagger_{-\mathbf{k},\downarrow}(\tau) c_{-\mathbf{k},\downarrow} \right\rangle\right\rangle \end{pmatrix}. \tag{3.84}$$

The matrix self-energy

$$\hat{\Sigma}\left(\mathbf{k}, \omega_n\right) = \left(\hat{g}^{(0)}\left(\mathbf{k}, \omega_n\right)\right)^{-1} - \hat{g}^{-1}\left(\mathbf{k}, \omega_n\right) \tag{3.85}$$

with $\hat{g}^{(0)}\left(\mathbf{k}, \omega_n\right) = \left(i\omega_n \tau_0 - \xi_{\mathbf{k}} \tau_3\right)^{-1}$. Here $\tau_{0,1,2,3}$ is a set of the Pauli matrices:

$$\tau_0 = \begin{pmatrix} 1 & 0 \\ 0 & 1 \end{pmatrix}$$
$$\tau_1 = \begin{pmatrix} 0 & 1 \\ 1 & 0 \end{pmatrix}$$
$$\tau_2 = \begin{pmatrix} 0 & -i \\ i & 0 \end{pmatrix}$$
$$\tau_3 = \begin{pmatrix} 1 & 0 \\ 0 & -1 \end{pmatrix}$$

The generalized equation for the matrix $\hat{\Sigma}$ is given by the same diagram as in the normal state, Fig.3.5, with only substitution $\tilde{\gamma}(\mathbf{q})\tau_3$ instead of $\tilde{\gamma}(\mathbf{q})$ and summation over Matsubara frequencies instead of integration:

$$\hat{\Sigma}\left(\mathbf{k}, \omega_n\right) = -T \sum_{\omega_{n'}} \int \frac{d\mathbf{q}}{(2\pi)^3} |\tilde{\gamma}(\mathbf{q})|^2 \tilde{\omega}_{\mathbf{q}} \tau_3 \hat{g}\left(\mathbf{k} - \mathbf{q}, \omega_{n'}\right) \tau_3 \tilde{d}\left(\mathbf{q}, \omega_n - \omega_{n'}\right) \tag{3.86}$$

The most important difference of Eq.(3.86) compared with the normal state Eq.(3.59) is the possibility of obtaining a finite value of the off-diagonal matrix elements $\sim < cc >$ within

the self-consistent solution, Fig.3.7. In the second $\left(\hat{g} \to \hat{g}^{(0)}\right)$ or in any finite order of the perturbation theory there are no anomalous averages from Eq.(3.86). That means that within the perturbation theory there is no superconducting phase transition. However if one sums all diagrams of Fig.3.7 which means solving Eq.(3.86)
self-consistently, one obtains the finite anomalous averages. To illustrate this we adopt a particular momentum dependence of the interaction constant as in the previous section and an approximate form of the phonon Green's function:

$$\tilde{d}\left(\mathbf{q}, \omega_n - \omega_{n'}\right) \simeq -1 \tag{3.87}$$

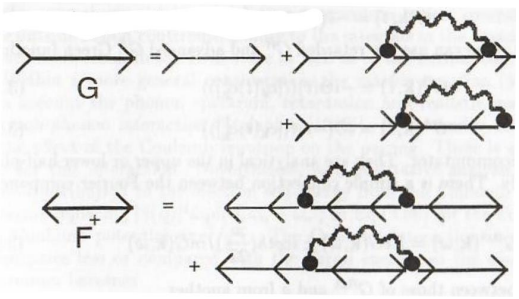

Fig.3.7. Normal G and anomalous F GFs of the BCS superconductor.

If there is no current in the system the phase of the order parameter can be chosen to be zero. In this case $\hat{\Sigma}$ is a sum of three Pauli matrices $\tau_{0,1,3}$ with the coefficients $(1-Z)i\omega_n, \Delta$ and χ respectively, which are the functions of frequency and momentum:

$$\hat{\Sigma}\left(\mathbf{k}, \omega_n\right) = (1-Z)i\omega_n\tau_0 + \Delta\tau_1 + \chi\tau_3. \tag{3.88}$$

Thus

$$\hat{g}^{-1}\left(\mathbf{k}, \omega_n\right) = Zi\omega_n\tau_0 - \Delta\tau_1 - \tilde{\xi}\tau_3 \tag{3.89}$$

and

$$\hat{g}\left(\mathbf{k}, \omega_n\right) = -\frac{Zi\omega_n + \Delta\tau_1 + \tilde{\xi}\tau_3}{Z^2\omega_n^2 + \tilde{\xi}^2 + \Delta^2} \tag{3.90}$$

with $\tilde{\xi} = \xi + \chi$. Substitution of Eq.(3.87,90) into the master equation (3.86) yields

$$(1-Z)i\omega_n = -\lambda T \int d\tilde{\xi} \sum_{\omega_{n'}} \frac{i\omega_{n'}Z}{Z^2\omega_{n'}^2 + \tilde{\xi}^2 + \Delta^2} = 0 \tag{3.91}$$

$$\chi = -\lambda T \int d\tilde{\xi} \sum_{\omega_{n'}} \frac{\tilde{\xi}}{Z^2\omega_{n'}^2 + \tilde{\xi}^2 + \Delta^2} = 0 \tag{3.92}$$

$$\Delta = \lambda T \int d\tilde{\xi} \sum_{\omega_{n'}} \frac{\Delta}{Z^2\omega_{n'}^2 + \tilde{\xi}^2 + \Delta^2} \tag{3.93}$$

It follows from Eq. (3.91, 92) that $Z = 1$ and $\chi = 0$. Applying the formula for tanh to the sum in Eq.(3.93) we obtain the familiar BCS equation for the order parameter

$$1 = \frac{\lambda}{2} \int \frac{d\xi}{\sqrt{\xi^2 + \Delta^2}} \tanh \frac{\sqrt{\xi^2 + \Delta^2}}{2T} \tag{3.94}$$

where the integration is restricted by the region $|\xi| < \omega_D$ because of the approximation, Eq.(3.87) for $\tilde{d}\,(\mathbf{q}, \omega_n - \omega_{n'})$.

There is no direct physical meaning of poles of the temperature GF. To derive the one-particle excitation spectrum one has to calculate the real-time GF determined at finite temperature as

$$G(\mathbf{k}, t) = -i \left\langle \left\langle T_t c_{\mathbf{k}}(t) c_{\mathbf{k}}^{\dagger} \right\rangle \right\rangle, \tag{3.95}$$

with the real time t. One can use the retarded G^R and advanced G^A Green functions:

$$G^R(\mathbf{k}, t) = -i\Theta(t) \left\langle \left\langle \left[c_{\mathbf{k}}(t) c_{\mathbf{k}}^{\dagger} \right] \right\rangle \right\rangle \tag{3.96}$$

$$G^A(\mathbf{k}, t) = i\Theta(-t) \left\langle \left\langle \left[c_{\mathbf{k}}(t) c_{\mathbf{k}}^{\dagger} \right] \right\rangle \right\rangle \tag{3.97}$$

where $[\ldots]$ is an anticommutator. They are analytical in the upper or lower half-plane of ω correspondingly. There is a simple connection between the Fourier components of G and $G^{R,A}$

$$G^{R,A}(\mathbf{k}, \omega) = \operatorname{Re} G(\mathbf{k}, \omega) \pm i \coth\left(\frac{\omega}{2T}\right) \operatorname{Im} G(\mathbf{k}, \omega) \tag{3.98}$$

from one side and between those of $G^{R,A}$ and g from another

$$G^R\left(\mathbf{k}, i\omega_n\right) = g\left(\mathbf{k}, \omega_n\right) \tag{3.99}$$

for $\omega_n > 0$ and

$$g\left(\mathbf{k}, -\omega_n\right) = g^*\left(\mathbf{k}, \omega_n\right) \tag{3.100}$$

In our case the temperature GF is

$$g(\mathbf{k}, \omega) = \frac{u_{\mathbf{k}}^2}{i\omega_n - \epsilon_{\mathbf{k}}} + \frac{v_{\mathbf{k}}^2}{i\omega_n + \epsilon_{\mathbf{k}}} \tag{3.101}$$

where $u_{\mathbf{k}}^2, v_{\mathbf{k}}^2 = \left(\epsilon_{\mathbf{k}} \pm \xi_{\mathbf{k}}\right)/2\epsilon_{\mathbf{k}}$ and $\epsilon_{\mathbf{k}} = \sqrt{\xi_{\mathbf{k}}^2 + \Delta^2}$. The analytical continuation of this expression to the upper half-plane yields

$$G^R(\mathbf{k}, \omega) = \frac{u_{\mathbf{k}}^2}{\omega - \epsilon_{\mathbf{k}} + i0^+} + \frac{v_{\mathbf{k}}^2}{\omega + \epsilon_{\mathbf{k}} + i0^+} \tag{3.102}$$

and with Eq.(3.98) one obtains

$$G(\mathbf{k}, \omega) = \operatorname{Re}\left(\frac{u_{\mathbf{k}}^2}{\omega - \epsilon_{\mathbf{k}}} + \frac{v_{\mathbf{k}}^2}{\omega + \epsilon_{\mathbf{k}}}\right) - i\pi \tanh\left(\frac{\omega}{2T}\right)\left(u_{\mathbf{k}}^2 \delta\left(\omega - \epsilon_{\mathbf{k}}\right) + v_{\mathbf{k}}^2 \delta\left(\omega + \epsilon_{\mathbf{k}}\right)\right) \tag{3.103}$$

At $T = 0, \tanh\left(\frac{\omega}{2T}\right) = \operatorname{sgn}(\omega)$ and

$$G(\mathbf{k}, \omega) = \frac{u_{\mathbf{k}}^2}{\omega - \epsilon_{\mathbf{k}} + i0^+} + \frac{v_{\mathbf{k}}^2}{\omega + \epsilon_{\mathbf{k}} - i0^+} \tag{3.104}$$

The poles of GF yield the BCS-quasiparticle energy

$$\epsilon_{\mathrm{k}} = \sqrt{\xi_{\mathrm{k}}^2 + \Delta^2(0)} \tag{3.105}$$

Thus the Migdal-Eliashberg theory reproduces the BCS results if a similar approximation for the attraction between electrons is made. The critical temperature and the BCS gap are

adiabatically small ($\sim \omega_D$) compared with the Fermi energy. Therefore, one can worry about the 'crossing' diagrams as in Fig. 3.6, which are neglected with the master equation, Eq.(3.86). However, the BCS state is essentially the same as the normal one outside the narrow momentum region around the Fermi surface. The outside region contribute mainly to the integrals in the crossing diagrams, which makes them small in the BCS state as well as in the normal one.

Within a more general consideration the master equation (3.86) takes properly into account the phonon spectrum, retardation and realistic matrix element of the electron-phonon interaction (Scalapino (1969)). In particular, it is useful in a study of the effect of the Coulomb repulsion on the pairing. There is no adiabatic parameter for this interaction. Nevertheless, in a qualitative analysis one can adopt the same contribution to the electron self-energy from the Coulomb interaction as from phonons replacing $|\tilde{\gamma}(\mathbf{q})|^2\tilde{\omega}_{\mathbf{q}}\tilde{d}\left(\mathbf{q},\omega_n-\omega_{n'}\right)$ in Eq.(3.86) for the Fourier component of the Coulomb potential $4\pi e^2/q^2\epsilon$. The Coulomb interaction is non-retarded for the frequencies less or compared with the Fermi energy, so the equation for the order parameter becomes

$$\Delta\left(\omega_n\right)=T\int d\xi\sum_{\omega_{n'}}K\left(\omega_n-\omega_{n'}\right)\frac{\Delta\left(\omega_{n'}\right)}{\omega_{n'}^2+\xi^2+\Delta^2\left(\omega_{n'}\right)} \tag{3.106}$$

where the kernel K is given by

$$K\left(\omega_n-\omega_{n'}\right)=\lambda\Theta\left(\omega_D-|\omega_n-\omega_{n'}|\right)-\mu_c\Theta\left(\mu-|\omega_n-\omega_{n'}|\right) \tag{3.107}$$

with μ_c the product of the Fourier component of the Coulomb potential and the normal density of states at the Fermi level. At $T=T_c$ one can neglect the second power of the order parameter in Eq.(3.106) and integrating over ξ obtain

$$\Delta\left(\omega_n\right)=\pi T_c\sum_{\omega_{n'}}K\left(\omega_n-\omega_{n'}\right)\frac{\Delta\left(\omega_{n'}\right)}{|\omega_{n'}|} \tag{3.108}$$

To solve this equation we adopt the BCS-like parametrization of the kernel

$$\begin{aligned}K\left(\omega_n-\omega_{n'}\right)\simeq{}&\lambda\Theta\left(2\omega_D-|\omega_n|\right)\Theta\left(2\omega_D-|\omega_{n'}|\right)\\&-\mu_c\Theta\left(2\mu-|\omega_n|\right)\Theta\left(2\mu-|\omega_{n'}|\right)\end{aligned} \tag{3.109}$$

and replace the summation by the integration

$$\pi T_c\sum\rightarrow\int_{\pi T_c}^{\infty}d\omega \tag{3.110}$$

lecause $T_c\ll\omega_D,\mu$. The solution can be found in the form

$$\Delta(\omega)=\Delta_1\Theta\left(2\omega_D-|\omega|\right)+\Delta_2\Theta(2\mu-|\omega|)\Theta\left(|\omega|-2\omega_D\right) \tag{3.111}$$

with constant but different values of the order parameter below (Δ_1) and above (Δ_2) the cul-off energy $2\omega_D$. Substitution of Eq.(3.109,111) into Eq.(3.108) yields for $\Delta_{1,2}$.

$$\Delta_1\left[1-(\lambda-\mu_c)\ln\frac{2\omega_D}{\pi T_c}\right]+\Delta_2\mu_c\ln\frac{\mu}{\omega_D}=0 \tag{3.112}$$

$$\Delta_1\mu_c\ln\frac{2\omega_D}{\pi T_c}+\Delta_2\left[1+\mu_c\ln\frac{\mu}{\omega_D}\right]=0 \tag{3.113}$$

The condition of the existence of a nontrivial solution of these coupled equations gives for T_c

$$T_c = \frac{2\omega_D}{\pi} \exp\left(-\frac{1}{\lambda - \mu_c^*}\right) \tag{3.114}$$

where

$$\mu_c^* = \frac{\mu_c}{1 + \mu_c \ln(\mu/\omega_D)} \tag{3.115}$$

is the Coulomb pseudopotential (Tolmachev (1958), Morel and Anderson (1962)). This is a remarkable result. It shows that even a large Coulomb repulsion $\mu_c > \lambda$ does not destroy Cooper pairs because its contribution is suppressed down to the value $\sim 1/\ln\frac{\mu}{\omega_D} \ll 1$. The retarded attraction mediated by phonons acts well after two electrons meet each other. This time delay is sufficient for two electrons to be separated by the relative distance, at which the Coulomb repulsion is small.

In the normal state the Coulomb correlations lead to a damping of excitations of order ξ^2/μ, which is relevant only in a narrow region around the Fermi surface of order $\omega_D\sqrt{m_e/M}$. Outside this region the damping due to the Fröhlich interaction dominates.

For metals and their alloys the empirical McMillan (1968) formula for T_c is adopted:

$$T_c = \frac{\omega_D}{1.45} \exp\left(-\frac{1.04(1+\lambda)}{\lambda - \mu_c^*(1+0.62\lambda)}\right) \tag{3.116}$$

which works well for low- T_c materials even if the estimated λ is large (> 1) as in Pb. However, already in materials with a moderate $T_c \sim 20K$ as in $A-15$ compounds (Nb_3Sn, V_3Si) the discrepancy between the values of λ estimated with Eq.(3.116) and the direct band-structure calculations exceeds by several times the limit allowed by the experimental and computation accuracy (Klein et al. (1978)) and therefore the credibility of the canonical BCS approach to these materials is low.

The Migdal-Eliashberg theory is based on the assumption that the Fermi liquid is stable and the adiabatic condition $\mu \gg \omega_D$ is satisfied. In original papers Migdal (1958) and Eliashberg (1960) restricted the region of the applicability of their approach by the value of the coupling $\lambda < 1$. We show in this book that the proper extension of the BCS theory to the strong coupling region $\lambda > 1$ inevitably involves small polaron formation.

5.3.5 3.5 Bloch states in semiconductors: Effective mass approximation

(this may be important since we always consider semiconductors)

Theory

Electron wave functions in semiconductors and narrow band metals differ significantly from plane waves, Eq.(3.26). Therefore, in general the band structure has to be calculated numerically. However, in doped semiconductors states in the vicinity of special points of the Brillouin zone matter only at low temperatures and doping. These are points where the energy dispersion $E_{\mathbf{k},n,s}$ of the conduction band has its minimum and the valence band energy has its maximum. While their positions and band edges are determined experimentally or with the numerical LDA calculations, the energy dispersion nearby can be determined analytically with ' $\mathbf{k}\cdot\mathbf{p}$ ' perturbation theory. (what is it??)

To show this we consider a simple cubic lattice having a nondegenerate band of s or d-like symmetry at $\mathbf{k} = 0(\Gamma)$ point lying above by an energy E_g three p-like bands degenerate at $\mathbf{k} = 0$

and transforming at this point like x, y and z under the rotation of the crystal space group. There is no spin-orbit interaction in this example, so spin is irrelevant. The Bloch theorem states that

$$\phi_{\mathbf{k},n}(\mathbf{r}) = e^{i\mathbf{k}\cdot\mathbf{r}} u_{\mathbf{k},n}(\mathbf{r}) \tag{3.117}$$

where $u_{\mathbf{k},n}(\mathbf{r})$ is periodic in $\mathbf{r}$ and satisfies to

$$\left(-\frac{1}{2m_e}\left(\nabla^2 + 2i\mathbf{k}\cdot\nabla\right) + V(\mathbf{r})\right) u_{\mathbf{k},n}(\mathbf{r}) = \left(E_{\mathbf{k},n} - \frac{k^2}{2m_e}\right) u_{\mathbf{k},n}(\mathbf{r}) \tag{3.118}$$

At the point $\mathbf{k} = 0$ this equation for $u_{0,n}(\mathbf{r})$ is

$$\left(-\frac{1}{2m_e}\nabla^2 + V(\mathbf{r})\right) u_{0,n}(\mathbf{r}) = E_{0,n} u_{0,n}(\mathbf{r}) \tag{3.119}$$

Thus $u_{0,n}$ has the symmetry of the crystal space group. For small k one can expand $u_{\mathrm{k},n}$ in series

$$u_{\mathbf{k},n}(\mathbf{r}) = \sum_{n'=s,x,y,z} a_{\mathbf{k},n'} u_{0,n'}(\mathbf{r}) \tag{3.120}$$

to obtain the secular equation

$$\det \begin{vmatrix} E_g + \frac{k^2}{2m_e} - E_{\mathbf{k}} & \frac{k_x p}{m_e} & \frac{k_y p}{m_e} & \frac{k_z p}{m_e} \\ \frac{k_x p}{m_e} & \frac{k^2}{2m_e} - E_{\mathbf{k}} & 0 & 0 \\ \frac{k_y p}{m_e} & 0 & \frac{k^2}{2m_e} - E_{\mathbf{k}} & 0 \\ \frac{k_z p}{m_e} & 0 & 0 & \frac{k^2}{2m_e} - E_{\mathbf{k}} \end{vmatrix} = 0 \tag{3.121}$$

with by symmetry $p \equiv \langle s| - i\nabla_x|x\rangle = \langle s| - i\nabla_y|y\rangle = \langle s| - i\nabla_z|z\rangle$. Different bra and ket correspond to the four different Γ-point Bloch functions $u_{0,n}(\mathbf{r})$. There are four solutions. Two of them correspond to conduction (c) and light hole (lh) valence bands

$$E_{\mathbf{k},c,lh} = \frac{k^2}{2m_e} + \frac{E_g}{2} \pm \sqrt{\frac{E_g^2}{4} + \frac{k^2 p^2}{m_e^2}} \tag{3.122}$$

and the other two, which are degenerate, correspond to heavy holes (hh)

$$E_{\mathbf{k},hh} = \frac{k^2}{2m_e} \tag{3.123}$$

One can split two degenerate heavy hole bands and change the sign of their effective mass if one includes states at Γ point split off from those under consideration by an mergy large in comparison with E_g, as shown with a thin line in Fig.3.8. The effective approximation follows from Eq.(3.122) for small $k \ll m_e E_g/p$

$$E_{\mathrm{k},c} - E_g \simeq \frac{k^2}{2m_c} \tag{3.124}$$

and

$$E_{\mathbf{k},lh} \simeq -\frac{k^2}{2m_{lh}} \tag{3.125}$$

with the effective mass

$$\frac{m_{c,lh}}{m_e} = \frac{1}{\frac{p^2}{m_e E_g} \pm 1} \tag{3.126}$$

In many semiconductors the interband dipole moment is large and the band gap is small so $p^2 \gg m_e E_g$. Therefore the band electron and hole masses can be significantly smaller than the bare mass,

$$\frac{m_c}{m_e} \simeq \frac{m_{lh}}{m_e} \ll 1. \tag{3.127}$$

As a result when experiment does not show very heavy carriers it does not necessary follow that the electron-lattice coupling is small, and the polaronic renormalisation of the band mass is absent.

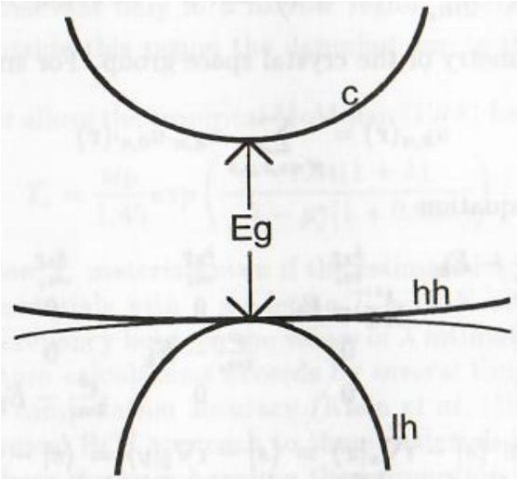

Fig.3.8. $\mathbf{k} \cdot \mathbf{p}$ energy band dispersion near the Γ point in a cubic lattice.

The effective mass approximation, Eq.(3.124,125) as well as $\mathbf{k} \cdot \mathbf{p}$ perturbation theory discussed above can be applied if the external field varies slowly in time and smoothly in space and the electron-phonon and electron-electron interactions are relatively weak, as in the case of large polarons, Chapter 1. If the external or internal fields are strong and contain high frequency and (or) short wave Fourier components they involve large momenta of order of the reciprocical lattice constant making all states of the electron band to be relevant to the problem. In this case a tight-binding approach is more appropriate.

5.3.6 3.6 Tight-binding approximation

Theory

For narrow band semiconductors and metals it is convenient to replace the Bloch states for the Wannier states with the canonical linear transformation of electron operators

$$c_i = \frac{1}{\sqrt{N}} \sum_{\mathbf{k}} e^{i\mathbf{k}\cdot\mathbf{m}} c_{\mathbf{k},s}, \tag{3.128}$$

where $i = (\mathbf{m}, n, s)$ includes both site $\mathbf{m}$, band n and spin s quantum numbers. Of course, i in the exponent is the imaginary i and not an index. The Wannier wave function, corresponding to the one-particle state $\{i\}$ is given by the linear combination of the Bloch states

$$w_i(\mathbf{r}) = \frac{1}{\sqrt{N}} \sum_{\mathbf{k}} e^{-i\mathbf{k}\cdot\mathbf{m}} \phi_{\mathbf{k},n,s}(\mathbf{r}). \tag{3.129}$$

In the new representation the periodic Hamiltonian H_e is written as

$$H_e = \sum_{i,j} \left(T(\mathbf{m}-\mathbf{n})\delta_{s,s'}\delta_{n,n'} - \mu\delta_{i,j}\right) c_i^\dagger c_j \tag{3.130}$$

with the bare hopping integral

$$T(\mathbf{m}) = \frac{1}{N} \sum_{\mathbf{k}} E_{\mathbf{k},n} e^{i\mathbf{k}\cdot\mathbf{m}} \tag{3.131}$$

$i = (\mathbf{m}, n, s)$ and $j = (\mathbf{n}, n', s')$.
(check!!!)

The idea behind the tight-binding approximation is to fit calculated numerically bands by using a finite number of the hopping integrals.

Many electronic structures, in particular perovskite ones can be fitted with only nearest-neighbor matrix elements between s, p and d-like orbitals (Harrison (1989)). (check that it is true in that paper)

The second-neighbor matrix elements are somewhat problematic. Their estimate from the nearest-neighbor formulae by scaling with the inter-site distance turns out to be inappropriate. (why??? some people use such models...)

Therefore one will not have occasion to use again the second-neighbor hopping integrals fitting well one particular band structure. (not explained, why?)

The hopping integrals could not be calculated by using tabulated atomic wave functions and potentials (which potentials?) estimated for the various solids. True atomic orbitals are not orthogonal for different sites and they do not provide a quantitative description of bands in solids. On the other hand atomiclike Wannier orbitals, Eq.(3.129) can provide a very good description already in the tight-binding (nearest-neighbor) approximation. For a nondegenerate band in a cubic lattice this approximation yields (derive???)

$$\begin{aligned} E_{\mathbf{k}} &= \sum_{|\mathbf{m}|=a} T(\mathbf{m}) e^{-i\mathbf{k}\cdot\mathbf{m}} \\ &= 2T(a)\left[\cos(k_x a) + \cos(k_y a) + \cos(k_z a)\right] \end{aligned} \tag{3.132}$$

if the middle of the band is taken to be zero, $T(0) = 0$. If the nearest-neighbor matrix element is negative, the bottom of the band lies at $\mathbf{k} = 0$, where the dispersion is parabolic with the band mass (why??)

$$m = \frac{1}{2a^2|T(a)|} \tag{3.133}$$

The half bandwidth is $D = z|T(a)|$, where the nearest- neighbor number $z = 6$ in this example. (???)

The electron-phonon interaction as well as the Coulomb correlation energy have a simple form in the Wannier representation if the corresponding matrix elements depend on the momentum transfer only, Eq.(3.23)

$$H_{e-ph} = \sum_{\mathbf{q},i} \omega_{\mathbf{q}} \hat{n}_i \left(u_i(\mathbf{q}) d_{\mathbf{q}} + h.c.\right) \tag{3.134}$$

$$H_{e-e} = \frac{1}{2} \sum_{i,j} V_c(\mathbf{m}-\mathbf{n}) \hat{n}_i \hat{n}_j \tag{3.135}$$

with the matrix element of the electron-phonon interaction

$$u_i(\mathbf{q}) = \frac{1}{\sqrt{2N}}\gamma(\mathbf{q})e^{i\mathbf{q}\cdot\mathbf{m}} \tag{3.136}$$

and the Coulomb interaction

$$V_c(\mathbf{m}) = \frac{1}{N}\sum_{\mathbf{q}} V_c(\mathbf{q})e^{i\mathbf{q}\cdot\mathbf{m}} \tag{3.137}$$

Here $\hat{n}_i = c_i^\dagger c_i$ is the density operator.

It follows from Eq.(3.134,135) that taking the interaction matrix elements depending only on the momentum transfer one neglects (why????) the terms of the electron-phonon and Coulomb interactions, containing the overlap of different site orbitals, which is a good approximation for narrow bands (why????), whose bandwidth $2D$ is less than the characteristic value of the crystal field.

As a result the Hamiltonian appropriate for semiconductors and narrow band metals is given by

$$\begin{aligned} H = &\sum_{i,j}\left(T(\mathbf{m}-\mathbf{n})\delta_{s,s'} - \mu\delta_{i,j}\right)c_i^\dagger c_j + \sum_{\mathbf{q},i}\omega_{\mathbf{q}}\hat{n}_i\left(u_i(\mathbf{q})d_{\mathbf{q}} + h.c.\right) \\ &+ \frac{1}{2}\sum_{i,j} V_c(\mathbf{m}-\mathbf{n})\hat{n}_i\hat{n}_j + \sum_{\mathbf{q}}\omega_{\mathbf{q}}\left(d_{\mathbf{q}}^\dagger d_{\mathbf{q}} + 1/2\right) \end{aligned} \tag{3.138}$$

We have just collected the terms above.

For narrow band metals this Hamiltonian can be treated at best as the bare one, in which all matrix elements and phonon frequencies have no direct physical meaning.

Phonons and the interaction matrix elements should be determined using a self-consistent LDA approach as described above. Fortunately, in doped semiconductors one can separate 'carriers' from 'inner' electrons. In this case parent dielectric compounds exist with well defined bare phonons ω_{q} and the electronic band structure $E_{\mathbf{k}}$.

The effect of carriers on the crystal field and on the dynamical matrix is negligible while the carrier density is much below the atomic one.

Therefore one can use the band structure and the crystal field of a parent insulator to calculate the parameters of the Hamiltonian, Eq.(3.138). (how???)

Depending on the particular phonon mode the interaction constant $\gamma(\mathbf{q})$ has different $q-$ dependence. For example, as discussed above

$$\begin{aligned} \gamma(\mathbf{q}) &\sim \frac{1}{q}, \\ &\sim \text{ constant }, \\ &\sim \frac{1}{\sqrt{q}} \end{aligned} \tag{3.139}$$

for optical, molecular ($\omega_{\mathbf{q}} \sim$ constant) and acoustic ($\omega_{\mathbf{q}} \sim q$) phonons, respectively in the long wave limit.

Example: values of coefficients of tight-binding model from other parameters of a model

(?????????? how to obtain them???)

5.4 4 The multi-polaron problem

5.4.1 4.1 Small-polaron instability within the Migdal approach

(this chapter relies on the ch. 3, so it is better start with it)

Theory

In doped semiconductors the carriers become small polarons or bipolarons at the intermediate value of the coupling constant $\lambda \geq 0.5$, Chapter 2. (why???)

However, within the adiabatic Migdal description of electrons and phonons coupled by the linear electron-phonon interaction there is no instability at any value of λ if the bare ionic plasmon mode is replaced by the acoustic phonon mode as described in Chapter 3. (what is known about such instabilities?)

The corrections to the normal state spectrum due to the coupling are adiabatically small ($\sim \omega_D/E_F$). In particular, the critical temperature of the BCS superconductor is adiabatically small, $T_c/E_F < \omega_D/E_F \ll 1$ for all relevant values of λ. (why is it "adiabatically"?)

The self-consistent Migdal-Eliashberg approach does not allow for the possibility to study the small-(bi)polaron formation in the intermediate and strong-coupling regime because of the following reason. The basic assumption of the canonical theory that GF is translationally invariant, thus $G(\mathbf{r}, \mathbf{r}', t) = G(\mathbf{r} - \mathbf{r}', t)$. This assumption excludes the possibility of the local violation of the translational symmetry due to the lattice deformation followed by the self-trapping. To enable the electron to relax into the lowest polaron state, one can introduce an infinitesimal translationally noninvariant potenlial, which should be set equal zero only in the final solution for GF (Alexandrov and Mazur (1989)). (it is not clear, how translational invariance is related to the possibility of change of state)

As in the case of the off-diagonal superconducting order parameter (when can it be???) a small potential, violating a translational symmetry drives the system into a new ground state at sufficiently large λ.

Setting it equal to zero in the solution to the equation of motion restore the translational symmetry but in a new polaronic band rather than in the electron one, which turns out to be an excited state. (why???)

In the Holstein model (????), in which electrons interact with the local (molecular) phonons (what are they?) one can notice the polaronic instability of the Fermi liquid at $\lambda \sim 1$ already within Migdal's diagrams for the electron self-energy.

The electron self-energy Σ in the Migdal approximation contains two contributions, Σ_M, Fig.3.3a and Σ_μ, IIg.3.3b. $\Sigma_M \simeq \lambda\omega$. (derive??!! add these figures also here)

Therefore it remains adiabatically small compared with the bandwidth $2D \simeq N(0)^{-1}$ in the relevant region of the coupling ($\lambda < D/\omega$), which guarantees the self-consistency of the approach. (read cheaper 3, learn why?)

On the other hand for the optical or molecular phonons $\Sigma_\mu \simeq D\lambda n$ is not small and it turns out to be comparable or larger than the Fermi energy already at $\lambda \sim 1$ for any filling of the band (n is the electron density per cell). (why???)

As a rule this diagram, which is momentum and frequency independent, is included in the definition of the chemical potential μ. (why??)

While this is justified for a weak-coupling regime, Σ_μ leads to an instability for a strong coupling. (why??)

To show this let us consider a one-dimensional chain in the tight-binding approximation with the nearest-neighbor hopping integral $D/2$. The renormalised chemical potential is given

by (why??)

$$\mu = D \sin\left(\frac{\pi(n-1)}{2}\right) - 2D\lambda n \tag{4.1}$$

The system is stable if $d\mu/dn$ is positive (never heard about this criterion), which yields the following region for the stability of the Migdal solution:

$$\lambda < \frac{\pi}{2}\cos\left(\frac{\pi(n-1)}{2}\right) \tag{4.2}$$

For two and three-dimensional lattices the numerical coefficient is different, but the critical value of λ remains of the order of unity. (????)

In doped semiconductors and metals optical phonons are screened and the diagram Σ_μ with the phonon momentum $\mathbf{q} \equiv 0$ vanishes as for the acoustical phonons. (check)

In that case one has to violate the translational symmetry to observe the instability of the bare band. Because the polaron level shift E_p is independent of the ion mass, the polaronic instability is essentially an adiabatic effect. Therefore, to see how the same self-energy diagram Σ_μ leads to the polaronic collapse independent of the type of phonons we consider the extreme adiabatic limit of the classical deformation field $\phi(\mathbf{r})$ coupled with electrons,

$$H = H_e + \int d\mathbf{r}d\mathbf{r}' \left[g\left(\mathbf{r}-\mathbf{r}'\right)\phi\left(\mathbf{r}'\right)\left\{\psi^\dagger(\mathbf{r})\psi(\mathbf{r}) - n^0(\mathbf{r})\right\} + \text{ h.c. } \right] + s^2|\nabla\phi(\mathbf{r})|^2 \tag{4.3}$$

Here s is the sound velocity, $g(\mathbf{r})$ is the coupling constant with the Fourier component $g_\mathbf{q} = \omega_\mathbf{q}^{3/2}\gamma(\mathbf{q})/\sqrt{2N}, n^0(\mathbf{r})$ is the periodic density of carriers respecting the translational symmetry, as defined by Eq.(3.9), and $\omega_\mathrm{q} = sq$. Minimising Eq.(4.3) with respect to the classical field $\phi^*(\mathbf{r})$ we obtain

$$s^2\nabla^2\phi(\mathbf{r}) = \int d\mathbf{r}' g^*\left(\mathbf{r}-\mathbf{r}'\right)\left\{n\left(\mathbf{r}'\right) - n^0\left(\mathbf{r}'\right)\right\} \tag{4.4}$$

The solution is

$$\phi(\mathbf{r}) = -\sum_\mathbf{q} \frac{g_\mathbf{q}^*}{s^2q^2} e^{i\mathbf{q}\cdot\mathbf{r}}\left\{n_\mathbf{q} - n_\mathbf{q}^0\right\} \tag{4.5}$$

where $n_\mathbf{q}$ is the Fourier component of the electron density $n(\mathbf{r}) \equiv \left\langle\psi^\dagger(\mathbf{r})\psi(\mathbf{r})\right\rangle$. Substituting Eq.(4.5) into the Hamiltonian Eq.(4.3) we find that the adiabatic lattice deformation leads to the lowering of the electron energy by the value

$$\delta\mu(\mathbf{r}) = -2\sum_\mathbf{q} \frac{|g_\mathbf{q}|^2}{\omega_\mathbf{q}^2} e^{i\mathbf{q}\cdot\mathbf{r}}\left\{n_\mathbf{q} - n_\mathbf{q}^0\right\} \tag{4.6}$$

If the electron density is periodic, $n_\mathbf{q} = n_\mathbf{q}^0$ the shift of the energy is zero. Otherwise, it is not. For example, one can consider a random statistically uncorrelated distribution
with the ansamble average $\langle n_\mathbf{q} n_{\mathbf{q}'}\rangle = Nn^2\delta_{\mathbf{q},-\mathbf{q}'}$. In that example the chemical potential is shifted by the value

$$\langle|\delta\mu|\rangle = n\left[\frac{1}{N}\sum_\mathbf{q}|\gamma(\mathbf{q})|^4\omega_\mathbf{q}^2\right]^{1/2} \simeq 2n\lambda D, \tag{4.7}$$

which is the same as in Eq.(4.1). However, now $\lambda D \equiv E_p = (1/2N)\sum_\mathbf{q}|\gamma(\mathbf{q})|^2\omega_\mathbf{q}$ depends on the phonon spectrum, integrated over all Brillouin zone rather than on zero momentum

phonons. Breaking of the translational symmetry lowers the energy by the value $2E_p$ per particle. The corresponding increase of the deformation energy is E_p. Therefore, the system prefers to relax into the selftrapped state if $E_p > D$. The vertex corrections neglected within the Migdal approach are not so crucial if the adiabatic parameter ω/D is small and $\lambda < D/\omega$.

This consideration shows that the extension of the Migdal approximation to the strong-coupling region $\lambda > 1$ is unacceptable. In the following we show that depending on the value of the Coulomb repulsion a many electron system strongly coupled with any bosonic field is a polaronic Fermi liquid or a bipolaronic Bose liquid.

5.4.2 4.2 Exact solution of the multi-polaron problem for $\lambda \to \infty$

Theory

In the case of large polarons the multi-polaron problem can be solved within the Migdal-Eliashberg approach discussed in Chapter 3. This is the weak coupling regime $\lambda < 1$, where large bipolarons, if they exist, transform into Cooper pairs at finite density.

In the small polaron regime, $\lambda \geq 1$ the kinetic energy remains smaller than the interaction energy and a self-consistent treatment of a many polaron system is possible with the ' $1/\lambda'$ expansion technique (Alexandrov (1992b)). (learn, what is it?)

This possibility results from the fact, known for a long time, that there is an exact solution for a single electron in the strong-coupling limit $\lambda \to \infty$. (where does it originates??)

Following Lang and Firsov (1962) one can apply the canonical transformation to diagonalise the tight-binding Hamiltonian of electrons and phonons if hopping coefficient between electrons $T(\mathbf{m}) = 0$ (or $\lambda = \infty$)

$$H = \sum_{\mathbf{q},i} \omega_{\mathbf{q}} \hat{n}_i \left(u_i(\mathbf{q}) d_{\mathbf{q}} + h.c. \right) + \frac{1}{2} \sum_{i,j} V_c(\mathbf{m} - \mathbf{n}) \hat{n}_i \hat{n}_j + \sum_{\mathbf{q}} \omega_{\mathbf{q}} \left(d^{\dagger}_{\mathbf{q}} d_{\mathbf{q}} + 1/2 \right) \tag{3.138}$$

by the transformation:

$$\tilde{H} = e^S H e^{-S}; \qquad S = \sum_{\mathbf{q},i} \hat{n}_i \left(u_i(\mathbf{q}) d_{\mathbf{q}} - \text{ h.c. } \right) \tag{4.9}$$

The electron operator transforms as

$$\tilde{c}_i = c_i \exp \left(\sum_{\mathbf{q}} u_i(\mathbf{q}) d_{\mathbf{q}} - h.c. \right) \tag{4.10}$$

and the phonon one as:

$$\tilde{d}_{\mathbf{q}} = d_{\mathbf{q}} - \sum_i \hat{n}_i u^*_i(\mathbf{q}) \tag{4.11}$$

From Eq.(4.11) it follows that the Lang-Firsov canonical transformation is the displacement transformation, Eq.(1.81) for the multi-polaron system shifting ions to the new equilibrium positions. (read ch. 1, understand it!)

In a more general sense it changes the boson vacuum. (????)

As a result:

$$\tilde{H} = \sum_{i,j} \left(\hat{\sigma}_{ij} - \mu \delta_{i,j} \right) c^{\dagger}_i c_j - E_p \sum_i \hat{n}_i + \frac{1}{2} \sum_{i,j} v_{ij} c^{\dagger}_i c^{\dagger}_j c_j c_i + \sum_{\mathbf{q}} \omega_{\mathbf{q}} \left(d^{\dagger}_{\mathbf{q}} d_{\mathbf{q}} + 1/2 \right) \tag{4.12}$$

where

$$\hat{\sigma}_{ij} = T(\mathbf{m}-\mathbf{n})\delta_{s.s'} \exp\left(\sum_{\mathbf{q}} \left[u_i(\mathbf{q}) - u_j(\mathbf{q})\right] d_{\mathbf{q}} - h.c.\right) \tag{4.13}$$

is the new hopping integral depending on the phonon variables,

$$v_{ij} = V_c(\mathbf{m}-\mathbf{n}) - 2\sum_{\mathbf{q}} \omega_{\mathbf{q}} \left(u_i(\mathbf{q}) u_j^*(\mathbf{q})\right) \tag{4.14}$$

is the polaron-polaron interaction comprising the direct Coulomb repulsion and the attraction via a nonretarded lattice deformation (second term of Eq.(4.14)).

(in which materials there is such a strong coupling???)

Proof. (???????)

□

In the extreme strong-coupling limit $\lambda \to \infty$ one can neglect the hopping term of the transformed Hamiltonian. The rest has analytically determined eigenstates and eigenvalues. The eigenstates $|\tilde{N}\rangle = |n_i, n_{\mathbf{q}}\rangle$ are classified with the polaron $n_{\mathbf{m},s}$ and phonon n_{q} occupation numbers and the energy levels are:

$$E = (T(0) - E_p - \mu)\sum_i n_i + \frac{1}{2}\sum_{i,j} v_{ij} n_i n_j + \sum_{\mathbf{q}} \omega_{\mathbf{q}} \left(n_{\mathbf{q}} + 1/2\right) \tag{4.15}$$

where $n_i = 0, 1$ and $n_{\mathrm{q}} = 0, 1, 2, 3, \ldots \infty$. The interaction term does not include the on-site interaction $i = j$ for parallel spins because of the Pauli principle.

Thus we conclude that the Hamiltonian Eq.(3.138) in zero order of the hopping describes localised polarons and independent phonons which are vibrations of ions relative to new equilibrium positions depending on the polaron occupation numbers. The phonon frequencies remain unchanged in this limit. The middle of the electronic band $T(0)$ falls down by E_p as a result of a potential well produced by the lattice deformation due to the self-trapping (see Fig.4.1).

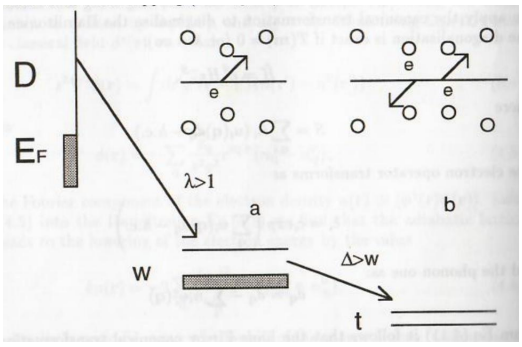

Fig.4.1. Polaron collapse of the electron band (a); bipolaron band (b).

5.4.3 4.3 Polaron band and self-energy

Theory

With the finite hopping term polarons tunnel in a narrow band because of the degeneracy of the zero order Hamiltonian relative the site position of a single polaron in a regular lattice. To show this self-consistently one can apply perturbation theory using $1/\lambda$ as a small parameter. Because of the degeneracy terms of the first order in $T(\mathbf{m})$ should be included in a zero order Hamiltonian H_0 :

$$H_0 = \sum_{i,j} \left(\sigma(\mathbf{m}-\mathbf{n}) - \mu\delta_{i,j}\right) c_i^\dagger c_j + \sum_{\mathbf{q}} \omega_{\mathbf{q}} \left(d_{\mathbf{q}}^\dagger d_{\mathbf{q}} + 1/2\right) \tag{4.16}$$

where

$$\sigma(\mathbf{m}-\mathbf{n}) = \langle\langle \hat{\sigma}_{ij} \rangle\rangle = T(\mathbf{m}-\mathbf{n})\delta_{s,s'} \exp\left[-g^2(\mathbf{m}-\mathbf{n})\right] \tag{4.17}$$

is the hopping integral averaged with the phonon equilibrium distribution. It is calculated by the use of the relation

$$e^{A+B} = e^A e^B e^{-[AB]/2} \tag{4.18}$$

which is valid for any operators A, B with a c-number commutator. For zero temperature one obtains

$$\begin{aligned}\sigma(\mathbf{m}-\mathbf{n}) = T(\mathbf{m}-\mathbf{n}) e^{-g^2(\mathbf{m}-\mathbf{n})} \\ \times \langle 0| \exp\left[-\sum_{\mathbf{q}} \left[u_i^*(\mathbf{q}) - u_j^*(\mathbf{q})\right] d_{\mathbf{q}}^\dagger\right] \exp\left[\sum_{\mathbf{q}} \left[u_i(\mathbf{q}) - u_j(\mathbf{q})\right] d_{\mathbf{q}}\right] |\mathcal{Q}\rangle\end{aligned} \tag{4,19}$$

where

$$g^2(\mathbf{m}-\mathbf{n}) = \frac{1}{2}\sum_{\mathbf{q}} \left(|u_i(\mathbf{q})|^2 + |u_j(\mathbf{q})|^2 - 2u_i^*(\mathbf{q})u_j(\mathbf{q})\right) \tag{4.20}$$

The bracket in Eq.(4.19) is equal unity for $T = 0$. The straightforward generalisation for finite temperatures yields

$$g^2(\mathbf{m}) = \frac{1}{2N}\sum_{\mathbf{q}} |\gamma(\mathbf{q})|^2 \coth\left(\frac{\omega_{\mathbf{q}}}{2T}\right) [1 - \cos(\mathbf{q}\cdot\mathbf{m})] \tag{4.21}$$

The renormalised position of the middle of the electron band is taken to be zero, so that $T(0) - E_p = 0$.

The interaction term in the transformed hamiltonian $\tilde{H} = H_0 + H_{\rm int}$ includes the residual interaction H_{p-ph} of polarons with phonons and the polaron-polaron interaction H_{p-p} :

$$H_{int} = H_{p-ph} + H_{p-p} \tag{4.22}$$

$$H_{p-ph} = \sum_{i,j} \left[\hat{\sigma}_{ij} - \sigma(\mathbf{m}-\mathbf{n})\right] c_i^\dagger c_j \tag{4.23}$$

$$H_{p-p} = \frac{1}{2}\sum_{i,j} v_{ij} c_i^\dagger c_j^\dagger c_j c_i \tag{4.24}$$

where
and

The polaron-phonon interaction leads to the polaron bandwidth and phonon frequency renormalisations and to the scattering of polarons. The polaron-polaron correlations are responsible for the scattering and in case of the attraction for the bipolaron formation. If the temperature is well above the temperature for the formation of bipolarons (see below) one can treat H_{p-ph} with the $1/\lambda$ perturbation expansion and H_{p-p} with the canonical random phase approximation (RPA). We consider first the effect of H_{p-ph} on the polaron self-energy Σ_p.

Because of the translation symmetry H_0 is diagonal in the Bloch-representation Eq.(3.128):

$$H_0 = \sum_{\mathbf{k},s} (\epsilon_{\mathbf{k}} - \mu)\, c^\dagger_{\mathbf{k},s} c_{\mathbf{k},s} + \sum_{\mathbf{q}} \omega_{\mathbf{q}} d^\dagger_{\mathbf{q}} d_{\mathbf{q}} \tag{4.25}$$

with a polaronic band

$$\epsilon_{\mathbf{k}} = \sum_{\mathbf{m}} \sigma(\mathbf{m}) e^{i\mathbf{k}\cdot\mathbf{m}} \tag{4.26}$$

From Eq.(4.26) we conclude that the polaronic band has the bandwidth $2w$ exponentially reduced compared with the bare electronic bandwidth as in the Holstein model, Chapter 1

$$w = De^{-g^2} \tag{4.27}$$

where g is determined in Eq.(4.21) for the nearest neighbor hopping $|\mathbf{m}| = a$. An increase of the effective mass $m^* = 1/wa^2$ is due to the phonon cloud surrounding a small polaron. The renormalisation factor $\exp(-g^2)$ is closely related to the wellknown Debye-Waller factor, determined by the mean-square displacement of atoms from their equilibrium positions.

To derive the polaron self-energy one can solve perturbatively the equation of motion for the polaronic temperature Green's function defined in the Wannier representation as

$$\tilde{g}_{ij}(\tau) = -\left\langle\left\langle T_\tau c_i(\tau) c^\dagger_j \right\rangle\right\rangle \tag{4.28}$$

with $c_i(\tau) = e^{\tilde{H}\tau} c_i e^{-\tilde{H}\tau}$. The double angular brackets correspond now to the quantum as well as statistical average over the eigenstates of the transformed Hamiltonian. Differentiating Eq.(4.28) we obtain

$$\frac{d\tilde{g}_{ij}(\tau)}{d\tau} - \mu \tilde{g}_{ij}(\tau) = -\delta(\tau)\delta_{i,j} + \sum_{i'} \left\langle\left\langle T_\tau \hat{\sigma}_{ii'}(\tau) c_{i'}(\tau) c^\dagger_j \right\rangle\right\rangle \tag{4.29}$$

where $\hat{\sigma}_{ii'}(\tau) = e^{\tilde{H}\tau} \hat{\sigma}_{ii'} e^{-\tilde{H}\tau}$.
For the Fourier component we have:

$$\hat{\tilde{g}}^{-1}(\omega_n) = \left(\hat{\tilde{g}}^{(0)}(\omega_n)\right)^{-1} - \hat{\Sigma}(\omega_n) \tag{4.30}$$

where $\hat{\tilde{g}}$ and $\hat{\Sigma}$ are matrices with respect to site indices i, j. The free polaron GF in determined by

$$\left(\tilde{g}^{(0)}(\omega_n)\right)^{-1}_{ij} = (i\omega_n + \mu)\,\delta_{i,j} - \sigma(\mathbf{m} - \mathbf{n}) \tag{4.31}$$

and the polaron self-energy by

$$\Sigma_{ij}(\omega_n) = \sum_{i',j'} \Gamma^{i'j'}_{ii'}(\omega_n)\, \hat{\tilde{g}}^{-1}_{j'j}(\omega_n) \tag{4.32}$$

where $\hat{\Gamma}(\omega_n)$ is the Fourier component of the polaron-phonon correlation function

$$\Gamma^{jj'}_{ii'}(\tau) = -\left\langle\left\langle T_\tau \left[\hat{\sigma}_{ii'}(\tau) - \sigma(\mathrm{m} - \mathrm{m}')\right] c_j(\tau) c^\dagger_{j'} \right\rangle\right\rangle. \tag{4.33}$$

This correlation function comprises the second and higher order terms with respect to the hopping integral, as follows from the corresponding equation of motion:

$$\frac{d\Gamma^{jj'}_{ii'}(\tau)}{d\tau} - \mu \Gamma^{jj'}_{ii'}(\tau) = \sum_{i''} \left\langle\left\langle T_\tau \left[\hat{\sigma}_{ii'}(\tau) - \sigma(\mathbf{m} - \mathbf{m}')\right] c_j(\tau) c^\dagger_{i''} \hat{\sigma}_{i''j'} \right\rangle\right\rangle. \tag{4.34}$$

To obtain Eq.(4.34) one can differentiate the function

$$\Gamma_{ii'}^{jj'}(-\tau) = -\left\langle\left\langle T_\tau \left[\hat{\sigma}_{ii'} - \sigma\left(\mathbf{m}-\mathbf{m}'\right)\right] c_j c_{j'}^\dagger(\tau)\right\rangle\right\rangle. \tag{4.35}$$

In the second order of the perturbation theory one can replace $\tilde{H}$ in Eq.(4.34) for H_0 to obtain

$$\Sigma_{ij}\left(\omega_n\right) = T\sum_{\omega_{n'}}\sum_{i',i'',j'} \tilde{\Phi}_{ii'}^{i''j'}\left(\omega_n - \omega_{n'}\right)\tilde{g}_{i'i''}^{(0)}\left(\omega_{n'}\right)\frac{\left(i\omega_n+\mu\right)\delta_{j',j} - \sigma\left(\mathbf{n}-\mathbf{n}'\right)}{i\omega_n+\mu} \tag{4.36}$$

where

$$\tilde{\Phi}_{ii'}^{jj'}\left(\Omega_n\right) = \Phi_{ii'}^{jj'}\left(\Omega_n\right) - \frac{1}{T}\sigma\left(\mathbf{m}-\mathbf{m}'\right)\sigma\left(\mathbf{n}-\mathbf{n}'\right)\delta_{\Omega_n,0} \tag{4.37}$$

and $\Phi_{ii'}^{jj'}\left(\Omega_n\right)$ is a Fourier component of the multiphonon correlator

$$\Phi_{ii'}^{jj'}(\tau) = \langle\langle T_\tau \hat{\sigma}_{ii'}(\tau)\hat{\sigma}_{jj'}\rangle\rangle \tag{4.38}$$

with $\tilde{H} = H_0$. Direct calculations yield

$$\Phi_{ii'}^{jj'}(\tau) = \sigma(\mathbf{a})\sigma(\mathbf{b})\exp\left(\frac{1}{N}\sum_{\mathbf{q}}\gamma^2(\mathbf{q})f_{\mathbf{q}}\frac{\cosh\left[\omega_{\mathbf{q}}\left(\frac{1}{2T}-|\tau|\right)\right]}{\sinh\frac{\omega_{\mathbf{q}}}{2T}}\right) \tag{4.39}$$

where $2f_{\mathbf{q}} = \cos(\mathbf{q}\cdot[\mathbf{c}-\mathbf{a}]) + \cos(\mathbf{q}\cdot[\mathbf{c}+\mathbf{b}]) - \cos(\mathbf{q}\cdot\mathbf{c}) - \cos(\mathbf{q}\cdot[\mathbf{c}-\mathbf{a}+\mathbf{b}])$ with $\mathbf{a} = \mathbf{m}-\mathbf{m}', \mathbf{b} = \mathbf{n}-\mathbf{n}'$ and $\mathbf{c} = \mathbf{n}'-\mathbf{m}'$. To simplify Eq.(4.36) further one can neglect all terms, containing a small exponent $e^{-g^2} \ll 1$. Omitting small terms the nelf-energy is diagonal, $\Sigma_{ij} \simeq \Sigma\delta_{i,j}$ where

$$\Sigma = T\sum_{\omega_{n'}}\sum_{\mathbf{a}}\frac{\tilde{\Phi}_{\mathbf{a}}\left(\omega_n - \omega_{n'}\right)}{i\omega_{n'}+\mu} \tag{4.40}$$

and

$$\tilde{\Phi}_{\mathbf{a}}\left(\Omega_n\right) = \frac{1}{2}\int_{-1/T}^{1/T} d\tau e^{i\Omega_n\tau}\tilde{\Phi}_{ii'}^{i'i}(\tau) \tag{4.41}$$

with $\Omega_n = 2\pi nT; n = 0, \pm1, \pm2, \ldots$. This Fourier component is readily calculated in the case of dispersionless phonons $\omega_{\mathrm{q}} = \omega$ expanding the exponent in Eq.(4.39)

$$\tilde{\Phi}_{\mathbf{a}}\left(\Omega_n\right) = \frac{2\sigma^2(\mathbf{a})}{\omega}\sum_{k=1}^{\infty}\sum_{p=0}^{k}\binom{k}{p}\frac{\sinh[(k-2p)\omega/2T]}{2^k k!\sinh^k(\omega/2T)}$$

$$\times\left(\frac{1}{N}\sum_{\mathbf{q}'}\gamma^2\left(\mathbf{q}'\right)\left[1-\cos\left(\mathbf{q}'\cdot\mathbf{a}\right)\right]^k\frac{(k-2p)\omega^2}{(k-2p)^2\omega^2+\Omega_n^2}\right. \tag{4.42}$$

The main frequency independent contribution is

$$\tilde{\Phi}_{\mathbf{a}}\left(\Omega_n\right) \simeq \frac{T^2(\mathbf{a})}{g^2(\mathbf{a})\omega_0} \tag{4.43}$$

Summation over frequencies in Eq.(4.40) yields

$$-T\sum_{\omega_{n'}}\frac{1}{i\omega_{n'}+\mu}=\frac{1}{2}\tanh\frac{\mu}{2T} \tag{4.44}$$

The chemical potential is determined via the atomic density of carriers n

$$\frac{2}{N}\sum_{\mathbf{k}}n_{\mathbf{k}}=n \tag{4.45}$$

with the Fermi-Dirac distribution function

$$n_{\mathbf{k}}=\frac{1}{\exp\left[\left(\epsilon_{\mathbf{k}}-\mu\right)/T\right]+1}\simeq\frac{1}{2}\left(1+\tanh\frac{\mu}{2T}\right) \tag{4.46}$$

By the use of Eq.(4.45) one obtains

$$\tanh\frac{\mu}{2T}\simeq n-1 \tag{4.47}$$

and

$$\Sigma\simeq-(1-n)\sum_{\mathbf{a}}\frac{T^2(\mathbf{a})}{2\omega_0 g^2(\mathbf{a})} \tag{4.48}$$

or in the nearest neighbor approximation with the definition $D=z|T(\mathbf{a})|$

$$\Sigma\simeq-\frac{(1-n)E_p}{2z\lambda^2} \tag{4.49}$$

This expression is a result of the summation of the second order in H_{p-ph} multiphonon diagrams as shown in Fig.4.2a. The contribution of the second order being negative lowers the polaron energy and increases the effective mass further (to show this one should calculate the frequency derivative of $\Sigma(\omega)$). Gogolin (1982) in the framework of a single polaron problem estimated also the third and higher order contributions to Σ, Fig. 4.2 b

$$\Sigma^{(3)}\sim+\frac{E_p}{\lambda^3} \tag{4.50}$$

The third order contribution is positive and leads to the reduction of the effective mass. Because the dispersion is exponentially small one can sum all diagrams, including the crossing ones. These results show that the consistent perturbation expansion in $1/\lambda$ exists with the small parameter

$$\frac{1}{2z\lambda^2}\ll 1 \tag{4.51}$$

where z is the nearest neighbor number. Therefore if the coupling constant $\lambda>1/\sqrt{2z}$, small polarons are stable and they tunnel in a narrow band, Eq.(4.26). This condition of the small polaron formation is independent of the adiabatic ratio ω/D. However, the term in front of the exponent in the bandwidth depends on this parameter. For the adiabatic small polaron ($\omega/D\ll 1$) it is different from D as follows from the numerical calculations, section 1.8.

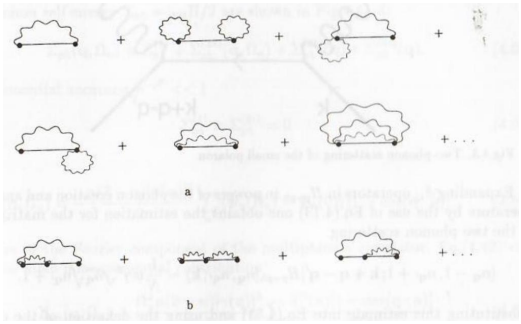

Fig.4.2. Polaron self-energy.

5.4.4 4.4 Temperature collapse of the polaron band

Theory

The self-energy effect is small at $T = 0$ if λ is of the order of unity or larger. However, the polaron bandwidth depends on the temperature according to Eq.(4.21). For high temperatures $T \gg \omega/2$ the band shrinks exponentially with increasing temperature

$$w \simeq D \exp\left(-\frac{2E_p T}{\omega^2}\right) \tag{4.52}$$

On the other hand the scattering of polarons within their narrow band becomes more important with the increasing temperature because of the simultaneous phonon emission and absorption. The absorption or emission of a single high-frequency phonon is forbidden by the energy conservation for the nonadiabatic small polaron with the bandwidth $2w \leq \omega$. However, two-phonon processes, Fig.4.3 with the simultanecum emission and absorption of different phonons are allowed at finite temperatures. These incoherent events tend to destroy the coherent polaron tunneling in the band. the corresponding scattering rate is given by the Fermi-golden rule, which for dis-
persionless phonons is

$$\frac{1}{\tau} = 2\pi \left\langle \sum_{\mathbf{q},\mathbf{q}'} \left| \langle n_{\mathbf{q}} - 1, n_{\mathbf{q}'} + 1; \mathbf{k} + \mathbf{q} - \mathbf{q}' | \, H_{p-ph} \, | n_{\mathbf{q}}, n_{\mathbf{q}'}; \mathbf{k} \rangle \right|^2 \delta\left(\epsilon_{\mathbf{k}} - \epsilon_{\mathbf{k}+\mathbf{q}-\mathbf{q}'}\right) \right\rangle \tag{4.53}$$

where $|n_{\mathbf{q}}; \mathbf{k}\rangle$ is an eigenstate of a noninteracting small polaron propagating with momentum k and n_{q} phonons.

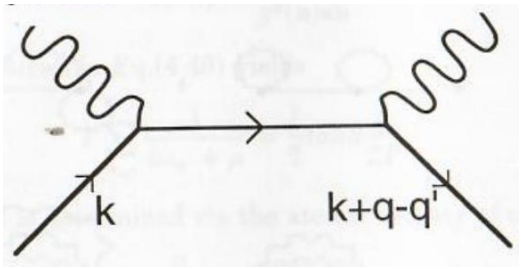

Fig.4.3. Two-phonon scattering of the small polaron.

Expanding $\hat{\sigma}_{ij}$ operators in H_{p-ph} in powers of the phonon creation and annihilation operators by the use of Eq.(4.13) one obtains the estimation for the matrix element of the two phonon scattering

$$\langle n_{\mathbf{q}}-1, n_{\mathbf{q}'}+1; \mathbf{k}+\mathbf{q}-\mathbf{q}'| \, H_{p-ph} \, |n_{\mathbf{q}}, n_{\mathbf{q}'}; \mathbf{k}\rangle \sim \frac{1}{N} w\gamma^2 \sqrt{n_{\mathbf{q}}}\sqrt{n_{\mathbf{q}'}+1} \tag{4.54}$$

Substituting this estimate into Eq.(4.53) and using the definition of the density of states in the polaron band

$$N_p(\xi) \equiv \frac{1}{N}\sum_{\mathbf{k}} \delta\left(\xi - \epsilon_{\mathbf{k}}\right) \simeq \frac{1}{2w} \tag{4.55}$$

we have

$$\frac{1}{\tau} \simeq w\gamma^4 n_\omega \left(1+n_\omega\right) \tag{4.56}$$

where $n_\omega = [\exp(\omega/T)-1]^{-1}$ is the phonon distribution function. The matrix element γ is taken momentum independent. The polaron band is well defined if

$$\frac{1}{\tau} < w \tag{4.57}$$

which is the case in a wide temperature range

$$T \leq \frac{\omega}{\ln \gamma^4} \tag{4.58}$$

below *ca.* half of the characteristic phonon frequency for the reasonable values of $\gamma^2 \leq 5$.

At higher temperatures the incoherent thermally activated hopping dominates in the polaron motion. Then the polaronic states cannot be classified with the momen tum.

5.4.5 4.5 Phonons in a strong-coupling system

Theory

An essential question, which arises within the adiabatic Migdal approach is that of the phonon instability and the applicability of the Fröhlich hamiltonian. Taking into account the polaron formation we show in this section that the phonon frequency softening is small and therefore the Fröhlich hamiltonian is applicable also in the strong coupling regime. The first and different second order diagrams in H_{p-ph} contributing to the phonon self energy $\Sigma_{ph} = \omega_{\mathbf{q}}\Pi/2$ are shown in Fig.4.4a-d:

$$\Sigma_{ph}\left(\mathbf{q}, \Omega_n\right) = \Sigma_{ph}^{(1)} + \Sigma_{ph}^{(2a)}\left(\mathbf{q}, \Omega_n\right) + \Sigma_{ph}^{(2b)}(\mathbf{q}) + \Sigma_{ph}^{(2c)}(\mathbf{q}). \tag{4.59}$$

With exponential accuracy, $e^{-g^2} \ll 1$

$$\Sigma_{ph}^{(1)} = \Sigma_{ph}^{(2c)} = 0 \tag{4.60}$$

and

$$\Sigma_{ph}\left(\mathbf{q}, \Omega_n\right) = -\frac{n(2-n)|\gamma(\mathbf{q})|^2}{2}\sum_{\mathbf{a}} \left(\Phi_{\mathbf{a}}\left(\Omega_n\right) - \Phi_{\mathbf{a}}(0)\right)\left[1-\cos(\mathbf{q}\cdot\mathbf{a})\right] \tag{4.61}$$

By the use of the Fourier component of the multiphonon correlator, Eq.(4.42) one obtains the main nonexponential contribution

$$\Sigma_{ph}\left(\mathbf{q}, \Omega_n\right) = \frac{\Omega_n^2 n(2-n)|\gamma(\mathbf{q})|^2}{2\omega^3}\sum_{\mathbf{a}} \frac{T^2(\mathbf{a})[1-\cos(\mathbf{q}\cdot\mathbf{a})]}{g^6(\mathbf{a})}$$

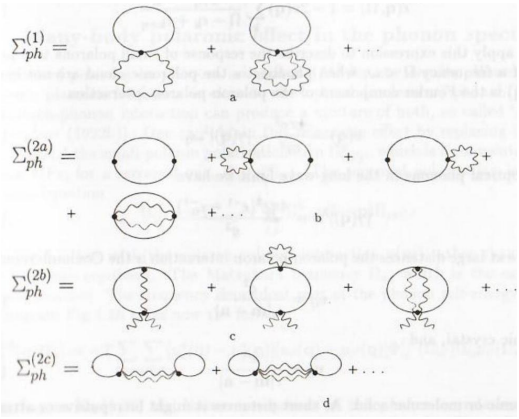

Fig. 4.4. Phonon self-energy in the strong-coupling limit.

The analytical continuation to the real frequencies is found by the simple substitution

$$i\Omega_n \to \tilde{\omega} + i0^+ \tag{4.63}$$

with the following result for the renormalised phonon frequency, which is a pole of the phonon GF:

$$\tilde{\omega}_{\mathbf{q}} \simeq \omega - \Delta(\mathbf{q}) \tag{4.64}$$

The phonon frequency softening

$$\Delta(\mathbf{q}) = \frac{n(2-n)|\gamma(\mathbf{q})|^2}{2\omega} \sum_{\mathbf{a}} \frac{T^2(\mathbf{a})[1-\cos(\mathbf{q}\cdot\mathbf{a})]}{g^6(\mathbf{a})} \tag{4.65}$$

is small compared with the frequency as $1/\lambda^2 \ll 1$. This result is consistent with the phonon frequency renormalisation in the two-site Holstein model, section 1.7. Phonons are stable in the strong-coupling regime. The ions change their equilibrium positions due to the electron-phonon coupling retaining their vibration frequencies practically unchanged.

5.4.6 4.6 Screening and polaronic plasmon

Theory

Polarons are coupled not only with phonons via the residual interaction H_{p-ph} but also between themselves. At sufficiently high temperatures above the bipolaronic instability (see Chapter 5) the effect of H_{p-p} is described by the dielectric response function $\epsilon(\mathbf{q}, \Omega)$, for which the canonical random phase approximation is adopted

$$\epsilon(\mathbf{q}, \Omega) = 1 - 2v(\mathbf{q}) \sum_{\mathbf{k}} \frac{n_{\mathbf{k}+\mathbf{q}} - n_{\mathbf{k}}}{\Omega - \epsilon_{\mathbf{k}} + \epsilon_{\mathbf{k}+\mathbf{q}}} \tag{4.66}$$

One can apply this expression to describe the response of small polarons to a perturbation of a frequency $\Omega < \omega$, when phonons in the polaronic cloud are not excited. Here $v(\mathbf{q})$ is the Fourier component of the polaron-polaron interaction

$$v(\mathbf{q}) = \frac{4\pi e^2}{\epsilon q^2} - |\gamma(\mathbf{q})|^2 \omega_{\mathbf{q}} \tag{4.67}$$

For the optical phonons in the long-wave limit we have

$$|\gamma(\mathbf{q})|^2\omega = \frac{4\pi e^2\left(\epsilon^{-1}-\epsilon_0^{-1}\right)}{q^2} \tag{4.68}$$

Therefore at large distances the polaron-polaron interaction is the Coulomb repulsion,

$$v_{ij} = \frac{e^2}{\epsilon_0|\mathbf{m}-\mathbf{n}|} \tag{4.69}$$

in an ionic crystal, and

$$v_{ij} = \frac{e^2}{\epsilon|\mathbf{m}-\mathbf{n}|} \tag{4.70}$$

in an atomic or molecular solid. At short distances it might be repulsive or attractive depending on the value of a short range ϵ.

In the static limit at large distances (or $q \to 0$) we obtain the usual Debye screening due to the repulsion with the static dielectric function

$$\epsilon(q,0) = 1 + \frac{q_s^2}{q^2} \tag{4.71}$$

where $q_s = \sqrt{2\pi e^2 n(2-n)/T\epsilon_0}$. This result is obtained for the temperature larger than the polaronic bandwidth using the expansion of the polaron distribution function:

$$n_{\mathbf{k}} \simeq \frac{n}{2}\left(1 - \frac{(2-n)\epsilon_{\mathbf{k}}}{2T}\right) \tag{4.72}$$

The polaron response becomes dynamic for a rather low frequency $\omega > w$,

$$\epsilon(\mathbf{q},\omega) = 1 - \frac{\omega_p^2(\mathbf{q})}{\omega^2} \tag{4.73}$$

with the temperature dependent plasma frequency

$$\omega_p^2(\mathbf{q}) = 2v(\mathbf{q})\sum_{\mathbf{k}} n_{\mathbf{k}}\left(\epsilon_{\mathbf{k}+\mathbf{q}} - \epsilon_{\mathbf{k}}\right) \tag{4.74}$$

which is proportional to the inverse temperature if $T \gg w$. This expression is applied to the polaronic plasmon with a frequency below or of the order of the characteristic phonon frequency, which is quite feasible due to a large value of the background dielectric constant and the enhanced effective mass. Otherwise, one should take into account the phonon shakeoff in the dielectric response function.

5.4.7 4.7 Many-body polaronic effect in the phonon spectrum

Theory

The effect of polarons on phonons is small as $1/\lambda^2$ for any density. However, if the polaronic plasmon frequency is close to the optical (molecular) phonon frequency the polaron-phonon interaction can produce a mixture of both, so called 'plasphon' (Alexandrov (1992b)). One can obtain this resonance effect by replacing in all diagrams Fig. 4.4 the small-polaron polarisation loop $\Pi^0_{iji'j'}$, which is a convolution of two polaron GFs, for a screened one, $\Pi_{iji'j'}(\Omega_n)$. The screened polarisation loop obeys the same equation

$$\Pi_{iji'j'} = \Pi^0_{iji'j'} + \sum_{l,p}\Pi^0_{ijll}v(\mathbf{l}-\mathbf{p})\Pi_{ppi'j'} \tag{4.75}$$

as in Fig.3.2, but with the polaron-polaron interaction $v(\mathbf{m})$ rather than with the bare Coulomb repulsion. The Matsubara frequency Ω_n, which is the same in all terms is omitted. The frequency dependent part of the phonon self-energy given by the diagram Fig.4.4b takes now the form

$$\Sigma_{ph}^{(2a)}(\mathbf{q},\Omega_n) = -T\sum_{\Omega_{n'}}\sum_{iji'j'}\left[u_i^*(\mathbf{q})-u_j^*(\mathbf{q})\right]\left[u_{i'}(\mathbf{q})-u_{j'}(\mathbf{q})\right]\Phi_{ij}^{i'j'}(\Omega_{n'})\,\Pi_{iji'j'}(\Omega_{n'}-\Omega_n)\,. \tag{4.76}$$

According to Eq.(4.37) the Fourier component of the phonon correlation function comprises the part Φ, which is almost frequency independent for $\Omega_n \ll E_p$, and the exponentially small term, which is nonzero only for $\Omega_n = 0$. The contribution of this second term to the self-energy is enhanced, however, if the resonance condition $\omega_p \simeq \omega$ is met. By the use of Eq.(4.37) one obtains

$$\Sigma_{ph}(\mathbf{q},\Omega_n) = \Sigma_{ph}^{res}(\mathbf{q},\Omega_n) - \Delta(\mathbf{q}) \tag{4.77}$$

where
$\Sigma_{ph}^{res}(\mathbf{q},\Omega_n) = -\sum_{iji'j'}\left[u_i^*(\mathbf{q})-u_j^*(\mathbf{q})\right]\left[u_{i'}(\mathbf{q})-u_{j'}(\mathbf{q})\right]\sigma(\mathbf{m}-\mathbf{n})\sigma(\mathbf{m}'-\mathbf{n}')\,\Pi_{iji'j'}(-\Omega_n)$.

The solution to Eq.(4.75) is obtained with the Fourier transformation of the polarisation loop

$$\Pi_{iji'j'} = \frac{1}{N}\sum_{\mathbf{k},\mathbf{k}',\mathbf{g}}\Pi(\mathbf{k},\mathbf{k}',\mathbf{g})\exp\left[-i\mathbf{k}\cdot(\mathbf{m}'-\mathbf{n})+i\mathbf{k}\cdot(\mathbf{n}'-\mathbf{m})+i\mathbf{g}\cdot(\mathbf{m}'-\mathbf{n}')\right] \tag{4.79}$$

The Fourier transformation of Eq.(4.75) yields

$$\Pi(\mathbf{k},\mathbf{k}',\mathbf{g}) = \Pi^0(\mathbf{k},\mathbf{k}')\left[N\delta_{\mathbf{g},0}+v(\mathbf{k}-\mathbf{k}')\sum_{\mathbf{g}'}\Pi(\mathbf{k}+\mathbf{g}'-\mathbf{g},\mathbf{k}'+\mathbf{g}'-\mathbf{g},\mathbf{g}')\right] \tag{4.80}$$

where

$$\Pi^0(\mathbf{k},\mathbf{k}') = 2\frac{n_{\mathbf{k}}-n_{\mathbf{k}'}}{i\Omega_n+\epsilon_{\mathbf{k}}-\epsilon_{\mathbf{k}'}} \tag{4.81}$$

One can replace k, k′ for k + g and k′ + g, respectively to obtain

$$\Pi(\mathbf{k}+\mathbf{g},\mathbf{k}'+\mathbf{g},\mathbf{g}) = \Pi^0(\mathbf{k}+\mathbf{g},\mathbf{k}'+\mathbf{g})\left[N\delta_{\mathbf{g},0}+v(\mathbf{k}-\mathbf{k}')A(\mathbf{k},\mathbf{k}')\right] \tag{4.82}$$

where $A(\mathbf{k},\mathbf{k}') \equiv \sum_{\mathbf{g}'}\Pi(\mathbf{k}+\mathbf{g},\mathbf{k}'+\mathbf{g}',\mathbf{g}')$ is found by taking the sum in Eq.(4.80) over $\mathbf{g}$

$$A(\mathbf{k},\mathbf{k}') = N\frac{\Pi^0(\mathbf{k},\mathbf{k}')}{\epsilon(\mathbf{k}-\mathbf{k}',i\Omega_n)} \tag{4.83}$$

As a result we find

$$\Pi(\mathbf{k},\mathbf{k}',\mathbf{g}) = N\Pi^0(\mathbf{k},\mathbf{k}')\left[\delta_{\mathbf{g},0}+v(\mathbf{k}-\mathbf{k}')\frac{\Pi^0(\mathbf{k},\mathbf{k}')}{\epsilon(\mathbf{k}-\mathbf{k}',i\Omega_n)}\right] \tag{4.84}$$

and
$\Sigma_{ph}^{res}(\mathbf{q},\Omega_n) = \frac{\gamma^2(\mathbf{q})}{2N^2}\sum_{\mathbf{k},\mathbf{g}}\left(\epsilon_{\mathbf{k}}\epsilon_{\mathbf{k}-\mathbf{q}-\mathbf{g}}+\epsilon_{\mathbf{k}-\mathbf{q}}\epsilon_{\mathbf{k}-\mathbf{g}}-\epsilon_{\mathbf{k}-\mathbf{g}}\epsilon_{\mathbf{k}-\mathbf{q}-\mathbf{g}}-\epsilon_{\mathbf{k}}\epsilon_{\mathbf{k}-\mathbf{g}}\right)\Pi(\mathbf{k},\mathbf{k}-\mathbf{q},\mathbf{g})$.

One can expand the unscreened polarisation $\Pi^0(\mathbf{k},\mathbf{k}')$ in powers of a small parameter $w/\omega \ll 1$ as

$$\Pi^0\left(\mathbf{k},\mathbf{k}'\right)=2\left(n_{\mathbf{k}}-n_{\mathbf{k}'}\right)\left[\frac{1}{i\Omega_n}+\frac{\epsilon_{\mathbf{k}}-\epsilon_{\mathbf{k}'}}{\Omega_n^2}+\ldots\right] \tag{4.86}$$

With this expansion we have

$$\Sigma_{ph}^{res}\left(\mathbf{q},\Omega_n\right)=-\frac{\beta(\mathbf{q})\omega_p^4(\mathbf{q})}{\omega\left[\Omega_n^2+\omega_p^2(\mathbf{q})\right]} \tag{4.87}$$

where $\beta(\mathbf{q})=\omega|\gamma(\mathbf{q})|^2/v(\mathbf{q})$ is the dimensionless plasmon-phonon coupling constant. The dispersion relation for the plasmon-phonon mixture is obtained by carrying out the analytical continuation of $\Sigma_{ph}\left(\mathbf{q},\Omega_n\right)$ to real frequencies by the substitution $i\Omega_n\to\Omega$,

$$\Omega_{\mathbf{q}}=\omega-\Delta(\mathbf{q})+\frac{\beta(\mathbf{q})\omega_p^4(\mathbf{q})}{\omega\left[\Omega_{\mathbf{q}}^2-\omega_p^2(\mathbf{q})\right]} \tag{4.88}$$

There are three solutions to Eq.(4.88)

$$\Omega_1=\frac{\tilde{\omega}}{3}+\frac{2}{3}\cos\left(\frac{\alpha}{3}\right)\left[\tilde{\omega}^2+\omega_p^2\right]^{1/2} \tag{4.89}$$

$$\Omega_{2,3}=\frac{\tilde{\omega}}{3}-\frac{2}{3}\cos\left(\frac{\alpha\pm\pi}{3}\right)\left[\tilde{\omega}^2+\omega_p^2\right]^{1/2} \tag{4.90}$$

with $\tilde{\omega}=\omega-\Delta$ and $\cos\alpha=\left[\tilde{\omega}^3-9\tilde{\omega}\omega_p^2+27\beta\omega_p^4/2\omega\right]/\left[\tilde{\omega}^2+3\omega_p^2\right]^{3/2}$. The dependence on $\mathbf{q}$ of all parameters is assumed. Only two solutions, $\Omega_{1,2}$ are real and positive. Consequently, instead of a single phonon mode, strongly coupled to carriers there are two branches of excitations describing the propagation of coupled phonon and polaronic plasmon, so called 'plasphons'. If the plasmon-phonon coupling is weak, $\beta\ll 1$ their dispersion is described by

$$\Omega_{1,2}\simeq\frac{1}{2}\left[\tilde{\omega}+\omega_p\pm\sqrt{\left(\tilde{\omega}-\omega_p\right)^2+2\beta\omega_p^3/\omega}\right] \tag{4.91}$$

In the limit $\beta\to 0\Omega_{1,2}$ describe the renormalised phonon with the frequency $\tilde{\omega}$ and the polaronic plasmon ω_p. However, for a finite β and $\tilde{\omega}\simeq\omega_p$ they are mixed and both contribute to the phonon GF

$$D(\mathbf{q},\Omega)=\sum_{i=1}^{3}\frac{P_i(\mathbf{q})}{\Omega-\Omega_i(\mathbf{q})} \tag{4.92}$$

The ratio of weights of two contributions is

$$\frac{P_2}{P_1}=\frac{\left(\Omega_2^2-\omega_p^2\right)\left(\Omega_3-\Omega_1\right)}{\left(\Omega_1^2-\omega_p^2\right)\left(\Omega_3-\Omega_2\right)} \tag{4.93}$$

It can be of the order of unity if the polaronic plasmon and phonon frequencies are close to each other.

5.4.8 4.8 Polaron thermodynamics

Theory

In the normal state for sufficiently high temperatures the polaron-polaron correlations are not very important and in the first approximation the small polaron heat capacity as well as the magnetic susceptibility are those of narrow band fermions. Moreover in the temperature range

$T < \omega/2$ the polaron bandwidth is temperature independent. For a narrow band Fermi-gas one obtains the heat capacity C_p :

$$C_p = 2T \int_{-w-\mu}^{w-\mu} d\xi N_p(\xi) \frac{df}{d\xi} \left(\frac{\xi}{T} \frac{d\mu}{dT} - \frac{\xi^2}{T^2} \right) \tag{4.94}$$

where $f(\xi) = \left(\exp\left(\frac{\xi}{T}\right) + 1\right)^{-1}$. This expression yields a linear temperature dependence $C_p(T)$ for low temperatures $T < 0.4w$ if the polaron density of states is energy independent, $N_p = 1/2w$

$$C_p = \frac{\pi^2 T}{3w} \tag{4.95}$$

and a power law decrease ($\sim T^{-2}$) for $T > w$:

$$C_p = \frac{w^2 n(2-n)}{6T^2}. \tag{4.96}$$

The numerical calculations in the intermediate temperature region reveal only a small change in the position T_m of the maximum of $C_p(T)$ with the variation of the filling factor $n, T_m \simeq 0.4w$, and a gradual increase of the maximum value from $C_p^m = 0.2$ at $n = 0.2$ to $C_p^m = 0.6$ at $n = 1$. The temperature dependence of the heat capacity is similar to the Schottky anomaly except for the low temperature region with the linear C_p instead of the exponential one of two-level systems.

In the polaronic system the narrow band includes all states of the Brillouin zone rather than a small part of them under a peak of the density of states as in a so-called 'van -Hove scenario' of high- T_c. This fact provides us with the possibility to get an absolute value of the spin susceptibility of polarons considerably higher than those of wide band electrons

$$\chi_s = -\frac{\mu_B^2}{w} \int_{-w-\mu}^{w-\mu} d\xi \frac{df}{d\xi} \tag{4.97}$$

where μ_B is the Bohr magneton. The chemical potential is determined through the density of polarons

$$\mu = T \ln \frac{\exp \frac{nw}{T} - 1}{\exp \frac{w}{T} - \exp \frac{(n-1)w}{T}}, \tag{4.98}$$

and

$$\chi_s = \frac{\mu_B^2}{w} \frac{\left(\exp \frac{nw}{T} - 1\right)\left(\exp \frac{(2-n)w}{T} - 1\right)}{\exp \frac{w}{T} - 1}. \tag{4.99}$$

Eq.(4.99) yields the Curie law in the high-temperature limit, $T \gg w$

$$\chi_s \simeq \frac{\mu_B^2 n(2-n)}{2T}, \tag{4.100}$$

and a temperature independent susceptibility enhanced due to the polaron narrowing of the band for $T < w$:

$$\chi_s = \frac{\mu_B^2}{w} \tag{4.101}$$

with w instead of D as in ordinary metals. The enhancement is the same as that of the specific heat ratio $\gamma = C_p/T$, Eq.(4.95) in contrast with the ordinary metals, where only the electronic heat capacity is increased by the electron-phonon interaction while the magnetic susceptibility remains unaffected.

5.4.9 4.9 Polaron kinetics: hopping transport

Theory

Transport properties of polarons depend strongly on the temperature. For temperature lower than the Debye temperature (or the characteristic phonon energy) polarons tunnel through the narrow band, however at higher temperatures the polaronic band collapses as discussed in section 4.4 and their transport is diffusive via thermally activated hopping (see e.g. Mott and Davis (1979)). There is extensive literature on the hopping transport of small polarons, in particular, the excellent reviews by Appel (1969) and Firsov (1975) and books by Klinger (1979) and Böttger and Bryksin(1985). Böttger and Bryksin also discussed in detail the hopping polaron transport in a random potential. These and other studies elucidated the value of the activation energy of the conductivity as well as the sign and the temperature behavior of the Hall effect in the hopping regime, $T \gg \omega/2$. In this regime the transport is due to thermally activated jumps of polarons from site to site. For such processes the diffusion coefficient is given by $D \simeq a^2 W$, where W is the hopping probability. The only term in the polaronic Hamiltonian, which changes the phonon occupation numbers is the polaron-phonon interaction H_{p-ph}. Applying the perturbation theory with respect to this interaction up to the second order one estimates the nearest neighbor hopping probability with the Fermi golden rule as

$$W = 2\pi \left\langle \sum_j \left| \langle j|H_{p-ph}|i\rangle \right|^2 \delta\left(\sum_{\mathbf{q}} \omega_{\mathbf{q}} \left(n^j_{\mathbf{q}} - n^i_{\mathbf{q}} \right) \right) \right\rangle , \tag{4.102}$$

where $|i\rangle$ and $|j\rangle$ are the eigenstates of H_0 corresponding to the polaron on site i with n^i_{q} phonons in each phonon mode and the polaron on the neighboring site j with n^j_{q} phonons, respectively. Representing the δ function in Eq.(4.102) by the integral and using the definition of the Heisenbeg operators we obtain in the second order with respect to the bandwidth

$$W = \int_{-\infty}^{\infty} dt \left[\Phi^{\mathbf{n},\mathbf{m}}_{\mathbf{m},\mathbf{n}}(t) - \sigma^2(\mathbf{a}) \right] e^{-i0^+|t|} \tag{4.103}$$

A real time multiphonon correlation function $\Phi^{i'j'}_{ij}(t)$ is the same as the Matsubara one, Eq.(4.39) with the substitution $|\tau| \to it$. Thus, we have

$$\Phi^{\mathrm{n,m}}_{\mathrm{m,n}}(t) = \sigma^2(\mathbf{a}) \exp\left(\frac{1}{N} \sum_{\mathbf{q}} |\gamma(\mathbf{q})|^2 [1 - \cos(\mathbf{q}\cdot\mathbf{a})] \frac{\cosh\left[\omega_{\mathbf{q}} \left(\frac{i}{2T} + t\right)\right]}{\sinh \frac{\omega_{\mathbf{q}}}{2T}} \right). \tag{4.104}$$

Substituting this expression into Eq.(4.103) and shifting the integration contour one obtains

$$W = T^2(\mathbf{a}) e^{-2g^2(\mathbf{a})} \int_{-\infty}^{\infty} dt \left[\exp\left(\frac{1}{N} \sum_{\mathbf{q}} |\gamma(\mathbf{q})|^2 [1 - \cos(\mathbf{q}\cdot\mathbf{a})] \frac{\cos(\omega_{\mathbf{q}} t)}{\sinh \frac{\omega_{\mathbf{q}}}{2T}} \right) - 1 \right] e^{-i0^+|t|} \tag{4.105}$$

The integrand here is an oscillating function. The integration with respect to t is performed by the use of the saddle-point approximation. This approximation is jusiified if a finite dispersion of the phonon frequency $\delta\omega$ is taken into account and the lemperature is so high that $T > \omega^2/2\gamma^2\delta\omega$. If this inequality is satisfied the integrand
decreases rapidly with increasing time. Then one can expand in the exponent $\cos(\omega t)$ in powers with respect to t up to the second order term. The unity in the integrand, Eq.(4.105), which compensates the divergence for $t \to \infty$ can be neglected. As a result one finds

$$W \simeq T^2(\mathbf{a}) e^{-E_a/T} \int_{-\infty}^{\infty} dt e^{-\delta t^2} \tag{4.106}$$

where the activation energy is

$$E_a = \frac{T}{N} \sum_{\mathbf{q}} |\gamma(\mathbf{q})|^2 [1 - \cos(\mathbf{q} \cdot \mathbf{a})] \tanh(\omega_{\mathbf{q}}/4T), \tag{4.107}$$

and

$$\delta = \frac{1}{2N} \sum_{\mathbf{q}} |\gamma(\mathbf{q})|^2 [1 - \cos(\mathbf{q} \cdot \mathbf{a})] \frac{\omega_{\mathbf{q}}^2}{\sinh(\omega_{\mathbf{q}}/2T)} \tag{4.108}$$

The activation energy is half of the polaronic level shift E_p, Eq.(1.98) if there is no dispersion of $\omega_{\mathbf{q}}$ and $\gamma(\mathbf{q})$. The dispersion diminishes the value of E_a further. By means of the Einstein relation $\sigma = ne^2 D/T$ the hopping conductivity in the hopping region $T \gg \omega/2$ is found to be

$$\sigma_h = ne^2 a^2 \frac{\sqrt{\pi} T^2(\mathbf{a})}{2T\sqrt{E_a T}} e^{-E_a/T} \tag{4.109}$$

The hopping mobility $\mu_h \equiv \sigma_h/ne \sim \exp(-E_a/T)$ can be below $ea^2 \simeq 1 cm^2/Vs$, which is the lowest limit for the Boltzmann theory to be applied. Within the Boltzmann theory such a low mobility corresponds to the mean free path $l < a$, which is not a reasonable result.

To calculate the transverse conductivity σ_{xy} and the Hall coefficient $R_H = \sigma_{xy}/H\sigma_{xx}^2$ of polarons one can introduce the vector potential $\mathbf{A}(\mathbf{r})$ of the external field with the Peierls substitution (Peierls (1933))

$$T(\mathbf{m} - \mathbf{n}) \to T(\mathbf{m} - \mathbf{n}) e^{-ie\mathbf{A}(\mathbf{m}) \cdot (\mathbf{m} - \mathbf{n})} \tag{4.110}$$

which is a fair approximation if the magnetic field is weak compared with the atomic field

$$eHa^2 \ll 1. \tag{4.111}$$

Here $\mathbf{A}(\mathbf{r})$ is the vector potential which can be also time dependent. Within the Boltzmann theory the sign of the Hall coefficient $R_H \simeq \pm 1/en$ depends on the type of carriers (holes or electrons) and the Hall mobility $\mu_H \equiv R_H \sigma_{xx}$ is the same as the drift mobility μ_t up to numerical factor of the order of unity. The calculations of a hopping Hall current similar to those of the hopping conductivity (Friedman and Holstein (1963), Friedman (1995)) shows that the Hall mobility depends on the symmetry of the crystal lattice and has nothing in common with the hopping mobility, neither with respect to the temperature dependence and even nor with respect to the sign. Thus, for hexagonal lattices three -site hops yield

$$\mu_H = ea^2 \frac{\sqrt{\pi} T(\mathbf{a})}{\sqrt{12 E_a T}} e^{-E_a/3T} \tag{4.112}$$

with the same sign for electrons and holes. The activation energy of the Hall mobility is three times less than that of the hopping mobility. In cubic crystals, the hopping Hall effect is governed by four-site hops. For the four-site case calculations by Emin (1971) gave a Hall mobility even more temperature independent with the sign depending on the type of carriers.

5.4.10 4.10 MIR conductivity of polarons

Theory

One of the hallmarks of polarons is the frequency and temperature dependence of their mid-infrared (MIR) conductivity $\sigma(\nu)$. In the low frequency and low temperature region, where the tunneling band transport operates the conductivity has the canonical Drude form

$$\sigma(\omega) = \frac{ne\mu_t}{1+(\nu\tau)^2}, \tag{4.113}$$

where the transport relaxation time τ may be frequency dependent because of the narrow band. For high mid-infrared frequencies well above the polaron bandwidth but below the inter-band gap the Drude law breaks down. In this frequency region one can apply the generalised Einstein relation $\sigma(\nu) = eD(\nu)/\nu$, where $D(\nu) = a^2W(\nu)$ and $W(\nu)$ is the hopping probability of the absorption of the energy quantum ν. The number of nearest neighbor transitions per second with the absorption of photon of the energy ν is given by the Fermi-golden rule

$$W^- = 2\pi \left\langle \sum_j \left| \langle j|H_{p-ph}|i\rangle \right|^2 \delta\left(\sum_{\mathbf{q}} \omega_{\mathbf{q}} \left(n^j_{\mathbf{q}} - n^i_{\mathbf{q}}\right) - \nu\right)\right\rangle, \tag{4.114}$$

and with the photon emission

$$W^+ = 2\pi \left\langle \sum_j \left| \langle j|H_{p-ph}|i\rangle \right|^2 \delta\left(\sum_{\mathbf{q}} \omega_{\mathbf{q}} \left(n^j_{\mathbf{q}} - n^i_{\mathbf{q}}\right) + \nu\right)\right\rangle. \tag{4.115}$$

As a result one gets

$$W(\nu) = W^- - W^+ = 2T^2(\mathbf{a})e^{-2g^2(\mathbf{a})}\sinh(\nu/2T) \times \int_{-\infty}^{\infty} dt e^{-i\nu t}\left[\exp\left(\frac{1}{N}\sum_{\mathbf{q}} |\gamma(\mathbf{q})|^2[1-\cos(\mathbf{q}\cdot\mathbf{a})]\frac{\cos(\omega t)}{\sinh\frac{\omega_{\mathbf{q}}}{2T}}\right) - 1\right] \tag{4.116}$$

An in the case of the *dc* hopping conductivity the integral over t is calculated using the saddle-point approximation (Böttger and Bryksin (1985)). The saddle point is lying on the imaginary axis, say, at $t = -iy$. Setting at this point the derivative of the exponent with respect to t equal zero one gets the following equation for y

$$\nu = \frac{1}{N}\sum_{\mathbf{q}} |\gamma(\mathbf{q})|^2[1-\cos(\mathbf{q}\cdot\mathbf{a})]\omega_{\mathbf{q}}\sinh\left(\omega_{\mathbf{q}}y\right). \tag{4.117}$$

If the frequency is not too high, $\nu \ll 4E_pT/\omega$ we can expand sinh in powers of ωy io find

$$y = \frac{\omega}{2\delta}, \tag{4.118}$$

where δ is defined by Eq.(4.108). Expanding the exponent in Eq.(4.116) in powers of t near the point $t = -iy$ and shifting the integration contour such that it passes through this point one obtains

$$\sigma(\nu) = \sigma_h \frac{T\sinh(\nu/2T)}{\nu} e^{\nu^2/4\delta}. \tag{4.119}$$

For high temperatures, $T \gg \omega/2$, this expression becomes

$$\sigma(\nu) = ne^2a^2 \frac{\sqrt{\pi}T^2(\mathbf{a})\left[1 - e^{-\nu/T}\right]}{2\nu\sqrt{E_aT}} \exp\left[-\frac{(\nu - 4E_a)^2}{16E_aT}\right]. \tag{4.120}$$

Consequently, the frequency dependence of the MIR conductivity has a form of an asymmetric Gaussian peak centered at $\nu = 4E_a \simeq 2E_p$ with the half-width $4\sqrt{E_aT}$ (Eagles (1963), Klinger (1963), Reik (1963)), Fig.4.6. According to the Franckthe principle, the position of the ions is not changed during an optical transiion. Therefore the frequency dependence of the Mir conductivity can be understood Fig.1.3. The polaron, say in the left adiabatic levels on two-site holstein model, Fig.1.3. tical transition ange in the the the the photon energy required to the from the sum of $\sigma(\nu)$, Eq. (4.120). The main control the order of max(T then comes the thin lines near the bottom with the energy of he of $2E_p \pm \sqrt{\text{ines}}$ in Fig.4.5. The corresponding photon energies are lying in the interval $2E_p \pm \sqrt{8E_pT}$ in agreement with the obtained formula. For low temperatures $T < \omega/2$ the half-width of the MIR maximum is of the order $\sqrt{E_p\omega}$ rather than $\sim \sqrt{E_pT}$.

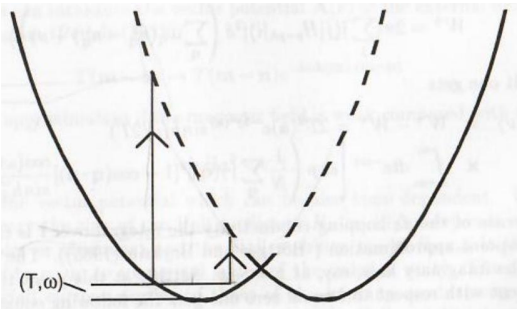

Fig.4.5. Optical transition between adiabatic levels of the two-site Holstein model.

The MIR absorption is due to the optical multiphonon transition within a single electron band. In the case of large polarons or electrons the MIR conductivity is much lower, if any. The analysis by Emin (1973, 1993) beyond the saddle-point approxima tion shows a more asymmetric and less temperature dependent MIR absorption of
large polarons compared with that of small polarons. Many perovskites have an intermediate value of the electron-phonon coupling $\lambda \sim 1$. It is, therefore, important to extend the theory of the MIR conductivity to the transition region from large to small polaron.

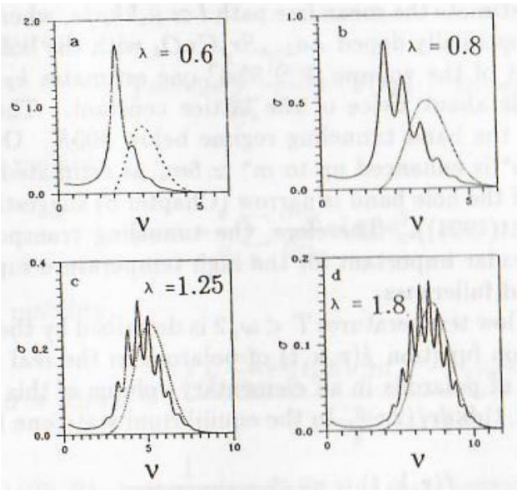

Fig.4.6. Small polaron MIR conductivity as a function of the frequency for different values of the electron-phonon coupling λ.

Such an extension is possible through the numerical calculations of $\sigma(\nu)$ of the finite size Holstein model by the exact diagonalisation procedure in the truncated space up to 50 excited phonons for the two site Holstein model and up to 20 phonons per each mode for the four site model (Alexandrov et al (1994b)). Conductivity occurs as energy is transferred between the electromagnetic field and the phonons via the charge carriers. The vibration energy must be capable of being dissipated. One has to introduce a continuous phonon density of states, which is not the case within the cluster model. However, one can avoid this problem introducing a lifetime τ_{ph} of phonons, which smears a δ-like density of their states, assuring the finite MIR conduclivity. The spectral shape of $\sigma(\nu)$ for the two-site Holstein model in the intermediate cegime ($\omega = 0.5J$) is shown in Fig.4.6 for $\tau_{ph}\omega = 2$. The main conclusions based on the numerical calculations are:

There is an agreement between the 'exact' $\sigma(\nu)$ and the analytical formula Eq.(4.119) in the strong coupling limit as far as the smooth part of the frequency dependence is concerned (dashed line).

The MIR conductivity is much more asymmetric in the intermediate coupling maion than that in the strong coupling regime;

The MIR conductivity shows an additional oscillating superstructure correspondling to a different spectral weight of the states with a different number of the virtual phanoms in the polaron cloud (section 4.12).

5.4.11 4.11 Polaron kinetics: band tunneling transport

Theory

The drift mobility μ_t along CuO 2 plane in high T_c copper oxides like $La_{2-x}Sr_xCuO_4$ is about 3 cm^2/Vs at room temperature. By the use of the transport relaxation time $\tau = \mu_t m^*/e$ one can estimate the mean free path $l \simeq \mu_t \hbar k_F/e$, where $\hbar k_F$ is the Fermi momentum. For the optimally doped $La_{2-x}Sr_xCuO_4$ with the hole density $n = x = 0.15$ per chemical unit of the volume $\Omega \simeq 95A^3$ one estimates $k_F \simeq 0.35 \times 10^8 A^{-1}$ and $l \simeq 6A$, which is about twice of the lattice constant. Therefore carriers in high T_c oxides are in the band tunneling regime below $300K$. On the other hand, their effective mass m^* is erhanced up to $m^* \simeq 5m_e$ as estimated from the London penetration depth and the hole band is narrow (Chapter 8) suggesting small polarons (Alexandrov and Mott(1994)). Therefore, the tunneling transport in

the narrow polaron band is particular important for the high temperature superconductors like copper oxides or doped fullerenes.

Polaron kinetics at low temperatures $T < \omega/2$ is described by the Boltzmann equation for the distribution function $f(\mathbf{r}, \mathbf{k}, t)$ of polarons in the real $\mathbf{r}$ and momentum k space. The number of polarons in an elementary volume of this space at time t is determined by $2f(\mathbf{r}, \mathbf{k}, t)d\mathbf{k}d\mathbf{r}/(2\pi)^3$. In the equilibrium state one has

$$f(\mathbf{r}, \mathbf{k}, t) = n_{\mathbf{k}} \equiv \frac{1}{\exp \frac{\epsilon_{\mathbf{k}} - \mu}{T} + 1} \tag{4.121}$$

The Boltzmann equation for polarons in an external electric $\mathbf{E}$ and magnetic $\mathbf{H}$ fields reads as

$$\frac{\partial f}{\partial t} + \mathbf{v}\frac{\partial f}{\partial \mathbf{r}} - e(\mathbf{E} + \mathbf{v} \times \mathbf{H})\frac{\partial f}{\partial \mathbf{k}} = \left(\frac{\partial f}{\partial t}\right)_c \tag{4.122}$$

where $\mathbf{v} = \partial\epsilon_{\mathbf{k}}/\partial\mathbf{k}$ is the group velocity. The collision integral for any elastic scattering is given by

$$\left(\frac{\partial f}{\partial t}\right)_c = 2\pi \sum_{\mathbf{q}} V_{sc}^2(\mathbf{q})\delta\left(\epsilon_{\mathbf{k}} - \epsilon_{\mathbf{k}+\mathbf{q}}\right)\left[f(\mathbf{r}, \mathbf{k} + \mathbf{q}, t) - f(\mathbf{r}, \mathbf{k}, t)\right] \tag{4.123}$$

where $V_{sc}(\mathrm{q})$ is the Fourier component of the scattering potential. The form of this integral does not depend on the statistics of particles because terms nonlinear in f_{k} are canceled. For a weak homogeneous electric and magnetic fields the Boltzmann equation can be solved by the substitution

$$f(\mathbf{r}, \mathbf{k}, t) = n_{\mathbf{k}} - \frac{\partial n_{\mathbf{k}}}{\partial \epsilon_{\mathbf{k}}}\mathbf{F}\left(\epsilon_{\mathbf{k}}\right) \cdot \mathbf{v} \tag{4.124}$$

We consider the case when the transport relaxation time defined as

$$\frac{1}{\tau\left(\epsilon_{\mathbf{k}}\right)} \equiv 2\pi \sum_{\mathbf{k}'} (1 - \cos\Theta) V_{sc}^2\left(\mathbf{k}' - \mathbf{k}\right)\delta\left(\epsilon_{\mathbf{k}'} - \epsilon_{\mathbf{k}}\right) \tag{4.125}$$

depends only on the energy. Here Θ is the angle between $\mathbf{v}'$ and $\mathbf{v}$. Then the Boltzmann equation for $\mathbf{F}(\epsilon)$ becomes

$$\mathbf{F}(\epsilon) \cdot \mathbf{v} = -e\tau(\epsilon)\left[\mathbf{E} \cdot \mathbf{v} - \mathbf{F}(\epsilon) \cdot \left(\mathbf{v} \times \mathbf{H} \cdot \nabla_{\mathbf{k}}\right)\mathbf{v}\right] \tag{4.126}$$

If the magnetic field is not too high, $\mu_t H \ll 1$, one can keep only terms linear in H with the following result for the nonequilibrium part of the distribution function

$$\mathbf{F}(\epsilon) \cdot \mathbf{v} = -e\tau(\epsilon)\left[\mathbf{E} \cdot \mathbf{v} + e\tau(\epsilon)\mathbf{E} \cdot \left(\mathbf{v} \times \mathbf{H} \cdot \nabla_{\mathbf{k}}\right)\mathbf{v}\right] \tag{4.127}$$

By the use of the current

$$\mathbf{j} = -2e \sum_{bfk} \frac{\partial n_{\mathbf{k}}}{\partial \epsilon_{\mathbf{k}}}\mathbf{v} \cdot \mathbf{F}\left(\epsilon_{\mathbf{k}}\right) \qquad \text{or cy7cis yer cnopu(4.128)}$$

we obtain the drift mobility

$$\mu_t = -\frac{e}{n} \sum_{\mathbf{k}} \frac{\partial n_{\mathbf{k}}}{\partial \epsilon_{\mathbf{k}}}\tau\left(\epsilon_{\mathbf{k}}\right) v_x^2 \tag{4.129}$$

as well as the Hall mobility

$$\mu_H \equiv R_H \sigma_{xx} = e \frac{\sum_{\mathbf{k}} \frac{\partial n_{\mathbf{k}}}{\partial \epsilon_{\mathbf{k}}} \tau^2 (\epsilon_{\mathbf{k}}) \left(v_y^2 m_{xx}^{-1} - v_y v_x m_{yx}^{-1} \right)}{\sum_{\mathbf{k}} \frac{\partial n_{\mathbf{k}}}{\partial \epsilon_{\mathbf{k}}} \tau (\epsilon_{\mathbf{k}}) v_x^2} \tag{4.130}$$

Here $m_{\alpha\beta}^{-1} = \partial^2 \epsilon(\mathbf{k}) / \partial k_\alpha \partial k_\beta$ is the polaron effective mass tensor.
The temperature dependence of the mobilities is determined not only by the temperature dependence of the relaxation time but also by the energy dispersion ϵ_{k} within the polaron band. At intermediate temperatures $w < T < \omega/2$ the finite bandwidth w becomes important. There are several (quasi)elastic scattering mechanisms, which normally restrict the relaxation time. In the strongly coupled electron-phonon sys1 cm the scattering due to the residual polaron-phonon interaction H_{p-ph} is primarily important. As we have discussed in section 4.4 two-phonon scattering due to the interaction with the high frequency phonons responsible for the polaron formadion becomes less effective at low temperatures $T \ll \omega/2$ because there are no such phonons available. On the other hand, impurities and thermal phonons contribute to Ule relaxation rate giving rise to the power temperature dependence of the polaronic mobilities rather than to the exponential one. Here we consider the scattering of twodimensional non-degenerate small polarons by the acoustical phonons (Alexandrov (1092c)). In this example, which is important for the normal state kinetics of high- T_c comper oxides the characteristic acoustic phonon frequency is $\omega_{\mathrm{q}} \leq s\sqrt{2m^*T}$ because Whe phonon momentum in the scattering is of the order of the polaron momentum $0\sqrt{2}m^*T$. The relevant phonon frequency turns out to be small compared with the temperature

$$\frac{\omega_{\mathrm{q}}}{T} \simeq \sqrt{\frac{m^* s^2}{T}} \ll 1 \tag{4.131}$$

Euri lor rather low temperatures of the order of $10K$ if $m^* < 10m_e$. Therefore the instituing is practically elastic with the square of the matrix element independent of line momentum and linear in temperature

$$V_{sc}^2(\mathbf{q}) = \frac{1}{2N} \left| \gamma_{ac}(\mathbf{q}) \omega_{\mathbf{q}} \right|^2 n_{\omega_{\mathbf{q}}} \sim T \tag{4.132}$$

Here $n_{\omega\mathbf{q}} \simeq T/\omega_{\mathbf{q}} \gg 1$ is the distribution function of thermal phonons. By the use of the isotropic spectrum $\epsilon_{\mathbf{k}} = \epsilon_k$ one obtains

$$\frac{1}{\tau_{ac}} \sim Tk \frac{dk}{d\epsilon_k} \tag{4.133}$$

The $2D$ density of states is energy independent, $kdk/d\epsilon_k = m^*$ and so is τ_{ac}. As a result the drift mobility of $2D$ nondegenerate carriers scattered by acoustic phonons is inversely proportional to the temperature and the resistivity is linear in temperature

$$\rho \sim 1/\mu_t \sim T \tag{4.134}$$

if the number of polarons is temperature independent.
Consequently, there is a duality of the kinetic properties of small polarons. At high temperatures they behave as localised particles propagating through the crystal by the thermally activated hopping. On the other hand at low temperatures they are in the Bloch states with well defined momenta propagating by tunneling. This duality can be seen in the temperature dependence of resistivity. In particular, at high temperatures the activation exponential drop of resistivity is expected, while below some characteristic temperature resistivity follows the power law, which is sensitive to the scattering mechanism and the polaron band dispersion. In high T_c oxides and doped fullerenes the high temperature activation region is ill defined because the relevant phonon frequency and the activation energy are of the same order, ca. $500 - 1000K$. On

the other hand, in several nonsuperconducting oxides with the lower phonon frequencies the crossover between the band tunneling and the hopping is observed, Chapter 8.

5.4.12 4.12 Electron Green's function and ARPES of polaronic systems

Theory

The extended-localised duality of small polarons and the band narrowing effect can be seen in the electron spectral function (Alexandrov and Ranninger (1992b)). The intensity of the coherent (i.e. angle-dependent) contribution to the spectral weight is expected to be strongly reduced due to a factor $\exp(-g^2)$ which plays the role of a step ' Z ' of the Fermi distribution function, while the broad featureless incoherent background should appear due to the phonon cloud, which constitutes a small polaron. To see these features we calculate the temperature electron Green's function under the condition of the polaron band narrowing

$$g(\mathbf{k},\omega_n) = -\frac{1}{2}\sum_{\mathbf{m}}\int_{-1/T}^{1/T} d\tau e^{i\omega_n\tau + i\mathbf{k}\cdot\mathbf{m}} \left\langle\left\langle T_\tau c_0(\tau) c^\dagger_{\mathbf{m}}\right\rangle\right\rangle \tag{4.135}$$

For convenience we omit spin. Applying the Lang-Firsov canonical transformation and neglecting the residual polaron-phonon coupling H_{p-ph} one obtains

$$g(\mathbf{k},\omega_n) = \frac{T}{N}\sum_{\omega_{n'},\mathbf{m},\mathbf{k}'} \frac{\sigma(\mathbf{m},\omega_{n'}-\omega_n)\, e^{i(\mathbf{k}-\mathbf{k}')\cdot\mathbf{m}}}{i\omega_{n'}-\xi_{\mathbf{k}'}} \tag{4.136}$$

with the Fourier component $\sigma(\mathbf{m},\omega_n)$ of the correlation function, determined as

$$\sigma(\mathbf{m},\tau) = \exp\left(\frac{1}{2N}\sum_{\mathbf{q}}|\gamma(\mathbf{q})|^2 f_{\mathbf{q}}(\mathbf{m},\tau)\right), \tag{4.137}$$

with

$$f_{\mathbf{q}}(\mathbf{m},\tau) = [\cos(\mathbf{q}\cdot\mathbf{m})\cosh(\omega_{\mathbf{q}}|\tau|) - 1]\coth\frac{\omega_{\mathbf{q}}}{2T} + \cos(\mathbf{q}\cdot\mathbf{m})\sinh(\omega_{\mathbf{q}}|\tau|)$$

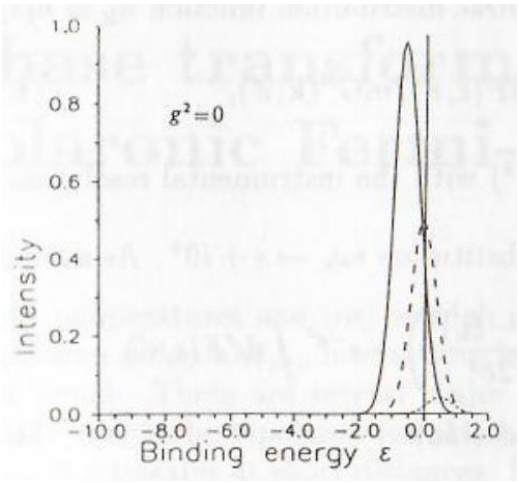

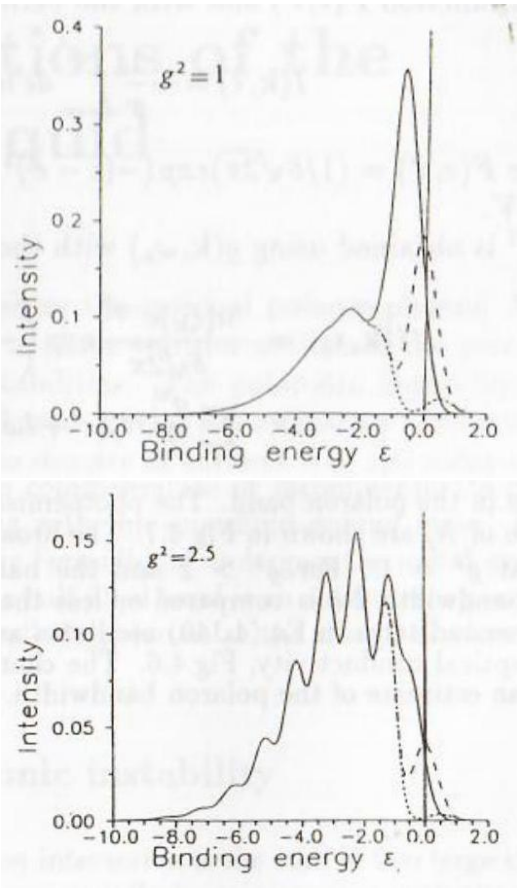

Fig 4.7 Polaron angle-resolved photoemission for three different angles and different coupling; ϵ is measured in units of ω.

Calculating the Fourier component of $\sigma(\mathbf{m},\tau)$ one obtains for the case of dispersiculess phonons ($\omega_{\mathbf{q}}=\omega$) and a constant $|\gamma(\mathbf{q})|^2=2g^2$

$$g\left(\mathbf{k},\omega_n\right)=\frac{e^{-g^2}}{i\omega_n-\xi_{\mathbf{k}}}+\frac{e^{-g^2}}{N}\sum_{l=1}^{\infty}\frac{g^{2l}}{l!}$$
$$\times\sum_{\mathbf{k}'}\left(\frac{n_{\mathbf{k}'}}{i\omega_n-\xi_{\mathbf{k}'}+l\omega}+\frac{1-n_{\mathbf{k}'}}{i\omega_n-\xi_{\mathbf{k}'}-l\omega}\right) \tag{4.138}$$

In the polaron regime the electron Green's function consists of two different contrihutiona. The first coherent term arises from the polaron band motion. The second is independent contribution describes the excitations accompanied by the emission
and absorption of phonons. It is this term which is responsible for the asymmetric background of the optical conductivity, Fig.4.6 and of the photoemission spectra (see below). We notice that the spectral density in the second term spreads over a wide frequency range of order of the polaron level shift $2g^2\omega$ or more. On the contrary the coherent term shows an angular dependence in a frequency range of order of the polaron bandwidth $2w$.

The angle-resolved photoemission spectroscopy (ARPES) measures the imaginary part of the retarded Green's function integrated with a Gaussian instrumental resolution function $F\left(\epsilon,\epsilon'\right)$ and with the Fermi-Dirac distribution function $n_{\mathbf{k}}\equiv n(\epsilon)$

$$I(\mathbf{k},\epsilon)=-\frac{1}{\pi}\int_{-\infty}^{\infty}d\epsilon' n\left(\epsilon'\right)F\left(\epsilon,\epsilon'\right)\operatorname{Im}G^R\left(\mathbf{k},\epsilon'\right) \tag{4.139}$$

where $F\left(\epsilon,\epsilon'\right)=\left(1/\delta\sqrt{2\pi}\right)\exp\left(-\left(\epsilon-\epsilon'\right)^2/2\delta^2\right)$ with the instrumental resolution $\delta\simeq 10$ meV.
G^R is obtained using $g\left(\mathbf{k},\omega_n\right)$ with the substitution $i\omega_n\to\epsilon+i0^+$. As a result

$$I(\mathbf{k},\epsilon)=\frac{n\left(\xi_{\mathbf{k}}\right)e^{-g^2}}{\delta\sqrt{2\pi}}\exp\left(-\frac{\left(\epsilon-\xi_{\mathbf{k}}\right)^2}{2\delta^2}\right)+e^{-g^2}\int d\epsilon' F\left(\epsilon,\epsilon'\right)$$
$$\times\sum_l\frac{g^{2l}}{l!}N_p\left(\epsilon'+l\omega\right)n\left(\epsilon'+l\omega\right) \tag{4.140}$$

with N_p the density of states in the polaron band. The photoemission spectra calculated with the Gaussian form of N_p are shown in Fig 4.7. The broadened asymmetric line shape occurs already at $g^2=1$. For $g^2>2$ and the bare half bandwidth $D=200$meV the polaron bandwidth $2w$ is compared or less than the phonon frequency. In this regime the second term in Eq.(4.140) oscillates as a function of the binding energy just as the optical conductivity, Fig.4.6. The characteristic angular dispersion of ARPES gives an estimate of the polaron bandwidth.

5.5 2 Large and small bipolaron

5.5.1 What Is Going On With Theories of Bipolarons?

(??? Virtor said that they are dead. So I'll write something about them)

5.5.2 2.1 Strong-coupling large bipolaron

Theory

Approaching the many polaron problem we first consider two carriers on a deformable lattice. As in the case of a single polaron we distinguish a strong and intermediatecoupling large bipolaron, formed by two large polarons in an ionic solid and a small bipolaron, formed by two small polarons in any solid if the electron-phonon interaction is sufficiently strong. A possibility of pairing of two large polarons was considered by Pekar (1951). He found that a large bipolaron does not exist for any value of the crystal parameters, ϵ and ϵ_0. Physically, one can reach this conclusion by scaling arguments (Emin (1995)) similar to those applied to a small polaron in the Introduction. The long range interaction with optical phonons is Coulomb like at large distances. Then the total energy, which must be minimised for a large polaron is

$$E_p(r)=\frac{\pi^2}{2mr^2}-\frac{e^2}{2\kappa r} \tag{2.1}$$

The first term in Eq.(2.1) is the minimum kinetic energy of a particle confined in a sphere of radius r, while the second term is the potential plus the deformation energy. Minimising Eq.(2.1) with respect to r one obtains the polaron radius

$$r_p=2\pi^2 a_B$$

and the energy

$$E_p=-\frac{1}{4\pi^2}\alpha^2\omega. \tag{2.3}$$

The numerical coefficient in Eq.(2.3) ($\simeq -0.025$) should be compared with a more realistic variational estimation -0.109 , Eq.(1.42). For a state of two carriers sharing the same orbital state within a common potential well the corresponding functional is

$$E_b(r)=2\frac{\pi^2}{2mr^2}-4\frac{e^2}{2\kappa r}+\frac{e^2}{\epsilon r} \tag{2.4}$$

where the first term is twice the polaron kinetic energy, the second term is four times the corresponding term for a polaron because the polarisation is twice as large as that for a polaron, and the last term describes the Coulomb repulsion between two
carriers. Minimising Eq.(2.4) we obtain for the bipolaron radius

$$r_b = r_p \frac{\epsilon_0 - \epsilon}{\epsilon_0 - 2\epsilon} \tag{2.5}$$

with r_p determined by Eq.(2.2). Thus a large bipolaron can only form if $\epsilon_0 > 2\epsilon$. The ground state energy is

$$E_b = -\frac{1}{2\pi^2}\alpha^2\omega \left(\frac{\epsilon_0 - 2\epsilon}{\epsilon_0 - \epsilon}\right)^2 \tag{2.6}$$

The large bipolaron is energetically stable with respect to dissociation into two separate large polarons if the binding energy is positive:

$$\Delta \equiv 2E_p - E_b > 0 \tag{2.7}$$

This however is not the case because

$$\Delta = 2\left|E_p\right| \left[\left(1 - \frac{\epsilon}{\epsilon_0 - \epsilon}\right)^2 - 1\right] < 0 \tag{2.8}$$

While a large portion of the Coulomb repulsion is neutralised by the Fröhlich interaction, this long-range interaction alone remains insufficient to produce a bound state. Approaching the problem from the weak-coupling limit Takada (1982) reached the same conclusion for the three-dimensional case. He introduced the effective retarded interaction between electrons with the Fourier component $V(\mathbf{q}, \nu)$ determined as

$$V(\mathbf{q}, \nu) = \frac{4\pi e^2}{q^2 \epsilon(\mathbf{q}, \nu)} \tag{2.9}$$

The dielectric function $\epsilon(\mathbf{q}, \nu) = \epsilon_0 \left(\omega^2 - \nu^2\right) / \left(\omega^2 - \epsilon_0 \nu^2/\epsilon\right)$ takes into account the retarded attraction, mediated by polar-optic phonons in a wide frequency region $\omega\epsilon/\epsilon_0 < \nu < \omega$. By the use of the two-particle vertex part one can derive the BetheSalpeter equation for the wave function $\phi_{\mathbf{p}}$, describing the relative motion of two electrons in the momentum representation

$$\left(\frac{p^2}{m} + \Delta\right)\phi_{\mathbf{p}} + \sum_{\mathbf{p}'} \frac{4\pi e^2}{\left|\mathbf{p} - \mathbf{p}'\right|^2 \epsilon} \frac{\left(p^2 + p'^2 + 2m\Delta + 2m\omega\epsilon/\epsilon_0\right)}{\left(p^2 + p'^2 + 2m\Delta + 2m\omega\right)} \phi_{\mathbf{p}'} = 0 \tag{2.10}$$

There are no solutions to this equation with a positive binding energy Δ in three dimensions. As is known from an elementary problem in quantum mechanics, a bound state can be formed more easily when the dimensionality is decreased. Since the state of the large bipolaron can be considered as the linear combination of longwave plane waves, the density of one-particle states near the bottom of the conduction band enters the problem. It should be large in order to bind two electrons. In a $3D$ system, however, the density of states vanishes at the bottom of the band and thus the bound state cannot be formed. Compared with a $3D$ system, a $2D$ system has a better chance to provide the bound state, because in a $2D$ system, the density of states is finite at the bottom of the band. In a $1D$ system, one can expect an even larger binding energy, because the density of states at the bottom of the band is infinite in this case. Takada found that in $1D$ and $2D$ system there is indeed a
bound solution of the Bethe-Salpeter equation with rather low binding energy. One can prove the absence of a bound state in three dimensions for any direct retarded interaction between electrons with the Fourier component of the form of Eq.(2.9) if the static dielectric function $\epsilon(\mathbf{q}, 0)$

is positive for all $\mathbf{q}$ (Khomskii (1995)). In the general case, however, the static electron-electron interaction can be attractive, which formally corresponds to the negative sign of $\epsilon(\mathbf{q},0)$ for finite q. This happens in some simple metals and, in particular, in complex compounds because short-wave acoustic and local vibration modes contribute to the electron-electron interaction. There are arguments, that a negative short-wave static dielectric function does not necessarily lead to a global instability (Dolgov et al (1981)). Moreover in a strongly polarisible lattice with $\epsilon_0/\epsilon \gg 1$ the bipolaron radius, Eq.(2.5) is close to the polaron one. The absolute value of the binding energy $|\Delta|$ in units of twice the polaron binding energy calculated by scaling is very small

$$\frac{|\Delta|}{2\,|E_p|} \simeq 2\frac{\epsilon}{\epsilon_0} \ll 1 \tag{2.11}$$

Therefore one can expect that two polaron wave functions strongly overlap and the quantum exchange interaction can stabilise Pekar's bipolaron even without any other attraction except the Fröhlich one. This was first realised by Vinetskii and Giterman (1958). The functional, which must be minimised is now

$$\begin{aligned} J_b\left(\Psi\left(\mathbf{r}_1,\mathbf{r}_2\right)\right) = \int d\mathbf{r}_1 \int d\mathbf{r}_2 \left[\frac{\left|\nabla_1\Psi\left(\mathbf{r}_1,\mathbf{r}_2\right)\right|^2}{2m} + \frac{\left|\nabla_2\Psi\left(\mathbf{r}_1,\mathbf{r}_2\right)\right|^2}{2m} + \frac{\left|\Psi\left(\mathbf{r}_1,\mathbf{r}_2\right)\right|^2}{\epsilon\left|\mathbf{r}_1-\mathbf{r}_2\right|}\right] \\ - \frac{4}{2ma_B}\iint d\mathbf{r}_1 d\mathbf{r}_1' \iint d\mathbf{r}_2 d\mathbf{r}_2' \frac{\left|\Psi\left(\mathbf{r}_1,\mathbf{r}_2\right)\right|^2\left|\Psi\left(\mathbf{r}_1',\mathbf{r}_2'\right)\right|^2}{\left|\mathbf{r}_1-\mathbf{r}_1'\right|} \end{aligned} \tag{2.12}$$

The minimum of Eq.(2.12) should be compared with twice of the minimum of a polaron functional $J(\psi(\mathbf{r}))$, Eq.(1.9). Then the bipolaron binding energy is

$$\Delta = 2\min(J) - \min\left(J_b\right) \tag{2.13}$$

Vinetskii and Giterman selected the variational singlet function in a symmetric form similar to that of the hydrogen molecule

$$\psi\left(\mathbf{r}_1,\mathbf{r}_2\right) = A\left[\psi\left(\mathbf{r}_1-\mathbf{a}/2\right)\psi\left(\mathbf{r}_2+\mathbf{a}/2\right) + \psi\left(\mathbf{r}_2-\mathbf{a}/2\right)\psi\left(\mathbf{r}_1+\mathbf{a}/2\right)\right] \tag{2.14}$$

where A is the normalisation factor and $\psi(\mathbf{r})$ is a single polaron function. Correlations between polarons are taken into account by assuming a nonzero distance $|\mathbf{a}|$ between them. For a small distance the polarisation attraction force depends differently on the distance compared with the Coulomb repulsion. Therefore the separation of two polaron clouds can stabilise a bipolaron. The simplest form of $\psi(\mathbf{r})$ as for Pekar's polaron, section 1.1

$$\psi(\mathbf{r}) = \frac{1}{\sqrt{\pi r_p^3}} e^{-r/r_p} \tag{2.15}$$

yields a positive binding energy if

$$\frac{\epsilon}{\epsilon_0} \leq 0.05 \tag{2.16}$$

The maximum binding energy at $\epsilon/\epsilon_0 \to 0$ is small:

$$\frac{\Delta}{2\,|E_p|} = 0.08 \tag{2.17}$$

and the distance between two polarons is about 1.5 of the polaron radius r_p. Vinetskii and Pashitskii (1983) extended this approach to a crystal having two-dimensional or one-dimensional

anisotropy of the carrier mass, either for easy movement in a plane $m_{\|} < m_{\perp}$ or for easy movement along an axis $m_{\|} > m_{\perp}$. Here $m_{\|}$is the in-plane and $m_{\perp}$ is the out-of-plane mass. A variational polaron wave function was taken in the Gaussian form

$$\psi(\mathbf{r}) = \beta^{1/2}\beta' \left(\frac{2}{\pi}\right)^{3/4} e^{-\beta^2 z^2 - \beta'^2 \rho^2} \tag{2.18}$$

where β, β' are variational parameters, z is the coordinate perpendicular to the plane and $\rho^2 = x^2 + y^2$. The effective mass anisotropy widens the range of existence of Pekar's bipolaron and increases its binding energy as shown in Fig.2.1 for the easy movement along the axis.

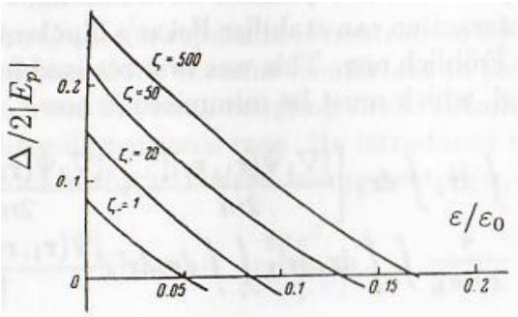

Fig.2.1. Dependence of the bipolaron binding energy on ϵ / ϵ_{0} for different values of the anisotropy

ξ, related to $m_{\|}/m_{\perp}$ by $2\xi^3 \left[\xi \ln\left(\sqrt{\xi^2-1}+\xi\right) - \sqrt{\xi^2-1}\right] / \left[\xi\sqrt{\xi^2-1} - \ln\left(\sqrt{\xi^2-1}+\xi\right)\right] = m_{\|}/m_{\perp}$.

It is seen from Fig.2.1 that when $m_{\|}/m_{\perp} \gg 1 (\xi \gg 1)$ a one - dimensional bipolaron can exist for a considerably larger ratio ϵ/ϵ_0 compared with the $3D$ case.

The variational approach to Pekar's bipolaron was improved by Mukhomorov (1982) and by Suprun and Moizhes (1982). Mukhomorov represented the two-particle wave function of the singlet state as a series of different polaron configurations including $|1s^2\rangle, |1s2p\rangle$ and $|2p^2\rangle$

$$\Psi(\mathbf{r}_1, \mathbf{r}_2) = A\left[\left|1s^2\right\rangle + C_1|1s2p\rangle + C_2\left|2p^2\right\rangle\right] \tag{2.19}$$

where different terms are symmetrised products of s-wave $\psi_s \sim (1+\beta r)\exp(-\beta r)$ and p-wave $\psi_p \sim rY_{10}(\Theta)\exp(-\beta' r)$ one-particle functions centered at the same site rather than at two different sites. This refinement of the variational wave function with four variational parameters $C_{1,2}, \beta$ and β' increases the binding energy up to $\Delta/2\,|E_p| = 0.195$ and the range of existence of the bipolaron up to $\epsilon/\epsilon_0 \leq 0.1$. Suprun and Moizhes found a simpler trial function with only two variational parameters β, β'

$$\Psi(\mathbf{r}_1, \mathbf{r}_2) \sim \psi_s(\mathbf{r}_1)\,\psi_s(\mathbf{r}_2)\,(1+\beta'|\mathbf{r}_1 - \mathbf{r}_2|), \tag{2.20}$$

which gives a lower binding energy and a wider region $\epsilon/\epsilon_0 \leq 0.14$ than those determined with Eq.(2.19). It can thus be expected that, if the electron correlations are taken into account, a large bipolaron can exist with rather low binding energy.

5.5.3 2.2 Intermediate-coupling large bipolaron

Theory

As in the case of the large polaron the continuum approximation for the lattice polarisation is unacceptable for low and intermediate values of the electron-phonon coupling constant α.

There is another problem with the variational estimation of the bipolaron binding energy in section 2.1 where the single-polaron energy E_p is estimated with the same shape of the polaron trial function as for the bipolaron one. Adamowskii (1989) noticed that the values of $2\,|E_p|$ obtained by the Pekar strongcoupling method were much too low compared with the best estimates based on the path-integral approach. After recalculating the variational results for Δ of section 2.1 with the use of the best estimate of a single polaron ground state energy $|E_p|$ one obtains no binding of two polarons, with an exception of very large α. Consequently, there is no reliable conclusion concerning the existence of a large bipolaron within the strong-coupling variational analysis. A more reliable conclusion can be reached by applying the LLP and displacement canonical transformations as in the case of a single intermediate-coupling polaron, section 1.4 (Bassani et al (1991)).

Here two electrons in interaction with a phonon field are described by the following Hamiltonian

$$H = \sum_{j=1.2}\left[-\frac{\nabla_j^2}{2m} + \sum_{\mathbf{q}}\left(V_{\mathbf{q}} d_{\mathbf{q}} e^{i\mathbf{q}\cdot\mathbf{r}_j} + h.c.\right)\right] + \frac{e^2}{\epsilon\,|\mathbf{r}_1 - \mathbf{r}_2|} + \sum_{\mathbf{q}} \omega_{\mathbf{q}}\left(d_{\mathbf{q}}^{\dagger} d_{\mathbf{q}} + 1/2\right) \tag{2.21}$$

Since the Hamiltonian commutes with the total linear momentum one can eliminate the center-of-mass coordinate and classify the relative motion of two polarons with the angular momentum L. Both linear and angular momenta include the phonon contribution. Their conservation constrains a possible shape of the trial functions. Introducing the relative coordinate $\mathbf{r} = \mathbf{r}_1 - \mathbf{r}_2$ and the position of the center of mass $\mathrm{R} = (\mathrm{r}_1 + \mathrm{r}_2)/2$ one can write the Hamiltonian in the form

$$II = -\frac{\nabla_{\mathbf{R}}^2}{4m} - \frac{\nabla_{\mathbf{r}}^2}{m} + 2\sum_{\mathbf{q}}\left[V_{\mathbf{q}} d_{\mathbf{q}} \cos(\mathbf{q}\cdot\mathbf{r}/2) e^{i\mathbf{q}\cdot\mathbf{R}} + h.c.\right] + \frac{e^2}{\epsilon r} + \sum_{\mathbf{q}} \omega_{\mathbf{q}}\left(d_{\mathbf{q}}^{\dagger} d_{\mathbf{q}} + 1/2\right) \tag{2.22}$$

The unitary LLP transformation $\exp S_{LLP}$ with

$$S_{LLP} = i\sum_{\mathbf{q}} (\mathbf{q}\cdot\mathbf{R}) d_{\mathbf{q}}^{\dagger} d_{\mathbf{q}} \tag{2.23}$$

diminates the center of mass coordinate from the Hamiltonian. To classify the eigenstates by the total angular momentum one can introduce new phonon operators

$$d_{q,l,m} = \frac{q}{(2\pi)^{3/2}} \int d\Omega_{\mathbf{q}} Y_{l,m}^{*}\left(\Omega_{\mathbf{q}}\right) d_{\mathbf{q}} \tag{2.24}$$

where $d\Omega_q$ is the element of solid angle $\Omega_{\mathbf{q}}$ of $\mathbf{q}$ and $Y_{l,m}$ is a spherical harmonic. The variational trial state $|L, M\rangle$, which is an eigenstates of L and $M \equiv L_z$, is constructed by the use of the displacement operator $\exp S(\mathbf{r})$ as

$$|L, M\rangle = R_L(r) Y_{L,M}\left(\Omega_{\mathbf{r}}\right) \exp S(\mathbf{r}) \tag{2.25}$$

Here

$$S(\mathbf{r}) = \sum_{l.m} \int_0^{\infty} dq\left[g_{q,l}(r) Y_{l.m}\left(\Omega_{\mathbf{r}}\right) d_{q,l,m} - h.c.\right] \tag{2.26}$$

and

$$R_L(r) = A r^{\beta} e^{-r/r_b} \tag{2.27}$$

The energy $\langle L, M|e^{S_{LLP}} H e^{-S_{LLP}}|L, M\rangle$ is minimised with respect to the variational parameters r_b, β and the variational function $g_{q,l}(r)$. The latter can be expressed analytically through the confluent hypergeometric functions. The total energy is calculated numerically and compared with twice the intermediate coupling polaron the two-dimensional case with the three-dimensional interaction $V_{\mathbf{q}} \sim 1/\sqrt{q}$ as well.

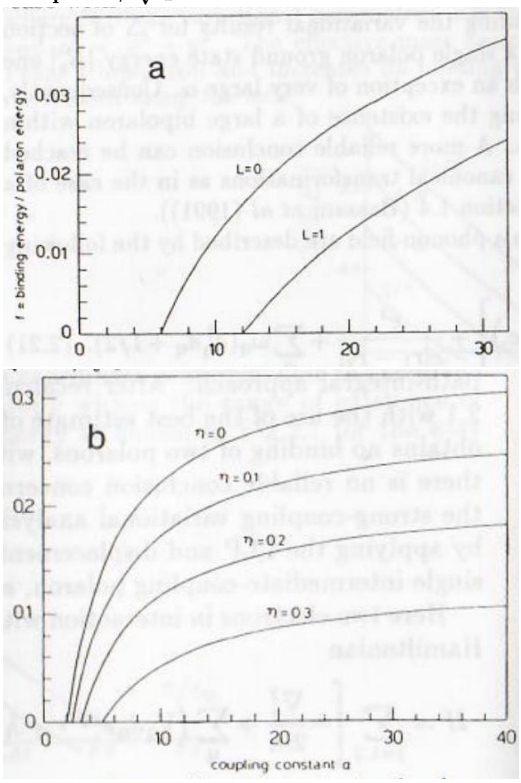

Fig.2.2 Dependence of the bipolaron binding energy on the coupling constant α in the threedimensional case for $\epsilon/\epsilon_0 = 0$ and $L = 0, 1(a)$ and in the two-dimensional case for different values of $\eta \equiv \epsilon/\epsilon_0(b)$.

Compared with the Pekar's variational approach there are several new features of the bipolaron formation in the intermediate coupling regime.

1. The large bipolaron exists ($\Delta > 0$) only if the electron-phonon coupling constant α is greater than a critical value α_c, which is ~ 6 in three dimensions and ~ 2 in two dimensions. The change in dimensionality increases the normalised binding energy by at least one order of magnitude as shown in Fig.2.2 a,b;

2. The largest value of ϵ/ϵ_0 for which $\Delta > 0$ depends on the coupling constant α being of the order of 0.05 in three dimensions and 0.4 in two dimensions.

3. The bipolaron radius is always of the order of a few polaron radii, i.e., in practical cases, of a few Å.

The latter means that a small bipolaron approach taking into account a finite bandwidth is more appropriate even in the case of the Fröhlich interaction.

5.5.4 2.3 Path integral approach to large bipolaron

Theory

A drawback of the variational formulation based on the canonical transformation is that it does not permit us to study well the bipolaron stability since the estimations of the single

polaron energy are poor compared to the path integral calculations. The variational method in the form of the path integral applied to the Fröhlich polaron by Feynman (1955) is known to give a very good variational estimates of the polaron ground state in the intermediate coupling regime. A large bipolaron problem was treated with path integrals by Kochetov et al (1977) in the $3D$ strong coupling limit, by Hiramoto and Toyozawa (1985) in three dimensions for optical and acoustic phonons and by Verbist et al (1991) for the whole coupling range in both two and three dimensions.

The path integral method allows for an exact elimination of the phonon coordinates. All thermodynamic quantities are known if one can calculate the partition function $Z = \mathrm{Tr}\left[e^{-\beta H}\right]$, where $\beta = 1/T$ is the inverse temperature in energy units ($k_B = 1$). The Hamiltonian at hand, Eq.(2.21) is the quadratic form with respect to the displacement (phonon) coordinates. Consequently, phonons can be eliminated exactly

$$Z = Z_b \prod_{\mathbf{q}} \left[2 \sinh\left(\frac{\beta\omega_{\mathbf{q}}}{2}\right)\right]^{-1} \tag{2.28}$$

where the bipolaron partition sum Z_b is a path integral in only the electron coordinates

$$Z_b = \prod_{j=1.2} \int d\mathbf{x}_j \iint_{\mathbf{r}_j(0)=\mathbf{x}_j}^{\mathbf{r}_j(\beta)=\mathbf{x}_j} D\mathbf{r}_j(t) e^{S[\mathbf{r}_1(t),\mathbf{r}_2(t)]} \tag{2.29}$$

The bipolaron action $S\left[\mathbf{r}_1(t), \mathbf{r}_2(t)\right]$ includes the kinetic energies, the retarded self and inter-electron attractive interaction, mediated by phonons, and the Coulomb repulsion

$$\begin{aligned} S\left[\mathbf{r}_1(\tau), \mathbf{r}_2(\tau)\right] = &- \int_0^\beta d\tau \left(\frac{m}{2}\dot{\mathbf{r}}_1^2(\tau) + \frac{m}{2}\dot{\mathbf{r}}_2^2(\tau) + \frac{U}{|\mathbf{r}_1(\tau) - \mathbf{r}_2(\tau)|}\right) \\ &+ \sum_{j,l=1,2;\mathbf{q}} \omega_{\mathbf{q}}^{-1} |V_{\mathbf{q}}|^2 \int_0^\beta d\tau \int_0^\beta ds d\left(\omega_{\mathbf{q}}, \tau - s\right) e^{i\mathbf{q}\cdot[\mathbf{r}_j(\tau) - \mathbf{r}_l(s)]}, \end{aligned} \tag{2.30}$$

where $U = e^2/\epsilon$ is a measure for the repulsion strength, and

$$d(\omega, \tau) = \frac{\omega \cosh\left(\frac{\beta\omega}{2} - \omega|\tau|\right)}{2 \sinh\left(\frac{\beta\omega}{2}\right)} \tag{2.31}$$

is the phonon Green's function, which Fourier component is defined in Chapter 3. The resulting path integral Z_b cannot be evaluated. However, the upper bound to the free energy $F_b = -T \ln Z_b$ can be estimated by the use of any trial quadratic action δ_0

$$F_b \leq F_0 - \frac{1}{\beta} \langle S - S_0 \rangle, \tag{2.32}$$

where $F_0 = -T \ln Z_0$ is the free energy corresponding to the trial action S_0, and brackets denote an average with weight $\exp S_0$ defined as

$$\langle \ldots \rangle = Z_0^{-1} \prod_{j=1.2} \int d\mathbf{x}_j \iint_{\mathbf{r}_j(0)=\mathbf{x}_j}^{\mathbf{r}_j(\beta)=\mathbf{x}_j} D\mathbf{r}_j(t) (\ldots) e^{S_0[\mathbf{r}_1(t),\mathbf{r}_2(t)]} \tag{2.33}$$

While Hiramoto and Toyozawa used the quadratic action S_0 with four variational parameters, Verbist et al allowed two polarons to fluctuate around a mean distance
a from each other. The Coulomb repulsion was approximated by a quadratic one with strength K. In analogy with the Feynman trial action for a single polaron, each electron interacts quadratically with a fictitious particle of mass M and oscillator strength k. Furthermore, a

quadratic interaction, with an oscillator strength k', between each electron and the oscillator of the other electron is also allowed. The Hamiltonian H_0 describing the model is

$$\begin{aligned} H_0 = & \sum_{j=1,2}\left[-\frac{\nabla_j^2}{2m}-\frac{\nabla_{\mathbf{R}_j}^2}{2M}+\frac{k}{2}\left(\mathbf{r}_j-\mathbf{R}_j\right)^2\right] \\ & +\frac{k'}{2}\left[\left(\mathbf{r}_1-\mathbf{R}_2-\mathbf{a}\right)^2+\left(\mathbf{r}_2-\mathbf{R}_1+\mathbf{a}\right)^2\right] \\ & -\frac{K}{2}\left(\mathbf{r}_1-\mathbf{r}_2-\mathbf{a}\right)^2 \end{aligned} \tag{2.34}$$

In analogy with the elimination of the phonon variables, the oscillator coordinates $\mathbf{R}_j$ can be eliminated to construct the trial action

$$\begin{aligned} S_0\left[\mathbf{r}_1(t),\mathbf{r}_2(t)\right] = & -\sum_{j=1,2}\int_0^\beta d\tau\frac{m}{2}\dot{\mathbf{r}}_j^2(\tau) \\ & -\frac{\left(k^2+k'^2\right)}{4M\nu^2}\sum_{j=1,2}\int_0^\beta d\tau\int_0^\beta dsd(\nu,\tau-s)\left[\mathbf{r}_j(\tau)-\mathbf{r}_j(s)\right]^2 \\ & -\int_0^\beta d\tau\int_0^\beta ds\left[\mathbf{r}_1(\tau)-\mathbf{r}_2(s)-\mathbf{a}\right]^2 \\ & \times\left[\frac{K}{2}\delta(\tau-s)-\frac{kk'd(\nu,\tau-s)}{M\nu^2}\right] \end{aligned} \tag{2.35}$$

where $\nu=\sqrt{\left(k+k'\right)/M}$ is the frequency of the free oscillator. The electrons now exhibit a quadratic self-interaction, the second term in Eq.(2.35).

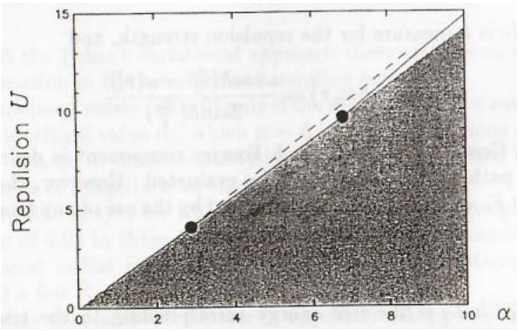

Fig.2.3. The stability region for large bipolaron formation in $3D$ and $2D$ (Verbist et al (1991)). Large bipolaron is formed below the curves, but above the shaded area.

They are bound together at an average distance $|\mathbf{a}|$ if the retarded attraction (the last term) is larger than the direct instanteneous repulsion, which is governed by the constant K. Minimising the right hand side of Eq.(2.34) with respect to the parameters M,k,k',K and $|\mathbf{a}|$ Verbist et al obtained a lower bipolaron energy
than with the canonical transformation method. The critical value of the coupling constant was found to be $\alpha_c\simeq 6.8$ in three dimensions. The path integral method gives not only a consistent description of a single polaron and bipolaron within the same physical picture, but also allows for a scaling relation for the free energy between different dimensions in the case when $\mathbf{a}=0$

$$F_{2D}(\alpha,U,\beta)=\frac{2}{3}F_{3D}\left(\frac{3\pi}{4}\alpha,\frac{3\pi}{4}U,\beta\right). \tag{2.36}$$

This means that the free energy in two dimensions can be calculated from the free energy in three dimensions by scaling the coupling constant α as well as the repulsion strength U with a factor $3\pi/4$. As a result the critical value of α in two dimensions is about 2.9. The space $(\alpha, \epsilon/\epsilon_0)$ in which large bipolaron exists in two (dashed curve) and three (solid curve) dimensions is presented in Fig. 2.3, where the nonphysical part is shaded. Our general conclusion is that the Fröhlich interaction can lead to a bound state if the coupling constant is sufficiently large and the ratio ϵ/ϵ_0 is sufficiently small. This is rather surprising because the Fröhlich interaction never overscreens the Coulomb repulsion. Nevertheless, a bound state can be formed due to the quantum exchange.

One can expect that the interaction with acoustic phonons and local vibrations acts to help the bipolaron formation against the direct Coulomb repulsion. In fact it plays a dominant role giving rise to the total direct attraction of two electrons.

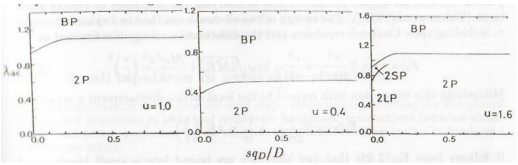

Fig.2.4 The critical acoustic phonon coupling constant for the small bipolaron formation as a function of the adiabatic ratio for three different values of the normalised Coulomb repulsion u.

As in the case of a single polaron, the deformation potential leads to the formation of small bipolarons rather than large bipolarons. By use of the path integral method and the effective mass (continuum) approximation for electrons Hiramoto and Toyozawa (1985) estimated the strength of the deformation potential, which binds two polarons. The continuum approach is sufficient for qualitative estimations if the Debye wave number $q_D \sim \pi/a$ is introduced as an upper limit cut-off in all sums in momentum space. The matrix element of the deformation potential depends on the momentum as $V_{\mathbf{q}} = E_d\sqrt{q/2NMs}$. The acoustic phonon frequency is $\omega_{\mathbf{q}} = sq$, where E_d the deformation potential, M the mass of a unit cell and s is the sound velocity. Applying the trial quadratic action similar to that with optical phonons Hiramoto and Toyozawa found the critical value of the acoustic phonon coupling

$$\lambda = \frac{E_p}{D}, \tag{2.37}$$

sufficient to form the small bipolaron. Here $E_p = E_d^2/2Ms^2$ is the polaron level shift calculated with Eq.(1.98) and $D = q_D^2/2m$ plays a role of the half bandwidth. When the characteristic Coulomb repulsion is small compared with the half bandwidth, $u \equiv 2e^2 q_D/\pi\epsilon D \ll 1$ the transition between two free electrons and a small bipolaron occurs at $\lambda \simeq 0.537$ that is a half of the critical value of λ_c at which the transition from large to small polaron takes place, $\lambda_c \simeq 1.075$ in the extreme adiabatic limit, $sq_D \ll D$. The effect of the adiabatic ratio sq_D/D on the critical value of λ was found to be small, Fig.2.4. The bipolaron mass was estimated to be enormous compared to the band mass in the extreme adiabatic limit while it is of the order of the band mass for $sq_D/D > 1$ as long as $\lambda = O(1)$. The deformation potential was found to be more effective for the bipolaron formation compared with the Fröhlich interaction. The mean distance between the two electrons in a bipolaron is usually about the lattice constant a. Consequently, the continuum approach does not work well in this type of problems. One would have to use a lattice small bipolaron model taking into account the finite bandwidth (Chapter 6).

5.5.5 2.4 Small bipolaron

Theory

Scaling arguments similar to those applied to the small polaron in the Introduction provide us with an elegant simple method of studying the formation of a small bipolaron (Cohen et al (1984)). The energy of two electrons confined in a sphere of radius r, including their Coulomb repulsion and the deformation energy is estimated as

$$E_b(u,r) = 2\frac{\pi^2}{2mr^2} + \frac{e^2}{\epsilon r} - 2x\omega\sqrt{2ME_p} + \frac{M\omega^2x^2}{2}\left(\frac{r}{a}\right)^3 \tag{2.38}$$

Minimising this expression with respect to the local lattice displacement x we obtain

$$E_b(r) = 2\frac{\pi^2}{2mr^2} + \frac{e^2}{\epsilon r} - 4E_p\left(\frac{a}{r}\right)^3 \tag{2.39}$$

It follows from Eq.(2.39) that two electrons are bound into a small bipolaron of radius $r = a\,(E_b(a) < 0)$ if the interaction with local and (or) acoustic vibrations is sufficiently strong

$$\lambda \geq 0.5 + u/8 \tag{2.40}$$

where $\lambda = 2ma^2E_p/\pi^2$ and u is the relative strength of the Coulomb repulsion, introduced in section 2.3. For sufficiently weak Coulomb interaction, the small bipolaron forms at twice lower coupling constant $\lambda \simeq 0.5$ than the small polaron, for which the critical value of λ estimated by scaling is about unity. This estimate is in perfect agreement with the path integral variational calculations, Fig.2.4. In ionic solids with a high value of the static dielectric constant $\epsilon_0 \gg 1$ polar optic phonons screen the Coulomb repulsion, rather than binds two electrons. Consequently, even the intermediate coupling, $\lambda > 0.5$ with acoustic phonons or (and) local vibrations is sufficient to form the small bipolaron in ionic solids, because u is replaced for $u\epsilon/\epsilon_0 \ll 1$.

Screening in solids and coupling with phonons are ill defined at large wave numbers of the order of the reciprocical lattice constant. Therefore, one has to postulate the existence of small bipolarons to explain some exotic properties of particular compounds rather than derive them from the first principles. Along this line Anderson
(1975) and Street and Mott (1975) introduced the concept of a small on-site localised bipolaron in glassy semiconductors (chalcogenide glasses) to explain their magnetic and electric properties. Though the ESR measurements did not reveal any considerable amount of localised states, other experiments showed their density about 10^{18} per cm^3. To explain these contradicting observations Street and Mott and Anderson proposed that the local lattice distortion is sufficiently strong for the reaction

$$2D^0 \rightarrow D^+ + D^- \tag{2.41}$$

to be exothermic. As a result in the ground state of chalcogenide glasses all donors are positively or negatively charged and D^0 are produced only by thermal excitation. The state D^-can be seen as a small bipolaron localised by the random potential.

Taking perturbatively into account the small polaron tunneling Alexandrov and Ranninger (1981a,b) introduced small bipolarons into the theory of superconductivity. This allowed for the prediction of the high T_c value about $100K$ (Alexandrov (1983), Alexandrov and Kabanov (1986)) and for the explanation of a number of kinetic and thermodynamic properties of high T_c superconducting oxides (Alexandov and Mott(1994), Chapter 8). The advantage of the perturbative approach is that in zero order the ground state can be studied without taking into account the electron kinetic energy, which is small perturbation due to the polaron band

narrowing (section 1.6 and Chapter 4). Consequently, one can obtain the binding energy and the size as well as geometry of the small bipolaron from the first principles by the use of the static lattice minimisation techniques (Catlow(1989)).

5.5.6 2.5 Small bipolaron in perovskite structures

Theory

Lattice minimisation techniques are used very extensively in modeling the energies of defects and impurities in ionic and semi-ionic insulators. Interactions between atoms in the lattice are presented by an effective potential including both Coulomb and short-range terms.

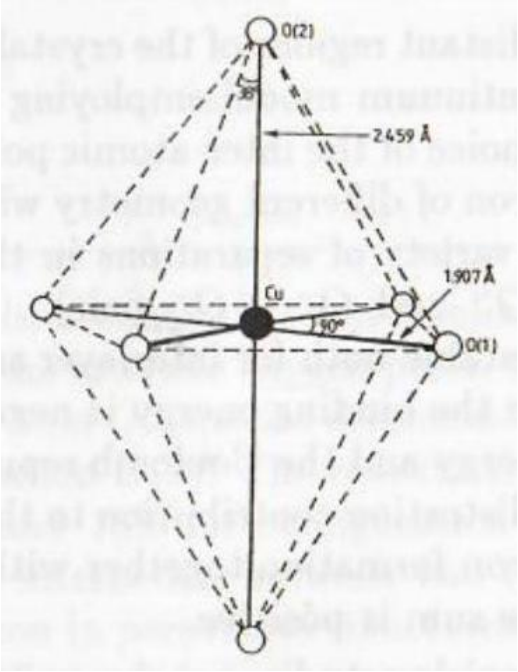

Fig. 2.5. CuO_{6} unit in La_2CuO_4.

This yields an equilibrium structure and phonon dispersion curves which are close to those observed experimentally. In their modeling of small bipolarons in doped Ca_3CuO_4 Zhang and Catlow (1991) treated holes as Cu^{3+} or O^{-}species placed in
the dielectric matrix with the CuO_6 unit, Fig.2.5. The energy of a region of the crystal surrounding the hole or the hole pair is then minimised with respect to the coordinates of the ions within the region containing ca. 200-300 ions.

Table 1$Cu^{3-} - Cu^{3+}$ pairs: configurations and energies				
configuration	number	separation of pair d/A	binding energy $-E_b$, eV	Coulomb
intralayer				
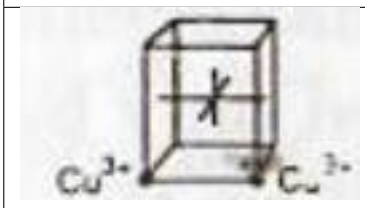	Cu(1)	3.81	0.414	0.135
Cu^{2-}	Cu(2)	5.41	0.254	0.095
c. $^{2+}$	Cu(4)	8.54	0.092	0.060
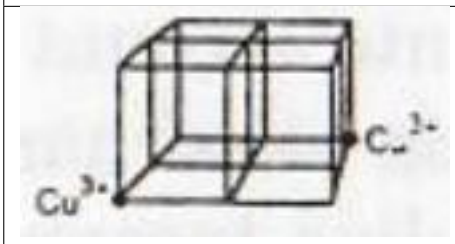	Cu(5)	10.81	0.120	0.048
interlayer				
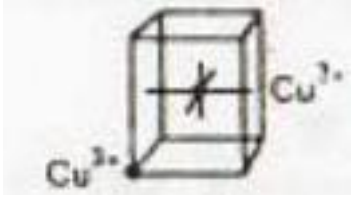	Cu(6)	7.10	0.046	0.073
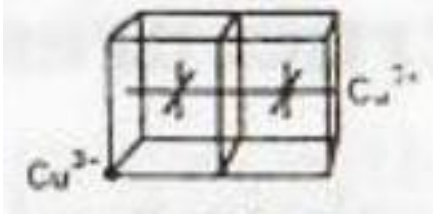	Cu(7)	10.74	0.036	0.058

The response of the more distant regions of the crystal is calculated using approximate procedures based on a continuum model employing the relative permittivity of the material. With a proper choice of the inter-atomic potentials one can find the binding energy of the small bipolaron of different geometry with accuracy within 0.01 eV. The pairing was studied for a variety of separations in three types of possible bipolaron ($Cu^{3+} - Cu^{3+}, Cu^{3+} - O^{-}$and $O^{-} -$ O^{-}pair). Intercopper and copper-oxygen intersite bipolarons are unstable both for interlayer and intralayer pairing, as one can see from Tables 1-3, where the binding energy is negative for all separations studied. The sum of the binding energy and the Coulomb repulsive energy in the Tables yields an estimate of the lattice distortion contribution to the pairing. If the sum is negative the lattice opposes bipolaron formation together with the Coulomb repulsion, and it favors bipolarons when the sum is positive.

The results of $O^{-} - O^{-}$pairing studies are shown in Table 4. Three stable bipolaron configurations were found. For configuration $O(1)$, the bipolaron is bound by *ca.* 0.06 eV , whereas bipolaron configuration $O(2)$ is bound by *ca.*0.12eV. These two bound oxygen pairs are situated at the nearest-neighbor sites ($d = 2.66$Å) and next-nearest-neighbor sites ($d = 3.11$Å). There is also a lightly bound bipolaron $O(4)$
with a binding energy of 0.001 eV at $d = 3.58$Å. When d is larger than 3.81Å all the configurations are energetically unfavorable.

In order to distinguish pairing from the phase separation of holes one can calculate in addition to the binding energy of two holes Δ, the binding energy of four holes Δ_4 with respect to hole pairs. If Δ_4 is positive then phase separation would be expected. In the nearest-neighbor

site pair and next-nearest-neighbor site pair Zhang and Catlow found, however, a positive Δ and a negative Δ_4, which promote bipolaronic superconductivity (Chapter 6) without phase separation.

Table $2Cu^{3+} - O^{-}$pairs (intralayer): configurations and energies

configuration	number	separation of pair d/A	binding energy $-E_b$/eV	Co
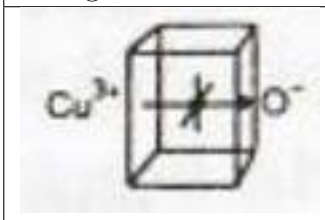	OCu(1)	1.91	1.010	0.2
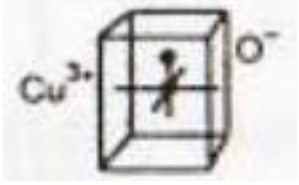	OCu(2)	2.46	0.228	0.2
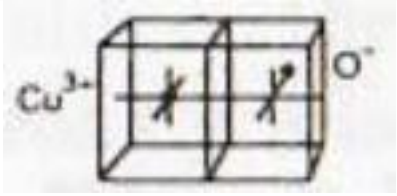	OCu(3)	4.31	0.237	0.1
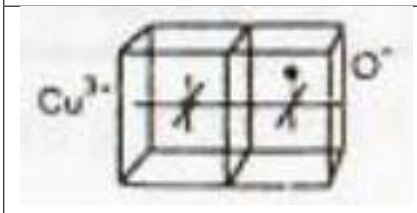	OCu(4)	4.64	0.129	0.1
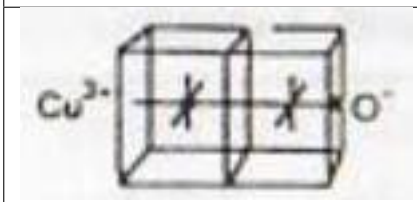	OCu(S)	5.72	0.114	0.0
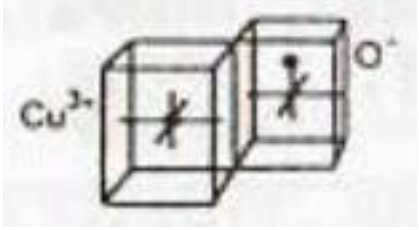	OCu(6)	5.79	0.053	0.0
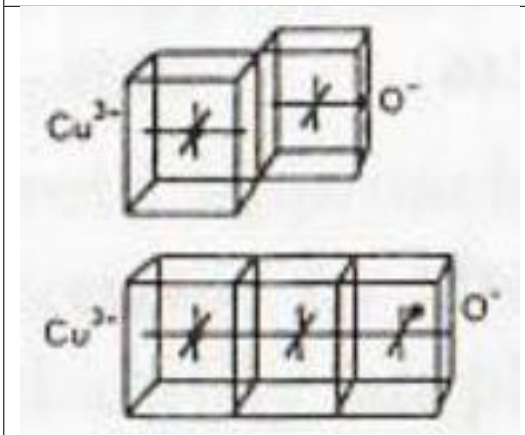	OCu(7)	6.89	0.145	0.0
	OCu(8)	7.87	0.078	0.0
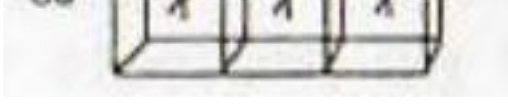	OCu(9)	7.89	0.137	0.0

Compared to the Coulomb repulsive energy the non-Coulombic lattice contribution is larger being ca. $0.2 - 0.3$eV for the intersite oxygen pairs. It was found that after latLice relaxation, the distance between O^-species decreases by 0.674Å in configuration $O(1)$ and by 0.564Å in configuration $O(2)$. The relative change of the pair distances in 25% for configuration $O(1)$ and 18% for configuration $O(2)$. This enhanced attraction is due to the covalent interaction between two O^-species. An important feature of the bipolaron formation in perovskite structures is that the bound state of the in-plane oxygen hole with the apex hole is more favorable. The binding energy of small bipolaron is strongly related not only to the distance of the pair but also to the detailed geometry of the site where the polaron is situated. Therefore, it is necessary to study the pairing mechanism of doped La_2CuO_4 using three-dimensional rather than two-dimensional models. The lattice contribution to the binding energy
is estimated to be larger than the characteristic antiferromagnetic exchange energy of the order of 0.1 eV. However, the latter is of the order of the binding energy Δ of the bipolaron and favors pairing further (Mott(1990)).

Table $3Cu^{3*} - O^+$pairs (interlayer): configurations and energies				
configuration	number	separation of pair d/A	binding energy $-E_b$/eV	Coulomb repulsive energy E_r, eV
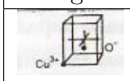	OCu(11)	4.92	0.061	0.105
	OCu(12)	6.75	0.006	0.076
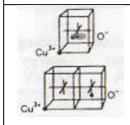	OCu(13)	7.23	0.096	0.071
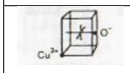	OCu(14)	7.76	0.079	0067
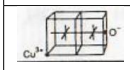	OCu(15)	10.17	0.041	0.060
configuration	number	separation of pair d/A	binding energy $-E_b$/eV	Coulomb repulsive energy E_r/eV
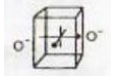	Ox($\hat{2}$)	2.66	-0.059	0.194
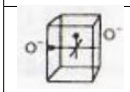	Ox(2)	3.11	-0.119	0.166
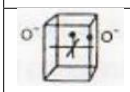	Ox(3)	3.17	0.036	0.163
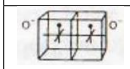	Ox(4)	3.58	-0.001	0.144
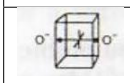	Ox(5)	3.81	0.228	0.135
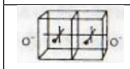	Ox(6)	3.81	0.127	0.135

In a similar study Allan and Mackrodt (1990) observed the difference in the bipolaron formation for Nd_2CuO_4 compared with La_2CuOO_4. They found no confining interactions in Nd_2CuO_4. It seems that the difference in bipolaron results for these two materials may arise from their structural difference (there is a $CuOO_6$ layer in La_2CuO_4 whereas there is a CuO_4 plane in Nd_2CuO_4). The detailed lattice structure may play an important role in the small bipolaron formation. As an example, the similar calculations performed on hole interactions in NiO revealed a much larger
repulsive interactions, and no configurations were found in which hole pairing might be ex-

pected. The lattice minimisation techniques show that the La_2CuO_4 structure is especially effective at screening of the Coulomb repulsion and the formation of intersite small bipolarons.

5.5.7 2.6 Effect of the kinetic energy on small-bipolaron formation

There is a finite probability for an electron to tunnel from one site of the lattice to the neighboring sites. The corresponding kinetic energy and the Coulomb repulsion oppose the small bipolaron formation. When the coupling constant is relatively large $\lambda > 1$, the hopping integrals are exponentially small as in the Holstein two-site model, section 1.6. Then the kinetic energy is a small perturbation and the static minimisation technique discussed above works perfectly well. However, in the intermediate coupling region $\lambda \leq 1$ the tunneling competes with the selftrapping and with the binding, trying to destroy both. The effect of the kinetic energy on the formation of small bipolaron depends on the lattice structure and geometry of the pair, because the binding energy is strongly related to them. In the case of a non-Bravais lattice such as the $CuOO_2$ plane of high T_c copper oxides some specific difficulties appear because of the multiband energy structure. A reasonable estimate of the kinetic energy effect on the small bipolaron can be obtained by solving a discrete Schrödinger equation for two electrons in the nearest neighbor approximation for a realistic crystal structure (Alexandrov and Kornilovitch (1993)). In this section we consider the solution of the two-particle problem on the CuO_2 plane modeling the repulsion by the positive Hubbard U term on copper, and the lattice mediated attraction by the negative term $-V$ on plane oxygen.

Within the discrete approach two electrons (holes) with opposite spins on the CuO_2 plane are described by the nine-component wave function $\phi_{\beta\gamma}(\mathbf{m}_1, \mathbf{m}_2)$. Each component is a probability amplitude to find one electron on a copper site ($\beta = 1$) or on two different plane oxygen sites ($\beta = 2, 3$) of the cell Fig.2.5 (the lattice vector $\mathbf{m}_1$), and the other electron on the site $\gamma = 1$ or 2,3 in the cell $\mathbf{m}_2$. The discrete Schrödinger equation is the infinite system of linear algebraic equations

$$E\phi_{\beta\gamma}(\mathbf{m}_1, \mathbf{m}_2) = -\sum_{\alpha,1}(-1)^{l_x/2+l_y/2}\left[\phi_{\alpha\gamma}(\mathbf{m}_1+1, \mathbf{m}_2) + \phi_{\beta\alpha}(\mathbf{m}_1, \mathbf{m}_2+1)\right] + U_\beta\delta_{\beta\gamma}\delta_{\mathbf{m}_1,\mathbf{m}_2}\phi_{\beta\gamma}(\mathbf{m}_1, \mathbf{m}_2) \tag{2.42}$$

where $U_1 \equiv U > 0$ and $U_2 = U_3 \equiv -V < 0$ and all energies are measured in units of the copper-oxygen nearest neighbor hopping integral $\tilde{J}$ renormalised by the electron-phonon interaction according to Eq.(1.118). The energy levels of p oxygen and d copper orbitals are taken to be equal for simplicity. The coefficient $(-1)^{l_x/2+l_y/2}$ of the kinetic energy term is due to the symmetry of two different $p_{x,y}$ oxygen in-plane orbitals hybridised with the $d_{x^2-y^2}$ copper orbital. The nearest $Cu-O$ distance is conveniently taken as unity, so the size of the cell is 2×2. Then the Fourier transform of Eq. (2.42) is

$$\left(\hat{H}_0 - E\right)\hat{\phi}(\mathbf{k}_1, \mathbf{k}_2) = \hat{C}(\mathbf{K}) \tag{2.43}$$

where

$$\hat{\phi}(\mathbf{k}_1, \mathbf{k}_2) = \frac{1}{N^2}\sum_{\mathbf{m}_1,\mathbf{m}_2}\phi_{\beta\gamma}(\mathbf{m}_1, \mathbf{m}_2)\, e^{-i\mathbf{k}_1\cdot\mathbf{m}_1 - i\mathbf{k}_2\cdot\mathbf{m}_2} \tag{2.44}$$

is the nine-component Fourier component of the wave function,

$$\hat{C}(\mathbf{K}) = -U_\beta\delta_{\beta\gamma}\sum_{\mathbf{q}}\phi_{\gamma\gamma}(\mathbf{q}, \mathbf{K}-\mathbf{q}) \tag{2.45}$$

is the interaction term with $\mathbf{K} = \mathbf{k}_1 + \mathbf{k}_2$ being conserving total momentum of the bipolaron. The kinetic energy of two electrons is given by the 9×9 matrix

$$\hat{H}_0 = \begin{bmatrix} \hat{T}_2 & 2i\hat{I}\sin k_{1y} & -2i\hat{I}\sin k_{1x} \\ -2i\hat{I}\sin k_{1y} & \hat{T}_2 & 0 \\ 2i\hat{I}\sin k_{1x} & 0 & \hat{T}_2 \end{bmatrix} \tag{2.46}$$

with

$$\hat{T}_2 = \begin{bmatrix} 0 & 2i\sin k_{2y} & -2i\sin k_{2x} \\ -2i\sin k_{2y} & 0 & 0 \\ 2i\sin k_{2x} & 0 & 0 \end{bmatrix} \tag{2.47}$$

and $\hat{I}$ being a unitary 3×3 matrix. Substitution of a formal solution of Eq.(2.43) into Eq.(2.45) yields three coupled equations with respect to C_{11}, C_{22} and C_{33}. From their consistency we find the standard secular equation for the eigenvalues $E(\mathbf{K})$

$$\det \begin{vmatrix} Ud_1 - 1 & Vd_2 & Vd_3 \\ -Ud_2 & -Vd_5 - 1 & Vd_4 \\ -Ud_3 & Vd_4 & -Vd_6 - 1 \end{vmatrix} = 0, \tag{2.48}$$

where

$$d_1 = \frac{1}{4}\sum_{\mathbf{q}} \left[R_{11} + R_{33} + R_{13} + R_{31}\right]$$

$$d_2 = \sum_{\mathbf{q}} \frac{\sin q_y \sin\left(K_y - q_y\right)}{E_{\mathbf{q}} E_{\mathbf{K}-\mathbf{q}}} \left[R_{11} + R_{33} - R_{13} - R_{31}\right]$$

$d_3 = d_2(y \to x)$,

$$\begin{aligned} d_4 = {} & 4\sum_{\mathbf{q}} \frac{\sin q_x \sin\left(K_x - q_x\right) \sin q_y \sin\left(K_y - q_y\right)}{E_{\mathbf{q}}^2 E_{\mathbf{K}-\mathbf{q}}^2} \\ & \times \left[2\left(R_{12} + R_{32} + R_{23} + R_{21}\right) - R_{11} - R_{33} - R_{13} - R_{31} - 4R_{22}\right] \\ d_5 = {} & \sum_{\mathbf{q}} \frac{4\sin^2 q_y \sin^2\left(K_y - q_y\right)}{E_{\mathbf{q}}^2 E_{\mathbf{K}-\mathbf{q}}^2} \left(R_{11} + R_{33} + R_{13} + R_{31}\right) \\ & + \frac{8\sin^2 q_y \sin^2\left(K_x - q_x\right)}{E_{\mathbf{q}}^2 E_{\mathbf{K}-\mathbf{q}}^2} \left(R_{12} + R_{32}\right) \\ & + \frac{1}{E_{\mathbf{q}}^2 E_{\mathbf{K}-\mathbf{q}}^2} \left[8\sin^2 q_x \sin^2\left(K_y - q_y\right)\left(R_{21} + R_{23}\right) + 16\sin^2 q_x \sin^2\left(K_x - q_x\right) R_{22}\right] \end{aligned}$$

$d_6 = d_5(y \to x)$. The one-particle spectrum is determined by

$$-E_1(\mathbf{k}) = E_3(\mathbf{k}) \equiv E(\mathbf{k}) = 2\sqrt{\sin^2 k_x + \sin^2 k_y}; E_2(\mathbf{k}) = 0, \tag{2.49}$$

and by

$$R_{\beta\gamma} = \frac{1}{E - E_\beta(\mathbf{q}) - E_\gamma(\mathbf{K} - \mathbf{q})}, \tag{2.50}$$

which is a free two-particle propagator. The bipolaron forms if the binding energy

$$\Delta(\mathbf{K}) = \min\left[E_\beta\left(\mathbf{k}_1\right) + E_\gamma\left(\mathbf{k}_2\right] - E(\mathbf{K}) = -4\sqrt{2} - E(\mathbf{K}) > 0. \tag{2.51}$$

The numerical solution of the secular equation, Eq.(2.48) shows that the pairs with $\mathbf{K} = 0$ are more stable, Fig.(2.6). For the center of the Brillouin zone, $K = 0$, the bipolaron exists if

$$V \geq \frac{8\sqrt{2}U}{4\sqrt{2} + 3U} \tag{2.52}$$

Therefore, there is a critical value of the attraction $V \simeq 3.8$ above which the bound state exists for any repulsion U.

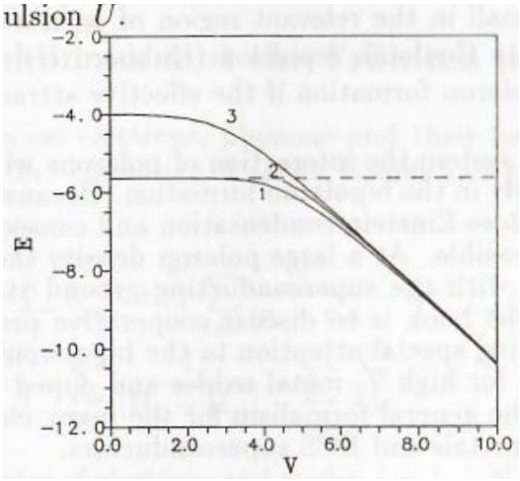

Fig.2.6. The energy of the bound state in units of the hopping integral versus the attractive potential V for (1) $K = U = 0$; (2) $K = 0, U = 1000$; (3) $K = (\pi/2, \pi/2)$ and U is arbitrary. The dashed line is the minimum of the kinetic energy of two electrons $(-4\sqrt{2})$.

The binding energy of a pair with the total momentum near the corners of the Brillouin zone does not depend on the repulsive potential at all, Fig.2.6. The reason for this is that near these points two particles interact on sites of only one and the wame type, so the repulsion on neighboring sites of another type does not affect the pairing.

The solution of the Schrödinger equation for two electrons enables us to calculate the bipolaron size r_b The space extension of the bipolaron wave function is determined by the sum

$$\phi_{\mathbf{K}}(\mathbf{r}_1, \mathbf{r}_2) \sim \sum_{\mathbf{q}} \frac{e^{i\mathbf{q}\cdot\mathbf{r}_1 + i(\mathbf{K}-\mathbf{q})\cdot\mathbf{r}_2}}{E^2 - \left[E_{\mathbf{q}} + E_{\mathbf{K}-\mathbf{q}}\right]^2}. \tag{2.53}$$

To derive the asymptotics at $\rho = \sqrt{x^2 + y^2} \to \infty$ one can apply the substitution

$$\frac{1}{E} = -i \int_0^\infty d\xi e^{\left(iE - 0^+\right)\xi} \tag{2.54}$$

to the sum, Eq.(2.53), which allows us to integrate over $\mathbf{q}$ with the following result for $K = 0$

$$\phi_0(x, y) \sim \int_0^\infty d\xi e^{\left(i\left[E^2/8 - 2\right] - 0^+\right)\xi} J_{x/2}(\xi) J_{y/2}(\xi). \tag{2.55}$$

Here $J_r(\xi)$ is the Bessel function and $x = x_1 - x_2, y = y_1 - y_2$. For the direction along $x = y$ we obtain

$$\phi_0(x, x) \sim Q_{x/2-1/2}\left(\left[E^2/8 - 2\right]^2/2 - 1\right) \tag{2.56}$$

where $Q_\nu(z)$ is the associated Legendre function with the exponential asymptotics for $\nu \to \infty$

$$\phi_0(x, x) \sim e^{-|x|/r_b} \tag{2.57}$$

The bipolaron radius is smaller than two lattice constants

$$r_b = \frac{2}{\operatorname{arccosh}\left(\left[E^2/8-2\right]^2/2-1\right)} \leq 4 \tag{2.58}$$

if the binding energy is not extremely small, $\Delta = |E + 4\sqrt{2}| > 0.01$. Thus we conclude that the bipolaron is small in the relevant region of on-site correlations within the CuO_2 plane. The on-site Coulomb repulsion (Hubbard U), no matter how strong, cannot prevent the bipolaron formation if the effective attraction on oxygen sites is relatively large $V \simeq 3.8$.

In the multi-polaron system the interaction of polarons with each other and with the lattice results not only in the bipolaron formation. Because of the bosonic character of bipolarons their Bose-Einstein condensation and consequently, the bipolaronic superconductivity are feasible. At a large polaron density the charge and (or) magnetic ordering compete with the superconducting ground state. Our intention for the remaining part of the book is to discuss cooperative properties of self-trapped carriers on a lattice paying special attention to the bipolaronic superconductivity as the natural explanation for high T_c metal oxides and doped fullerenes. In the next Chapter we introduce the general formalism for the many electron-phonon problem Chapter we introduce the generar BCS and apply it to normal metals and BCS superconductors.

5.6 5 Phase transformations of the polaronic Fermi-liquid

At low temperatures and (or) at high densities the residual polaron-phonon H_{p-ph} and polaron-polaron H_{p-p} interactions lead to phase transformations of the polaronic Fermi-liquid. There are several major instabilities. The polaronic Fermi-liquid is unstable versus the bipolaron formation followed by the Bose-Einstein condensation if H_{p-p} is attractive at short distances. If the density of carriers is of the order of the atomic density the commensurate or incommensurate charge-density wave (CDW) develops competing with the superfluid ground state. If the Coulomb repulsion is atrong the polaronic Fermi liquid undergoes the metal-insulator Mott transition. The ground state for the half-filled band is an antiferromagnetic insulator, which, if doped, has spin-lattice small (bi)polarons as the charge carriers.

5.6.1 5.1 Bipolaronic instability

Theory

The polaron-polaron interaction is the sum of two large contributions of the opposite Aign, Eq.(4.14). It is generally large compared with the polaron bandwidth. This is just the opposite regime to that of the BCS superconductor where the Fermi energy in the largest one. In polar solids the Coulomb repulsion is perfectly screened by the lons. Then the acoustical and (or) molecular phonons make the short-range interaction between polarons to be attractive. As discussed in Chapter 2 two polarons furm a small bipolaron at intermediate value of the electron-phonon coupling $\lambda \geq 0.5$, practically independent off the value of the Coulomb potential. In the multi-polaron matem the formation of bipolarons is manifested as a pole in the two-particle vertex part at large q corresponding to the pairing of small polarons. For a short distance (large q) the Fourier component of the interaction $v(\mathbf{q}) \equiv U$ might be positive or (???)live. Because the polaron bandwidth is normally smaller than $|U|$ we can consider this static dielectric function defined by Eq.(4.66). For $(T \gg w)$ we have

$$\epsilon(\mathbf{q}, 0) = 1 + \frac{n(2-n)U}{2T} \tag{5.1}$$

A screened short-range interaction is given by

$$\tilde{U} = \frac{U}{\epsilon(\mathbf{q},0)} = \frac{UT}{T \pm T^{**}} \tag{5.2}$$

with the characteristic temperature

$$T^{**} = \frac{|U|n(2-n)}{2} \tag{5.3}$$

The upper sign corresponds to the repulsion $U > 0$ while the lower sign (-) to the attraction, $U < 0$. One can see that in the temperature region $w < T \ll T^{**}$ the short range repulsion is sufficiently suppressed by the screening. The two-body correlations lead to a modification of polaron trajectories, which reduces the Coulomb self-energy to a magnitude of the order of the polaronic bandwidth if $T \simeq w$. In the case of the attraction the pole occurs in the effective interaction $\tilde{U}$ at $T = T^{**}$. Therefore, in this case T^{**} is the critical temperature of the bipolaron formation. For a half-filled band $(n \simeq 1)T^{**}$ is of order of the attraction itself and might be as high as $10^3 K$, section 2.5.

5.6.2 5.2 Cooper pairing of nonadiabatic carriers

Theory

For an intermediate value of $\lambda \simeq 1$ the effective interaction of polarons can be comparable or even less than the polaron bandwidth, both being less or of the order of the characteristic phonon frequency. If a pair binding energy Δ is small compared with the renormalised bandwidth $2w$, polarons constituting a pair tunnel through many sites during the characteristic time $1/\Delta$. Therefore a pair spreads over a large number of sites. Such 'extended' bipolarons consisting of two small polarons are overlapped similar to Cooper pairs if their density is compared with the atomic one. This is a narrow region of the coupling where the BCS approach is applied to nonadiabatic carriers with a nonretarded attraction. Bipolarons are then Cooper pairs formed by two small polarons (Alexandrov (1983)). The appropriate Hamiltonian is the extended Hubbard Hamiltonian taking into account the polaron narrowing of the band

$$H_p = \sum_{i,j} \left(\sigma(\mathbf{m}-\mathbf{n}) - \mu\delta_{i,j} \right) c_i^\dagger c_j + \frac{1}{2} v_{ij} c_i^\dagger c_j^\dagger c_j c_i \Bigg) \tag{5.4}$$

where $\sigma(\mathbf{m})$ is determined with Eq.(4.17) for the nonadiabatic system ($\omega > D/z$), or with Eq.(1.135) in the opposite case. For simplicity one can keep only the on-site v_0 and the nearest neighbor intersite v_1 interactions. At least one of them should be attractive to ensure the superconducting ground state. By introducing two order parameters

$$\Delta_0 = -v_0 \langle c_{\mathbf{m},\uparrow} c_{\mathbf{m},\downarrow} \rangle \tag{5.5}$$

$$\Delta_1 = -v_1 \langle c_{\mathbf{m},\uparrow} c_{\mathbf{m}+\mathbf{a},\downarrow} \rangle \tag{5.6}$$

and transforming to k -space one arrives at the usual BCS Hamiltonian

$$H_p = \sum_{\mathbf{k},s} \xi_{\mathbf{k}} c_{\mathbf{k},s}^\dagger c_{\mathbf{k},s} + \sum_{\mathbf{k}} \left[\Delta(\mathbf{k}) c_{\mathbf{k},\uparrow}^\dagger c_{-\mathbf{k},\downarrow}^\dagger + \text{ h.c. } \right] \tag{5.7}$$

where $\xi_{\mathbf{k}} = \epsilon_{\mathbf{k}} - \mu$ is the kinetic energy of the polaron tunneling with momentum $\mathbf{k}$ and

$$\Delta(\mathbf{k}) = \Delta_0 - \Delta_1 \frac{\xi_{\mathbf{k}} + \mu}{w} \tag{5.8}$$

is the order parameter corresponding to a singlet pairing. In general a triplet p-wave pairing is also possible with the Hamiltonian, Eq.(5.4).

Applying the standard diagonalisation procedure to the Hamiltonian one obtains for the order parameter

$$\langle c_{\mathbf{k},\uparrow} c_{-\mathbf{k},\downarrow} \rangle = \frac{\Delta(\mathbf{k})}{2\sqrt{\xi_{\mathbf{k}}^2 + \Delta(\mathbf{k})^2}} \tanh \frac{\sqrt{\xi_{\mathbf{k}}^2 + \Delta(\mathbf{k})^2}}{2T} \tag{5.9}$$

and with the definition Eq.(5.5,6)

$$\Delta_0 = -\frac{v_0}{N} \sum_{\mathbf{k}} \frac{\Delta(\mathbf{k})}{2\sqrt{\xi_{\mathbf{k}}^2 + \Delta(\mathbf{k})^2}} \tanh \frac{\sqrt{\xi_{\mathbf{k}}^2 + \Delta(\mathbf{k})^2}}{2T} \tag{5.10}$$

$$\Delta_1 = -\frac{v_1}{Nw} \sum_{\mathbf{k}} \frac{\Delta(\mathbf{k})\,(\xi_{\mathbf{k}} + \mu)}{2\sqrt{\xi_{\mathbf{k}}^2 + \Delta(\mathbf{k})^2}} \tanh \frac{\sqrt{\xi_{\mathbf{k}}^2 + \Delta(\mathbf{k})^2}}{2T} \tag{5.11}$$

The last two equations are equivalent to the BCS one for $\Delta(\mathbf{k}) = \Delta(\xi)$ with the potential depending on energy and with the half bandwidth w as a cutoff of the integral instead of the Debye temperature,

$$\Delta(\xi) = \int_{-w-\mu}^{w-\mu} d\xi' N_p\left(\xi'\right) V\left(\xi, \xi'\right) \frac{\Delta\left(\xi'\right)}{2\sqrt{\xi'^2 + \Delta\left(\xi'\right)^2}} \tanh \frac{\sqrt{\xi'^2 + \Delta\left(\xi'\right)^2}}{2T} \tag{5.12}$$

with $V\left(\xi, \xi'\right) = -v_0 - z v_1 \frac{(\xi+\mu)(\xi'+\mu)}{w^2}$. The polaron density of states is enhanced due to the polaron narrowing effect:

$$N_p(\xi) \equiv \frac{1}{N} \sum_{\mathbf{k}} \delta\left(\xi - \xi_{\mathbf{k}}\right) \tag{5.13}$$

luing of order of $1/2w$ instead of $1/2D$ for a bare band. The on-site and intersite interaction terms are both attractive (< 0) or one of them (on-site) may be repulsive.

5.6.3 5.3 High T_c polaronic superconductivity

Theory

The critical temperature T_c of a polaronic superconductor is determined from the Imo linearised equations in the limit $\Delta_{0,1} \to 0$:

$$\left(1 + A\left(\frac{v_0}{z v_1} + \frac{\mu^2}{w^2}\right)\right)\Delta - \frac{B\mu}{w}\Delta_1 = 0 \tag{5.14}$$

$$-\frac{A\mu}{w}\Delta + (1+B)\Delta_1 = 0 \tag{5.15}$$

where $\Delta = \Delta_0 - \Delta_1 \frac{\mu}{w}$ and

$$A = \frac{z v_1}{2w} \int_{-w-\mu}^{w-\mu} \frac{d\xi \tanh \frac{\xi}{2T_c}}{\xi} \tag{5.16}$$

$$B = \frac{z v_1}{2w} \int_{-w-\mu}^{w-\mu} \frac{d\xi \xi \tanh \frac{\xi}{2T_c}}{w^2} \tag{5.17}$$

These equations are applied only for a weak and intermediate polaron-polaron coupling $|v_{0,1}| < w$. In the limit of the weak coupling one obtains from Eq.(5.14,15)

$$T_c \simeq 1.14w\sqrt{1-\frac{\mu^2}{w^2}}\exp\left(\frac{2w}{v_0+zv_1\frac{\mu^2}{w^2}}\right) \tag{5.18}$$

The expression Eq.(5.18) plays the same role in the polaronic superconductivity as the BCS one for the low temperature superconductors. It predicts superconductivity even in the case of on-site repulsion $v_0 > 0$ if this repulsion is less than the total intersite attraction $z\,|v_1|$. It also predicts a nontrivial dependence of T_c on the doping. With the constant density of states within the polaron band the Fermi level μ is expressed through the number of polarons per atom n

$$\mu = w(n-1) \tag{5.19}$$

and

$$T_c \simeq 1.14w\sqrt{n(2-n)}\exp\left(\frac{2w}{v_0+zv_1(n-1)^2}\right) \tag{5.20}$$

T_c has two maxima as a function of n separated by a deep minimum for the half filled band ($n = 1$) when the nearest neighbor contributions to the pairing are mutually compensated.

The basic phenomenon that allows a high value of T_c is that the polaronic narrowing of the band, which eliminates the small exponential factor in the BCS or McMillan's formula Eq.(3.116). To show this we rewrite Eq.(5.20) in a slightly differ ent form separating the phonon mediated attraction and the Coulomb repulsion and taking explicitly into account the polaronic narrowing effect:

$$T_c \simeq \tilde{D}\exp\left(-g^2-\frac{\exp\left(-g^2\right)}{\lambda-\mu_c}\right) \tag{5.21}$$

where $\tilde{D} = 1.14D\sqrt{n(2-n)}$,

$$\lambda = \frac{2E_p + z(n-1)^2\sum_{\mathbf{m}=\mathbf{a}}\gamma^2(\mathbf{q})\omega_{\mathbf{q}}e^{i\mathbf{q}\cdot\mathbf{m}}}{2D} \tag{5,22}$$

and

$$\mu_c = \frac{U+z(n-1)^2V_c}{2D} \tag{5.23}$$

with U and V_c the onsite and intersite Coulomb repulsion, respectively. There are four independent parameters which determines the value of T_c, in particular the bare bandwidth D, the polaronic level shift E_p, the number of phonons g^2 in a polaronis
cloud, and the Coulomb repulsion μ_c. They correspond to the four independent parameters of the Fröhlich Hamiltonian: the electron kinetic energy $E_F \sim D$, the matrix element of the electron-phonon interaction $\gamma \sim g$, the characteristic phonon frequency $\omega = E_p/g^2$, and the Coulomb (pseudo)potential. Because only g^2 (or ω) depends on the ion mass one can determine the maximum value of T_c with respect to g^2 keeping D, λ and μ constant. Differentiating Eq.(5.21) with respect to g^2 we obtain for the maximum T_c^*

$$T_c^* = \tilde{D}\frac{\lambda-\mu_c}{e} \tag{5.24}$$

The applicability of this formula is restricted by the intermediate region of the interaction constant $\lambda - \mu_c < 1$ because of the formation of bipolarons in the large λ limit (Chapter 6).

However, if bipolarons are intersite and their effective mass is of the order of the polaron effective mass the expression Eq.(5.21) also describes the Bose-Einstein condensation of bipolarons, as we discuss in Chapter 6.

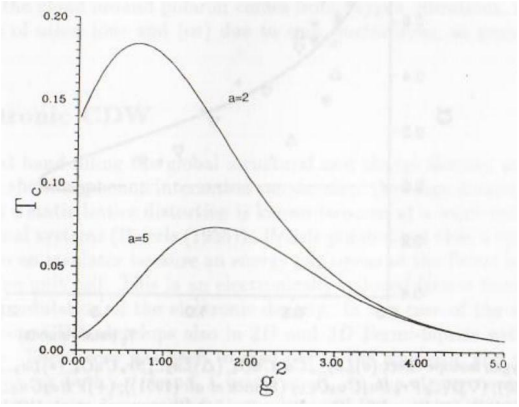

Fig.5.1. Critical temperature of a polaronic superconductor (in units of $\tilde{D}$) as a function of the interaction constant g^2 for two different values of the attraction between polarons, $a = 1/(\lambda - \mu_c)$.

T_8^* is limited by the condition of the small polaron formation $\lambda > 1/\sqrt{2z}$ (section (1)), which restricts the maximum value of D in Eq.(5.24). The value of g^2, at which I_c reaches its maximum is $g^2 = \ln(\lambda - \mu_c)^{-1}$, so

$$D < \sqrt{2z}\omega \ln(\lambda - \mu_c)^{-1} \tag{5.25}$$

and

$$T_c^* < \omega \frac{\sqrt{2z}(\lambda - \mu_c)\ln(\lambda - \mu_c)^{-1}}{e} \tag{5.26}$$

Une maximum value of the critical temperature of order of $\omega/3$ is reached in the Inimon of the intermediate coupling $g^2 \simeq 1$, Fig.5.1, where on the contrary the BCS superconductor has rather low T_c of order of 0.1ω. The absolute value depends on Wand can be as high as $200 - 300K$ depending on the value of the optical phonon
frequency. At large value of the coupling T_c of the bipolaronic superconductor drops because carriers become very heavy. Therefore we conclude that the highest T_c is in the transition region from polaronic to bipolaronic superconductivity. The fact that due to the polaron nonadiabaticity the short-range Coulomb pseudopotential μ_c is not suppressed contrary to the BCS case with μ_c^* rather than μ_c does not change this conclusion if $\lambda - \mu_c$ is positive.

With the formula for T_c, Eq.(5.21) interpolating between polaronic and bipolaronic superconductivity one can explain the unusual oxygen isotope effect in superconducting oxides, in particular its large value in low T_c oxides, an overall trend to lower value as T_c increases, and a negative α at high T_c, Fig.5.2. As it is shown below negative values of the isotope effect suggest that in some high- T_c oxides polaronic (rather than bipolaronic) superconductivity may exist.

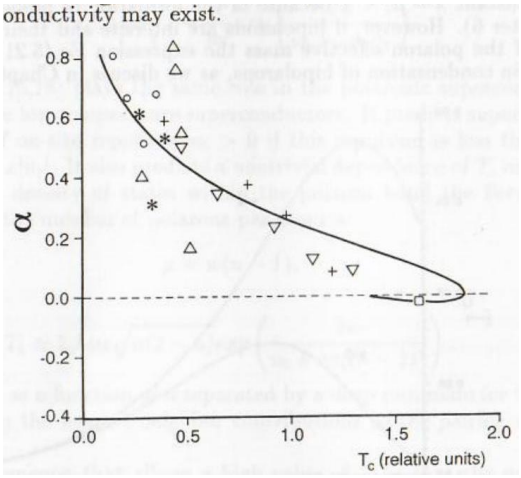

Fig.5.2. Oxygen isotope effect:(o) $La_{2-x}Ca_xCuO_4$, ($\triangle$)$La_{2-x}Sr_xCuO_4$, ($*$)$La_{2-x}Ba_xCuO_4$ (Craw ford et al. (1990)); (∇) $Y_{1-x}Pr_xBa_2Cu_3O_{6.92}$ (Franck et al. (1991)); ($+$) $YBa_2Cu_{4-x}Ni_xO_8$ (Bornemann et al. (1991a)); ($\square$) $Bi-Pb-Ca-Sr-Cu-O$ (Bornemann et al. (1991b)). Theoretical curve after Alexandrov (1992a).

As far as the oxygen mass dependence is concerned the formula Eq.(5.21) is applied both to the BCS-like polaronic superconductor and to the Bose-Einstein condensation of intersite bipolarons with the effective mass depending exponentially on the electron-phonon coupling $g : m^{**} \simeq m^* \sim \exp(g^2)$ (Chapter 6). As mentioned above the only quantity, which depends on the oxygen isotope mass M is g :

$$g^2 = \text{ const } \sqrt{M} + g_s^2 \tag{5.27}$$

where g_s^2 is a possible contribution to the mass renormalisation from the vibrations of other ions and from spin fluctuations. Differentiating Eq.(5.21) one obtains

$$\alpha = \frac{\beta g^2}{2}\left(1 - \frac{e^{-g^2}}{\lambda - \mu_c}\right), \tag{5.28}$$

where $\beta = 1 - g_s^2/g^2$ measures the relative contribution of oxygen to the small polaron cloud. Expressing T_c in units of $\tilde{D}$ we find

$$T_c = \exp\left(-g^2 - \frac{e^{-g^2}}{\lambda - \mu_c}\right) \tag{5.29}$$

With the equations (5.28, 29) one can analyse the correlation between the critical temperature and the isotope shift, Fig.5.2. It follows from our considerations that with the isotope effect one can distinguish the BCS like polaronic superconductivity $\alpha < 0$ from the Bose-Einstein condensation of small bipolarons $\alpha > 0$. With the increasing ion mass in the bipolaronic superconductor the bipolaron mass increases and the Bose-Einstein condensation temperature T_c decreases. On the contrary in polaronic superconductors the increase of the ion mass leads to the band narrowing and to the enhancement of the polaron density of states and therefore of T_c. The value of $\beta \simeq 1/3$ obtained from the fit to the experiment, Fig.5.2 shows that more than 30% of the cloud around polaron comes from oxygen vibrations, the rest is due to vibrations of other ions and (or) due to spin fluctuations, as proposed by Mott (1990).

5.6.4 5.4 Polaronic CDW

Theory

At substantial band-filling the global structural and charge density wave instability driven by the electron-phonon interaction can develop. A charge density wave (CDW) together with a static lattice distortion is known to occur at a wave vector $q = 2k_F$ in one-dimensional systems (Peierls (1955)). Peierls pointed out that a one-dimensional metal turns to an insulator because an energy gap opens at the Fermi level due to the doubling of the unit cell. This is an electronically induced lattice instability accompanied by a modulation of the electronic density. In the case of the weak electron-phonon coupling CDW develops also in $2D$ and $3D$ Fermi-liquids with the 'nested' Fermi surface. The theory has been worked out in the adiabatic and weak coupling approximations for both ω/D and λ being small. In the strong coupling limit the CDW ground state was discussed by Alexandrov and Ranninger (1981a). The central question is the electron excitation spectrum. The ground state is a charge ordered state of on-site small bipolarons. Taking into account the nonadiabatic corrections one should expect that the lowest charge excitation mode corresponds to the bipolaron conneling to the nearest neighbor site as discussed in Chapter 6. The dimerization of a half-filled Holstein chain of molecules in the strong coupling regime has been studied by Hirsch and Fradkin (1983) by means of the Monte-Carlo simulations. One of their conclusions is that the CDW order parameter is reduced gradually with the increasing adiabatic ratio ω/D due to the quantum fluctuations. Nasu (1985, 1991) and Zheng et al (1989) developed the variational approach to the Holstein $1D$ HamilImian describing the multi-electron system locally coupled to dispersionless phonons

$$\mathit{\Pi} = -t\sum_i \left(c_i^\dagger c_{i+1} + h.c.\right) - g\omega \sum_i \left(\hat{n}_i - 1/2\right)\left(d_i^\dagger + d_i\right) + \omega \sum_i \left(d_i^\dagger d_i + 1/2\right). \tag{5.30}$$

Here $\hat{n}_1 = c_1^\dagger c_i$ and t is the value of the nearest neighbor hopping integral. The muilibrium position of every oscillator is taken $\pm g\sqrt{2/M\omega}, 0$ if $n_{\mathbf{m}\uparrow} + n_{\mathbf{m}\downarrow} = 0, 2, 1,$
respectively. One can apply three successive unitary transformations with three variational parameters. The first one is a coherent state transformation for every phonon mode,

$$\exp S_1 = \exp\left[\sum_i (-1)^{i+1} m_0 \sqrt{M\omega/2}\left(d_i^\dagger - d_i\right)\right] \tag{5.31}$$

where m_0 is the first variational parameter, which measures the phonon-staggered ordering. As a result of the first transformation the equilibrium position of molecules becomes $(-1)^{i+1}m_0$ (for $\sum_s n_i = 1$). The second transformation is

$$\exp S_2 = \exp\left[\delta \sum_i g\left(\hat{n}_i - 1/2\right)\left(d_i^\dagger - d_i\right)\right] \tag{5.32}$$

which is an 'incomplete' Lang-Firsov polaronic transformation referring to the phononstaggered ordering state rather to the original homogeneous liquid. The variational parameter $\delta \leq 1$ measures the thickness of the phonon cloud around polaron, presumably allowing to consider the weak-coupling Migdal and polaron regimes within the same variational approach. However, differently from the displacement transformation of the Lee-Low-Pines theory (Chapter 1) or from the complete Lang-Firsov transformation, applied within the $1/\lambda$ expansion technique (Chapter 4), the 'incomplete' transformation, Eq.(5.32) leaves the substantial part ΔH_{e-ph} of the strong electron-phonon interaction in the transformed Hamiltonian

$$\Delta H_{e-ph} = -g\omega(1-\delta)\sum_i \left(\hat{n}_i - 1/2\right)\left(d_i^\dagger + d_i\right) \tag{5.33}$$

Finally, one can partly offset the polaronic narrowing effect, which is less favorable in the multi-polaron system compared with a single polaron one, by the third unitary transformation, the so-called 'squeezing' transformation (Zheng (1988))

$$\exp S_3 = \exp\left[\alpha \sum_i \left(d_i^\dagger d_i^\dagger - d_i d_i\right)\right] \tag{5.34}$$

This transformation generates a two-phonon coherent state with α being a third variational parameter. At this point Nasu and Zheng et al neglect the off-diagonal interaction ΔH_{e-ph} averaging the transformed Hamiltonian with respect to phonons. Thus the polaron and the phonon subsystems are decoupled with the effective Hamil tonian

$$\begin{aligned}\tilde{H}_{eff} \equiv \left\langle e^{S_3} e^{S_2} e^{S_1} H e^{-S_1} e^{-S_2} e^{-S_3} \right\rangle_{ph} &= -\rho t \sum_i \left(c_i^\dagger c_{i+1} + h.c.\right) \\ &+ \sum_i \hat{n}_i \left[\left(2\delta - \delta^2\right) g^2\omega + (-1)^{i+1}(1-\delta) g\omega m_0 \sqrt{2M\omega}\right] \\ &- 2\left(2\delta - \delta^2\right) g^2\omega \sum_i \hat{n}_{\mathbf{m}\uparrow}\hat{n}_{\mathbf{m}\downarrow} + NE_d \end{aligned} \tag{5.35}$$

where

$$\rho = \exp\left[-g^2\delta^2 e^{-4\alpha}\right] \tag{5.36}$$

is a new band narrowing factor and

$$E_d = \frac{\omega\cosh(4\alpha)}{2} + \frac{M\omega^2 m_0^2}{2} + \left(\delta^2 - 2\delta\right) g^2\omega \tag{5.37}$$

is the deformation energy per site. The effective Hamiltonian can be diagonalised with the Bloch representation for electrons. The ground state energy is minimised with respect to m_0, δ and α. It appears from the results of these calculations that because of the multi-polaron nature of the problem and the squeezing effect the band narrowing is not so dramatic as in a single polaron system. No order-disorder transition has been found and CDW ordering prevails for the half-filling for all values of the adiabatic ratio ω/D. This result is in agreement with the Monte Carlo simulations. However, the excitation spectrum is less reliable because the large off-diagonal interaction ΔH_{e-ph} is neglected in the effective variational Hamiltonian. It can have a drastic effect on the excitation spectrum.

As in the case of the polaronic Fermi-liquid the phonon excitation spectrum of the polaronic CDW state can be studied analytically by the use of the $1/\lambda$ expansion technique (Göbel et al (1994)). The CDW state of the half-filled chain of molecules in the strong coupling adiabatic regime has the following configuration

$$

$$

The phonon operators are now replaced by new operators describing the vibrations around the new equilibrium positions: $d_i \to d_i + \alpha_i$. After the substitution the Hamiltonian reads as

$$\begin{aligned} H = &-t\sum_i \left(c_i^\dagger c_j + h.c.\right) - 2g\omega \sum_i \hat{n}_i\alpha_i - g\omega \sum_i \left(\hat{n}_i - \alpha_i/g\right)\left(d_i^\dagger + d_i\right) \\ &+ \omega \sum_i \left(d_i^\dagger d_i + 1/2 + \alpha_i^2\right) \end{aligned} \tag{5.38}$$

The last term represents the energy of the frozen distortion. The remaining terms give rise to the definition of two new electronic energy bands resulting from the broken symmetry of the ground state. The interaction terms are now supplemented by a term involving phonon operators only. The reason is that due to the buildup of CDW the occupation number n_i no longer has lattice periodicity. The supplemented term serves to cancel the expectation value of the interaction energy

$$n_i - \alpha_i/g = 0 \tag{5.39}$$

IIy defining $\alpha_{2i} \equiv \alpha$ and $\alpha_{2i+1} = \beta$ the new band structure is obtained by reverting to the reciprocical space shrinking the Brillouin zone from 2π to π (the lattice constant is taken as unity):

$$E_k^t = -g(\alpha - \beta) + \frac{t_k + t_{k+\pi}}{2} \pm \left[\frac{(t_k - t_{k+\pi})^2}{4} + g^2\omega^2(\alpha - \beta)^2 \right]^{1/2} \tag{5.40}$$

Where $t_h = -2$ tcos k and the momentum k has range $[-\pi/2, \pi/2]$. The parameters α, β Hacribing the distortion are now to be determined self-consistently. By minimising
the total energy with respect to α and β the lattice distortion depending on the coupling can be calculated. The contribution from the interaction term is expected to be small if Eq.(5.39) is satisfied. The amount of symmetry breaking is measured by $\Delta \equiv (\alpha - \beta)/g$. Introducing the familiar coupling constant $\lambda = g^2\omega/2t$ we obtain as a result of the minimisation of $\langle H \rangle$

$$\Delta = \frac{4}{\pi} \int_{-\pi/2}^{\pi/2} dk \frac{\lambda\Delta}{[\cos k + \lambda^2\Delta^2]^{1/2}} \tag{5.41}$$

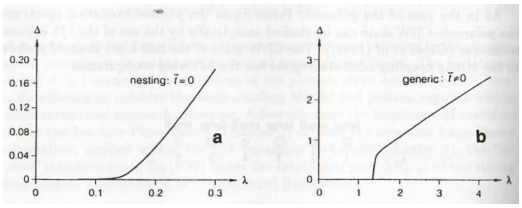

Fig.5.3. Distortion with (a) and without (b) nesting.

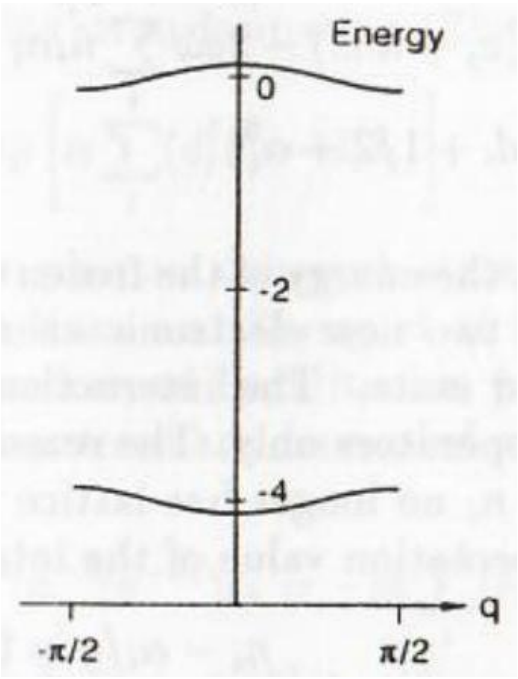

Fig.5.4. Electron energy bands of $1 D \mathrm{CDW}$ insulator for $\lambda \gg 1$.

Besides the trivial solution $\Delta = 0$ there is a nonvanishing one for every value of λ which gives the global minimum of the energy, Fig.5.3a. For large values of $\lambda > 1$ we have $\Delta \simeq 2 - 1/8\lambda^2$. In this range of λ the two energy bands become very flat and are separated by a huge 'Peierls' gap of the order of $4g^2\omega$, Fig.5.4. The immediate breaking of symmetry regardless of the value of λ, Fig.5.3a is an artificial feature particularly pertinent to one dimension. It is related to Fermi surface nesting and completely removed in higher dimensions with the realistic Fermi surface. To see the
general picture one can consider two dimensions with a pattern of symmetry breaking of the form

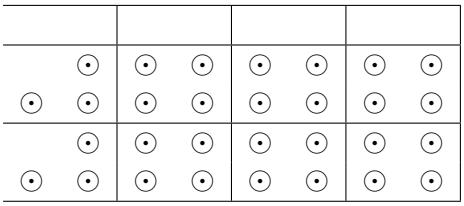

After symmetry breaking there will now arise four energy bands. However, the coupling must exceed a critical value λ_c for symmetry breaking to take place unless there is Fermi surface nesting. This can be verified with the bare kinetic energy dispersion of the form

$$E_{\mathbf{k}} = -2t\left(\cos k_x + \cos k_y\right) + \bar{t}\left(\cos 2k_x + \cos 2k_y\right) \tag{5.42}$$

For $\bar{t} = 0$ there is Fermi surface nesting and symmetry is broken for every value of the coupling, Fig.5.3a. On the other hand the general case $\bar{t} \neq 0$ shows no such pathological feature, Fig.5.3b. By expanding the static ground state energy about the equilibrium value of Δ up to the second order one finds for $\lambda > 1$ the renormalised phonon frequency $\tilde{\omega} = \omega\left(1 - O\left(1/\lambda^2\right)\right)$ similar to that of the two-site Holstein model, Eq.(1.129). With increasing λ the phonon frequency decreases to the left of the critical point $\lambda < \lambda_c$, vanishes at the phase transition and increases rapidly afterwards, as shown in Fig.5.5. This behavior of the phonon frequency is reminiscent of that of the finite size cluster, Fig.1.6. The spurious kink in the curve $\tilde{\omega}(\lambda)$

immediately after the phase transition, Fig.5.5 is due to a static approximation for the energy. Calculation done with the polarization loop (GF) smoothes out this part of the curve. The static energy result are then reproduced with the lowest order in the adiabatic parameter ω/t.

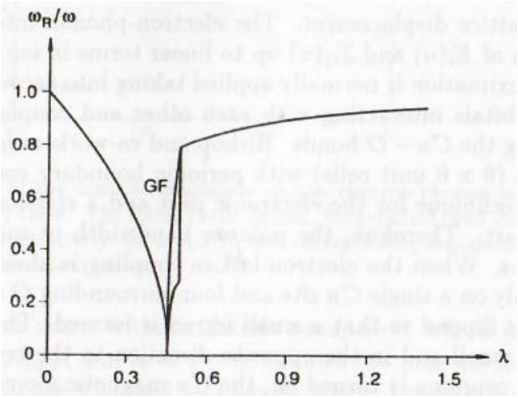

Iig.5.5. Renormalisation of the phonon frequency.

5.6.5 5.5 Small polarons in doped Mott insulators

Theory

I he formation and dynamics of polarons and bipolarons in strongly correlated narrow hand metals became fascinating topics because of renewed importance on account of its application to the high temperature superconductors. The behavior of a doped 'Mott' insulator - that is an antiferromagnetic material in which the moments have value $S = 1/2$ is still an unsolved problem; but we do not consider this to be the case for the antiferromagnetic materials in general. In magnetic materials the carriers in the conduction band form spin polarons - sometimes called ferrons (Nagaev (1979)); that is a group of moments oriented antiparallel to that of the carrier. This entity has a mass increasing exponentially with the number of moments it contains. One can assume that this remains so for the simple Mott insulator such as La_2CuO_4, if holes in the oxygen $2p$ band are introduced by doping with strontium. Then polarons must be of complex hybrid type. In the centre is a spin polaron, containing perhaps from 4 to 8 moments. But-in these highly dielectric materials, they will polarise the lattice. Both spin and lattice will contribute to the mass enhancement (Mott (1993)). Consequently, the problem combines aspects of coupled fields with distinct time scales (electrons, phonons and spin fluctuations), electron-electron interaction, lattice discreteness and, in real solids, competition between trapping in a random potential and the self-trapping.

The qualitative effects of the lattice- and spin-polaronic distortion upon doping into an antiferromagnetic stoichiometric background can be studied with the extended Peierls-Hubbard model (Bishop and Salkola (1995)). In particular case of CuO 2 plane of high- T_c copper oxides, Fig. 2.5 the model takes into account both the electron-phonon interaction (via the modulation of the atomic level E_i as well as the hopping integral T_{ij}) and the on-site (Hubbard U) and nearest-neighbor repulsion terms (V)

$$H = \sum_i E_i(u)\hat{n}_i + \sum_{\langle i \neq j \rangle} T_{ij}(u) c_i^\dagger c_j + \sum_{\mathbf{m}} U_{\mathbf{m}} \hat{n}_{\mathbf{m}\uparrow} \hat{n}_{\mathbf{m}\downarrow} + \sum_{\langle i \neq j \rangle} V_{ij} \hat{n}_i \hat{n}_j + \sum_{\mathbf{q}} \omega_{\mathbf{q}} \left(d_{\mathbf{q}}^\dagger d_{\mathbf{q}} + 1/2 \right) \tag{5.43}$$

where u is the lattice displacement. The electron-phonon interaction is introduced by the expansion of $E_i(u)$ and $T_{ij}(u)$ up to linear terms in ion displacements u. The three-band approximation is normally applied taking into account holes in $Cud_{x^2-y^2}Op_x$ and Op_y orbitals

interacting with each other and coupled with the motion of oxygen ions along the $Cu-O$ bonds. Bishop and co-workers made their calculations on large clusters (6×6 unit cells) with periodic boundary conditions by the use of a Hartree-Fock technique for the electronic part and a classical adiabatic treatment for the lattice part. Therefore, the polaron bandwidth or mass remains outside of these calculations. When the electron-lattice coupling is absent, each added hole in localised primarily on a single Cu site and four surrounding O sites. The spin density at this Cu site is flipped so that a small ferron is formed. The spin densities at the four O sites are small and in the opposite direction to the central Cu spin. As the electron-phonon coupling is turned on, the Cu magnetic moment is reduced and the O atoms are displaced toward the central Cu. At the Cu site, where a small polaron resides, reduction of the magnetic moment results in strong mixing of the four O with the Cu. Then, substantially below a critical value of the electron-phonon coupling $\lambda \leq 1$ for destruction of the global antiferromagnetic state the magnetic moment of the central Cu collapses. Finally, above the critical value of λ the antiferromagnetic undoped ground state is replaced by a non-magnetic (lattice) small polaron state.

Under certain conditions the three-band Hubbard model discussed above in to
duced to a single-band $t-J$ model, in which the hole, constrained to a projected Hilbert space without double occupancy of sites, interacts with the spin density (for references see Dagotto (1994)). The formation of small polarons and bipolarons in the Holstein $t-J$ model was examined by Fehske et al (1995) by means of a variational diagonalisation technique on finite square lattices, up to 18 effective sites in size. The Hamiltonian of the $2D$ Holstein $t-J$ model is given by

$$H = -t \sum_{\langle i\neq j\rangle, s=s'} \left(c_i^{\dagger} c_j + h.c. \right) + J \sum_{\langle i\neq j\rangle} \left(\mathrm{S}_i \cdot \mathrm{S}_j - \frac{1}{4} \hat{n}_i \hat{n}_j \right)$$
$$- g\omega \sum_i h_i \left(d_i^{\dagger} + d_i \right) + \omega \sum_i \left(d_i^{\dagger} d_i + 1/2 \right). \qquad (5.44))$$

0.04

Fig.5.6. Dependence of the transfer amplitude on the electron-phonon coupling for the onehole (a) and two- hole (b) cases. The solid, chain-dashed, long-dashed, and dashed curves refer to $\omega/l = 0.1, 0.8, 3.0, 10.0$, respectively. At $\omega = 0.1t$, the corresponding dependence for noncorrelated carriers is presented by the dotted curve.

II acts in a Hilbert space without double occupancy, where $\hat{n}_i = \sum_s c^{\dagger}_{\mathbf{m},s} c_{\mathbf{m},s}$, $\mathrm{H}_i = (1/2)\sum_{ss'} c^{\dagger}_{\mathrm{m},s} \tau_{ss'} c_{\mathrm{m},s'}$, and $h_i = 1 - \hat{n}_i$ denotes the hole number operator. The linet two terms represent the standard $t-J$ model, where J measures the antiferromagnelic exchange interaction and t denotes hopping processes between nearest-neighbor colls on a square lattice. The third and fourth terms take the electron-phonon interaction and the phonon energy into account. The physics of the Holstein $t-J$ model 10 governed by two effects: the strong Coulomb correlations (due to J/t and the consiraint of no double occupancy), and the polaronic band renormalisation depending in $\lambda = g^2\omega/4t$ and ω/t. Including static displacement field, 'incomplete' polaron diccasing and squeezing effect and averaging over the transformed phonon vacuum as
described above, Fehske et al investigate numerically the ground state properties of the resulting polaronic $t-J$ model. As a measure of the phonon- induced band renormalisation the effective transfer amplitude

$$t_{eff} = \frac{E_t(g,J)}{E_t(0,J)} \qquad (5.45)$$

is introduced. Here

$$E_t = -\frac{\rho t}{N} \left\langle \sum_{\langle ij \rangle} \left(c_i^\dagger c_j + h.c. \right\rangle \right. \tag{5.46}$$

denotes the kinetic energy with the reduction factor ρ, determined in Eq.(5.36). The effective transfer amplitude, calculated for $J/t = 0.4$ is shown in Fig 5.6a for the one hole case and in Fig.5.6b for the two hole case for different values of the adiabatic ratio ω/t. As in the noncorrelated system for low frequencies ($\omega < t$), one can distinguish the free hole if $\lambda \leq 0.2$ and the adiabatic small polaron for larger coupling with phonons. Increasing the electron-phonon interaction, the mobility of the hole ($\sim t_{eff}$) is strongly reduced when the small polaron is formed. To discuss the effect of the electronic correlations on the self-trapping transition, the noncorrelated case of spinless fermions is also considered. Obviously, the transition from large to small polaron is obtained at a much larger critical value of $\lambda_c \simeq 1$, which corresponds to the polaronic shift of the order of half the bare bandwidth, Fig.5.6a,b (dotted line). For the nonadiabatic case ($\omega \geq t$) there are small polarons at all values of λ, and the transfer amplitude decreases smoothly with increasing λ. As we have mentioned in section 5.4 the drawback of the variational approach is that a large part of the electron-phonon interaction is neglected because of the averaging with respect to phonons. However, the conclusion that the critical coupling strength λ for the selftrapping of the carriers in the doped Mott insulator is considerably reduced by the antiferromagnetic exchange interaction seems to be reasonable. Both lattice and spin distortions drive the system towards localisation. Therefore a rather weak electron-phonon interaction ($\lambda \geq 0.2$) can cause polaron band narrowing in strongly correlated phoriz electron system supporting a prominent role of the lattice degree of freedom in the cuprates.

5.7 6 Bipolaronic liquid

As we have mentioned in Chapter 5 the onsite or intersite attractive energy of two small polarons is generally larger than the polaron bandwidth. At this condition real space pairs of polarons i.e. small bipolarons form if temperature is not very high, $T < T^{**}$. Then the polaronic Fermi liquid transforms into a bipolaronic liquid. The latter is stable at low density of bipolarons because the effective bipolaron-bipolaron interaction is repulsive for all distances (see below). At large density the bipolaronic CDW state competes with the superfluid.

5.7.1 6.1 Coherent tunneling and repulsion of bipolarons

A small parameter $w/\Delta \ll 1$ where Δ is the bipolaron binding energy, of order of the attractive energy provides us with a consistent treatment of the bipolaronic systems (Alexandrov and Ranninger (1981a,b)). Under this condition the hopping term in the transformed Hamiltonian $\tilde{H}$ is a small perturbation to the ground state of immobile bipolarons and free phonons:

$$\tilde{H} = H_0 + H_{\text{pert}} \,, \tag{6.1}$$

where

$$H_0 = \frac{1}{2} \sum_{i,j} v_{ij} c_i^\dagger c_j^\dagger c_j c_i + \sum_{\mathbf{q}} \omega_{\mathbf{q}} \left(d_{\mathbf{q}}^\dagger d_{\mathbf{q}} + 1/2 \right) \tag{6.2}$$

and

$$H_{pert} = \sum_{i,j} \hat{\sigma}_{ij} c_i^\dagger c_j \tag{6.3}$$

Under the condition $\Delta \gg w$ there are no unbound polarons in the ground state, and the bipolaron motion can be described with a new canonical transformation $\exp(S_2)$. This transformation eliminates the first order of H_{pert} , which destroys the bipolaron and therefore has no diagonal contribution:

$$(S_2)_{f,p} = \sum_{i,j} \frac{\langle f|\hat{\sigma}_{ij} c_i^\dagger c_j|p\rangle}{E_f - E_p} \tag{6.4}$$

where $E_{f,p}$ and $|f\rangle, |p\rangle$ are the energy levels and the eigenstates of H_0. Neglecting the terms of higher order than $(w/\Delta)^2$ one obtains

$$(H_b)_{ff'} = \left(e^{S_2} \tilde{H} e^{-S_2}\right)_{ff'} \tag{6.5}$$

$$\begin{aligned}(H_b)_{ff'} \simeq (H_0)_{ff'} - \frac{1}{2} \sum_{\nu} \sum_{i,i';j,j'} \langle f|\hat{\sigma}_{ii'} c_i^\dagger c_{i'}|\nu\rangle\langle\nu|\hat{\sigma}_{jj'} c_j^\dagger c_{j'}\,|f'\rangle \\ \times \left(\frac{1}{E_\nu - E_{f'}} + \frac{1}{E_\nu - E_f}\right)\end{aligned} \tag{6.6}$$

The nonzero matrix elements of S_2 act between a localised bipolaron state and a state of two unpaired polarons localised in different cells or sites (in case of on-site pairs). The expression (6.6) determines the matrix elements of the transformed (bipolaronic) Hamiltonian H_b in the subspace $|f\rangle, |f'\rangle$ without unpaired polarons. On the other hand $|\nu\rangle$ refers to configurations involving two unpaired polarons, so that

$$E_f - E_\nu = -\Delta + \sum_{\mathbf{q}} \omega_{\mathbf{q}} \left(n_{\mathbf{q}}^f - n_{\mathbf{q}}^\nu\right) \tag{6.7}$$

where $n_{\mathrm{q}}^{f,\nu}$ are the phonon occupation numbers $(0, 1, 2, 3 \ldots)$. This equation is an explicit definition of the bipolaron binding energy Δ, which takes into account the interaction between bipolarons as well as between two unpaired polarons. The lowest eigenstates of H_b are in the subspace which involves only doubly occupied $c_{\mathbf{m},s}^\dagger c_{\mathbf{m},s'}^\dagger|0\rangle$ or empty $|0\rangle$ states. The bipolaron tunneling takes place via a transition to a virtual unpaired state implying a single polaron tunneling to the adjacent cell. The subsequent tunneling of a second polaron of a pair restores the initial energy state of the system. Because the bipolaron band is narrow (see below) there are no high-frequency phonons emitted or absorbed. Hence one can average H_b with the phonon density matrix

$$H_b = H_0 - i \sum_{i,i';j,j'} c_i^\dagger c_{i'} c_j^\dagger c_{j'} \int_0^\infty dt e^{-i\Delta t} \Phi_{ii'}^{jj'}(t) \tag{6.8}$$

with the real time t in the multiphonon correlator Φ determined in section 4.3. The difference between the 'exact' and averaged Hamiltonians can be treated perturbatively as the bipolaron-phonon interaction (section 6.3). Taking into account that there are only bipolarons in the subspace in which H_b operates one can rewrite the bipolaron Hamiltonian in terms of the creation $b_i^\dagger = c_{\mathbf{m}\uparrow}^\dagger c_{\mathbf{m},\downarrow}^\dagger$ and annihilation singlet bipolaron operators

$$H_b = -\sum_{\mathbf{m}} \left(\Delta + \frac{1}{2} \sum_{\mathbf{m}'} v^{(2)}_{\mathbf{m},\mathbf{m}'} \right) n_{\mathbf{m}} + \sum_{\mathbf{m} \neq \mathbf{m}'} \left(-t_{\mathbf{m},\mathbf{m}'} b^{\dagger}_{\mathbf{m}} b_{\mathbf{m}'} + \frac{1}{2} \bar{v}_{\mathbf{m},\mathbf{m}'} n_{\mathbf{m}} n_{\mathbf{m}'} \right) \tag{6.9}$$

where $n_{\mathrm{m}} = b^{\dagger}_{\mathrm{m}} b_{\mathrm{m}}$ is the bipolaron occupation number operator,

$$\bar{v}_{\mathrm{m},\ \mathrm{m}'} = 4 v_{\mathrm{m},\ \mathrm{m}'} + v^{(2)}_{\mathrm{m},\ \mathrm{m}'} \tag{6.10}$$

is the bipolaron-bipolaron interaction including the direct (density-density) Coulomb repulsion (V_c), the attraction via phonons between two small polarons in different cells and a second order correction

$$v^{(2)}_{\mathbf{m},\mathbf{m}'} = 2i \int_0^{\infty} dt \Phi^{\mathbf{m}'\mathbf{m}}_{\mathbf{m}\mathbf{m}'}(t) \exp(-i\Delta t) \tag{6.11}$$

which is repulsive. The origin of this repulsion is that a virtual hop of one of the polarons of a pair is forbidden when the neighboring cell is occupied by another pair. The bipolaron transfer integral is of the second order in the electron kinetic energy $T(\mathbf{m})$

$$t_{\mathbf{m},\mathbf{m}'} = 2i \int_0^{\infty} dt \Phi^{\mathbf{m}\mathbf{m}'}_{\mathbf{m}\mathbf{m}'}(t) \exp(-i\Delta t) \tag{6.12}$$

To calculate t and $v^{(2)}$ one can use the explicit form of the multiphonon correlator, $\Phi^{m'm}_{mm'}$, Eq.(4.104). For $\Phi^{m'}_{mm'}$ the expression is the same, but with the opposite sign of the argument of the second exponent. If $T = 0$ and phonons are dispersionless the calculation yields (Alexandrov and Kabanov (1986))

$$t_{\mathbf{m},\mathbf{m}'} = \frac{2T^2(\mathbf{a})}{\Delta} e^{-2g^2} \sum_{k=0}^{\infty} \frac{(-2g^2)^k}{k!(1 + k\omega/\Delta)} \tag{6.13}$$

and

$$v^{(2)}_{\mathbf{m},\mathbf{m}'} = \frac{2T^2(\mathbf{a})}{\Delta} e^{-2g^2} \sum_{k=0}^{\infty} \frac{(+2g^2)^k}{k!(1 + k\omega/\Delta)} \tag{6.14}$$

with $\mathbf{a} = \mathbf{m} - \mathbf{m}'$. If $\Delta < \omega$ both the bipolaron hopping and the second order repulsion are about w^2/Δ. However, for large binding energy $\Delta \gg \omega$ the bipolaron bandwidth dramatically decreases being proportional to e^{-4g^2} in the limit $\Delta \to \infty$. This limit is, however, not realistic because $\Delta \simeq 2E_p - V_c \leq 2g^2\omega$. Therefore, a more realistic regime is $\omega < \Delta < 2g^2\omega$, where

$$t_{\mathbf{m},\mathbf{m}'} \simeq \frac{2\sqrt{2\pi} T^2(\mathbf{a})}{\sqrt{\omega\Delta}} \exp\left[-2g^2 - \frac{\Delta}{\omega} \left(1 + \ln \frac{2g^2\omega}{\Delta} \right) \right] \tag{6.15}$$

On the contrary the bipolaron-bipolaron repulsion increases, $v^{(2)} \sim D^2/\Delta$ in the limit $\Delta \to \infty$. For dispersionless molecular or optical phonons the intermolecular attraction via phonons (the second term in Eq.(4.14)) is zero. Therefore the direct Coulomb and the second order $v^{(2)}$ repulsive terms lead to a total repulsive interaction between bipolarons, preventing the formation of droplets. At finite temperatures the denominator of the second order terms of the bipolaronic Hamiltonian, Eq.(6.6) turns out to be zero if the resonance condition $N\omega = \Delta$ is met ($N = 1, 2, 3, \ldots$). This divergence is eliminated by taking into account the phonon frequency dispersion and (or) by including the higher terms of the $1/\lambda$ perturbation expansion.

The high temperature behavior of the bipolaron transfer integral is just opposite to that of the small polaron bandwidth. While the polaron band collapses with increasing temperature as described in section 4.4 the bipolaron band becomes wider [24] found by Bryksin and Gol'tsev (1988)

$$t_{\mathrm{m},\ \mathrm{m}'} \sim T^{-1/2} \exp\left[-\frac{E_p + \Delta}{2T}\right] \tag{6.16}$$

for $T > \omega$.

In the case of inter - site bipolarons, which are the bound states of two small polarons on neighboring sites, there are two additional points. First of all an intersite bipolaron can be formed with a nonzero spin $S = 1$ (triplet state) and with the energy $J \sim w^2/U$ above the singlet state $S = 0$. This should be taken into account by introducing additional spin quantum numbers $S = 1; l = 0, \pm 1$ in the definition of $b_{\mathbf{m}}$. The second point is that in a simple square or cubic lattice the inter-site bipolaron tunnels via the next neighbor hopping of a single polaron rather than via two-particle (Josephson-like) tunneling, described with Eq.(6.12). This 'crablike' tunneling results in a bipolaron bandwidth of the same order as the polaron one. In the perovskite structures the apex bipolaron is the ground state as discussed in section 2.5. Its band structure is described below. In general, H_b in the form of Eq.(6.9) is applied not only to on-site bipolarons but also to inter-site or more extended nonoverlapping pairs if $\mathbf{m}$ includes the spin, and $t_{\mathbf{m},\mathbf{m}'}$ is considered as a phenomenological parameter. The site index $\mathbf{m}$ should be generally considered as a position of the centre of mass of the bipolaron.

5.7.2 6.2 Bipolaron anisotropic flat bands in high- T_c copper oxides

Consideration of particular lattice structures shows that small inter-site bipolarons can be perfectly mobile even when the electron-phonon coupling is strong and the bipolaron binding energy is large (Alexandrov (1995)). Here we analyse the important case of copper based high-T_c oxides. The existence of the 'parent' Mott insulators suggest that high- T_c superconductors are in fact doped semiconductors with narrow electron bands. Therefore, different types of bipolarons can be found with computer simulation techniques based on the minimization of the ground state energy, Eq. (4.15) without the kinetic energy term, section 2.5. The intersite pairing of the in-plane oxygen hole with the apex one is energetically favorable in the perovskite structures with the binding energy $\Delta = 0.119$eV for La_2CuO_4, Table 4. Obviously, this apex bipolaron can tunnel from one cell to another via a direct single polaron tunneling from one apex oxygen to its apex neighbor as shown in Fig.6.1.

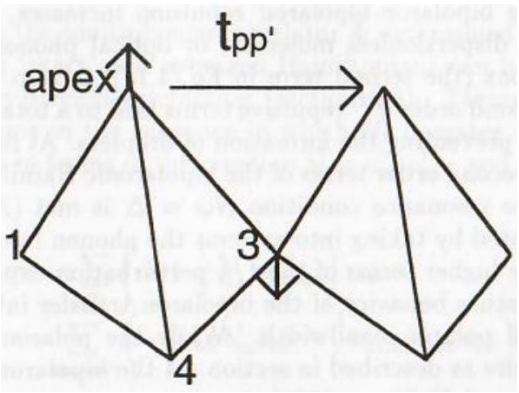

Fig.6.1. Apex bipolaron tunneling in perovskites.

To show this we consider the model Hamiltonian, including the oxygen-oxygen and oxygen-copper hopping integrals

$$H = \sum_{i,j} T_{ij} c_i^\dagger c_j + \sum_{\mathbf{q},j} \omega_{\mathbf{q}} \hat{n}_j \left(u_j(\mathbf{q}) d_{\mathbf{q}} + h.c. \right) + \sum_{\mathbf{q}} \omega_{\mathbf{q}} \left(d_{\mathbf{q}}^\dagger d_{\mathbf{q}} + 1/2 \right) + \sum_{i,j} V_{ij} \hat{n}_i \hat{n}_j \tag{6.17}$$

where T_{ij} determines the bare band structure in the site representation; c_i, c_j are hole annihilation operators for oxygen or copper sites $i, j; \hat{n}_j = c_j^\dagger c_j$ is the number operator, V_{ij} is the direct Coulomb repulsion, which does not include the on-site term $i = j$ for parallel spins. Oxides are strongly polarizable materials, so coupling with optical phonons dominates in the electron-phonon interaction

$$\gamma(\mathbf{q}) = -\frac{i\sqrt{8\pi\alpha}}{\sqrt{\Omega}(2m\omega)^{1/4} q} \tag{6.18}$$

The lattice polarization is coupled with the electron density, therefore the interaction is diagonal in the site representation and the coupling constant does not depend on the particular orbital. In doped oxides optical phonons are partially screened. Then molecular and acoustical phonons also contribute to the interaction. The canonical displacement transformation eliminates an essential part of the electron-phonon interaction. The transformed Hamiltonian is given by

$$\tilde{H} = SHS^{-1} = (T_p - E_p) \sum_{i(p)} n_{i(p)} + (T_d - E_d) \sum_{i(d)} n_{i(d)} + \sum_{i \neq j} \hat{\sigma}_{ij} c_i^\dagger c_j + \sum_{\mathbf{q}} \omega_{\mathbf{q}} \left(d_{\mathbf{q}}^\dagger d_{\mathbf{q}} + 1/2 \right) - \frac{1}{2} \sum_{\mathbf{q},i,j} \left(2\omega_{\mathbf{q}} u_i(\mathbf{q}) u_j^*(\mathbf{q}) - V_{ij} \right) \hat{n}_i \hat{n}_j \tag{6.19}$$

The first oxygen (p) and the second copper (d) diagonal terms include the polaronic level shift, which is the same for oxygen and copper ions

$$E_p = E_d = \sum_{\mathbf{q}} |u_j(\mathbf{q})|^2 \omega_{\mathbf{q}} \tag{6.20}$$

The transformed hopping term involves phonon operators

$$\hat{\sigma}_{ij} = T_{ij} \exp \left(\sum_{\mathbf{q}} u_i^*(\mathbf{q}) d_{\mathbf{q}}^\dagger - \text{ h.c. } \right) \exp \left(\sum_{\mathbf{q}} u_j(\mathbf{q}) d_{\mathbf{q}} - \text{ h.c. } \right). \tag{6.21}$$

There are two major effects of the electron-phonon interaction. The first one is the band narrowing due to a phonon cloud surrounding the hole. In case of a large charge Iransfer gap $E_g \gg \omega$ the bandwidth narrowing factor is the same for the direct $t_{pp'}$ and the second order via copper $t_{pp'}^{(2)}$ oxygen-oxygen transfer, Fig.6.2a,b

$$t_{pp'} \equiv \langle 0 | \hat{\sigma}_{pp'} | 0 \rangle = T_{pp'} e^{-g_{pp'}^2} \tag{6.22}$$

$$t_{pp'}^{(2)} \equiv \sum_{\nu} \frac{\langle 0 | \hat{\sigma}_{pd} | \nu \rangle \langle \nu | \hat{\sigma}_{dp'} | 0 \rangle}{E_0 - E_\nu} \simeq \frac{T_{pd}^2}{E_g} e^{-g_{pp'}^2}, \tag{6.23}$$

where $|\nu\rangle, E_\nu$ are eigenstates and eigenvalues of the transformed Hamiltonian, Eq.(6.19) without the third hopping term, $|0\rangle$ the phonon vacuum, and the reduction factor is

$$g^2_{pp'} = \frac{1}{2N}\sum_{\mathbf{q}} |\gamma(\mathbf{q})|^2 \left(1 - \cos\left[\mathbf{q}\cdot(\mathbf{m}_p - \mathbf{m}_{p'})\right]\right) \tag{6.24}$$

These expressions are the result of the straightforward calculations described below. The direct hopping is given by

$$t_{pp'} = T_{pp'}\langle 0|\exp\left(\sum_{\mathbf{q}} u^*_p(\mathbf{q})d^\dagger_{\mathbf{q}} - \text{ h.c. }\right)\exp\left(\sum_{\mathbf{q}} u_{p'}(\mathbf{q})d_{\mathbf{q}} - \text{ h.c. }\right)|0\rangle \tag{6.25}$$

With the help of $e^{A+B} = e^A e^B e^{-[AB]/2}$ one obtains

$$t_{pp'} = T_{pp'}e^{-g^2_{pp'}}\langle 0|\exp\left(\sum_{\mathbf{q}} u^*_p(\mathbf{q})d^\dagger_{\mathbf{q}}\right)\exp\left(-\sum_{\mathbf{q}} u_{p'}(\mathbf{q})d^\dagger_{\mathbf{q}}\right)|0\rangle \tag{6.26}$$

where

$$g^2_{ij} = \frac{1}{2}\sum_{\mathbf{q}}\left(|u_i(\mathbf{q})|^2 + |u_j(\mathbf{q})|^2 - 2u^*_i(\mathbf{q})u_j(\mathbf{q})\right) \tag{6.27}$$

The bracket in Eq.(6.26) is equal to unity. Then Eq.(6.22) follows from Eq.(6.26) using the definition of $u_j(\mathbf{q})$.

Taking into account that $E_\nu - E_0 = E_g + \sum_{\mathrm{q}} \omega_{\mathrm{q}} n_{\mathrm{q}}$ the second order indirect hopping Eq.(6.23) is written as

$$t^{(2)}_{pp'} = i\int_0^\infty dt e^{-iE_g t}\langle 0|\hat{\sigma}_{pd}(t)\hat{\sigma}_{dp'}|0\rangle \tag{6.28}$$

where

$$\hat{\sigma}_{pd}(t) = T_{pd}\exp\left(\sum_{\mathbf{q}} u^*_p(\mathbf{q},t)d^\dagger_{\mathbf{q}} - h.c.\right)\exp\left(\sum_{\mathbf{q}} u_d(\mathbf{q},t)d_{\mathbf{q}} - h.c.\right) \tag{6.29}$$

Here $u_j(\mathbf{q},t) \equiv u_j(\mathbf{q})\exp(i\omega_{\mathbf{q}}t)$ and $n_{\mathbf{q}} = 0, 1, 2, \ldots$ the phonon occupation numbers. Calculating the bracket in Eq.(6.28) one obtains

$$\langle \ldots \rangle = e^{-g^2_{pd}}e^{-g^2_{dp'}}\exp\left(-\sum_{\mathbf{q}}\left[u_p(\mathbf{q}) - u_d(\mathbf{q})\right]\left[u^*_d(\mathbf{q}) - u^*_{p'}(\mathbf{q})\right]e^{-i\omega\mathbf{q}^t}\right) \tag{6.30}$$

If $\omega_{\mathbf{q}}$ is $\mathbf{q}$-independent, the integral in Eq.(6.28) is calculated by the expansion of the exponent in Eq.(6.30):

$$t^{(2)}_{pp'} = \frac{T^2_{pd}}{E_g}e^{-g^2_{pd}}e^{-g^2_{dp'}}\sum_{k=o}^{\infty}\frac{(-1)^k\left(\sum_{\mathbf{q}}\left[u_p(\mathbf{q}) - u_d(\mathbf{q})\right]\left[u^*_d(\mathbf{q}) - u^*_{p'}(\mathbf{q})\right]\right)^k}{k!\,(1 + k\omega/E_g)} \tag{6.31}$$

Then Eq.(6.23) is obtained in the limit $E_g \gg \omega$.
Substitution of Eq.(6.18) into Eq.(6.24) yields

$$g^2_{pp'}, g^2 = \frac{E_p}{\omega}\left(1 - \frac{Si\,(q_d m)}{q_d m}\right) \tag{6.32}$$

if the Debye approximation for the Brillouin zone is applied. Here $\mathrm{Si}(x) = \int_0^x \sin(t)dt/t$, $m = a/\sqrt{2}$ and $m = a$ for the in-plane reduction factor $g^2_{pp'}$ and for the apex-reduction factor g^2, respectively. For $LSCO$ with $q_d \simeq 0.7\text{Å}^{-1}$ and $a \simeq 3.8$Å one obtains $g^2_{pp'} \simeq 0.2E_p/\omega$ and $g^2 \simeq 0.3E_p/\omega$ where E_p is given by Eq.(1.99). Because the nearest neighbor oxygen-oxygen distance in copper oxides is less than the lattice constant the calculations yield a remarkably lower value of $g^2_{pp'} \simeq 0.2E_p/\omega$ than one can expect with a naive estimate ($\simeq E_p/\omega$).

The other effect of the electron-phonon coupling is the attraction between two polarons given by the last term in Eq.(6.19). For the Fröhlich interaction the polaron level shift in $La_{2-x}Sr_xCuO_4$ is estimated to be as large as $E_p \simeq 0.6$eV, section 1.5. Then with $\omega = 0.06$eV one obtains $g^2_{pp'} \simeq 2$. As a result a large attraction between two polarons of the order of $2E_p \geq 1$eV is possible accompanied by only one order of magnitude mass enhancement. Such a possibility is a result of the particular lattice structure and the phonon dispersion.

The bipolaron hopping integral t is obtained by projecting the Hamiltonian, Eq.(6.19) onto the reduced Hilbert space containing only empty or doubly occupied elementary cells. The wave function of the apex bipolaron localised, say in the cell $\mathbf{m}$ is written as

$$|\mathrm{m}\rangle = \sum_{i=1}^{4} A_i c_i^\dagger c_{apex}^\dagger |0\rangle \tag{6.33}$$

where i denotes the $p_{x,y}$ orbitals and spins of the four plane oxygen ions in the cell m , Fig. 2.5 and $c^\dagger_{\mathrm{apex}}$ is the creation operator for the hole on one of the three apex oxygen orbitals with the spin, which is same or opposite to the spin of the plane hole, depending on the total spin of the bipolaron. The probability amplitudes A_i are normalised by the condition $|A_i| = 1/2$ because only four plane orbitals p_{x1}, p_{y2}, p_{x3} and p_{y4} are relevant within the three band model. The matrix element of the Hamiltonian Eq.(6.19) of the first order with respect to the transfer integral responsible for the bipolaron tunneling to the nearest neighbor cell (m + a) is

$$t = \langle \mathbf{m}|\tilde{H}|\mathbf{m}+\mathbf{a}\rangle = \frac{1}{4} T^{apex}_{pp'} e^{-g^2} \tag{6.34}$$

where $T^{apex}_{pp'}$ is the single polaron hopping between two apex ions,

$$g^2 = \frac{1}{2N} \sum_{\mathbf{q}} |\gamma(\mathbf{q})|^2 \left[1 - \cos\left(q_x a\right)\right] \tag{6.35}$$

is the polaron narrowing factor, and a is the in-plane lattice constant, which is also the nearest neighbor apex-apex distance. As a result the hole bipolaron energy spectrum in the tight binding approximation consists of two bands $E^{x,y}$ formed by the overlap of p_s and p_y apex polaron orbitals, respectively, Fig.6.2b:

$$E^x_{\mathbf{k}} = -t\cos\left(k_x\right) + t'\cos\left(k_y\right) \tag{6.36}$$
$$E^y_{\mathbf{k}} = t'\cos\left(k_x\right) - t\cos\left(k_y\right) \tag{6.37}$$

where the in-plane lattice constant is taken to be $a = 1, t$ is the renormalized hopping integral, Eq.(6.34) between p orbitals of the same symmetry elongated in the direction of the hopping ($pp\sigma$) and t' is the renormalised hopping integral in the perpendicular direction ($pp\pi$). Their ratio $t/t' = T^{apex}_{pp'}/T^{appex}_{pp'} = 4$ as follows from the tables of hopping integrals in solids (Harrison (1989)).

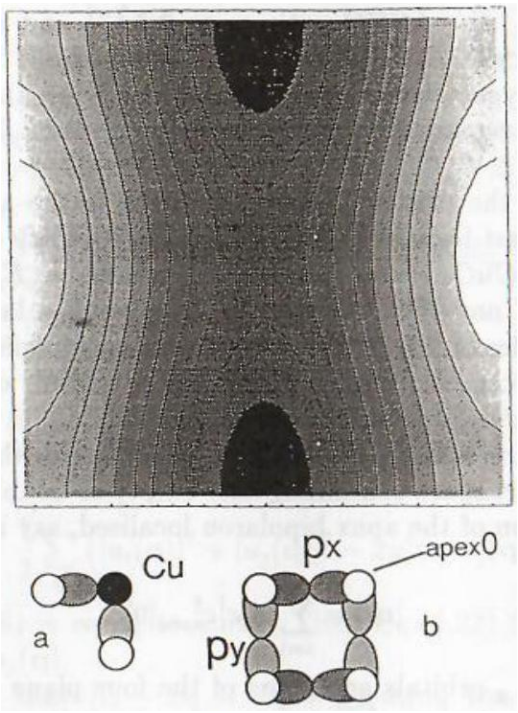

Fig.6.2. Counterplot of the 'x'-bipolaron dispersion $E_{\mathbf{k}}^{x}$. Dark regions correspond to the bottom of the band. $E_{\mathbf{k}}^{y}$ energy surfaces are obtained by $\pi/2$ rotation. Three-band model (a) and two-band

apex bipolaron model (b).

Two different bands are not mixed because $T_{p_x,p'_y}^{apex} = 0$ for the nearest neighbors. The random potential does not mix them either if it varies smoothly on the lattice scale. Consequently, we can distinguish ' x ' and ' y ' bipolarons with a lighter effective mass in x or y direction, respectively. The apex ' z ' bipolaron, if formed, is *ca.* four times less mobile than the x and y bipolarons. The bipolaron bandwidth is of the same order as the polaron one, which is a specific feature of the inter-site bipolaron discussed above. For a large part of the Brillouin zone near $(0, \pi)$ for ' x ' and $(\pi, 0)$ for ' y ' bipolaron, Fig.6.2 one can adopt the effective mass approximation

$$E_{\mathbf{k}}^{x,y} = \frac{k_x^2}{2m_{x,y}} + \frac{k_y^2}{2m_{y,x}} \tag{6.38}$$

with $k_{x,y}$ taken relative to the band bottom positions and $m_x = 1/t, m_y = 4m_x$. The bipolaron mass anisotropy has an important impact on the value of the Hall effect in high- T_c oxides (Chapter 8).

5.7.3 6.3 Bipolaron kinetics

As in the case of small polarons discussed in Chapter 4, bipolarons interact with phonons via the residual bipolaron-phonon interaction, which is a difference of the
exact and averaged with respect to phonons bipolaronic Hamiltonians

$$H_{b-ph} = \sum_{\mathbf{m}\neq\mathbf{m}'} \left(t_{\mathbf{m},\mathbf{m}'} - \hat{t}_{\mathbf{m},\mathbf{m}'}\right) b^{\dagger}_{\mathbf{m}} b_{\mathbf{m}'} + \frac{1}{2} \sum_{\mathbf{m}\neq\mathbf{m}'} \left(v^{(2)}_{\mathbf{m},\mathbf{m}'} - \hat{v}^{(2)}_{\mathbf{m},\mathbf{m}'}\right) n_{\mathbf{m}} \left(1 - n_{\mathbf{m}'}\right) \tag{6.39}$$

where

$$\hat{t}_{\mathbf{m},\mathbf{m}'} = i \int_0^{\infty} e^{-\left(i\Delta + 0^+\right)t} \left[\hat{\sigma}_{\mathbf{m},\mathbf{m}'}(t)\hat{\sigma}_{\mathbf{m},\mathbf{m}'} + \hat{\sigma}_{\mathbf{m},\mathbf{m}'}\hat{\sigma}_{\mathbf{m},\mathbf{m}'}(-t)\right] \tag{6.40}$$

and

$$\hat{v}^{(2)}_{\mathbf{m},\mathbf{m}'} = i \int_0^{\infty} e^{-\left(i\Delta + 0^+\right)t} \left[\hat{\sigma}_{\mathbf{m},\mathbf{m}'}(t)\hat{\sigma}_{\mathbf{m}',\mathbf{m}} + \hat{\sigma}_{\mathbf{m},\mathbf{m}'}\hat{\sigma}_{\mathbf{m}',\mathbf{m}}(-t)\right]. \tag{6.41}$$

The interaction is of the second order in the transfer integral $T(\mathbf{m})$, so it can be treated perturbatively by the $1/\lambda$ expansion technique. In particular, one can calculate the hopping conductivity of bipolarons in the high temperature regime $T > \omega/2$ (Bryksin and Gol'tsev (1988)). As in the case of small polarons the hopping bipolaron contribution to the conductivity is expressed in terms of the diffusion coefficient $D_b = 2a^2 W_b$. Then the drift mobility is found from the Einstein relationship $\mu_b = 2eD_b/T$, where an additional 2 appears because the bipolaron charge is $2e$. The probability W_b of a jump to the nearest neighbor site per second in the lowest fourth order with respect to the hopping integral $T(\mathbf{m})$ is found by the use of the Fermi-golden rule with the interaction term H_{b-ph} rather than with H_{p-ph}

$$W_b = \int_{-\infty}^{\infty} dt \left[\left\langle \hat{t}_{\mathbf{m},\mathbf{n}}(t)\hat{t}_{\mathbf{n},\mathbf{m}}\right\rangle - t^2_{\mathbf{m},\mathbf{n}}\right] e^{-0^+|t|} \tag{6.42}$$

Here $|\mathbf{m} - \mathbf{n}| = a$ and $\hat{t}_{\mathbf{m},\mathbf{n}}(t) = \exp\left(iH_{ph}t\right)\hat{t}_{\mathbf{m},\mathbf{n}} \exp -iH_{ph}t$ is the Heisenberg hopping operator. If there is a phonon frequency dispersion, only the first saddle-point contributes to the integral in Eq.(6.42) with the following result

$$\mu_b \simeq ea^2 \frac{64\pi^{3/2} T^4(\mathbf{a})}{\omega^2 \sqrt{TE_a}\left(\Delta + 4E_a\right)} \exp\left[\frac{-\left(\Delta + 4E_a\right)^2}{16E_a T}\right], \tag{6.43}$$

where E_a is a single polaron activation energy, determined in Eq.(4.107). Because of the small exponential term in Eq.(6.43) the on-site bipolaron hopping mobility is lower compared with the contribution of the thermally excited polaron despite the fact that the polaron density is exponentially small ($\sim \exp(-\Delta/2T)$) compared with the bipolaron one. The on-site bipolaron contribution to the *dc* conductivity is small compared with the polaron contribution as $\sigma_b/\sigma_p \sim \exp\left(-\Delta^2/16E_aT\right)$. However, as the frequency of the electric field increases, the dominant role in conductivity is gradually transferred to bipolarons, as discussed in the next section. In the absence of the Coulomb repulsion the bipolaron binding energy is $\Delta \simeq 2E_p \simeq 4E_a$ and consequently, the bipolaron mobility obeys the law $\mu_b \sim \exp\left(-4E_a/T\right)$. This has a simple explanation because in this case the bipolaron jump is equivalent to a single polaron jump but with a double coupling constant with phonons. Of course, internite bipolarons with the activation energy of the same order as the single polaron activation energy dominate both in the *dc* and *ac* transport at all temperatures $T < T^{"}$. Also, at low temperatures $T < \omega/2$ we expect that the tunneling mechanism
will play the dominant role. In this temperature range bipolaron kinetics is that of charged bosons on a lattice, while the tunneling contribution of the thermally excited single polarons is frozen out. Low temperature bipolaron kinetics is discussed in Chapter 7.

5.7.4 6.4 MIR conductivity of small bipolarons

The frequency dependence of the MIR bipolaron conductivity can be estimated using the two-site Holstein model with two electrons and the Franck-Condon principle, which states that optical transitions take place instantaneously without any change in the nuclear configuration. Consequently, the optical transition between adiabatic levels takes place vertically as in the case of a single polaron, Fig.4.5. The corresponding qualitative analysis by Bryksin and Voloshin (1984) shows that the absorption coefficient of light by the on-site bipolaron has three Gaussian peaks located at frequencies $\nu_1 = 4E_a, 8E_a - U$ and $16E_a$. The lowest peak corresponds to the absorption by single thermally excited polarons. The highest peak is due to the shakeoff of phonons without dissociation of the bipolaron while the main central peak is the absorption involving dissociation. The value of the lowest single polaron peak is exponentially small ($\sim \exp(-2E_a/T)$) compared with the two high frequency absorption maxima, while the highest peak is smaller compared with the main central peak due to an additional factor $\sim J^2$. The width of the high-frequency peak, which is $\sim 8\sqrt{E_a T}$ is twice the width of the two low-frequency peaks. If the on-site Coulomb repulsion is absent, $U = 0$ the main maximum of the MIR conductivity is shifted relative to the maximum of the single polaron conductivity, section 4.10 by the value $\simeq 2E_p$ towards the high frequency region. The explanation is that the polaron shift of the atomic level is proportional to the square of the ion displacement, as is always the case in the harmonic approximation. Consequently, the polaron shift becomes $4E_p$ for two electrons on the same site compared with $2E_p$ when the electrons occupy different sites.

The exact diagonalisation of the two-site Holstein model in the truncated Hilbert space up to 50 phonons allows us to carry out the quantitative analysis of the bipolaronic MIR conductivity (Alexandrov et al (1994b)). In the case of two electrons in a two-site cluster the ground state changes essentially due to the formation of a bipolaron. If the electron-electron repulsion is weak optical properties will be determined by the excitation of a bipolaron in the state of two unpaired electrons. On the other hand, in the case of strong Hubbard U, the ground state corresponds to unpaired electrons and the main peak in $\sigma(\nu)$ is expected to be for $\nu \sim U$. The evolution of $\sigma(\nu)$ with increasing for two-site cluster with two electrons is shown in Fig.6.3 for $T = 0$. For $U = 0$ (Fig.6a) we found one peak in $\sigma(\nu)$ in the high energy region $\nu \simeq 4E_p$. This peak also shows the additional phonon superstructure, Other peaks are absent. If U increases, peak in $\sigma(\nu)$ shifts to the lower value of ν. This is due to the fact that the finite value of U reduces the binding energy of the the peak has well defined asymmetry (Fig. Further increase of U round

of U leads to the change of the ground state. A bipolaron is no longer the ground state. It leads to the appearance of an additional peak in $\sigma(\nu)$. These two peaks state. It leads to the appearance of an additional peak in $\sigma(\nu)$. These two peak (Fig.6c,d) correspond to the excitation of an electron from the unpaired ground state to bonding and antibonding paired states $|\phi_\pm\rangle \sim \left(c^+_{1\uparrow}c^+_{2\downarrow} \pm c^+_{1\downarrow}c^+_{2\uparrow}\right)|0\rangle$. The lineshape in that case is also asymmetric. The observed spectral shape of the spectrum and the

phonon superstructure strongly suggest small lattice polarons as the common origin of the MIR conductivity in all perovskite materials, Chapter 8. If one accepts that the high energy MIR maximum at $\nu \simeq 0.7$eV in the high- $T_c YBCO$ is due to inter-site bipolarons and the gap, observed with the tunneling, IR reflectivity, photoemission, and with the electron energy loss spectroscopy $2\Delta \simeq 8T_c$ is the bipolaron binding energy one can estimate E_p and the characteristic inter-site Coulomb repulsion V_c. If we adopt in a qualitative analysis a similar shape of the on-site and the inter-site bipolaron absorption the position of the maximum of the inter-site bipolaron absorption is given by $\nu = 4E_p - V_c$ and $2\Delta = 2E_p - V_c$. With $\nu = 0.7$eV and $2\Delta = 0.07$eV we obtain $E_p \simeq 0.3$eV and $V_c = 0.5$eV. This value of E_p is close to that obtained with ther the appropriate electron-phonon interaction constant ($\lambda \sim 1 - 2$). The value of V_c is close to the estimation of the inter-site Coulomb repulsion with the high-frequency dielectric constant $\epsilon = 5$.

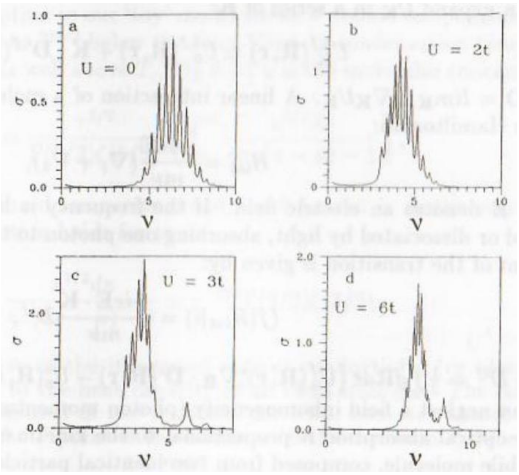

Fig.6.3. Two-site bipolaronic optical conductivity for different values of the on-site Hubbard repulsion $U, \omega = 0.5J$, and $\lambda = 0.8$.

5.7.5 6.5 Effect of superconducting phase transition on MIR conductivity

It is difficult to study the temperature dependence of the MIR conductivity on the temperature scale compared with the critical temperature of the superconducting phase transition T_c within the finite cluster model. Also, in the qualitative connideration of the preceding section the tunneling transport of bipolarons is ignored. Nevertheless, the temperature dependence of the integrated bipolaronic MIR conductivity can be studied by the use of the Kubo sum rule (Alexandrov et al (1993)). Let us discuss first a simple but rather general model which show a hundred percent decrease of the optical absorption while temperature changes from T_c to zero: an ideal gas of molecules, composed of two identical particles (electrons) on a lattice. To stabilize their bound state one should assume that the pair attraction operates, compensating the Coulomb repulsion. All molecules are in the ground internal state
with the binding energy being much higher than temperature. The periodic crystal field is assumed to be large compared with the binding energy, so all molecular states, including continuum, are built from the single-band single-electron Bloch wave functions.

Because of the translation symmetry the molecular wave function is a two-particle Bloch function described with the total quasi-momentum $\mathbf{K}$:

$$\Psi^{i,f}(\mathbf{r}_1, \mathbf{r}_2) = \exp(i\mathbf{K} \cdot \mathbf{R}) U^{i,f}_{\mathbf{K}}(\mathbf{R}, \mathbf{r}) \tag{6.44}$$

where $\mathbf{R} = (\mathbf{r}_1 + \mathbf{r}_2)/2, \mathbf{r} = \mathbf{r}_1 - \mathbf{r}_2$, and $U_{\mathbf{K}}(\mathbf{R}, \mathbf{r})$ is periodic with the lattice translations. At low temperatures only states with small K (near Γ point) are relevant, so one can expand $U_{\mathbf{K}}$ in a series of $\mathbf{K}$:

$$U^{i,f}_{\mathbf{K}}(\mathbf{R}, \mathbf{r}) \simeq U^{i,f}_0(\mathbf{R}, \mathbf{r}) + \mathbf{K} \cdot \mathbf{D}^{i,f}(\mathbf{R}, \mathbf{r}) \tag{6.45}$$

with $\mathbf{D} = \lim_{\mathbf{K}\to 0} \nabla_{\mathbf{K}} U_{\mathbf{K}}$. A linear interaction of a molecule with light is described by the Hamiltonian:

$$H_{int} = \frac{-ie\mathbf{E}}{m\nu} (\nabla_1 + \nabla_2) \tag{6.46}$$

where $\mathbf{E}$ denotes an electric field. If the frequency is high enough the molecule is excited or dissociated by light, absorbing one photon to the final state f. The matrix element of the transition is given by:

$$\langle f|H_{int}|i\rangle = \frac{-ie\mathbf{E}\cdot\mathbf{K}}{m\nu}D^{if} \tag{6.47}$$

where $D^{if} = \frac{1}{3}\int d\mathbf{R}d\mathbf{r}\left(U_0^f(\mathbf{R},\mathbf{r})^*\nabla_{\mathbf{R}}\cdot\mathbf{D}^i(\mathbf{R},\mathbf{r}) - U_0^i(\mathbf{R},\mathbf{r})\nabla_{\mathbf{R}}\cdot\mathbf{D}^f(\mathbf{R},\mathbf{r})^*\right)$. As usual one can neglect a field inhomogeneity (photon momentum). From Eq.(6.47) the rate of the optical absorption is proportional to the kinetic energy of a molecule, and an immobile molecule, composed from two identical particles cannot absorb, which is a trivial consequence of parity and spin conservation. The dipole matrix element for the Γ point is equal zero because all singlet states of a molecule with $\mathbf{K} = 0$ are even and all triplets are odd under the inversion transformation, $\mathbf{R}, \mathbf{r} \to -\mathbf{R}, -\mathbf{r}$, for a lattice with the inversion symmetry. This is similar to the dipole-forbidden singleelectron transitions in semiconductors. The matrix element, Eq.(6.47), increases with increasing K. It is now the essence of our argument that the occupancy at $K \neq 0$ is a thermodynamic function, which 'sees' the Bose condensation and, thus, allows us to measure the condensation directly via optical absorption. The Fermi-golden rule yields the optical conductivity:

$$\sigma(\nu) = \frac{4\pi e^2}{3m\nu}E_k\sum_f \left|D^{if}\right|^2\delta\left(\epsilon_f - \epsilon_i - \nu\right) \tag{6.48}$$

where $\epsilon_{i,f}$ is the energy spectrum of a single molecule, including its continuous part and

$$E_k = \sum_{\mathbf{K}}\frac{K^2}{4m}n(\mathbf{K}) \tag{6.49}$$

is the kinetic energy of all molecules, which obey the Bose-Einstein distribution with the chemical potential $\mu, n(\mathbf{K}) = \left(\exp\frac{K^2/4m-\mu}{T} - 1\right)^{-1}$. Integrating Eq.(6.48) over the frequency we obtain the conductivity sum rule for our system:

$$I(T) = \int_0^\infty d\nu\sigma(\nu) = \pi e^2 a^2 E_k \tag{6.50}$$

where

$$a^2 = \frac{4}{3m}\sum_f \frac{\left|D^{if}\right|^2}{\epsilon_f - \epsilon_i} \tag{6.51}$$

and a is a temperature independent characteristic length of the order of the molecular radius (a cubic lattice is assumed).

Thus the optical absorption in our 'toy' model shows a drastic temperature dependence, being proportional to $T^{5/2}$ below the Bose-Einstein condensation temperature $T_c = 3.3n^{2/3}/2m$ and linear well above T_c, Fig. 6.4 (n is the molecular concentration),

$$\frac{I(T)}{I\left(T_c\right)} = \frac{\tau^{5/2}}{\Gamma(5/2)\zeta(5/2)}\left(\int_0^\infty \frac{x^{3/2}dx}{\exp(x-\mu)-1}\right) \tag{6.52}$$

where $\tau = T/T_c$ is the reduced temperature and $\mu = 0$ for $\tau < 1$. In the normal state ($\tau > 1$) the following equation holds for μ :

$$\int_0^\infty \frac{x^{1/2}dx}{\exp(x-\mu)-1} = \tau^{-3/2}\Gamma(3/2)\zeta(3/2) \tag{6.53}$$

The temperature derivative of the integrated optical conductivity (or absorption), $dI(T)/dT$ is proportional to the heat capacity of an ideal Bose-gas. The condensed fraction of molecules,

composed of two identical particles, does not absorb light, if bosons are condensed at the Γ point of the lattice with the inversion symmetry.

Toy model

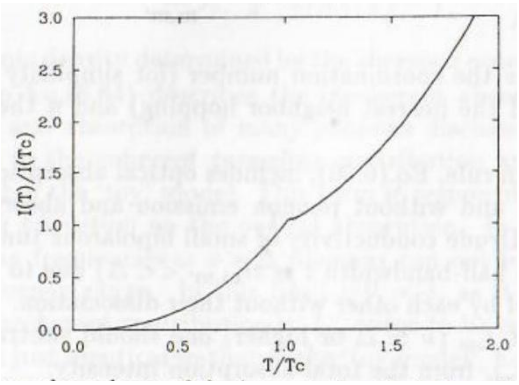

Fig.6.4. Temperature dependence of the integrated optical absorption of free bosons composed from two identical particles on a lattice.

To analyse the temperature dependence of the integrated MIR conductivity of bipolarons we apply the Kubo (1957) sum rule. The real part of the conductivity is

$$\sigma_{xx}(\nu) = \pi \sum_f |\langle 0|J_x|\, f\rangle|^2 \frac{\delta\left(\nu - E_f + E_0\right)}{E_f - E_0} \tag{6.54}$$

where $|0\rangle$ and $|f\rangle$ are the ground and excited states of the total Hamiltonian, including the electron-phonon interaction term. The current operator is

$$\mathbf{J} = ie \sum_{\mathbf{m},\mathbf{m}',s} (\mathbf{m}' - \mathbf{m})\, T\left(\mathbf{m} - \mathbf{m}'\right) c^{\dagger}_{\mathbf{m},s} c_{\mathbf{m}',s} \tag{6.55}$$

It satisfies the equation

$$\mathbf{J} = ie[H, \mathbf{X}] \tag{6.56}$$

where $\mathbf{X}$ is the sum of the position operators of the electrons:

$$\mathbf{X} = \sum_{\mathbf{m},s} \mathbf{m} c^{\dagger}_{\mathbf{m},s} c_{\mathbf{m},s} \tag{6.57}$$

Integrating over frequency Eq.(6.54) and using the identity Eq.(6.56) one obtains:

$$\int_0^{\infty} \sigma_{xx}(\nu) d\nu = \frac{ie\pi}{2} \langle 0|\,[X, J_x]\,|0\rangle \tag{6.58}$$

which yields after the direct substitution of Eq.(6.55,57)

$$I(T) = \frac{\pi e^2 a^2}{2} \left\langle - \sum_{\mathbf{m},\mathbf{m}',s} T\left(\mathbf{m} - \mathbf{m}'\right) c^{\dagger}_{\mathbf{m},s} c_{\mathbf{m}'s} \right\rangle \tag{6.59}$$

where a is the lattice constant. To calculate the kinetic energy of the strongly coupled electron-phonon system up to the second order in the transfer integral with the accuracy $\sim 1/\lambda^2$ one can apply the polaronic S and bipolaronic S_2 canonical transformations to Eq.(6.59) with the following result:

$$I(T) = \frac{\pi e^2 a^2}{2}\left(2v^{(2)}\left(n - \langle n_{\mathbf{m}} n_{\mathbf{m+a}}\rangle\right) + 2\left\langle \sum_{\mathbf{m},\mathbf{m}'} t_{\mathbf{m},\mathbf{m}'} b^{\dagger}_{\mathbf{m}} b_{\mathbf{m}'}\right\rangle\right) \tag{6.60}$$

with $v^{(2)} = z v^{(2)}_{\mathbf{m},\mathbf{m+a}}, z$ the coordination number (for simplicity we consider cubic or quadratic lattice and the nearest neighbor hopping) and n the bipolaron atomic density.

The conductivity sum rule, Eq.(6.60), includes optical absorption due to the bipolaron dissociation with and without phonon emission and absorption. It includes also the low-frequency Drude conductivity of small bipolarons tunneling in the bipolaron narrow band (the half-bandwidth $t = z t_{\mathbf{m},\mathbf{m}'} \ll \Delta$) due to their scattering by phonons, impurities and by each other without their dissociation. If one is interested only in the optical part $I_{\rm opt}$ ($\nu \simeq \Delta$ or higher) one should subtract the bipolaronic Drude contribution $I_{\rm Drude}$ from the total absorption intensity:

$$I(T) = I_{\rm opt}\,(T) + I_{\rm Drude}\,(T) \tag{6.61}$$

To derive the integrated bipolaronic Drude conductivity, $I_{\rm Drude}$ one can apply the sum rule to the bipolaronic Hamiltonian, Eq.(6.9), keeping in mind that bipolarons have charge $2e$

$$I_{\rm Drude}\,(T) = \frac{4\pi e^2 a^2}{2}\left\langle \sum_{\mathbf{m},\mathbf{m}'} t_{\mathbf{m},\mathbf{m}'} b^{\dagger}_{\mathbf{m}} b_{\mathbf{m}'}\right\rangle \tag{6.62}$$

Subtracting Eq.(6.62) from Eq.(6.60) one obtains:

$$I_{opt} = \pi e^2 a^2\left[v^{(2)}\left(n - \langle n_{\mathbf{m}} n_{\mathbf{m+a}}\rangle\right) - \left\langle \sum_{\mathbf{m},\mathbf{m}'} t_{\mathbf{m},\mathbf{m}'} b^{\dagger}_{\mathbf{m}} b_{\mathbf{m}'}\right\rangle\right] \tag{6.63}$$

Let us consider a low-density regime. As we shall discuss in section 6.7 the ground state of our system is a homogeneous Bose-liquid, in which the tendency to charge order is suppressed by quantum fluctuations if $n < n_c$. The critical value of the dencity n_c above which the charge density wave develops turns out to be independent of the repulsion if the latter is strong $v + v^{(2)} \gg t$, where $t = z t(\mathbf{a})$ is the half width of the bipolaronic band. For a cubic lattice $n_c \simeq 0.08$. If the repulsion between bipolarons has a moderate value $v + v^{(2)} < 3t$ the homogeneous Bose-liquid is stable versus the charge ordering practically in the whole density region. In a homogeneous repulsive Bose-liquid the short range pair correlation function $g(r) = \langle n(0) n(r)\rangle / n^2$ is small. As example in liquid $He^4 g(r) < 0.2$ for $r < 2.5A$. The temperature dependent part of this correlator is even smaller. Thus the contribution to the conductivity sum rule, Eq.(6.63) of the term quadratic in the bipolaron density is practically temperature independent and negligible for the homogeneous strongly repulsive Bose-liquid. In the dilute limit one can also neglect the corrections to the free particle energy spectrum, which are small while the gas parameter is small. These simplifications yield:

$$I_{opt}(T) = \pi e^2 a^2\left[\left(v^{(2)} - t\right) n(T) + \int_0^{2t} \frac{\epsilon N_b(\epsilon) d\epsilon}{y^{-1}\exp(\epsilon/T) - 1}\right] \tag{6.64}$$

where $N_b(\epsilon)$ is the density of states in a narrow bipolaronic band, and

$$n(T) = \int_0^{2t} \frac{N_b(\epsilon) d\epsilon}{y^{-1}\exp(\epsilon/T) - 1} \tag{6.65}$$

is the bipolaron atomic density determined by the chemical potential $\mu, y = \exp(\mu/T)$. The first term in Eq.(6.64) describes the incoherent absorption of light accompanied by emission and absorption of many phonons discussed in section 6.4. The second term is due to the coherent tunneling contribution and is identical to that discussed above within the 'toy' model. This

term is responsible for the influence of the superconducting transition on the optical absorption. In the limit of very high diaracteristic phonon frequencies $\omega \gg \Delta$ phonons can not be emitted or absorbed in the relevant frequency range. In this limit $v^{(2)} = t$, as it was shown in section 6.1. If $v^{(2)} = t$ the incoherent contribution to $I_{\rm opt}$ turns to be zero, and the integrated optical absorption is just identical to that of the 'toy model', Eq.(6.52), at least in the low-temperature region, when the band energy dispersion is practically parabolic. In diis case $I_{\rm opt}\,(0) = 0$. On the other hand if the phonon frequencies are comparable or leas than the bipolaron binding energy, $v^{(2)}$ does not contain the polaronic narrowing factor and is larger than t. In this more realistic case the absorption at $T = 0$ is finite and the coherent contribution is not very large, less than 10% of the total intensity.

To describe the temperature dependence of the infrared absorption in a wide temperature range in the normal state, compared with Δ one has to take into account the Inermal dissociation of the bipolaron on two small polarons. Restricting ourselves by
the quasi two-dimensional lattice with the constant density of polaronic and bipolaronic states within the polaronic and bipolaronic bands $N_p(\epsilon) = 1/2w, N_b(\epsilon) = 1/2t$ respectively, one obtains

$$\frac{I_{opt}(T)}{I_{opt}(0)} = \frac{2n(T)}{n_e} + \delta_c \frac{T^2}{T_c^2} \int_0^{2t/T} \frac{xdx}{y^{-1}\exp(x) - 1} \tag{6.66}$$

with

$$\delta_c = \frac{T_c^2}{t\,(v^{(2)} - t)\,n_e}. \tag{6.67}$$

The parameter δ_c determines the relative contribution of the coherent motion to the kinetic energy of the system and because normally $v^{(2)} \gg t > T_c/n_e$ this parameter is small, of the order of 0.1 or less. Here n_e is the electron (hole) atomic density, which is assumed to be temperature independent. Taking into account the upper polaronic band with the half bandwidth $w = tm^{**}/m^*$ one obtains the following equation for the chemical potential in the normal state ($T > T_c$):

$$\ln\left(\frac{1 - y\exp(-2t/T)}{1-y}\right) + \frac{m^*}{m^{**}} \ln\left(\frac{1 + \sqrt{y}\exp(-\Delta/2T)}{1 + \sqrt{y}\exp\left(-\Delta/2T - 2tm^{**}/m^*T\right)}\right) = \frac{tn_e}{T}. \tag{6.68}$$

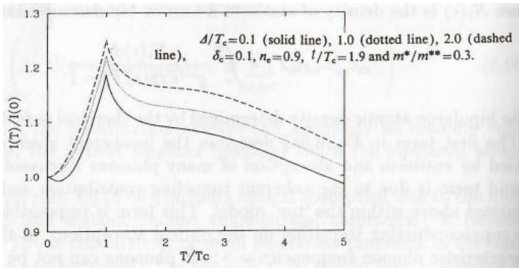

Fig.6.5. Temperature dependence of the integrated optical absorption of onsite small bipolarons

The ratio of the polaronic m^* and bipolaronic m^{**} effective masses is small in the case of onsite bipolarons. This fact enables us to neglect the polaronic contribu tion to the integrated optical absorption. The polaronic absorption is shifted to the low-frequency (Drude) region. In the superconducting phase $T < T_c$ the chemical potential is zero, so $y = 1$. The temperature dependence of the integrated intensity

$$\frac{I_{opt}(T)}{I_{opt}(0)} = 1 - \frac{m^*T}{2tm^{**}} \ln\left(\frac{1+\sqrt{y}\exp(-\Delta/2T)}{1+\sqrt{y}\exp\left(-\Delta/2T - 2tm^{**}/m^*T\right)}\right)$$
$$+\delta_c \frac{T^2}{T_c^2}\int_0^{2t/T} \frac{xdx}{y^{-1}\exp(x)-1} \tag{6.69}$$

calculated for three different values of the binding energy Δ/T_c is shown in Fig.6.5. Because the relative density of states in the polaronic band is small ($\sim m^*/m^{**}$) the temperature dependence of the on-site bipolaron concentration is weak except in the case of a very low binding energy.

It is well known that for frequencies much higher than the superconducting energy gap no change with temperature in optical absorption is expected within the BCS theory. However, a rather significant change with temperature of the MIR absorption is expected at the superconducting transition as a result of the Bose-Einstein condensation of small bipolarons in bipolaronic superconductors.

5.7.6 6.6 Pseudospin representation of the bipolaronic Hamiltonian

Bipolarons are not perfect bosons. In the subspace of pairs their commutation relations are those of Pauli matrices. Therefore, the 'pseudospin' representation of the bipolaronic Hamiltonian is convenient (Alexandrov and Ranninger (1981a)). We rewrite the bipolaronic Hamiltonian for a perfect lattice in the form

$$H_b = -\mu\sum_{\mathbf{m}} n_{\mathbf{m}} + \sum_{\mathbf{m}\neq\mathbf{m}'}\left(\frac{1}{2}\bar{v}_{\mathbf{m}\mathbf{m}'}n_{\mathbf{m}}n_{\mathbf{m}'} - t_{\mathbf{m}\mathbf{m}'}b^\dagger_{\mathbf{m}}b_{\mathbf{m}'}\right), \tag{6.70}$$

where the energy of a single localised bipolaron is included in the definition of the bipolaron chemical potential μ. The bipolaron operators obey the mixed commutation rules in a subspace of empty or doubly occupied sites (cells)

$$b_{\mathrm{m}}b^\dagger_{\mathrm{m}} + b^\dagger_{\mathrm{m}}b_{\mathrm{m}} = 1 \tag{6.71}$$

and

$$b_{\mathbf{m}}b^\dagger_{\mathbf{m}'} - b^\dagger_{\mathbf{m}'}b_{\mathbf{m}} = 0 \tag{6.72}$$

for $\mathbf{m} \neq \mathbf{m}'$. This makes useful the pseudospin analogy

$$b^\dagger_{\mathrm{m}} = S^x_{\mathrm{m}} - iS^y_{\mathrm{m}} \tag{6.73}$$

and

$$b^\dagger_{\mathrm{m}}b_{\mathrm{m}} = \frac{1}{2} - S^z_{\mathrm{m}} \tag{6.74}$$

with the spin(pseudo)1/2 operators $S^{x,y,z} = \frac{1}{2}\tau_{1,2,3}$. $S^z = 1/2$ corresponds to an empty cell and $S^z = -1/2$ to a cell occupied by a bipolaron. The spin operators preserve the bosonic character of bipolarons if they are on different cells and their fermionic (or hard core) internal structure. Replacing bipolarons for the spin operacore we transform the bipolaronic Hamiltonian into the familiar anisotropic Heisenberg Hamiltonian

$$H_b = \mu\sum_{\mathbf{m}} S^z_{\mathbf{m}} + \sum_{\mathbf{m}\neq\mathbf{m}'}\left(\frac{1}{2}\bar{v}_{\mathbf{m}\mathbf{m}'}S^z_{\mathbf{m}}S^z_{\mathbf{m}'} - t_{\mathbf{m}\mathbf{m}'}\left(S^x_{\mathbf{m}}S^x_{\mathbf{m}'} + S^y_{\mathbf{m}}S^y_{\mathbf{m}'}\right)\right) \tag{6.75}$$

with the bipolaron chemical potential playing the role of an external magnetic field. This Hamiltonian has been investigated in detail as a relevant form for magnetism and also for quantum solids like a lattice model for He^4. However, while in those cases the magnetic field is an independent thermodynamic variable, in our case it is fixed by the total 'magnetization' because the bipolaron density n is conserved

$$\frac{1}{N}\sum_{\mathrm{m}}\langle\langle S^z_{\mathrm{m}}\rangle\rangle = \frac{1}{2} - n \tag{6.76}$$

That leads to an important difference in the phase diagram and the excitation spectrum.

5.7.7 6.7 Superfluid versus charged ordered ground state

For the ground state one can apply a mean field approach introducing an average magnetic field $\mathbf{H_m}$ acting on a spin $\mathbf{m}$. In the nearest-neighbor approximation

$$\mathbf{H_m} = -\left(\mu + 2\bar{v}\left\langle S^z_{\mathbf{m}'}\right\rangle\right)\mathbf{e} + 2t\left\langle \mathbf{S}^{\perp}_{\mathbf{m}'}\right\rangle \tag{6.77}$$

where $\bar{v} = \frac{z}{2}\bar{v}_{\mathbf{mm}'}, t = zt_{\mathbf{mm}'}, \mathbf{m}' = \mathbf{m} + \mathbf{a}, \mathbf{e}$ is a unit vector in the z-direction, and $\mathbf{S}^{\perp}_{\mathbf{m}}$ is a spin component perpendicular to z. In the absence of the macroscopic current $\langle S^y\rangle = 0$ and at $T = 0$

$$\langle S^z_{\mathrm{m}}\rangle = \frac{1}{2}\cos\Theta \tag{6.78}$$

$$\langle S^x_{\mathrm{m}}\rangle = \frac{1}{2}\sin\Theta \tag{6.79}$$

where Θ is the angle between z-axis and spin. The ground state has $\langle\mathbf{S_m}\rangle$ parallel to $\mathbf{H_m}$ and we arrive at the following set of equations for Θ and μ

$$\sin\Theta = \frac{t\sin\Theta'}{\sqrt{\left(\mu + \bar{v}\cos\Theta'\right)^2 + t^2\sin^2\Theta'}} \tag{6.80}$$

$$\cos\Theta = -\frac{\mu + \bar{v}\cos\Theta'}{\sqrt{\left(\mu + \bar{v}\cos\Theta'\right)^2 + t^2\sin^2\Theta'}} \tag{6.81}$$

$$\cos\Theta + \cos\Theta' = 2(1-2n) \tag{6.82}$$

where Θ' is the angle for the nearest neighbors.
Two solutions to Eq.(6.80-82) are possible. The first one is a 'ferromagnetic' solution

$$\cos\Theta = \cos\Theta' = 1 - 2n \tag{6.83}$$

and

$$\mu = -(1-2n)(\bar{v} + t) \tag{6.84}$$

In the 'ferromagnetic' state bipolarons are distributed uniformly over the lattice willi the density per site n. The total energy of this state

$$\frac{E_f}{N} = -\frac{t}{4}\left(1 + (1-2n)^2\left(1 + \frac{\bar{v}}{t}\right)\right) \tag{6.85}$$

The second solution is an 'antiferromagnetic' one with two sublattices with different Θ and Θ',

$$\cos\Theta = 1 - 2n + \sqrt{1 + (1-2n)^2 - \frac{2(1-2n)\bar{v}}{\sqrt{\bar{v}^2 - t^2}}} \tag{6.86}$$

$$\cos\Theta' = 1 - 2n - \sqrt{1 + (1-2n)^2 - \frac{2(1-2n)\bar{v}}{\sqrt{\bar{v}^2 - t^2}}} \tag{6.87}$$

It exists if only $\bar{v} > t$ and the density is sufficiently high

$$n > n_c = \frac{1}{2}\left(1 - \sqrt{\frac{\bar{v}-t}{\bar{v}+t}}\right) \tag{6.88}$$

In the region of its existence the 'antiferromagnetic' state is a ground state because

$$E_a = -\frac{\bar{v}N}{4} < E_f \tag{6.89}$$

The conclusion is that the bipolarons exist at $T = 0$ in two states: as a homogeneous quantum liquid resembling He^4 or at high density as a mixture of an inhomogeneous Bose-Einstein condensate ($\sin\Theta \neq \sin\Theta' \neq 0$) and a charge density wave $\cos\Theta \neq \cos\Theta'$. At a very low density the Wigner crystallization of charged bipolarons is feasible because of their long-range Coulomb repulsion.

5.7.8 6.8 Excitation spectrum of the bipolaronic liquid

One can expect that the excitation spectrum is similar to that of a Heisenberg magnet and one-particle excitations are 'magnons'. At $T = 0$ one can write down the equation of the 'spin' motion

$$\frac{d\mathbf{S_m}}{dt} = \mathbf{H_m} \times \mathbf{S_m} \tag{6.90}$$

We allow each 'spin' besides its static component Eq. (6.78, 79) to have a small time and space dependent part

$$\delta\mathbf{S}\exp(i\mathbf{k}\cdot\mathbf{m} - i\omega t) \tag{6.91}$$

Irom Eq.(6.90) one obtains

$$-i\omega\delta S^x = -t\delta S^y \sin\Theta' \cot\Theta + (t - E_\mathbf{k})\,\delta S'^y \cos\Theta \tag{6.92}$$

$$-i\omega\delta S^y = t\delta S^x \sin\Theta' \cot\Theta - (t - E_\mathbf{k})\,\delta S'^x \cos\Theta$$
$$- t\delta S^z \sin\Theta' - \frac{\bar{v}}{t}(t - E_\mathbf{k})\,\delta S'^z \sin\Theta \tag{6.93}$$

$$-i\omega\delta S^z = t\delta S^y \sin\Theta' - (t - E_\mathbf{k})\,\delta S'^y \sin\Theta \tag{6.94}$$

Where $E_\mathbf{k} = \sum_{\mathbf{m}'} t_{\mathbf{m}\mathbf{m}'}\left[1 - \exp\left(i\mathbf{k}\cdot(\mathbf{m} - \mathbf{m}')\right)\right]$ is the energy dispersion of a single hipularon on a lattice. The condition of the existence of a nontrivial solution yields Hee excitation spectrum of the 'ferromagnetic' ground state $\omega = \epsilon_\mathrm{k}$:

$$\epsilon_\mathbf{k} = \sqrt{E_\mathbf{k}\left(t + [\bar{v} - (1-2n)^2(\bar{v}+t)]\left(1 - \frac{E_\mathbf{k}}{t}\right)\right)} \tag{6.95}$$

with **k** varying in the first Brillouin zone (for intersite bipolarons in a simple lattice it is half of the original one). In the long-wave limit $k \to 0$ this spectrum is sound-like like as in He^4, Fig.6.6f,

$$\epsilon_{\mathrm{k}} = sk \tag{6.96}$$

with the 'sound' velocity

$$s = 2a\sqrt{\frac{t(\bar{v}+t)n(1-n)}{z}} \tag{6.97}$$

The linear dispersion is, of course, the consequence of the nearest neighbor approximation, used here. The long-range Coulomb interaction yields the plasma gap in three dimensions and the square root dispersion in $2D$ (Chapter 7).

When the density is critical $n = n_c$, the spectrum is given by

$$\epsilon_{\mathbf{k}} = \sqrt{E_{\mathbf{k}}\,(2t - E_{\mathbf{k}})} \tag{6.98}$$

and the critical velocity $v_c = \min \frac{\epsilon_k}{k}$ is zero, Fig 6.6f.

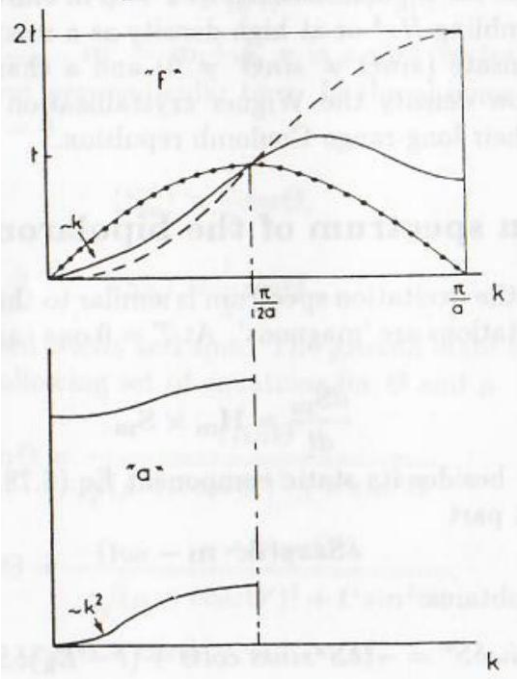

Fig.6.6. The excitation spectrum (solid lines) of $BS(f)$ and $M(a)$ ground states. Dashed line refers to a single bipolaron, dotted line to $n=n_{c}$.

Above n_c the charge density wave develops and the excitation spectrum consists of two branches

$$\epsilon^{\pm}_{\mathbf{k}} = \sqrt{\gamma^2 t^2 + E_{\mathbf{k}}\,(2t - E_{\mathbf{k}}) \pm \gamma t\sqrt{\gamma^2 t^2 + 2E_{\mathbf{k}}\,(2t - E_{\mathbf{k}})}} \tag{6,99}$$

with

$$\gamma^2 = 2\frac{\bar{v}^2 - t^2}{t^2}\left(1 + (1-2n)^2 - 2(1-2n)\frac{\bar{v}}{\sqrt{\bar{v}^2 - t^2}}\right) \tag{6.100}$$

and k varying in a new Brillouin zone, Fig.6.6a. In the long-wave limit

$$\epsilon^{+} = t\gamma\sqrt{2} \tag{6.101}$$

and

$$\epsilon^{-} \sim k^2 \tag{6.102}$$

The gap in the spectrum is of order of $\bar{v}$ if $\bar{v} \gg t$.

5.7.9 6.9 $T - n$ phase diagram of the bipolaronic liquid

At finite temperatures thermal as well as quantum fluctuations are important. It is clear that under the condition $\bar{v} \gg t$ the off-diagonal long range order ($ODLRO$) (i.e. the Bose-Einstein condensate) disappears first with increasing temperature at $T \sim t$, followed by the disappearance of the charge ordered state ($DLRO$) at $T \sim \bar{v}$. At temperatures $\bar{v} < T < T^{**}$ an unusual metal of nondegenerate bipolarons exists with an elementary charge $2e$. As a result the $T - n$ phase diagram of a bipolaronic liquid consists of four phases. Two of them are the low-temperature phases: a bipolaronic superfluid (BS) and a mixed phase (M) with $ODLRO$, described above and two high-temperature phases, one of them is an unusual metal (N) and the other is a charge-ordered state (CO).

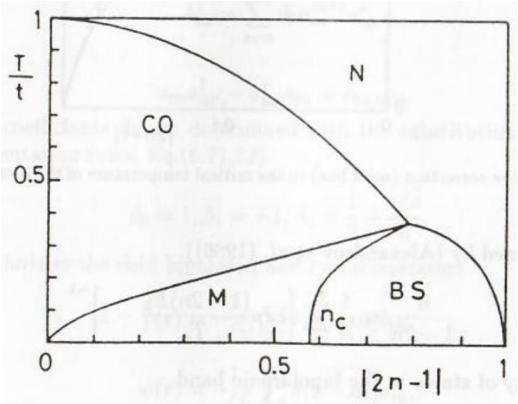

Fig.6.7. Mean-field $T - n$ phase diagram of bipolarons, $\bar{v} / t=2$.

In an extreme limit of a very high phonon frequency $\omega \gg \Delta$ the bipolaron liandwidth t and a short-range component of the repulsion $v^{(2)}$ are of the second under in the polaron bandwidth w for on-site bipolarons. In this limit the on-site hipolaron Hamiltonian can be mapped on the negative U Hubbard Hamiltonian if the long-range Coulomb interaction is screened. In a more realistic case of long-range butica and (or) $\omega < \Delta$ no such mapping is possible. Nevertheless in a qualitative analysis of the phase diagram we can use the finite temperature mean-field (MFA) anil random phase approximations (RPA), developed for the negative U Hubbard IInmiltonian by Robaszkiewicz et al (1981).

The MFA phase diagram is shown in Fig.6.7 for $\bar{v} = 2t$. Quantum fluctuations ('magnons'), which can be taken into account with the RPA equation of motion for the 'spin-spin' correlation function lead to a significant modification of the critical density n_c. Quantum fluctuations extend the region of the existence of the BS phase, which turns out to be the ground state ($T = 0$) even in the limit $\bar{v}/t \to \infty$ if the density is low,

$$n < 0.078 \tag{6.103}$$

for a simple cubic lattice.

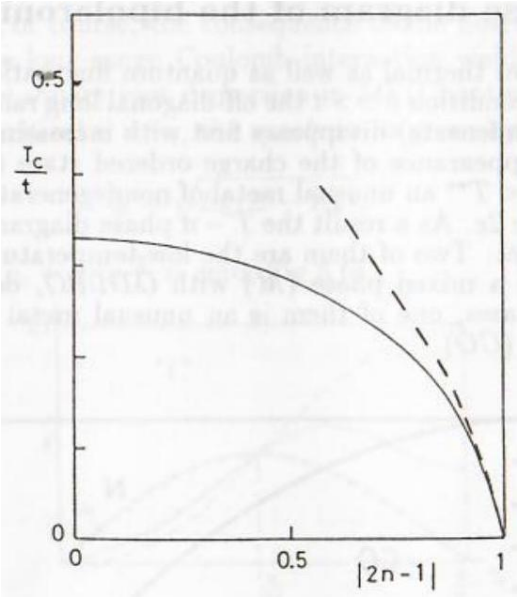

Fig.6.8. Hard-core correction (solid line) to the critical temperature of the ideal Bose gas (dashed line).
T_c is determined by (Alexandrov et al. (1986))

$$\frac{n}{1-2n} = \frac{1}{N}\sum_{\mathbf{k}} \left[\exp \frac{(1-2n)E_{\mathbf{k}}}{T_c} - 1\right]^{-1} \tag{6.104}$$

With the density of states in the bipolaronic band

$$N_b(E) = \frac{1}{N}\sum_{\mathbf{k}} \delta\left(E - E_{\mathbf{k}}\right)$$

this equation takes the form of the condition for the Bose-Einstein condensation of the ideal Bose gas if $n \ll 1$,

$$n = \int dE \frac{N_b(E)}{\exp\left(E/T_c\right) - 1} \tag{6.105}$$

At higher density a hard core correction appears, Fig.6.8,

$$T_c \simeq \frac{3.31 n^{2/3}}{m^{**}a^2}\left(1 - 0.54 n^{2/3}\right) \tag{6.100}$$

T_c is independent of the dynamical repulsion of bipolarons $\bar{v}$. This is an artifact of the random phase and nearest neighbor approximations.Taking into account the next neighbor interaction Kubo and Takada (1983) found two new phases of bipolaronic liquid: an incommensurate CO phase and an incommensurate M phase. A detailed study of the charge ordered bipolaronic states is given by Aubry (1995) in the adiabatic limit $\omega = 0$.

We believe, however, that in real solids the long range Coulomb repulsion of bipolarons is the only relevant term for low-energy kinetics and thermodynamics. That favors the homogeneous charged Bose-liquid for all realistic values of the Coulomb interaction and densities. A mapping of the bipolaronic Hamiltonian on a charged Bose gas is useful in this case.

5.7.10 6.10 Mapping on a charged Bose gas

One can transform the bipolaronic Hamiltonian to a representation containing only Bose operators $a_{\mathbf{m}}, a^{\dagger}_{\mathbf{m}}$

$$b_{\mathbf{m}} = \sum_{k=0}^{\infty} \beta_k a_{\mathbf{m}}^{\dagger k} a_{\mathbf{m}}^{k+1} \tag{6.107}$$

$$b_{\mathbf{m}}^{\dagger} = \sum_{k=0}^{\infty} \beta_k a_{\mathbf{m}}^{\dagger k+1} a_{\mathbf{m}}^{k} \tag{6.108}$$

with

$$a_{\mathbf{m}} a_{\mathbf{m}'}^{\dagger} - a_{\mathbf{m}'}^{\dagger} a_{\mathbf{m}} = \delta_{\mathbf{m},\mathbf{m}'} \tag{6.109}$$

The first few coefficients β_k are determined with the substitution of Eq.(6.107,108) into the commutation rules, Eq.(6.71,72)

$$\beta_0 = 1, \beta_1 = -1, \beta_2 = \frac{1}{2} + \frac{\sqrt{3}}{6} \tag{6.110}$$

We introduce further the field bipolaron and boson operators

$$\phi(\mathbf{r}) = \frac{1}{\sqrt{N}} \sum_{\mathbf{m}} \delta(\mathbf{r} - \mathbf{m}) b_{\mathbf{m}} \tag{6.111}$$

$$\psi(\mathbf{r}) = \frac{1}{\sqrt{N}} \sum_{\mathbf{m}} \delta(\mathbf{r} - \mathbf{m}) a_{\mathbf{m}} \tag{6.112}$$

where $\delta(\mathrm{r} - \mathrm{m})$ is the eigenfunction of the coordinate operator. The transformation for the field operators takes the form

$$\phi(\mathbf{r}) = \left(1 - \frac{\psi^{\dagger}(\mathbf{r})\psi(\mathbf{r})}{N} + \frac{(1/2 + \sqrt{3}/6)\psi^{\dagger}(\mathbf{r})\psi(\mathbf{r})\psi(\mathbf{r})}{N^2} + \dots\right)\psi(\mathbf{r}) \tag{6.113}$$

The bipolaronic Hamiltonian is now

$$H_b = -\int d\mathbf{r} d\mathbf{r}' \psi^{\dagger}(\mathbf{r}) \left[t\left(\mathbf{r} - \mathbf{r}'\right) + \mu\right] \psi\left(\mathbf{r}'\right) + H_{int} \tag{6.114}$$

with

$$H_{int} = H_l + H_s \tag{6.115}$$

where H_l is the dynamic part of the interaction,

$$H_l = \frac{1}{2} \int d\mathbf{r} d\mathbf{r}' \bar{v}\left(\mathbf{r} - \mathbf{r}'\right) \psi^{\dagger}(\mathbf{r}) \psi^{\dagger}\left(\mathbf{r}'\right) \psi(\mathbf{r}) \psi\left(\mathbf{r}'\right) \tag{6.116}$$

H_s describes the kinematic hard-core effect,

$$\begin{aligned} H_s = \frac{2}{N} t\left(\mathbf{r} - \mathbf{r}'\right) \big(&\psi^{\dagger}(\mathbf{r}) \psi^{\dagger}\left(\mathbf{r}'\right) \psi\left(\mathbf{r}'\right) \psi\left(\mathbf{r}'\right) \\ &+ \psi^{\dagger}(\mathbf{r}) \psi^{\dagger}(\mathbf{r}) \psi(\mathbf{r}) \psi\left(\mathbf{r}'\right)\big) + H^{(3)} \end{aligned} \tag{6.117}$$

Here

$$t\left(\mathbf{r}-\mathbf{r}'\right)=\sum_{\mathbf{k}}\left(t-E_{\mathbf{k}}\right)e^{i\mathbf{k}\cdot\left(\mathbf{r}-\mathbf{r}'\right)} \tag{6.118}$$

$$\bar{v}\left(\mathbf{r}-\mathbf{r}'\right)=\frac{1}{N}\sum_{\mathbf{k}}\bar{v}_{\mathbf{k}}e^{i\mathbf{k}\cdot\left(\mathbf{r}-\mathbf{r}'\right)} \tag{6.119}$$

and $\bar{v}_{\mathbf{k}}=\sum_{\mathbf{m}'\neq\mathbf{m}}\bar{v}_{\mathbf{m},\mathbf{m}'}\exp(i\mathbf{k}\cdot\mathbf{m})$ is the Fourier component of the bipolaron repulsion. The term $H^{(3)}$ contains powers of the field operators higher than four. The essential physics of bipolarons is controlled by the two-particle interaction, which includes a short-range kinematic part $t\left(\mathbf{r}-\mathbf{r}'\right)$ as well. Because $\bar{v}$ contains also the short range part $v^{(2)}$ this kinematic contribution can be included in the definition of $\bar{v}$. As a result H_b is the Hamiltonian of the interacting charged bosons tunneling in a band.

5.7.11 6.11 Bipolaron electrodynamics

To describe electrodynamics of bipolarons one can take into account the vector potential $\mathbf{A}(\mathbf{r})$ of the external field with the Peierls substitution (Peierls (1933))

$$t_{\mathbf{m},\mathbf{m}'}\rightarrow t_{\mathbf{m},\mathbf{m}'}e^{-i2e\mathbf{A}(\mathbf{m})\cdot(\mathbf{m}-\mathbf{m}')} \tag{6.120}$$

which is a fair approximation if the magnetic field is weak compared with the atomic field

$$eHa^2\ll 1 \tag{6.121}$$

Here $\mathbf{A}(r)$ is a vector potential, which can be also time dependent. This yields in real space

$$t\left(\mathbf{r},\mathbf{r}'\right)=\sum_{\mathbf{k}}\left(t-E_{\mathbf{k}+2e\mathbf{A}}\right)e^{i\mathbf{k}\cdot\left(\mathbf{r}-\mathbf{r}'\right)} \tag{6.122}$$

If the condition Eq.(6.121) is satisfied one can expand $E_{\mathbf{k}}$ in the vicinity of $\mathbf{k}=0$ to obtain

$$t\left(\mathbf{r},\mathbf{r}'\right)\simeq\left(t+\frac{\left[\nabla-2ie\mathbf{A}(\mathbf{r})\right]^2}{2m^{**}}\right)\delta\left(\mathbf{r}-\mathbf{r}'\right) \tag{6,121}$$

where

$$\frac{1}{m^{**}}=\frac{d^2E_{\mathbf{k}}}{d\mathbf{k}^2}$$

at $k\rightarrow 0$. As a result the Hamiltonian of fermions strongly coupled with any bosonic field (i.e. phonons) reduces to

$$\begin{aligned}H_b=&-\int d\mathbf{r}\psi^{\dagger}(\mathbf{r})\left[\frac{\left(\nabla-2ie\mathbf{A}(\mathbf{r})\right)^2}{2m^{**}}+\mu\right]\psi(\mathbf{r})\\&+\frac{1}{2}\int d\mathbf{r}d\mathbf{r}'\bar{v}\left(\mathbf{r}-\mathbf{r}'\right)\psi^{\dagger}(\mathbf{r})\psi^{\dagger}\left(\mathbf{r}'\right)\psi(\mathbf{r})\psi\left(\mathbf{r}'\right)\end{aligned} \tag{6.124}$$

if three-body and higher order interactions are neglected. The hard core effect is taken into account by the definition of the repulsion $\bar{v}$ as described above, and the constant t in Eq.(6.122) is included in the chemical potential μ. At large distances the bipolaron-bipolaron interaction is the Coulomb one ($\bar{v}\sim 1/\epsilon r$ in the atomic solids or $\bar{v}\sim 1/\epsilon_0 r$ in the ionic compounds).

We have shown in this Chapter that the Fermi-liquid behavior is destroyed by the strong electron-phonon interaction. The ground state of carriers strongly coupled with phonons in a

doped band and Mott insulators is the bipolaronic charged Boseliquid. We proposed bipolarons as a key element for the understanding of the high- T_c phenomenon in metal oxides and doped fullerenes (Alexandrov and Mott (1994)). The key point for the bipolaronic mechanism of high- T_c superconductivity is the possibility of the coherent tunneling of (bi)polarons with a reasonable value of the effective mass. Several authors assert that their bandwidth should not exceed $10^{-4}-10^{-5}$eV, and then the maximal T_c attainable with small bipolarons should be a few K or less. However, we believe this is an erroneous conclusion based on an incorrect estimate of the bipolaron mass. For the intermediate value of the coupling constant $\lambda \simeq 1$ and the high-frequency phonons $\omega \simeq 0.1$eV. the polaron binding energy is large ($E_p = 0.2-0.6$eV) and the value of the bare electronic bandwidth compatible with the small polaron formation is large enough being of the order of 1.0 eV. In this case the estimate of the small polaron bandwidth yields the value of w as large as a few hundred K and the same for T_c. Taking into account the phonon frequency dispersion in the the perovskite crystal structure one can find the effective mass of intersite small bipolarons of the order of $10m_e$ as discussed in section 6.2. Of course, a short-range intersite Coulomb repulsion should be below $2E_p$ to ensure the formation of mobile intersite bipolarons. That is quite feasible because the highfrequency dielectric constant in metal oxides is large, normally $\epsilon \sim 5$ and larger. The low-frequency dielectric constant is extremely large in oxides. As a result, optical phonons perfectly screen the Coulomb repulsion. Then the deformation potential as well as molecular vibrations give rise into a net short-range attraction between small polarons as discussed in Chapter 2.

At low temperatures $T < \omega/2, T^{**}$ and low frequencies of an external field $\nu \ll \omega$ the internal structure of the bipolaron including its phonon cloud can not be observed. Therefore their low-temperature and low-frequency kinetics is that of charged bosons. An we have discussed (Alexandrov and Mott (1994)) the internal symmetry of the hipolaron should be distinguished from that of the macroscopic off-diagonal order parameter ψ_0(r) (see below). While the internal symmetry depends on the short-range allraction between two polarons and the unit cell geometry, the 'external' symmetry of 1/0 is determined by the long-range repulsion between bipolarons. Also the excitaIon spectrum of the superfluid bipolaronic liquid depends on the bipolaron-bipolaron mpulsion rather than on the internal bipolaron structure. Therefore, as an example, (lie nymmetry observed by the Josephson tunneling may be different from that observed with another technique. Low-energy physics of bipolarons can be studied within a simplified charged Bose-gas model. The Coulomb repulsion between bipolarons is significantly reduced in oxides by the ionic screening and the dimensionlees interaction r_s is not large even for heavy particles.

5.8 7 Charged Bose gas

A charged Coulomb Bose-gas (CBG) is a fundamental reference system in manyparticle physics with a superfluid phase transition. It has been studied by several authors and recently became of particular interest motivated by the bipolaron theory of high temperature superconductivity. As we have discussed in Chapter 6 the long-wave excitations of the bipolaronic liquid are those of charged bosons with the Coulomb repulsion between them. Schafroth (1955) demonstrated that an ideal gas of charged bosons exhibits the Meissner-Ochsenfeld effect (expulsion of a magnetic field) below the ideal Bose-gas condensation temperature. Later on the one-particle excitation spectrum at $T = 0$ was calculated by Foldy (1961), who worked at zero temperature using the Bogoliubov (1947) approach. The Bogoliubov method leads to the result that the ground state of the system has a negative correlation energy, whose magnitude increases with the density of bosons. Perhaps more interesting is the fact that the elementary excitations of the system have, for small momenta, energies characteristic of plasma oscillations which pass over smoothly for large momenta to the energies characteristic of single particle ex-

citations. Further investigations have been carried out at or near T_c, the transition temperature for the gas. These works has been concerned with the critical exponents (Bishop (1974)) and the change in the transition temperature from that of the ideal gas (Bishop (1974), Fetter (1971)). The RPA dielectric response function and screening in CBG have been studied in the high-density limit (Hore and Frankel (1975, 1976), including a low-dimensional ($2D$) CBG (Hines and Frankel (1979), Gold (1991)). In this Chapter we verify superfluid properties of charged bosons with the Bogoliubov-de Genes type equations derived for CBG by Alexandrov and Beere (1995) and discuss superconducting as well as normal state CBG kinetics.

5.8.1 7.1 Bogoliubov-de Gennes equations for CBG

The superfluid properties of charged bosons as well as their excitation spectrum and the response function can be studied by the use of the Bogoliubov-de Genes (BdG) type equations, fully taking into account the interaction of quasiparticles with the condensate. The Hamiltonian for a system of charged bosons on an oppositely charged liar ckround (to ensure charge neutrality) in an external field is given by

$$H = \int d\mathbf{r}\psi^{\dagger}(\mathbf{r}) \left[-\frac{(\nabla - i2e\mathbf{A})^2}{2m^{**}} + \mu \right] \psi(\mathbf{r}) + \frac{1}{2} \int d\mathbf{r} \int d\mathbf{r}' V\left(\mathbf{r}-\mathbf{r}'\right) \psi^{\dagger}(\mathbf{r}) \psi(\mathbf{r}) \psi^{\dagger}\left(\mathbf{r}'\right) \psi\left(\mathbf{r}'\right) \tag{7.1}$$

For $3D$ charged bosons the Fourier component of the Coulomb potential $V(\mathbf{r})$ is $V(\mathbf{k}) = 16\pi e^2/k^2\epsilon_0$ with ϵ_0 a dielectric constant of the background and bosonic charge $2e$. For $2D$ system with a three dimensional interaction $V(\mathbf{k}) = 8\pi e^2/k\epsilon_0$. To respect electroneutrality one takes $V(\mathbf{k} \equiv 0) = 0$.

The equation of motion for the field operator, ψ, is derived using this Hamiltonian,

$$i\frac{\partial}{\partial t}\psi(\mathbf{r},t) = [H, \psi(\mathbf{r},t)] = \left[-\frac{(\nabla - i2e\mathbf{A})^2}{2m^{**}} + \mu \right] \psi(\mathbf{r},t) + \int d\mathbf{r}' V\left(\mathbf{r}-\mathbf{r}'\right) \psi^{\dagger}\left(\mathbf{r}',t\right) \psi\left(\mathbf{r}',t\right) \psi(\mathbf{r},t) \tag{7.2}$$

If the interaction is weak one can expect that the occupation numbers of one-particle states are not very much different from those in the ideal Bose-gas. In particular the state with zero momentum $k = 0$ remains to be macroscopically occupied and the corresponding Fourier component of the field operator $\psi(\mathbf{r})$ has anomalously large matrix element between the ground states of the system containing $N + 1$ and N bosons. It is convenient to consider a grand canonical ansamble, introducing a chemical potential μ. In this case the quantum state is a superposition of states $|N\rangle$ with slightly different total numbers of bosons. The weight of each state is a smooth function of N which is practically constant near the average number $\bar{N}$ on the scale $\pm\sqrt{N}$. Because ψ changes the number of particles only by one its diagonal matrix element coincides with the off-diagonal, calculated for the states with fixed $N = N + 1$ and $N = \bar{N}$. Following Bogoliubov (1947) one can separate the large diagonal matrix element ψ_0 from ψ by treating the rest ψ as a small fluctuation

$$\psi(\mathbf{r},t) = \psi_0(\mathbf{r},t) + \tilde{\psi}(\mathbf{r},t). \tag{7.3}$$

The anomalous average $\psi_0(\mathrm{r},t) = \langle\psi(\mathrm{r},t)\rangle$ is equal to $\sqrt{n_0}$ in a homogeneous system, where n_0 is the condensate density.

Substituting the Bogoliubov displacement transformation, Eq.(7.3) into the equa tion of motion and collecting c - number terms of ψ_0, and supracondensate boson operators $\tilde{\psi}$ we obtain a set of the BdG-type equations. The macroscopic condensale wave function, which plays the role of the order parameter obeys to the following equation

$$
\begin{aligned}
i\frac{\partial}{\partial t}\psi_0(\mathbf{r},t) = & \left[-\frac{(\nabla - i2e\mathbf{A})^2}{2m^{**}} + \mu\right]\psi_0(\mathbf{r},t) \\
& + \int d\mathbf{r}' V(\mathbf{r}-\mathbf{r}')\, n(\mathbf{r}',t)\,\psi_0(\mathbf{r},t) + \int d\mathbf{r}' V(\mathbf{r}-\mathbf{r}') \\
& \times \left[\left\langle \tilde{\psi}^\dagger(\mathbf{r}',t)\,\tilde{\psi}(\mathbf{r},t)\right\rangle \psi_0(\mathbf{r}',t) + \left\langle \tilde{\psi}(\mathbf{r}',\mathbf{t})\,\tilde{\psi}(\mathbf{r},\mathbf{t})\right\rangle \psi_0^*(\mathbf{r}',\mathbf{t})\right]
\end{aligned} \tag{7.4}
$$

Taking explicitly into account the interaction of supracondensate bosons with the con densate and applying the Hartree approximation for the interaction between super condensate particles we obtain

$$
\begin{aligned}
i\frac{\partial}{\partial t}\tilde{\psi}(\mathbf{r},t) = & \left[-\frac{(\nabla - i2e\mathbf{A})^2}{2m^{**}} + \mu\right]\tilde{\psi}(\mathbf{r},t) + \int d\mathbf{r}' V(\mathbf{r}-\mathbf{r}')\, n(\mathbf{r},t)\tilde{\psi}(\mathbf{r},t) \\
& + \int d\mathbf{r}' V(\mathbf{r}-\mathbf{r}')\left[\psi_0^*(\mathbf{r}',t')\,\psi_0(\mathbf{r},t) + \left\langle \tilde{\psi}^\dagger(\mathbf{r}',t)\,\tilde{\psi}(\mathbf{r},t)\right\rangle\right]\tilde{\psi}(\mathbf{r}',t) \\
& + \int d\mathbf{r}' V(\mathbf{r}-\mathbf{r}')\left[\psi_0(\mathbf{r}',t)\,\psi_0(\mathbf{r},t) + \left\langle \tilde{\psi}(\mathbf{r}',t)\,\tilde{\psi}(\mathbf{r},t)\right\rangle\right]\tilde{\psi}^\dagger(\mathbf{r}',t) \\
& + \int d\mathbf{r}' V(\mathbf{r}-\mathbf{r}')\left[\tilde{\psi}^\dagger(\mathbf{r}',t)\,\tilde{\psi}(\mathbf{r}',t) - \left\langle \tilde{\psi}^\dagger(\mathbf{r}',t)\,\tilde{\psi}(\mathbf{r}',t)\right\rangle\right]\psi_0(\mathbf{r},t) \\
& + \int d\mathbf{r}' V(\mathbf{r}-\mathbf{r}')\left[\tilde{\psi}^\dagger(\mathbf{r}',t)\,\tilde{\psi}(\mathbf{r},t) - \left\langle \tilde{\psi}^\dagger(\mathbf{r}',t)\,\tilde{\psi}(\mathbf{r},t)\right\rangle\right]\psi_0(\mathbf{r}',t) \\
& + \int d\mathbf{r}' V(\mathbf{r}-\mathbf{r}')\left[\tilde{\psi}(\mathbf{r}',t)\,\tilde{\psi}(\mathbf{r},t) - \left\langle \tilde{\psi}(\mathbf{r}',t)\,\tilde{\psi}(\mathbf{r},t)\right\rangle\right]\psi_0^*(\mathbf{r}',t)
\end{aligned} \tag{7.5}
$$

Here

$$
n(\mathbf{r},t) = |\psi_0(\mathbf{r},t)|^2 + \left\langle \tilde{\psi}^\dagger(\mathbf{r},t)\tilde{\psi}(\mathbf{r},t)\right\rangle \tag{7.6}
$$

is the boson density.
In the high density limit $r_s \ll 1$ for the temperature close to zero the number of bosons $\tilde{n}$ pushed up from the condensate by the repulsion is small. Therefore the contribution of terms nonlinear in $\tilde{\psi}$ is negligible. Applying a linear Bogoliubov transformation for $\tilde{\psi}$

$$
\tilde{\psi}(\mathbf{r},t) = \sum_n u_n(\mathbf{r},t)\alpha_n + v_n^*(\mathbf{r},t)\alpha_n^\dagger \tag{7.7}
$$

where α_n and $\alpha_n^\dagger$ are bosonic quasiparticle operators for the one-particle quantum state n, and omitting nonlinear terms we obtain two coupled Schrödinger equations for the wave functions $u(\mathbf{r},t)$ and $v(\mathbf{r},t)$

$$
\begin{aligned}
i\frac{\partial}{\partial t}u(\mathbf{r},t) = & \left[-\frac{(\nabla - i2e\mathbf{A})^2}{2m^{**}} + \mu\right]u(\mathbf{r},t) \\
& + \int d\mathbf{r}' V(\mathbf{r}-\mathbf{r}')\left[|\psi_0(\mathbf{r}',t)|^2\, u(\mathbf{r},t) + \psi_0^*(\mathbf{r}',t)\,\psi_0(\mathbf{r},t)u(\mathbf{r}',t)\right] \\
& + \int d\mathbf{r}' V(\mathbf{r}-\mathbf{r}')\,\psi_0(\mathbf{r}',t)\,\psi_0(\mathbf{r},t)v(\mathbf{r}',t)
\end{aligned} \tag{7.8}
$$

and

$$-i\frac{\partial}{\partial t}v(\mathbf{r},t)=\left[-\frac{(\nabla+i2e\mathbf{A})^2}{2m^{**}}+\mu\right]v(\mathbf{r},t)$$
$$+\int d\mathbf{r}'V\left(\mathbf{r}-\mathbf{r}'\right)\left[\left|\psi_0\left(\mathbf{r}',t\right)\right|^2 v(\mathbf{r},t)+\psi_0\left(\mathbf{r}',t\right)\psi_0^*(\mathbf{r},t)\right]v\left(\mathbf{r}',t\right)$$
$$+\int d\mathbf{r}'V\left(\mathbf{r}-\mathbf{r}'\right)\psi_0^*\left(\mathbf{r}',t\right)\psi_0^*(\mathbf{r},t)u\left(\mathbf{r}',t\right) \tag{7.9}$$

There is also the sum rule,

$$\sum_n\left[u_n(\mathbf{r},t)u_n^*\left(\mathbf{r}',t\right)-v_n(\mathbf{r},t)v_n^*\left(\mathbf{r}',t\right)\right]=\delta\left(\mathbf{r}-\mathbf{r}'\right), \tag{7.10}$$

which retain the Bose commutation relations for all operators. The set of BdG equadions (7.4,8-10) plays the same role as the time-dependent Ginzburg-Landau equations for the BCS superconductors.

5.8.2 7.2 Excitation spectrum and ground state energy of CBG

For the homogeneous case and $\mathbf{A}=0$ the excitation wave functions are plane waves

$$u_{\mathbf{k}}(\mathbf{r},t)=u_{\mathbf{k}}e^{i\mathbf{k}\cdot\mathbf{r}-i\epsilon_{\mathbf{k}}t} \tag{7.11}$$

and

$$v_{\mathbf{k}}(\mathbf{r},t)=v_{\mathbf{k}}e^{i\mathbf{k}\cdot\mathbf{r}-i\epsilon_{\mathbf{k}}t} \tag{7.12}$$

The condensate wave function is (r,t) independent, $\psi_0=\sqrt{n_0}$, so the solution to Eq.(7.4) is

$$\mu=0 \tag{7.13}$$

Substitution of Eqs.(7.11-13) into the BdG set yields

$$\epsilon_{\mathbf{k}}u_{\mathbf{k}}=\frac{k^2}{2m^{**}}u_{\mathbf{k}}+n_0V(\mathbf{k})\left[u_{\mathbf{k}}+v_{\mathbf{k}}\right] \tag{7.14}$$
$$-\epsilon_{\mathbf{k}}v_{\mathbf{k}}=\frac{k^2}{2m^{**}}v_{\mathbf{k}}+n_0V(\mathbf{k})\left[u_{\mathbf{k}}+v_{\mathbf{k}}\right] \tag{7.15}$$

and from Eq.(7.10)

$$\left|u_{\mathbf{k}}\right|^2-\left|v_{\mathbf{k}}\right|^2=1. \tag{7.16}$$

As a result we find

$$u_{\mathrm{k}}^2=\frac{1}{2}\left(1+\frac{\xi_{\mathrm{k}}}{\epsilon_{\mathrm{k}}}\right) \tag{7.17}$$
$$v_{\mathrm{k}}^2=-\frac{1}{2}\left(1-\frac{\xi_{\mathrm{k}}}{\epsilon_{\mathrm{k}}}\right) \tag{7.18}$$
$$u_{\mathrm{k}}v_{\mathrm{k}}=-\frac{V(\mathrm{k})n_0}{2\epsilon_{\mathrm{k}}} \tag{7.19}$$

where $\xi_{\mathbf{k}} = k^2/2m^{**} + V(\mathbf{k})n_0$. The elementary excitation energy is

$$\epsilon_{\mathbf{k}} = \sqrt{\frac{k^4}{4\left(m^{**}\right)^2} + \frac{k^2 V(\mathbf{k}) n_0}{m^{**}}}. \tag{7,20}$$

With the Fourier component of the Coulomb interaction this makes (Foldy (1961))

$$\epsilon_{\mathbf{k}} = \sqrt{\frac{k^4}{4\left(m^{**}\right)^2} + \omega_{p0}^2} \tag{7,21}$$

with a gap $\omega_{p0} = \sqrt{16\pi e^2 n_0/\epsilon_0 m^{**}}$, which is the classical plasma frequency for 4 plasma of density n_0, Fig.7.1a. In a two-dimensional system $V(\mathbf{k}) = 8\pi e^2/c_0 k$ and the Bogoliubov spectrum is gapless, Fig.7.1b,

$$\epsilon_{\mathbf{k}} = E_s \sqrt{k/q_s + k^4/q_s^4} \tag{7,\mu}$$

with $E_s = q_s^2/2m^{**}, q_s = \left(32\pi e^2 n_0/\epsilon_0\right)^{1/3}$ a two-dimensional screening wave-number and n_0 is the $2D$ density. The density of bosons pushed up from the condensate by the Coulomb repulsion at $T = 0$ is

$$\tilde{n} = \left\langle \tilde{\psi}^\dagger(\mathbf{r})\tilde{\psi}(\mathbf{r}) \right\rangle = \sum_{\mathbf{k}} v_{\mathbf{k}}^2 \tag{7.23}$$

which is small compared with the total density n,

$$\frac{\tilde{n}}{n} \simeq 0.2 r_s^{3/4} \sim 1 \quad r_s = \frac{s}{a_0}$$

if the latter is high, so $r_s \ll 1$.

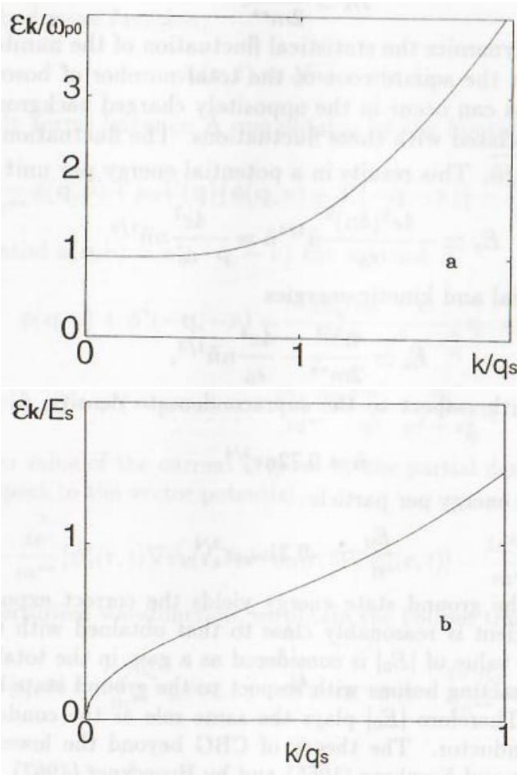

Fig.7.1. Excitation spectrum of a $3D(a)$ and $2D(b)$ charged Bose gas at $T = 0$.

The ground state $|0\rangle$ is a vacuum for the elementary excitations, $\alpha_{\mathbf{k}}|0\rangle = 0$. The ground state energy E_0 is obtained by substitution of Eq.(7.7) into the Hamiltonian and neglecting higher order terms than quadratic in α,

$$E_0 \equiv \langle 0|H|0\rangle = \frac{1}{2}\sum_{\mathbf{k}} (\epsilon_{\mathbf{k}} - \xi_{\mathbf{k}}) \tag{7.25}$$

This can be written per particle in terms of the plasma frequency ω_{p0}

$$\frac{E_0}{n} = \frac{2^{3/2}}{3^{1/4}\pi}\omega_{p0} r_s^{3/4} \int_0^\infty dk k^2 \left[\sqrt{k^4+1} - k^2 - 1/2k^2\right] \simeq -0.23\omega_{p0} r_s^{3/4} \tag{7.26}$$

The negative value of the ground state energy is due to the oppositely charged background. That can be shown by a simple estimation. The ground state energy is estimated as the zero-point energy of supracondensate bosons plus the potential energy arising from statistical fluctuations of their density. The zero-point energy is calculated as the kinetic energy of a single supracondensate boson confined to the average volume occupied of each of them ($\sim 1/\tilde{n}$). This produces an energy per unit volume of

$$E_k \simeq \frac{\tilde{n}^{5/3}}{2m^{**}} \tag{7.27}$$

From classical thermodynamics the statistical fluctuation of the number of bosons in a given volume goes as the square root of the total number of bosons within that volume. No fluctuations can occur in the oppositely charged background, producing a potential energy associated with these fluctuations. The fluctuation in the number of particles is $\delta n = \sqrt{n/\tilde{n}}$. This results in a potential energy per unit volume of

$$E_p \simeq -\frac{4e^2(\delta n)^2}{\epsilon_0}\tilde{n}^{1/3}\tilde{n} = -\frac{4e^2}{\epsilon_0} n\tilde{n}^{1/3} \tag{7.28}$$

The sum of the potential and kinetic energies

$$E_0 \simeq \frac{\tilde{n}^{5/3}}{2m^{**}} - \frac{4e^2}{\epsilon_0} n\tilde{n}^{1/3} \tag{7.29}$$

is then minimised with respect to the supracondensate density, $\tilde{n}$, producing the solution

$$\tilde{n} = 0.72 n r_s^{3/4} \tag{7.30}$$

and the ground state energy per particle

$$\frac{E_0}{n} \simeq -0.31\omega_{p0} r_s^{3/4} \tag{7.31}$$

This estimation of the ground state energy yields the correct exponent of r_s and the numerical coefficient is reasonably close to that obtained with the Bogoliubov transformation. The value of $|E_0|$ is considered as a gain in the total energy due to condensation of interacting bosons with respect to the ground state energy ($= 0$) of an ideal Bose gas. Therefore $|E_0|$ plays the same role as the condensation energy of the BCS superconductor. The theory of CBG beyond the lowest order in $r_0^{3/4}$ was discussed by Lee and Feenberg (1965) and by Brueckner (1967). They obtained the next order correction to the ground state energy. Woo and Ma (1967) found numerically the correction to the Bogoliubov excitation spectrum.

5.8.3 7.3 Linear-response function

The linear response function is defined as

$$J_m(\mathbf{q},\omega) = K^{mn}(\mathbf{q},\omega) a_n(\mathbf{q},\omega) \tag{7.32}$$

where $\mathbf{J}(\mathbf{q},\omega)$ and $\mathbf{a}(\mathbf{q},\omega)$ are the Fourier transforms of the current and vector potential, respectively. It is important that the vector potential $\mathbf{A}$ is defined as an external vector potential. The internal Coulomb field is explicitly taken into account by the Bogoliubov transformation. The use of the effective internal field $\mathbf{A}$ rather than the external one results in reducible diagrams for the polarisation, and thus in the double counting of the Coulomb interaction. To calculate the response to the leading order of the condensate density, n_0, we need only consider equation Eq.(7.4) with $\hat{\psi} = \mu = 0$

$$i\frac{\partial}{\partial t}\psi_0(\mathbf{r},t) = -\frac{(\nabla - i2e\mathbf{A})^2}{2m^{**}}\psi_0(\mathbf{r},t) + \int d\mathbf{r}' v\left(\mathbf{r}-\mathbf{r}'\right)\left|\psi_0^*\left(\mathbf{r}',t\right)\right|^2\psi_0(\mathbf{r},t) \tag{7.33}$$

Using a perturbed wave function,

$$\psi_0(\mathbf{r},t) = \sqrt{n_0} + \phi(\mathbf{r},t) \tag{7.34}$$

and keeping only terms linear in $\mathbf{A}$ one obtains by the Fourier transformation

$$\nu\phi(\mathbf{q},\nu) = \frac{q^2}{2m^{**}}\phi(\mathbf{q},\nu) + n_0 V(\mathbf{q})\left\{\phi(\mathbf{q},\nu) + \phi^*(-\mathbf{q},-\nu)\right\} - \frac{2e\sqrt{n_0}}{2m^{**}}\mathbf{q}\cdot\mathbf{a}(\mathbf{q},\nu) \tag{7.35}$$

For a real potential $\mathbf{a}(\mathbf{q},\nu) = \mathbf{a}^*(-\mathbf{q},-\nu)$ the solution is

$$\phi(\mathbf{q},\nu) + \phi^*(-\mathbf{q},-\nu) = -\frac{2e\sqrt{n_0}}{m^{**}}\frac{\nu}{\nu^2-\epsilon_{\mathbf{q}}^2}\mathbf{q}\cdot\mathbf{a}(\mathbf{q},\omega) \tag{7.36}$$

$$\phi(\mathbf{q},\nu) - \phi^*(-\mathbf{q},-\nu) = -\frac{2e\sqrt{n_0}}{m^{**}}\frac{2m^{**}}{q^2}\frac{\epsilon_{\mathbf{q}}^2}{\nu^2-\epsilon_{\mathbf{q}}^2}\mathbf{q}\cdot\mathbf{a}(\mathbf{q},\omega) \tag{7.37}$$

The expectation value of the current is given by the partial derivative of the Hamiltonian with respect to the vector potential,

$$\mathbf{J}(\mathbf{r},t) = -\frac{ie}{m^{**}}\left[\psi_0^*(\mathbf{r},t)\nabla\psi_0(\mathbf{r},t) - \psi_0(\mathbf{r},t)\nabla\psi_0^*(\mathbf{r},t)\right] - \frac{4e^2n_0}{m^{**}}\mathbf{A}(\mathbf{r},t) \tag{7.38}$$

Applying the perturbed wavefunction, we obtain the Fourier transform of the current as,

$$\mathbf{J}(\mathbf{q},\nu) = \frac{e\sqrt{n_0}}{m^{**}}\mathbf{q}\left[\phi(\mathbf{q},\nu) - \phi^*(-\mathbf{q},-\nu)\right] - \frac{4e^2n_0}{m^{**}}\mathbf{a}(\mathbf{q},\nu) \tag{7.39}$$

Hence

$$K^{mn}(\mathbf{q},\nu) = \frac{4e^2n_0}{m^{**}}\left[\delta^{mn}\frac{\nu^2}{\epsilon_{\mathbf{q}}^2-\nu^2} + \left(q^mq^n - \delta^{mn}q^2\right)\frac{\epsilon_{\mathbf{q}}^2}{q^2\left(\epsilon_{\mathbf{q}}^2-\nu^2\right)}\right] \tag{7.40}$$

This response function has been split into a longitudinal $K_l \sim \delta^{mn}$ and transverse $K_1 \sim (q^mq^n - \delta^{mn}q^2)$ parts.

The longitudinal response to the field $(\mathbf{D}\|\mathbf{q})$ is expressed in terms of the so-called external conductivity σ_{ex} as

$$\mathbf{J}_l(\mathbf{q},\nu) = \sigma_{ex}(\mathbf{q},\nu)\mathbf{D}(\mathbf{q},\nu) \tag{7.41}$$

where $\mathbf{D}$ is the external electric field. By the use of Eq.(7.40) we find

$$\sigma_{ex}(\mathbf{q},\nu)=\frac{K_l}{i\nu}=\frac{i\epsilon_0\nu\omega_{p0}^2}{4\pi\left(\nu^2-\epsilon_{\mathbf{q}}^2\right)} \tag{7.42}$$

The Kubo conductivity sum rule is satisfied

$$\int_0^\infty d\nu\Re\sigma_{ex}(\nu)=\frac{\pi e^2 n_0}{2m^{**}} \tag{7.43}$$

The conductivity in the transverse electromagnetic field ($\mathbf{D}\perp\mathbf{q}$) is

$$\sigma_t=\frac{i}{4\pi\lambda_H^2\nu} \tag{7.44}$$

where

$$\lambda_H=\left[\frac{m^{**}}{16\pi e^2 n_0}\right]^{1/2} \tag{7.45}$$

This expression is the same as that for the BCS superconductor. Combined with the Maxwell equation it describes the Meissner-Ochsenfeld effect in CBG with the London penetration depth λ_H. Consequently, a charged Bose gas is a superconductor.

5.8.4 7.4 Collective excitations and screening

The dielectric response function $\epsilon(\mathbf{q},\nu)$ is defined as

$$\frac{1}{\epsilon(\mathbf{q},\nu)}=1+\frac{\rho(\mathbf{q},\nu)}{\rho_{ex}(\mathbf{q},\nu)} \tag{7.46}$$

The Fourier component of the boson charge density $\rho_b(\mathbf{q},\nu)$ obeys the continuity equation

$$qJ_l(\mathbf{q},\nu)-\nu\rho_b(\mathbf{q},\nu)=0 \tag{7.47}$$

Combining the Maxwell

$$iqD(\mathbf{q},\nu)=4\pi\frac{\rho_{ex}}{\epsilon_0} \tag{7.48}$$

and continuity equations we find the total density $\rho=\rho_{ex}+\rho_b$ and the dielectric function of CBG

$$\frac{1}{\epsilon(\mathbf{q},\nu)}=1-4\pi\frac{K_l(\mathbf{q},\nu)}{\nu^2} \tag{7,49}$$

or

$$\epsilon(\mathbf{q},\nu)=1-\frac{\omega_{p0}^2}{\nu^2-q^4/4\left(m^{**}\right)^2} \tag{7.50}$$

This expression is the same as derived for an ideal charged Bose gas by Hore and Frankel (1975).

The zeros of $\epsilon(\mathbf{q},\nu)$ describe collective excitations of the system. These turn out to be the same as the Bogoliubov single-particle excitations in agreement with the general arguments (Pines (1961)). The screening in the condensed CBG goes like $\epsilon(q,0)\sim 1/q^4$ in the long-wave limit. It produces a screened potential, which goes as

$$\tilde{V}(r)\sim\frac{\cos\left(q_s r/\sqrt{2}\right)}{r}e^{-q_s r/\sqrt{2}} \tag{7.51}$$

where $q_s = \sqrt{2m^{**}\omega_{p0}}$ is the inverse screening length.
For two-dimensional condensed bosons ($T = 0$) the dielectric response function can easily be derived in the same way,

$$\epsilon(\mathbf{q}, \nu) = 1 - \frac{E_s^2 q/q_s}{\nu^2 - E_s^2 q^4/q_s^4} \tag{7.52}$$

Zeros of $\epsilon(\mathbf{q}, \omega)$ yield the gapless collective branch, which is the same as the Bogoliubov mode, Eq.(7.22).

There is a direct analogy between excitations of CBG and of the BCS superconductor. The only difference is that in the former the plasmon mode is identical with the Bogoliubov quasiparticle, while in the BCS superconductor the collective plasmon mode lies well above the BCS quasiparticle gap.

5.8.5 7.5 Superconducting kinetics of CBG: $2D$ heat superconductor

The long-wave excitations are responsible for the kinetic properties of CBG at low temperatures differently from normal metals or BSC superconductors where the characteristic wavelength is of the order of the lattice constant. As we have discussed above the condensate screens perfectly well the scattering potential. Therefore, in CBG one can expect a strong enhancement of the scattering rate below T_c. For near $2D$ bosons this leads to an infinite thermal conductivity (Alexandrov and Mott (1993)).

The elastic scattering of excitations is described by the Hamiltonian:

$$H_s = \sum_{\mathbf{k},\mathbf{k}'} v\left(\mathbf{k}, \mathbf{k}'\right) \alpha^{\dagger}_{\mathbf{k}'} \alpha_{\mathbf{k}} \tag{7.53}$$

with

$$v\left(\mathbf{k}, \mathbf{k}'\right) = \frac{v_0\left(\mathbf{k} - \mathbf{k}'\right)\left(u_{\mathbf{k}} u_{\mathbf{k}'} + v_{\mathbf{k}} v_{\mathbf{k}'}\right)}{\epsilon\left(\mathbf{k} - \mathbf{k}', 0\right)} \tag{7.54}$$

a screened scattering potential and the coherence factors $u_{\mathrm{k}}, v_{\mathrm{k}}$ determined by Eq.(7.1719). Here $v_0(\mathbf{q})$ is the Fourier component of a bare (unscreened) boson -impurity or boson- acoustic phonon interactions. Because the characteristic excitation energy is of the order of temperature the boson-acoustic phonon scattering is practically elastic if the temperature is not extremely low, $T > m^{**}s^2/2$ as we have discussed in section 4.11. The static dielectric function of $2D$ charged bosons $\epsilon(q, 0)$ depends on q at low temperatures as

$$\epsilon(q, 0) = 1 + \left(\frac{q_s}{q}\right)^3 \tag{7.55}$$

With the Fermi golden rule and the Boltzmann equation one obtains the elastic transport relaxation rate for excitations in the usual way:

$$1/\tau(k) = 2\pi \sum_{\mathbf{k}'} \frac{k_x - k'_x}{k_x} v^2\left(\mathbf{k}, \mathbf{k}'\right) \delta\left(\epsilon_{\mathbf{k}} - \epsilon_{\mathbf{k}'}\right) \tag{7.56}$$

or

$$1/\tau(k) = \frac{k}{\pi} \frac{dk}{d\epsilon_{\mathbf{k}}} \left(u_{\mathbf{k}}^2 + v_{\mathbf{k}}^2\right)^2 \int_0^{\pi} d\phi (1 - \cos(\phi)) \frac{v_0^2(k\sqrt{2(1 - \cos(\phi))})}{\epsilon^2(k\sqrt{2(1 - \cos(\phi)}, 0)} \tag{7.57}$$

For the scattering by acoustic phonons (or by point defects) v_0 is independent of q. For charged impurities $v_0^2(q) \sim 1/q^2$.

By the use of the spectrum of low-energy $2D$ Bogoliubov excitations with $k < q_s$, $\epsilon_{\mathbf{k}} = E_s\sqrt{k/q_s}$ we obtain for the acoustic phonon

$$\tau^s_{ac}(k) \sim \left(\frac{q_s}{k}\right)^{9/2} \tag{7.58}$$

and

$$\tau^s_{im}(k) \sim \left(\frac{q_s}{k}\right)^{5/2} \tag{7.59}$$

for the impurity scattering. Both τ_{ac} and τ_{im} are infinite in the long-wave limit $k \to 0$ because of screening and of a large group velocity of the $2D$ Bogoliubov mode, $d\epsilon/dk$, which is divergent as $k^{-1/2}$ in this limit. Due to this singularity of the group velocity, which is a common feature of surface waves, and the due to the screening by the condensate the $2D$ Bogoliubov mode is a perfect heat carrier. In fact, the thermal conductivity is infinite. To show this we write the expression for the heat flow, taking into account that in the superconducting state both the chemical and the electrical potentials are zero:

$$\mathbf{Q} = -\sum_{\mathbf{k}} \frac{d\epsilon_{\mathbf{k}}}{d\mathbf{k}} \epsilon_{\mathbf{k}} \frac{\partial n(\mathbf{k})}{\partial T} \tau^s(k) \left(\frac{d\epsilon_{\mathbf{k}}}{d\mathbf{k}} \nabla T\right) \tag{7.60}$$

where $n(\mathbf{k})$ is the Bose-Einstein distribution function with zero chemical potential and

$$\tau^s = \frac{\tau^s_{ac}\tau^s_{im}}{\tau^s_{ac} + \tau^s_{im}} \tag{7.61}$$

Substitution of Eq.(7.61) into Eq.(7.60) yields the superconducting-state thermal conductivity:

$$K_s \sim \frac{1}{T^8} \int_0^{E_s/T} dx \frac{1}{x^2 \sinh^2(x)\left(x^4 + \eta/T^5\right)} = \infty \tag{7,62}$$

where η is a temperature independent constant, proportional to the ratio of the iii purity and phonon scattering cross-sections. The infinite thermal conductivity it $2D + \epsilon$CBG is quite unexpected compared with the usual s-wave BCS supercon ductor, which has exponentially suppressed thermal conductivity due to a gap the excitation spectrum. Three-dimensional corrections to the spectrum cancel ii
'infrared' divergence of K_s. As a result the temperature shape of the thermal conductivity curve of near $2D$ bosons below their condensation temperature is controlled by the simultaneous increase of 'diffusivity' of the Bogoliubov excitations due to the screening of the scattering potential as well as due to the long-wave singularity of the group velocity and by the decrease of the heat capacity, $C_b \sim T^4$. This shape is in global qualitative agreement with the experimental data for high- T_c copper oxides which show the in-plane thermal conductivity enhancement in the superconducting state.

5.8.6 7.6 BEC of charged bosons in a random potential

Kinetic properties of charged bosons in real solids depend on their localization in a random potential. The intuitive picture of hard - core bosons filling up all localized single-particle states and Bose-condensing into the first extended state is known in the literature. To calculate the density of localised bosons $n_L(T)$ one should take into account the repulsion between them. One cannot ignore the fact that the localization length ξ generally varies with energy and diverges at the mobility edge. One would expect that the number of hard - core bosons in a localized state near the mobility edge diverges in a way similar to the localization length. Therefore,

it is still not clear how the hard-core bosons form a true (extended) Bose-Einstein condensate (BEC) in the random field.

However, in the case of CBG the Coulomb repulsion restricts the number of bosons in each localised state, so that the distribution function will show a mobility edge E_c (Mott (1993)). The number of bosons in a single potential well is determined by the competition between their long-range Coulomb repulsion $\simeq 4e^2/\xi$ and the binding energy $E_c - \epsilon$. If the localization length diverges with the critical exponent $\nu < 1 : \left(\xi \sim (E_c - \epsilon)^{-\nu}\right)$, one can apply a 'single well-single particle' approximation assuming that one can place only one boson in each potential well. In doped semiconductors the exponent ν depends on the degree of compensation varying from $\nu = 0.5$ in SiP to $\nu \simeq 1.0$ in amorphous $NbSi$. In an extreme case of the hydrogen atom the average electron-nucleus distance is proportional to the inverse binding energy, i.e. $\nu = 1$.

In two dimensions any random potential yields localised states, independent of its strength. Here we consider BEC of quasi-two dimensional bosons by the use of the 'single well-single particle' approximation (Alexandrov et al (1994)). Within this approximation localized charged bosons obey the Fermi-Dirac statistics:

$$n_L(T) = \int_{-\infty}^{E_c} \frac{N_L(\epsilon) d\epsilon}{\exp\left(\frac{\epsilon-\mu}{T}\right) + 1} \tag{7.63}$$

where $N_L(\epsilon)$ is the density of localized states. Near the mobility edge it remains constant $N_L(\epsilon) \simeq \frac{n_L}{\gamma}$ with γ of order of a binding energy in a single random potential well and n_L the total number of localized states per unit cell. We chose the position of the mobility edge as zero, $E_c = 0$. Then for $n \geq n_L$ the number of empty localised states turns out to be linear as a function of temperature in a wide temperature range $T < \gamma, 2t$ because the chemical potential is pinned in this temperature region to the mobility edge, $\mu \simeq E_c = 0$ ($2t$ is the bandwidth). This follows from the conservation
of the total number of bosons $n = n_b(T) + n_L(T)$, which yields for the chemical potential:

$$\frac{T}{2t} \ln \frac{1}{1-y} - \frac{n_L T}{\gamma} \ln\left(1 + y^{-1}\right) = n - n_L \tag{7.64}$$

If $T \ll (\gamma, 2t)$, the solution of this equation is $y \simeq 1$ with an exception of a very narrow region of concentration $n - n_L \ll T/2t$, where y decreases to about 0.6. The density of extended bosons n_b depends on y logarithmically,

$$n_b(T) = \frac{T}{2t} \ln\left(\frac{1 - ye^{-2t/T}}{1-y}\right) \tag{7.65}$$

Therefore its temperature dependence remains practically linear up to $T \simeq \gamma$:

$$n_b(T) = n - n_L + n_L bT, \tag{7.66}$$

with temperature independent $b = \ln 2/\gamma$.
It turns out that the decrease of the density of extended bosons with the temperature lowering (up to zero for $T = 0$ and $n_L = n$) does not prevent the Bose-Einstein condensation. There is no true Bose condensate in two dimensions. Therefore we introduce a three-dimensional correction to the free boson energy spectrum as

$$E_{\mathrm{k}} = \frac{k_\parallel^2}{2m^{**}} + 2t_\perp \left(1 - \cos\left(k_\perp d\right)\right) \tag{7.67}$$

Then the density of the extended states $N(\epsilon)$ is given by

$$N(\epsilon) = \frac{1}{2t\pi} \arccos\left(1 - \frac{\epsilon}{2t_\perp}\right) \tag{7.68}$$

for $0 < \epsilon < 4t_\perp$ and $N(\epsilon) = 1/2t$ for $4t_\perp < \epsilon < 2t$ with $t_\perp \ll t$ the inter-plane hopping, d the interplane distance, and $m^{**} \simeq \pi/ta^2$ the in-plane effective mass.

The BEC temperature is found by the use of

$$n_b(T) = \int_0^\infty dE \frac{N(E)}{\exp(E/T) - 1}, \tag{7.69}$$

which for $T_c \ll 2t$ can be written as

$$\frac{T_c}{2t\pi} \int_0^{4t_\perp/T_c} dx \frac{\arccos\left(1 - xT_c/2t_\perp\right)}{\exp(x) - 1} - \frac{T_c}{2t} \ln\left[1 - \exp\left(-\frac{4t_\perp}{T_c}\right)\right] = n - n_L + \frac{T_c n_L \ln 2}{\gamma}$$

This equation is simplified if $T_c \gg t_\perp$:

$$\frac{T_c}{2t} \ln\left[\frac{T_c \exp\left(1 - 2n_L t \ln 2/\gamma\right]}{2t_\perp}\right] = n - n_L \tag{7.71}$$

Depending on the 'compensation', $n - n_l, T_c$ changes from

$$T_c = \frac{2t\left(n - n_L\right)}{L} \tag{7.72}$$

for

$$n - n_L \gg \frac{t_\perp \exp\left(\frac{2n_L t \ln 2}{\gamma} - 1\right)}{t} \tag{7.73}$$

with

$$L = \ln\left[\frac{(n - n_L)\,\mathrm{texp}\left(1 - \frac{2n_L t \ln 2}{\gamma}\right)}{t_\perp}\right] \tag{7.74}$$

to

$$T_c \simeq 2t_\perp \exp\left(\frac{2n_L t \ln 2}{\gamma} - 1\right) \tag{7.75}$$

if $n = n_L$.T_c depends on the compensation $n - n_L$ practically linearly, Fig.7.2.

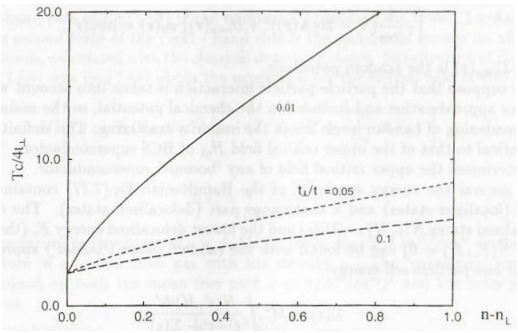

Fig.7.2. T_{c} of CBG in a random potential as a function of the compensation $n - n_L$.

In general, statistics of localised bosons is different from both the Fermi and BoseEinstein statistics. The shallow potential wells can accommodate more than one boson, so the profile of

the density of states just below the mobility edge is important for the low temperature CBG kinetics.

Charged bosons like ordinary carriers in doped semiconductors screen the random potential. The screening radius at $T = 0$ is given by the value $q_s^{-1} = \sqrt{2m^{**}\omega_{po}}$. Therefore, we would expect that the Mott criterion for the metal-insulator transition

$$n_{im}^{1/3} a_B \simeq 0.26, \tag{7.76}$$

to be valid with $2n_{im}$ instead of n_{im} and $a_B \simeq \epsilon_0/m^{**}(2e)^2$. With $\epsilon_0 \sim 100$ and $m^{**} \sim 10m_e$ this yields $n_{im} \sim 10^{22}$ cm^{-3}.

5.8.7 7.7 BEC of charged bosons in a magnetic field

As noted by Schafroth(1955) an ideal charged Bose-gas in a magnetic field cannot be condensed because of the one-dimensional character of particle motion within the
lowest Landau level. However, the interacting charged Bose-gas is condensed in a field lower than a certain critical value H^* because the interaction with impurities or between bosons broadens the Landau levels and thereby eliminates the one-dimensional singularity of the density of states (Alexandrov (1993)). As we discuss below the critical field of BEC has an unusual positive curvature near $T_{c0}, H^*(T) \sim (T_c - T)^{3/2}$. At low impurity concentration it diverges at $T \to 0$. The localization can drastically change the low-temperature behavior of $H^*(T)$, so at high concentration of impurities the re-entry effect to the normal state occurs.
H^* is determined as the field in which the first nonzero solution of the linearized stationary equation for the macroscopic condensate wave function $\psi_0(\mathbf{r}) = \langle N|\hat{\psi}(\mathbf{r},\tau) \mid N+1\rangle, (N \to \infty, N/V = n = \text{const})$ appears:

$$\left[-\frac{1}{2m}(\nabla - 2ie\mathbf{A}(\mathbf{r}))^2 + U_{imp}(\mathbf{r})\right]\psi_0(\mathbf{r}) = \mu\psi_0(\mathbf{r}) \tag{7.77}$$

where $U_{imp}(\mathbf{r})$ is the random potentials.
We suppose that the particle-particle interaction is taken into account within the Hartree approximation and included in the chemical potential, so the main origin of the broadening of Landau levels lies in the impurity scattering. This definition of H^* is identical to that of the upper critical field H_{c2} of BCS superconductors. Therefore H^* determines the upper critical field of any 'bosonic' superconductor.

In general the energy spectrum of the Hamiltonian Eq.(7.77) contains discrete levels (localized states) and a continuous part (delocalised states). The density of delocalised states $\tilde{N}(\epsilon, H) \sim \Im\Sigma(\epsilon)$ and the lowest delocalised energy E_c (the mobility edge, $\tilde{N}(E_c, H) = 0$) can be found with the random phase ('ladder') approximation for the one-particle self-energy:

$$\Sigma(\epsilon) = M^2 \int \frac{N(\epsilon', H)\, d\epsilon'}{\epsilon - \epsilon' - \Sigma(\epsilon)} \tag{7.78}$$

where M^2 is the squared matrix element for the boson-impurity scattering multiplied by the impurity density, and

$$N(\epsilon, H) = \frac{\sqrt{2}\,(m^{**})^{3/2}\,\omega}{4\pi^2} \Re \sum_{N=0}^{\infty} \frac{1}{\sqrt{\epsilon - \omega(N + 1/2)}} \tag{7.79}$$

is the density of states for a noninteracting system with $\omega = 2eH/m^{**}$.
The solution of Eq.(7.78) yields for the lowest Landau level ($N = 0$)

$$\tilde{N}_0(\epsilon, H) = \frac{\sqrt{6}\,(m^{**})^{3/2}\,\omega}{8\pi^2\sqrt{\Gamma_0}} \left[\left(\frac{\tilde{\epsilon}^3}{27} + \frac{1}{2} + \sqrt{\frac{\tilde{\epsilon}^3}{27} + \frac{1}{4}} \right)^{1/3} - \left(\frac{\tilde{\epsilon}^3}{27} + \frac{1}{2} - \sqrt{\frac{\tilde{\epsilon}^3}{27} + \frac{1}{4}} \right)^{1/3} \right] \quad (7.80)$$

and

$$E_c = \frac{\omega}{2} - \frac{3\Gamma_0}{2^{2/3}} \quad (7{,}81)$$

Here $\Gamma_0 = 0.5\left(2M^2 eH\sqrt{m^{**}}/\pi\right)^{2/3}$ is the characteristic broadening of the lowest Lan dau level and $\tilde{\epsilon} = (\epsilon - \omega/2)/\Gamma_0$.

Because the singularity of the density of states is integrated out for all levels except $N = 0$, one can neglect their quantization using the zero field density of states for $\epsilon > \omega$,

$$N(\epsilon) \simeq \frac{(m^{**})^{3/2}\sqrt{\epsilon}}{\sqrt{2}\pi^2} \quad (7.82)$$

The first nontrivial extended solution of Eq.(7.77) appears at $\mu = E_c$. Thus the critical curve $H^*(T)$ is determined from the conservation of the number of particles n_b under the condition that the chemical potential coincides with the mobility edge:

$$\int_{E_c}^{\infty} \frac{\tilde{N}_0\,(\epsilon, H^*)\,d\epsilon}{\exp\left(\frac{\epsilon - E_c}{T}\right) - 1} = n\left[1 - (T/T_{c0})^{3/2} - \frac{n_L(T)}{n}\right] \quad (7.83)$$

The left-hand side of Eq.(7.83) is the number of bosons on the lowest Landau level, while the second term of the right - hand side is the number of bosons on all upper Landau levels, calculated with the classical density of states. Substitution of Eq.(7.80) and Eq.(7.63) into Eq.(7.83) yields the expression for the critical field of BEC:

$$H^*(T) = H_d\,(T_{c0}/T)^{3/2}\left[1 - (T/T_{c0})^{3/2} - \frac{T n_L}{\gamma n}\beta(T/\gamma)\right]^{3/2} \quad (7.84)$$

with

$$\beta(x) = \sum_{k=0}^{\infty} \frac{(-1)^k}{x + k} \quad (7.85)$$

and temperature independent $H_d = \phi_0/2\pi\xi_0^2$. Here $T_{c0} \simeq 3.3n^{2/3}/m^{**}$ is the BEC temperature of an ideal Bose gas with the density n. The 'coherence' length ξ_0 is determined by both the mean free path $l = \pi/M^2\,(m^{**})^2$ and the inter-particle distance as

$$\xi_0 \simeq 0.8(l/n)^{1/4} \quad (7.86)$$

Here $\phi_0 = \pi/e$ is the flux quantum.
Using the asymptotic $\beta(x) \simeq (2x)^{-1}$ at temperature $T > \gamma$ one obtains:

$$H^* = H_d\sqrt{1 - \frac{n_L}{2n}}\left(\frac{1}{\tau} - \sqrt{\tau}\right)^{3/2} \quad (7.87)$$

where $\tau \equiv T/T_c$ is the reduced temperature and

$$T_c = T_{c0}\left(1 - \frac{n_L}{2n}\right)^{2/3} \quad (7.88)$$

is the critical temperature of BEC in a random potential for zero magnetic field.
Thus $H^*(T)$ has the positive ' 3/2 ' curvature near T_c. This curvature is a universal feature of CBG, which does not depend on a particular scattering mechanism and on approximations made. The number of bosons at the lowest Landau level is proportional to the density of states near the mobility edge $\tilde{N}_0 \sim H/\sqrt{\Gamma(H)}$, where the 'width' of the Landau level is also proportional to the same density of states $\Gamma(H) \sim H/\sqrt{\Gamma(H)}$. Hence $\Gamma(H) \sim H^{2/3}$ and the number of condensed bosons is proportional to $H^{2/3}$. On the other hand this number in the vicinity of T_c should
be proportional to $T_c - T$ (the total number minus the number of thermally excited bosons). That gives the ' 3/2 ' law for $H^*(T)$.

At low temperatures $T \ll \gamma$ the temperature dependence of H^* turns to be different for different impurity concentration. If $0 < n_L < n$ the critical field diverges at $T \to 0$,

$$H^* \simeq H_d \left(T_{co}/T\right)^{3/2} \left(1 - \frac{n_L}{n}\right)^{3/2} \tag{7.89}$$

because the number of localized states is smaller then the number of bosons. In this case only the paramagnetic limit restricts the value of $H^*(0)$ if bosons are composed from two fermions with the opposite spins. If $n_L = n$ the critical field reaches its maximum at $T = 0$:

$$H^* \simeq H_d \left(T_{c0} \ln 2/\gamma\right)^{3/2} \left(1 - \frac{\pi^2 T}{8\gamma \ln 2}\right). \tag{7.90}$$

And finally, if $n < n_L < 2n$ there is a re-entry effect to the normal state at temperature below some T^*, so $H^* = 0$ for $T < T^*$, Fig.7.3.

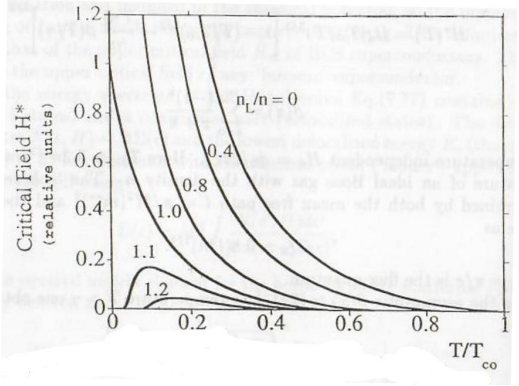

If the number of localized states is large, $n_L > 2n$ Bose condensation is impossible: $T_c = 0$.

Deriving Eq.(7.84) for H^* we expand the exponent in the left hand side of Eq.(7.83) and assume that the scattering amplitude is energy independent. The ultra-low ($T \ll \Gamma_0$) temperature behavior of H^* depends on these assumptions. In this temperature regime one can expect $T^{-9/2}$ behavior of H^* rather than $T^{-3/2}$. It depends also on the shape of the localised level distribution $N_L(\epsilon)$ as we shall discuss in Chap ter 8. However, the gross features like the divergent behavior at $T \to 0$ and the re-entry effect for the sufficiently large impurity density ($n_L > n$) are independent of the model and approximation made.

In contrast to the Fermi liquid, in which the long-range Coulomb interaction in screened and high-energy plasmons are not relevant for the low-frequency kinetic,
allowance for the Coulomb interaction at finite temperatures in CBG is a more complicated matter because plasmon and one particle excitation are essentially the same in the long-wave limit. However, the residual interaction between low-energy excitations of CBG is also screened, if we integrate out the high-energy excitations from the action. Therefore, one can assume that the mixed state of CBG in an external magnetic field can be described by the equation similar to that of the Ginsburg-Landau (GL) theory for the BCS superconductors, which is obtained from

the BdG set if we replace the long-range Coulomb potential for a short-range one $v_0(\mathbf{r}) \simeq v_q\delta(\mathbf{r})$ and neglect fluctuations of the order of $\tilde{\psi}^2$ (Alexandrov et al (1987))

$$\left[-\frac{1}{2m}(\nabla - 2ie\mathbf{A}(\mathbf{r}))^2 - \mu + v_0\left|\psi_0(\mathbf{r})\right|^2\right]\psi_0(\mathbf{r}) = 0 \tag{7.91}$$

This equation is supplemented by the expression for the superfluid current, Eq.(7.38) and by the Maxwell equation. Recognizing that the chemical potential of a homogeneous system is $\mu = nv_0$, the characteristic lengths in the problem are

$$\lambda_H = \sqrt{\frac{m^{**}}{16\pi ne^2}}, \tag{7.92}$$

which is the field penetration depth and

$$\xi = \frac{1}{\sqrt{2m^{**}nv_0}} \tag{7.93}$$

the GL coherence length. The GL ratio is $\kappa \equiv \lambda_H/\xi = m^{**}\left(v_0/8\pi e^2\right)^{1/2}$. Because $\left(v_0/16\pi e^2\right)^{1/2}$ is of the order of the screening radius q_s^{-1} the GL ratio is very large

$$\kappa \sim \frac{m^{**}c}{q_s} \gg 1, \tag{7.94}$$

where c is the light velocity. Therefore CBG is the extreme type -II superconductor. The lower critical field, in which a first normal vortex appears is given by the canonical Abrikosov (1957) expression

$$H_{c1}(0) \simeq \frac{\phi_0 \ln\kappa}{4\pi\lambda_H^2} \tag{7.95}$$

In particular, for $T = 0$ we estimate

$$H_{c1}(0) \simeq \frac{4\pi en}{m^{**}}\ln\kappa \tag{7.96}$$

In order to calculate the thermodynamic critical field H_c, in which the homogeneous superconducting state is in the thermal equilibrium with the normal phase, we assume that the ground state energy E_0 is determined by the interaction energy in both phases. The normal state is a homogeneous phase, in which bosons are on the lowest Landau level. Allowance for only the interaction energy in this state is equivalent to neglecting of small diamagnetism. The kinetic energy of the superconducting phase is small because the supracondensate density is small. Thus for the normal state we obtain per unit volume

$$E_0^n = n^2v_0 \tag{7.97}$$

and

$$E_0^s = \frac{1}{2}n^2v_0 \tag{7.98}$$

for the superconducting state. Doubling the energy of the normal state compared with the superconducting state is explained by the exchange contribution in the normal state, which is positive, in contrast to the Fermi gas. As a result, the thermodynamic critical field is

$$H_c(0) \equiv \sqrt{8\pi\left(E_0^n - E_0^s\right)} = \left(4\pi v_0\right)^{1/2}n \tag{7.99}$$

One can compare H_c of CBG with that of noninteracting charged bosons, calculated by Schafroth (1955), $H_0 = 2\pi ne/m^{**}$. Their ratio is

$$\frac{H_c}{H_0} \sim \kappa \gg 1 \tag{7.100}$$

Thus the diamagnetic energy is negligible.

5.8.8 7.8 Normal state kinetics of CBG

Above T_c the boson gas is nondegenerate. Therefore their kinetic properties are those of the nondegenerate carriers in doped semiconductors and can be studied by solving the Boltzmann equation taking into account the scattering by acoustical phonons, by each other and by unscreened random potential. As a result one obtains the canonical expressions for the Hall coefficient R_H and the resistivity ρ :

$$R_H = \frac{\langle \tau^2 \rangle}{2en_b(T)\langle \tau \rangle^2} \tag{7.101}$$

$$\rho = \frac{m^{**}}{4e^2 n_b(T)\langle \tau \rangle} \tag{7.102}$$

where $\langle \ldots \rangle$ means an average with energy and the derivative of the Bose-Einstein distribution function

$$\langle A(E) \rangle \equiv \frac{\int dE N(E) E A(E) n'(E)}{\int dE N(E) E n'(E)} \tag{7.103}$$

for the simplest case of isotropic energy spectrum with the density of states $N(E)$. Here $n'(E) = \partial n(E)/\partial E$.

The case of quasi-two dimensional bosons is important for high- T_c copper oxides. In the normal state the characteristic boson momentum is large compared with the inverse screening length $q > q_s$ and therefore the scattering potential is not screened, $\epsilon(q, 0) = 1$. The transport relaxation rate due to the two-dimensional acoustic phonon scattering is energy independent and linear in temperature (Section 4.11)

$$\frac{1}{\tau_{b-ac}} = m^{**} C_{ac} T \tag{7.104}$$

where the constant C_{ac} is proportional to the deformation potential.

In case of the classical statistics umklapp scattering can be neglected, so the scattering between bosons in extended states does not contribute to the resistivity. However, in the random potential the inelastic scattering of an extended boson by localised bosons makes a contribution because the momentum is not conserved in two-particle collisions. Therefore the boson-boson scattering contributes to the transport relaxation rate in disordered solids. In a 'single well-single particle approximation' the role of the Pauli exclusion principle is played by the dynamical repulsion between bosons. That is why the boson-boson relaxation rate has the same temperature dependence as the fermion-fermion scattering. In particular, the relaxation rate is proportional to the temperature squared because only localized bosons within the energy shell of the order of T near the mobility edge contribute to the scattering and because the number of the final states is proportional to temperature,

$$\frac{1}{\tau_{b-b}} = \frac{\alpha e^2 b n_L}{m^{**}} T^2 \tag{7.105}$$

with α a constant.
As a result one obtains

$$R_H = \frac{1}{2e\left(n - n_L + bn_L T\right)} \tag{7.106}$$

$$\rho = \left[\left(m^{**}\right)^2 C_{ac}/4e^2\right] \frac{T + \sigma_b T^2}{n - n_L + bn_L T} \tag{7.107}$$

where $\sigma_b = \alpha e^2 b n_L / \left(m^{**}\right)^2 C_{ac}$ is the relative boson-boson scattering cross-section. The density of extended bosons is temperature dependent as discussed in section 7.6, which leads to the temperature dependent Hall constant and to the linear resistivity. The boson-phonon scattering is mainly responsible for the linear temperature dependence of ρ at low temperatures while the boson-boson scattering and the temperature dependent density $n_b(T)$ are responsible for the linear ρ at higher temperatures. The residual resistivity is taken to be zero. Any nondegenerate carriers on a two-dimensional lattice have the same temperature and doping dependencies of their kinetic properties, so decomposition of the boson into two fermions at high temperatures does not change the temperature dependencies of R_H and ρ. As regards the Hall angle Θ_H above T_c the number of carriers increases linearly with T, while the boson-boson scattering gives the relaxation rate $1/\tau \sim nT$, so that $\rho \sim 1/n\tau \sim T$ and $\cot\Theta_H \sim 1/\tau \sim T^2$ in full agreement with many experimental observations in highT_c copper oxides (Alexandrov and Mott (1994)). At high temperatures ($T \gg \gamma$) the density of extended bosons eventually saturates, as measurements of the Hall coefficient in several copper oxides show.

Finally, we calculate the thermal conductivity K_n of $2D$ bosons in the normal state applying the standard kinetic theory, developed for metals and semiconductors, by replacing the Fermi distribution function for the Bose function. As a result one obtains the Wiedemann-Franz law

$$K_n = L_B \sigma T \tag{7.108}$$

where σ is the normal state conductivity, and

$$L_B = \left(\frac{k_B}{2e}\right)^2 \frac{3B_0(z)B_2(z) - 4B_1^2(z)}{B_0^2(z)} \tag{7.109}$$

is a bosonic Lorentz number with

$$B_\nu(z) = \int_0^\infty \frac{x^\nu dx}{\exp(x - z) - 1} \tag{7.110}$$

Here zT is the chemical potential and k_B is the Boltzmann constant. The transport relaxation time is assumed to be energy independent. In the classical high-temperature limit, $T \gg T_c$ we obtain:

$$L_B = 2\left(\frac{k_B}{2e}\right)^2 \tag{7.111}$$

The boson Lorentz number, Eq.(7.109), should be compared with the electron one, $L_e = \pi^2 k_B^2/3e^2$, which does not depend on the scattering mechanism or on the dimensionality for degenerate carriers. Their ratio is very small mainly due to the double elementary charge of a boson. It is given by

$$\frac{L_B}{L_e} = \frac{6}{4\pi^2} \tag{7.112}$$

which is approximately 0.152. Taking this into account one can explain the near equality of the thermal conductivity of superconducting and insulating crystals of $YBCO$ in the temperature range above 100 K (Alexandrov and Mott (1993)).

5.9 8 Evidence for mobile small polarons and bipolarons

5.9.1 8.1 Small versus large polarons

Over the last decades many materials with rather high density of carriers $n \geq 10^{20}$ cm^{-3} and low mobility of the order or even less than the Mott-Ioffe-Regel limit ($ea^2/\hbar \sim 1cm^2/Vs$) were discovered. In our book we have put forward the multipolaron theory of low-mobility solids, which cannot be understood within the framework of the canonical theory of metals. This Chapter is intended to discuss several experiments supporting the theory.

There is some confusion in the literature, particularly about the use of the terms 'large' and 'small' polarons and bipolarons. Some authors define the 'large polaron' as a mobile electron moving together with the self-induced extended polarization in an ionic crystal and the 'small polaron' as an immobile object completely localised within a unit cell (site). This is physically and historically incorrect. It has been known for four decades starting from pioneering work by Tjablikov (1952) and Holstein (1959) that the small polaron can tunnel in a narrow band because of the translational symmetry. Now a clear 'borderline' between large and small polarons and bipolarons is established with the scaling analysis, Monte-Carlo, cluster, variational and analytical calculations as we have discussed in Chapters 1,2 and 4. If one determines a dimensionless coupling constant

$$\lambda = \frac{E_p}{D} \tag{8.1}$$

which is essentially the same as the BCS one, large bipolarons can exist in ionic crystals at

$$\lambda \leq 0.5 \tag{8.2}$$

and small bipolarons exist in all crystals at

$$\lambda \geq 0.5 \tag{8.3}$$

Here $E_p \equiv g^2\hbar\omega$ is the Frank-Condon (or polaronic) shift, D is a bare half-bandwidth and ω is the characteristic phonon frequency. Therefore, $1/\lambda$ characterises the size of a polaron. The second dimensionless constant $g^2 = E_p/\hbar\omega$, which is the number of
phonons in a cloud around the polaron, determines the small polaron half-bandwidth w

$$w \sim D \exp\left(-g^2\right) \tag{8.4}$$

This is definitely nonzero and can be as high as several hundred K if high frequency phonons $\omega_0 \sim 0.05 - 0.1$eV are involved in the polaron formation and the bare adiabatic ratio $D/\hbar\omega$ is not very large: $D/\hbar\omega < 10$. Moreover, the calculations of the bandwidth beyond the Holstein model show that the narrowing factor g^2 is considerably reduced compared with a naive estimate ($\simeq E_p/\omega$) because of the dispersion. As we have discussed in section 6.2, $g^2 \sim 0.2E_p/\omega$ is quite feasible in copper based oxides.

As stressed by Shluger and Stoneham (1993) much of the single polaron theory is based on highly idealised models, often essentially a continuum description with a single vibrational frequency. These models ignore much of the wealth of the experimental data, which find interpretation in many atomistic simulations. The continuum description leads to the collapse of large polarons at an intermediate value of the coupling $\lambda \sim 1$. As a result, one can discuss

large polarons in ionic crystals only if the coupling with phonons is not large. The carrier density should also be small to avoid the overlap of the extended deformation fields as well as their screening. We believe that when the density of carriers is about 10^{21} cm^{-3} or higher, so the number of polarons per unit cell is above few percent, large bipolarons cannot survive because of screening. A simple estimation of the screening length r_s yields for the quasi-two dimensional Fermi gas

$$r_s \simeq \frac{\hbar}{2}\sqrt{\frac{\epsilon_0 d}{m^* e^2}} < 4\text{Å} \tag{8.5}$$

with the static dielectric constant $\epsilon_0 \sim 100, m^* = 5m_e$ and the interplane distance $d \sim 5A$. This estimate remains valid also for three dimensions if the carrier density $n \geq 10^{21}$ cm^{-3}. Therefore any extended lattice distortion and large polarons are ruled out by screening. In this case the many body effects including superconductivity should be described by the Migdal-Eliashberg theory, so the superconducting state at $\lambda \leq 0.5$ is the BCS superconductor.

On the other hand small mobile polarons form in the strong coupling regime $\lambda > 0.5$ at any doping. Their hallmarks are

- a low but finite mobility,
- the coherent band motion at temperatures below the characteristic phonon frequency and the activated mobility above it,
- a mid-infrared maximum of optical conductivity with a descrete multiphonon structure,
- the polaron band narrowing.

Being rather heavy they readily form small bipolarons if a short range attraction due to the local lattice deformation overcomes the Coulomb repulsion. Because in ionic solids the essential part of the Coulomb repulsion is screened by optical phonons, the deformation potential and molecular vibrations can easily bind two small polarons at a short distance. The hallmarks of small bipolarons are those of small polarons, plus

- superfluid phase transition similar to that of He^4,
- spin gap in the magnetic susceptibility, that is $\chi_s \to 0$ at $T \to 0$ if a singlet is the ground state ,
- electrodynamics of the charged Coulomb Bose gas,
- double elementary charge $2e$ in the normal state.

However, the absence of some of these properties does not tell us that carriers are not small (bi)polarons. As an example, proceeding from the absence of the activated mobility in doped copper oxides and from an estimation of the effective mass based on a Drude-like fit to the optical conductivity some workers interpret kinetic and optical data for copper oxides in terms of large polarons with $m^* \simeq 2m_e$ or free electrons. However, the value of the effective mass itself cannot be used to distinguish large and small polarons. In case of small polarons the mass enhancement is the same as the band narrowing factor, and is generally larger than an increase of the band mass due to the large polaron formation. However, in both cases the band mass can be and often is significantly smaller than the free electron mass m_e as discussed in section 3.5. Therefore, the absolute value of the effective mass does not yield the value of the band mass renormalisation. Moreover, a low effective mass of the order of $2m_e$ might be, in our view, an artifact of the Drude-like fit to the optical conductivity which definitely fails to describe

the multiphonon midinfrared maxima. The Drude formula is meaningless if the effective mass as well as the relaxation rate are frequency dependent. Their frequency dependence is itself a small polaronic feature. Low field measurements of the London penetration depth in high-T_c superconductors consistently yield larger m^* for polarons($\simeq 5m_e$) and $m^{**} \geq 10m_e$ for bipolarons. With a low value of the effective mass ($\sim 2m_e$) one fails to explain a low value of the *dc* mobility. Also the absence of the activation law in oxides at high temperatures is compatible with small polarons because the characteristic phonon frequency is very high ($\sim 1000K$), of the order of the activation energy, so the activation hopping can not be verified.

Here we present a discriminating selection of kinetic, optical, and photoemission experimental data, which unequivocally show that carriers in different insulating and superconducting oxides are small polarons and small bipolarons.

5.9.2 8.2 Small-polaron transport in TiO_2 and NiO

The comprehensive investigation of the small polaron transport has been performed in rutile TiO_2 by Bogomolov et al (1967). The small polaron transport mechanism was also proposed for NiO (Appel (1968), Austin and Mott (1969)). From experimental investigation of the drift and Hall mobilities, the infrared absorption, the thermoelectric power and comparison with the small polaron theory one gets quite convincing evidence for the small polaron transport in TiO_2. Figure 8.1 shows the drift and Hall mobilities for lightly reduced rutile above $100K$. The small value of the mobility is the most characteristic feature of TiO_2. For conduction perpendicular to the *c* axis the drift mobility shows an increase above room temperature with an activation energy of 0.13 eV. For conduction along the *c* axis the activation energy is 0.07 eV. The curve of the drift mobility has a minimum around room temperature, which is characteristic of small polarons if the activation region of parameters, $\omega < T \ll E_0$ is realised. The Hall depends depends on temperature, which is also characterister agreement with that in the high temperature region $\mu_H/\mu_d < 1$ is in agreement with that expected for
the adiabatic small polaron (Böttger and Bryksin (1985)). Normally, the activated behaviour of μ_H sets in at higher temperatures than for μ_d with a smaller activation energy. Thus the absence of an activated temperature dependence of μ_d only indicates that its activation region is not reached in the experiment. A striking feature in TiO_2 is that the Hall mobility is very small (~ 1 cm$^2/Vs$) above room temperature but rises to large value at temperatures below about $50K$. The drift mobility increases also with the temperature lowering up to the value about 50 cm$^2/Vs$ at 30 K , which also with the which, he explanation was given by Austin and Mott (1969). As we have discussed in Chapter 4 the polaron behaves like a heavy particle in a narrow band below $T \sim \omega_D/2$, and the relaxation time is determined by phonon and impurity scattering. The estimated polaron bandwidth is very small in rutile (see below), therefore single-phonon optical scattering is prohibited and twophonon contribution is frozen out. Thus a large increase in mobility is predicted at low temperatures, if the impurity scattering is not too strong.

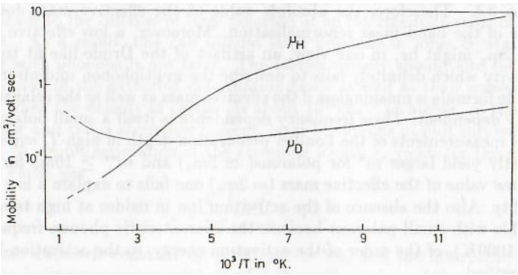

Fig.8.1. Hall μ_{H} and drift μ_d mobilities in TiO_2 as a function of the inverse temperature.

Semiconducting samples of TiO_2 show an absorption peak at ~ 0.8eV which correlates in intensity with the magnitude of the conductivity. At temperatures above 50 K a single peak in the absorption is independent of the nature of the donor centres and attributed to small free polarons. Below $10K$, a single peak is observed at $\sim$ 1eV, the exact position depending on the nature of the donor centres, and this is attributed to bound polarons. The frequency and temperature dependence of the absorption coefficient of TiO_2 doped with Nb , measured by Kudinov et al (1969) agrees well with the MIR conductivity of small polarons (Böttger and Bryksin (1985)). From the analysis of the optical data the estimated characteristics of the small polaron are

$$E_p \simeq 0.4\text{eV}; E_a \simeq 0.2\text{eV}; g^2 = 4. \tag{8.6}$$

With the value of the transfer integral $T(\mathbf{a}) \simeq 0.1$eV estimated from band structure calculations one obtains by the use of the non-adiabatic small polaron theory (Chapter 4)

$$\sigma(\mathbf{a}) = T(\mathbf{a})e^{-g^2} \simeq 2meV, \tag{8.7}$$

and the effective mass enhancement

$$\frac{m^*}{m_e} \simeq 150 \tag{8.8}$$

The measurements of the line width of ESR on defect centres in TiO_2 for different carrier densities confirmed this estimation of the effective mass (Bogomolov et al (1968)).

As it was discussed by Austin and Mott (1969) nickel oxide is a Mott insulator, which becomes a p-type semiconductor when doped with lithium or partially reduced. The measured values of the drift and Hall mobilities are below 1 cm^2/V s at room temperature. However, because $\omega_D/2$ is rather high (about $400K$) the thermally activated hopping is hardly expected. Nevertheless, there is some evidence of hopping conduction to the thermally activated polaron hopping in Li-doped NiO. The estimated value of the polaronic level shift is $\sim$ 0.7eV, the polaron radius is 1Å, the bare transfer integral $T(\mathbf{a})$ is estimated at 0.3 eV contrasted with 0.1 eV for TiO_2. The polaron transfer integral is $\sigma(\mathbf{a}) < 12$meV which corresponds to $m^* > 30m_e$. The study of the polaronic transport in doped nickel oxide is complicated by the magnetic fluctuations. In NiO, μ_H shows an anomalous behaviour near the Neel point and the Hall constant changes sign. It seems certain that the sign reversal is associated with the onset of magnetic disorder cal absorption measurements are complicated by the state between 1 and 5 eV. An observed NIR absorptions

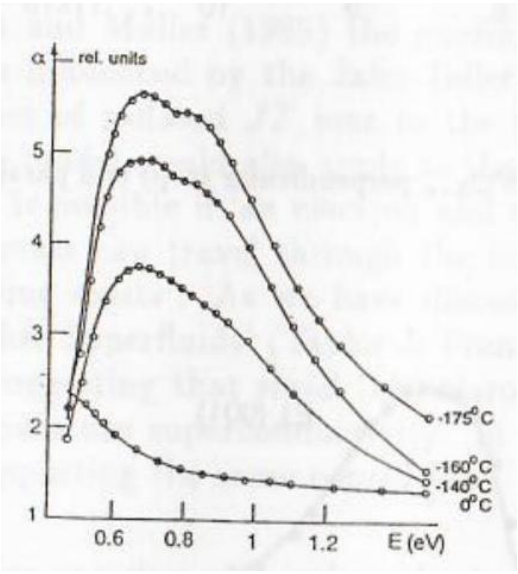

Fig.8.2. The absorbance of WO_{3-x} at low temperatures. Upon cooling poor metal $\delta - \mathrm{WO}_{3-x}$ transforms into (bi)polaronic semiconductor $\epsilon - WO_{3-x}$.

5.9.3 8.3 Mobile polarons and bipolarons in WO_{3-x}

Tungsten oxide, WO_{3-x}, studied in detail by a Cambridge group (Salje (1995)) shows properties of charge carrier transport, which cannot be described by those of free electrons. It is an almost ideal model compound for studies of polaronic transport because carriers can easily be generated or destroyed by chemical reactions or doping of WO_3 with $\mathrm{H, V, Mo}$ or implantation/removal of oxygen. They are not pinned to structural defects in crystals with reduced oxygen content because point defects are locally compensated. Formation of small polarons is specific for some structural
phases of WO_{3-x} but not for all. At room temperature and above $\delta - WO_{3-x}$ behaves as a poor metal. Its electronic transport is due to carriers with slightly enhanced mass and the Hall coefficient well in agreement with the predictions of almost free carriers with weak electron-phonon coupling, i.e. large polarons.

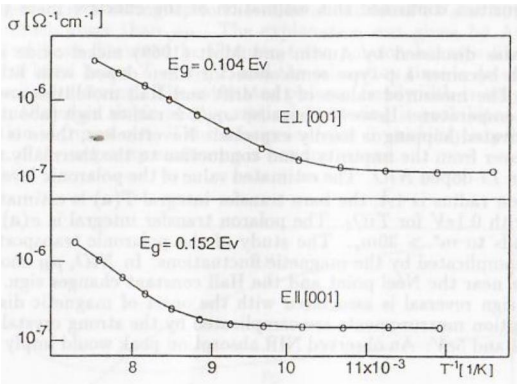

Fig.8.3. The conductivity of ϵ-WO_{3-x} perpendicular (top) and parallel (bottom) to the c-axis.

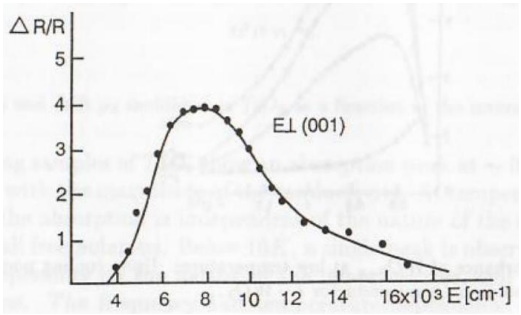

Fig.8.4. The energy dependence of the ESR photoeffect. $\Delta R/R$ is the relative change in ESR signal generated by illumination through splitting of bipolarons into pairs of small polarons ($T = 20K$).

The optical properties are dominated by Drude absorption and a fundamental absorption edge with $E_g = 2.77$eV, Fig.8.2. At temperatures close to 250 K , the crystal transforms on cooling into $\epsilon - WO_{3-x}$, which is insulating with a larger gap $E_g = 3.05$eV. The Drude absorption disappears. Instead, the optical absorption spectra display the (bi)polaronic profile, as shown in Fig.8.2. The experimentally observed profile shows a maximum at 0.71 eV , which corresponds to $E_p \simeq 0.3$eV, if
the IR conductivity is due to small polarons. The phonon energy results from the linewidth (section 4.11) and $\omega = 0.07$eV, i.e. in the expected spectral range of phonon modes of the WO_6 octahedra. The *dc* conductivity of $\epsilon - WO_{3-x}$ clearly shows the small (bi)polaron characteristics. The transport is thermally activated at $T \geq 100K$ with the activation energy $ca.E_p/2$ and tunneling in a (bi)polaronic band appears to occur at lower temperatures, Fig.8.3. When WO_3 is cooled in the dark, no ESR signal is observed in the ϵ-phase. This experimental result shows that all spins are paired in the ground state. The optical absorption shows a signal similar to that of polarons but shifted to higher energies about 1 eV. Single polarons are either generated thermally or, more conveniently, by photoexcitation of bipolarons. The fingerprint of single polarons is a strong ESR signal under illumination of $\epsilon - WO_{3-x}$ with the spectral dependence shown in Fig.8.4. The maximum efficiency occurs near 1 eV. The close similarity between the low-temperature absorption spectra and the spectral dependence of the ESR photoeffect suggests that the optical absorption is due to excitation of bipolarons. As the transport properties are highly two-dimensional ($\sigma_{ab} > 100\sigma_c$), it appears that bipolarons are confined to the $a - b$ plane, favoring the idea of disc-shaped bipolarons rather than spherical ones.

5.9.4 8.4 Small polarons in high- T_c oxides

According to Bednorz and Müller (1988) the guiding idea in searching for high- T_c superconductivity was influenced by the Jahn-Teller polaron model. Based on the experience from studies of isolated JT ions in the perovskite insulators, their assumption was that the model would also apply to the oxides, if they could be turned into conductors. This is possible if 'an electron and a surrounding lattice distortion with a high effective mass can travel through the lattice as a whole, and a strong electron-phonon coupling exists'. As we have discussed in 'High Temperature Superconductors and Other Superfluids' (Taylor & Francis (1994)) there is now a large body of experiments suggesting that small (bi)polarons are responsible for the phenomenon of high temperature superconductivity. In this section we discuss several recent observations supporting the same conclusion.

5.9.5 8.4.1 High- T_c oxides are doped semiconductors

The existence of 'parent' Mott insulators, which are spin ' 1/2 ' antiferromagnets suggest that high- T_c superconductors are, in fact, doped semiconductors. There is now a growing consensus that the dopant-induced charge carriers in high T_c oxides exhibit a significant dressing due to spin and lattice distortion. Studies of strongly correlated models like the Holstein $t-J$ model show that the critical electron-phonon coupling strength for polaron formation is considerably reduced by an antiferromagnetic exchange interaction compared to that in the uncorrelated model (section 5.5).

On the other hand, it has been suggested that optimally doped and overdoped oxides are metals with a large Fermi surface as follows from $ARPES$, the T^2 temperature dependence of resistivity, and from the small value of the Hall constant. However, the progress in elucidating the normal state of the prototypical cuprate $La_{2-x}Sr_xCuO4$ (Batlogg et al (1995), Hwang et al (1994)) leads us to the conclusion that optimally doped and overdoped copper oxides remain to be semiconductors. In
particular, semiconductor-like scaling with x of dc conductivity in $La_{2-x}Sr_xCuO_4$ for a wide temperature and doping region, Fig.8.5, has been observed.

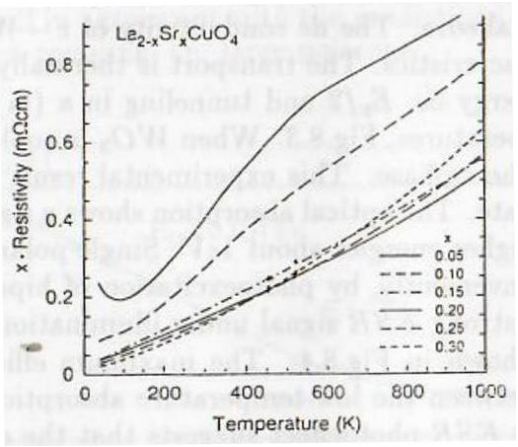

Fig.8.5. Resistivity of $\mathrm{La}_{2-x}\mathrm{Sr}_x\mathrm{CuO}_4$ multiplied by x covering the wide span of hole concentration from under to overdoping (Batlogg et al (1995)).

A plot of resistivity ρ multiplied by x brings $\rho(T)$ for various values of x on a similar scale, suggesting that the in-plane conductivity is dominated by holes, introduced with Sr, and that copper electrons remain localized even in overdoped oxides because of the large Hubbard U on copper and the local lattice deformation, which prevents their hopping.

Sometimes it is argued that unusual features of overdoped high- T_c oxides can be understood as a result of a strong magnetic pair-breaking if the spin-flip mean free path l_s is shorter than the coherence length ξ_0. However high- T_c oxides are at a 'clean' limit, the mean free path l is larger than ξ_0. This makes the magnetic pair breaking irrelevant for high- T_c because the strong inequality $l_s \ll l$ is unrealistic; normally $l_s \gg l$.

5.9.6 8.4.2 Low mobility

A low value of the in-plane mobility in high- T_c copper oxides is now well established. The Hall coefficient, dc conductivity, and hence the mobility in the CuO 2 planes were reported by MIT group (Chen et al (1995)) for single crystals of the prototypical cuprate La_2CuO_4 containing a few holes ($\sim 0.2\%$ per mole). In particular, they presented transport measurements

for current in the CuO 2 planes for two crystals. One of them, La_2CuO_{4+y}, referred to as $LCO-1$ in Fig.8.6, contained only enough oxygen accet a acce istic of undoped La_2CuO_4. The other, $La_{1.998}Sr_{0.002}CuO_4$ labeled as LSCO(295 K), has been reduced after growth to eliminate all excess oxygen. It contained about the same density of acceptors as $LCO-1$ and had almost the same Néel temperature. The in-plane mobilities are shown in Fig.8.6. Despite the different magnitudes of the mobilities the temperature dependencies are very similar and the absolute values are about 1 cm^2/Vs in the relevant temperature range near the superconducting transition in doped samples. A low effective mass of the oxygen-induced hole of only $\sim 2m_e$, as suggested by the Drude-like fit to the optical conductivity requires a surprisingly short scattering time and the concentration of ionized acceptors ten times larger than expected. Therefore, we believe that the effective mass of (bi)polarons in $LSCO$ should be enhanced up to $10m_e$ or more and (bi)polarons are small. This
conclusion is confirmed by the observation of an oxygen isotope effect on the Néel temperature in the insulating La_2CuO_4 suggesting the oxygen-mass dependence of the superexchange J (Zhao et al (1994))

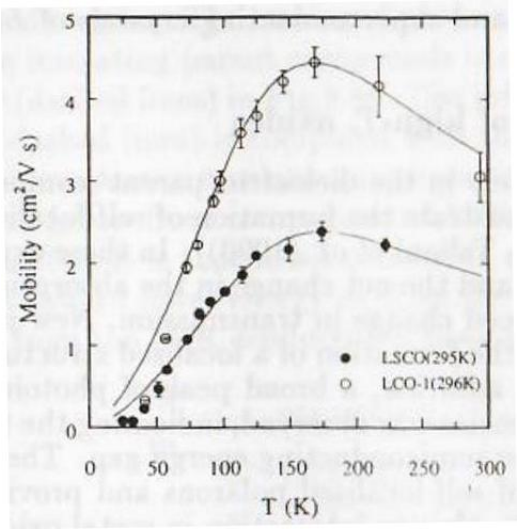

Fig.8.6. The in-plane mobilities of $LCO-1$ and $LSCO(295K)$ determined from Hall and conductivity measurements by Chen et al (1995).

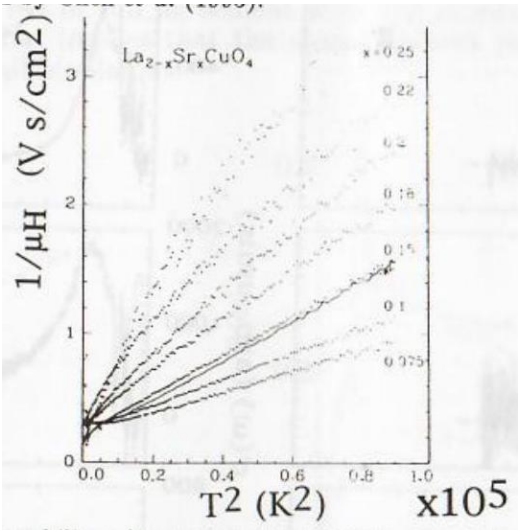

The latter is determined by the bandwidth and because of the small polaron band narrowing it depends on the phonon spectrum. This clear-cut experiment verified the crucial role of apex oxygen ions for the bipolaron formation in $LSCO$ in agreement with the first-principles calculations by Zhang and Catlow (1991), section 2.5. On the other hand, Mott (1995) has argued, that the polarons will necessarily produce also excited holes, which could be observed as light carriers.

The Hall mobilities of superconducting poly and single-crystals of $L_{2-x}Sr_xCuO_4$ were measured by Hwang et al (1994) over a wide temperature ($4 - 500$ K) and composition ($0 < x < 0.35$) range, Fig.8.7. For $x \leq 0.15$, the data follows a T^2 fit for $T > 100K$, with the systematic trend that the coefficient of the T^2 term increases with doping. This is in line with the bipolaron $2D$ kinetics as discussed in
section 7.8. The mobility value is between 1 cm$^2/Vs$ and 5 cm$^2/Vs$ for all measured temperatures and compositions. The Mott-Ioffe-Regel limit for the in-plane CuO_2 mobility is $ea^2/\hbar \simeq 2.5$ cm$^2/Vs(a \simeq 3.8$Å$)$. Therefore carriers are small polarons or bipolarons both in insulating and superconducting crystals of $LSCO$.

5.9.7 8.4.3 MIR conductivity of high- T_c oxides

Studies of photoinduced carriers in the dielectric 'parent' compounds like La_2CuO_4, $YBa_2Cu_3O_6$ and others demonstrate the formation of self-localised small polarons or bipolarons (Kim et al. (1988), Taliani et al. (1990)). In these experiments the sample was pumped by a laser beam and the net change in the absorption coefficient was determined from the photoinduced change in transmission. New photoinduced phonon modes were found indicating the formation of a localised structural distortion around a photogenerated carrier. In addition, a broad peak of photoinduced absorption in the electronic region of frequencies was observed, indicating the formation of localised electron states deep inside the semiconducting energy gap. These two aspects of the data confirm the formation of self-localised polarons and provide direct evidence of the importance of the electron-phonon interaction in metal oxides.

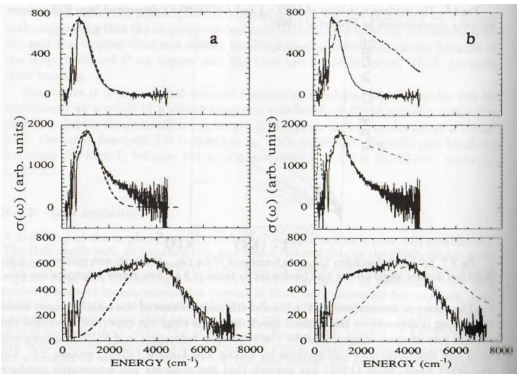

Fig.8.8 The photoinduced MIR conductivity in the insulator precursors for $\mathrm{Tl}_{2}\mathrm{Ba}_{2}\mathrm{CaCu}_{2}\mathrm{O}_{8}$ (top), $YBa_2Cu_3O_7$ (middle), and $La_{2-x}Sr_xCuO_4$ (bottom) compared with the polaron MIR conductivity (dashed line) (*a*); *b* : superconducting samples (dashed lines) compared with (*a*).

Mihailovic et al. (1990) described the spectral shape of the photoconductivity with the small polaron transport theory. They also argued that the similar spectral shape and systematic trends in both photoconductivity of optically doped dielectric samples and infrared conductivity of chemically doped high- T_c oxides indicate that carriers in the concentrated (metallic) regime retain much of the character of carriers in the dilute (photoexcited) regime. The measured photoinduced infrared conductivity $\sigma(\nu)$ (solid lines) in the insulating parent compounds is compared with the small-polaron MIR conductivity (dashed lines) in Fig.8.8a. The infrared conductivity of the high- T_c superconductors (dashed lines) is compared with the photoinduced infrared conductivity (solid lines) in respective insulator precursors in Fig.8.8b. One of the qualitative observations, which follow from comparison of MIR conductivities of insulating and superconducting materials is that in all perovskite exhibiting superconductivity, the peak energy shifts toward lower energy as T_c of the material increases. The polaron masses estimated from the MIR conductivity peak are

$$\begin{aligned} \frac{m^*}{m_e} &= 23(LSCO) \\ &= 13(YBCO) \\ &= 11\,(Tl_2Ba_2CaCu_2O_8) \end{aligned} \tag{8.9}$$

The critical temperature of the superconducting transition turns out to be inversely proportional to m^* in full agreement with the bipolaron theory of high- T_c superconductivity. That implies that the charge carriers in the normal state of high- T_c cuprates are small bipolarons.

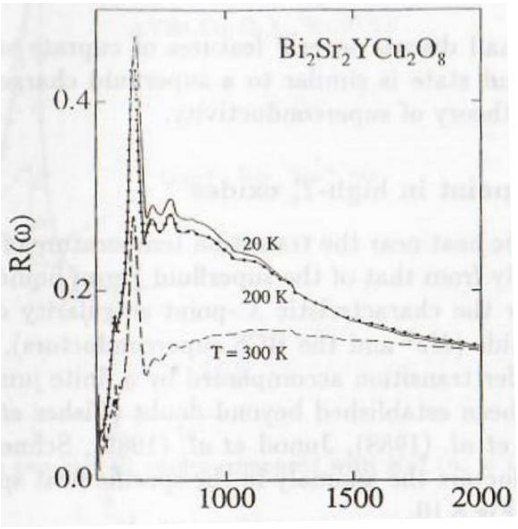

Fig.8.9. MIR reflectivity $R(\nu)$ for BSYCO single crystal at three different temperatures.

It follows from two upper curves of Batlogg's scaling of resistivity with x, Fig. 8.7 that the self-trapped (bi)polarons can be trapped by impurities. Falk et al (1993) measured the temperature dependence of the MIR reflectivity of lightly-doped La_2CuO_4. They found the large difference between the optical 0.13 eV and thermal 0.035 eV ionization energy. This observation as well as the line shape and the temperature dependence of the MIR peak are consistent with absorption from polaronic impurity states.

Calvani et al (1994, 1995) in a series of papers reported a fine structure of the MIR conductivity in several copper oxides, as predicted by the numerical calculations of the optical conductivity of the Holstein clusters (Alexandrov et al (1994b)), Fig.4.6. As an example, the MIR reflectivity of a single crystal of insulating $Bi_2Sr_2YCu_2O_8(BSYCO)$ is shown in Fig. 8.9 for three different temperatures. Therein, a strong infra-red band is observed, with a clear and T - dependent fine structure, together with the phonon peak at 610 cm^{-1}. Starting from $300K$, the amplitude of the IR band increases by a factor of two for T decreasing to $200K$, then it saturates. For the same temperature variation, the phonon peak at 640 cm^{-1} increases by less than 20%. The fine structure has been explained in terms of overtones of additional modes, which strongly depend on doping and temperature. These modes correspond to vibration of the locally perturbed lattice and are quite general features, as they appear also in the metallic phases of several high- T_c oxides. The finding that in the metallic phases of many cuprates the polaron band in the optical absorption is superimposed on a normal Drude term, implies that the carriers, responsible for superconductivity could represent either a normal Fermi liquid coexisting with a substrate of small polarons, or the coherent part of a small-polaron fluid. The correlation of the position of the MIR peak with the value of T_c favors the second scenario.

5.9.8 8.5 Small bipolarons in high- T_c oxides

We now shall discuss several features of cuprate superconductors which show that their ground state is similar to a superfluid charged Bose gas, as predicted by the bipolaron theory of superconductivity.

5.9.9 8.5.1 λ-point in high- T_c oxides

The specific heat near the transition temperature of the superfluid Bose liquid differs significantly from that of the superfluid Fermi liquid. Bose liquids (or more precisely He^4) show the characteristic λ-point singularity of their specific heat. Superfluid Fermi liquids (He^3 and the BCS superconductors), on the contrary, exhibit a sharp second order transition accompanied by a finite jump in the specific heat.

It has been established beyond doubt (Fisher et al. (1988), Loram et al. (1988), Inderhees et al. (1988), Junod et al. (1989), Schnelle et al. (1990)) that in high T_c superconductors the anomaly in the specific heat spreads to about $|T - T_c| / T_c \sim 0.1$ or larger, Fig.8.10.

The estimations with the canonical gaussian fluctuations yield an unusually small coherence volume, Table 8.1, comparable with the unit cell volume, $\Omega \simeq 167 \mathring{A}^3$ in $YBCO$ (Loram et al. (1992)). That means that the overlap of pairs is small (if any). Moreover it was stressed by Salamon et al (1990) that the heat capacity anomaly is logarithmic, and consequently, cannot be adequately treated by gaussian corrections to the mean field BCS heat capacity.

On the other hand one can rescale the absolute value of the specific heat and the temperature to compare the experimentally determined specific heat of He^4 with that of high- T_c oxides (Alexandrov and Ranninger (1992a)), Fig.8.10. The specific heat per boson in the two high T_c oxides practically coincides with that of He^4 ($n_b = 1$) in the entire region of the λ singularity. In fact for the 2223 compound the λ shape is experimentally better verified than in He^4 itself because of the fifty times larger value

Table 8.1: The coherence volume Ω in $\dot{A}^{3}$, the in-plane ξ_{ab} and out- of- plane ξ_c coherence lengths derived from a Ginzburg-Landau analysis of the specific heat (Loram et al. (1992)).

Compound	Ω	$\xi_{ab}^2, \left(\mathring{A}^2\right)$	$\xi_c, (\mathring{A})$
$YBa_2Cu_3O_7$	400	125	3.2
$YBa_2Cu_3O_{7-0.025}$	309	119	2.6
$YBa_2Cu_3O_{7-0.05}$	250	119	2.1
$YBa_2Cu_3O_{7-0.1}$	143	119	1.2
$Ca_{0.8}Y_{0.2}Sr_2Tl_{0.5}Pb_{0.5}Cu_2O_7$	84	70	1.2
$Tl_{1.8}Ba_2Ca_{2.2}Cu_3O_{10}$		40	< 0.9

of the critical temperature. The density of nonlocalised bosons $n_b(T_c)$ determined from the heat capacity fit to He^4 is very close to that determined from the Hall measurements:

$$n_b \simeq 1.8 \times 10^{21} \text{ cm}^{-3} \tag{8.10}$$

in the optimally doped $YBCO$. The specific heat of a single crystal of $YBa_2Cu_3O_7$ was measured with the magnetic fields up to $8T$ providing strong evidence for the critical exponents consistent with those observed in He^4 (Overend et al. (1994)).

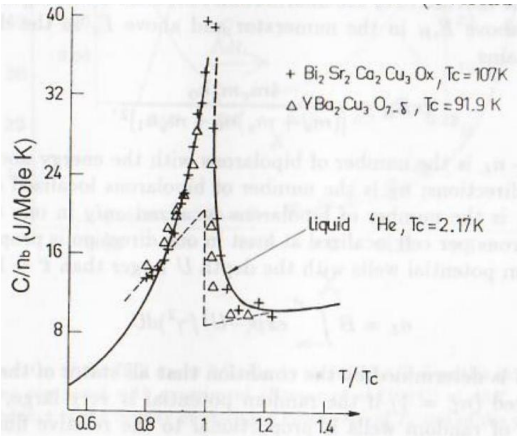

Fig.8.10. Heat capacity anomaly in two high- \$T_{c}\$ oxides compared with He^4 ($n_b = 1$), solid line

and with the BCS curve, dashed line.

5.9.10 8.5.2 Doping dependence of R_H, T_c and λ_H

The two-band bipolaron model discussed in section 6.2 allows us to explain an outstanding problem of the metal-semiconductor duality of overdoped copper oxides and the doping dependence of the critical temperature and the London penetration depth (Alexandrov (1995)).

It is well known that the effective mass anisotropy of energy ellipsoids in a square (or cubic) lattice diminishes the value of the Hall constant as in Si or Ge. In the presence of disorder an ' x ' -bipolaron can be localized in the y direction tunneling
practically freely along x and a ' y '-bipolaron can be localized in the x direction remaining free along y. That gives a very low metallic-like R_H, which presumably is due to bipolarons with the energy above the Hall mobility edge, $E > E_{cH}$. At the same time the dc conductivity remains proportional to the number of bipolarons above the mobility edge, which lies below, $E_c < E_{cH}$. To support this conclusion quantitatively one can adopt the effective mass approximation, Fig. 6.2

$$E_{\mathbf{k}}^{x,y} = \frac{k_x^2}{2m_{x,y}} + \frac{k_y^2}{2m_{y,x}} \tag{8.11}$$

with $m_x = 1/t$ and $m_y = 4m_x$. The Boltzmann equation in the relaxation time approximation yields (section 4.11)

$$R_H \sim \frac{\sum_{\mathbf{k},n=x,y} n'\left(E_{\mathbf{k}}^n\right)\left(\frac{\partial^2 E_{\mathbf{k}}^n}{\partial k_x^2}\left(\frac{\partial E_{\mathbf{k}}^n}{\partial k_y}\right)^2 - \frac{\partial E_{\mathbf{k}}^n}{\partial k_y}\frac{\partial E_{\mathbf{k}}^n}{\partial k_x}\frac{\partial^2 E_{\mathbf{k}}^n}{\partial k_y \partial k_x}\right)}{\left(\sum_{\mathbf{k},n} n'\left(E_{\mathbf{k}}^n\right)\left(\frac{\partial E_{\mathbf{k}}^n}{\partial k_x}\right)^2\right)^2}, \tag{8.12}$$

where $n'\left(E_{\mathbf{k}}^n\right)$ is the derivative of the distribution function. Counting bipolarons (n_0), with the energy above E_{cH} in the numerator and above E_c in the denominator of Eq.(8.12) one obtains

$$2eR_H = \frac{4m_x m_y n_0}{\left[\left(m_x + m_y\right) n_0 + m_y n_1\right]^2} \tag{8.13}$$

where $n_0 = x/2 - n_L$ is the number of bipolarons with the energy above E_{cH}, which are free in both directions; n_L is the number of bipolarons localized at least in one direction, and

n_1 is the number of bipolarons localized only in one direction. The number of bipolarons per cell localized at least in one direction is proportional to the number of random potential wells with the depth U larger than $t' \sim 1/m_y$

$$n_L = B \int_{-\infty}^{-t'} \exp\left(-U^2/\gamma^2\right) dU \tag{8.14}$$

The coefficient B is determined by the condition that all states of the Brillouin zone should be localized ($n_L = 1$) if the random potential is very large, $\gamma \gg t'$. The average depth γ of random wells is proportional to the relative fluctuation of the dopant density, which is the square root of the mean density x

$$\gamma = \gamma_0 \sqrt{x}. \tag{8.15}$$

Here γ_0 is the characteristic binding energy independent of the dopant density. That yields $B = \frac{2}{\gamma\sqrt{\pi}}$ and

$$n_0 = x/2 + \mathrm{erf}(\kappa/\sqrt{x}) - 1 \tag{8.16}$$

with $\kappa = t'/\gamma_0$. The number of bipolarons, $n_0 + n_1$, above the mobility edge E_c contributing to the longitudinal conductivity remains practically equal to the chemical density $x/2$ in a wide range of κ which can be verified with Eq.(8.14) replacing t' for $t = 4t'$. As a result, the Hall density $n_H = 1/2eR_H$ to the chemical density ratio is given by

$$\frac{n_H}{x/2} = \frac{[5x + 2\,\mathrm{erf}(\kappa/\sqrt{x}) - 2]^2}{16x[x + 2\,\mathrm{erf}(\kappa/\sqrt{x}) - 2]} \tag{8.17}$$

with $\mathrm{erf}(z) = \frac{2}{\sqrt{\pi}} \int_0^z \exp\left(-\xi^2\right) d\xi$. The agreement with the experiment is almost perfect for $\kappa = 0.57$, Fig.8.11. Due to the mass anisotropy the low temperature 'physical' density n_H remains c.1.6 times larger than the chemical $x/2$ even for low doping when $n_L \ll x/2$. The dc conductivity scales with x in overdoped samples as observed, Fig.8.5. because $n_0 + n_1 \simeq x/2$ for all x. On the contrary, the density n_0 of carriers extended in both directions falls rapidly in overdoped samples, Fig.8.11 (inset), due to increasing random potential fluctuations, proportional to $\sqrt{x}$. The mass anisotropy of the order of 4 can be seen commonly in doped semiconductors. However the anisotropy increases rapidly in overdoped samples. In fact, we believe that the large Hall to chemical density ratio, Fig.8.11 is a measure of this anisotropy and has nothing to do with a large Fermi surface.

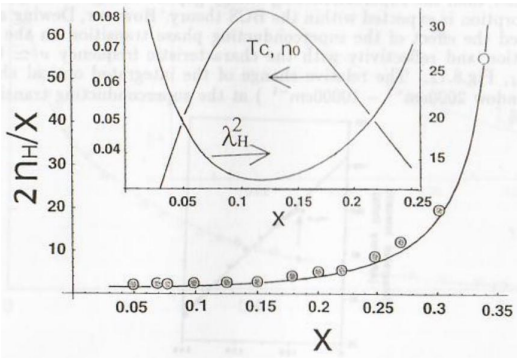

Fig.8.11. The ratio of the Hall $n_{H}=1 / 2 e R_{H}$ to chemical $x/2$ densities in $La_{2-x}Sr_xCuO_4$ as a function of doping compared with experiment (Hwang et al (1994)) at $40K$. Inset represents the theoretical dependence of the density of extended bosons n_0, of T_c and of the penetration depth (in relative units).

The critical temperature for the condensation of CBG is proportional and the London penetration depth squared is inversely proportional to the density n_0 of delocalised bosons in $2+\epsilon$ dimensions. Therefore

$$T_c \sim x + 2\,\mathrm{erf}(\kappa/\sqrt{x}) - 2$$

and

$$\lambda_H^2(0) \sim \frac{1}{x + 2\,\mathrm{erf}(\kappa/\sqrt{x}) - 2} \tag{8.19}$$

With these equations one can easily explain the doping dependence of $T_c(x)$ in superconducting oxides as well as the so-called 'Uemura' plot $T_c \sim 1/\lambda_H^2$ verified experimentally in underdoped and overdoped samples (Uemura (1995)), Fig.8.11 (insert).

As a result the metallic value of the Hall effect and the semiconducting scaling of *dc* conductivity in overdoped high- T_c oxides as well as the doping dependence of the critical temperature and of the London penetration depth can be explained by taking into account the localization of bipolarons in a random potential. Then both underdoped and overdoped high- T_c oxides are doped semiconductors with oxygen bipolarons as carriers partly localized by disorder.

5.9.11 8.5.3 NIR absorption in $YBCO$

Another piece of evidence for bipolarons in high - T_c oxides and their Bose-Einstein condensation comes from the near infrared (NIR) absorption in the high frequency region ($\nu \sim 0.5 - 0.7$eV) (Afexandrov et al. (1993)). It is well known that for frequencies much higher than the superconducting energy gap no change with temperature in optical absorption is expected within the BCS theory. However, Dewing and Salje (1992) observed the effect of the superconducting phase transition on the near infrared absorption and reflectivity with the characteristic frequency $\nu \simeq 0.7$eV in $YBa_2Cu_3O_{7-\delta}$, Fig.8.12. The relative change of the integrated optical absorption (frequency window 2000 $\mathrm{cm}^{-1} - 10000$ cm^{-1}) at the superconducting transition was as high as 10%.

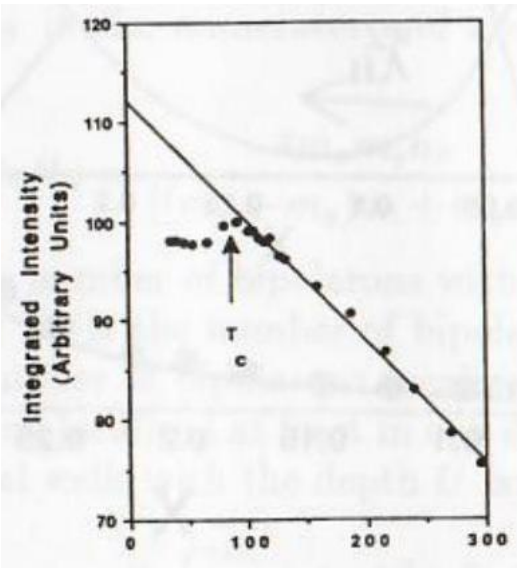

Fig.8.12. The temperature dependence of the NIR absorption near 5000 cm^{-1} in $YBa_2Cu_3O_7$.

This observation is in line with the temperature dependence of the optical bipolaronic conductivity, as discussed in section 6.5. The effect of the superconducting phase transition on NIR absorption is explained by the Bose-Einstein condensation of small bipolarons. Triplet intersite bipolarons, which are thermally activated, are responsible for the temperature dependence of the NIR conductivity in the normal state. The temperature dependence of the MIR and NIR reflectance and transmittance of thin Y *BCO* films was found to be consistent with the powder absorbance measurements (Yagil et al (1995)). In these regimes the optical energy is much higher than both temperature and superconducting energy gap, therefore the temperature dependence in the normal and in the superconducting states is anomalous and cannot be explained within a normal Fermi liquid approach.

5.9.12 8.5.4 Upper critical field of high- T_c oxides

The superconducting transition in a magnetic field for a wide temperature range starting from mK-level up to T_c has been reported by Mackenzie et al. (1993) in overdoped Tl-based cuprate. Resistively determined H_{c2} values from $T/T_c = 0.0025$ to $T/T_c = 1$ in a $T_c = 20$ K single crystal of $Tl_2Ba_2CuO_{6+\delta}$ follow the temperature dependence that is in good qualitative agreement with the type of curve for CBG, Fig.7.3 for $n_L/n \simeq 1$.

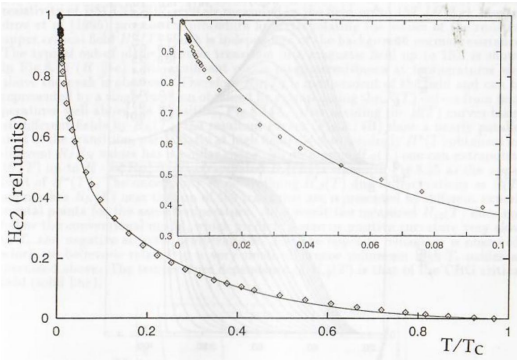

Fig.8.13. The upper critical field of \$\mathrm{Tl}*{2}* *\mathrm{Ba}*{2}*\mathrm{CuO}*_{6+\delta}\$ compared with the critical field $H^*(T)$ of CBG.

Osofsky et al. (1993) also observed the divergent upward temperature dependence of the upper critical field $H_{c2}(T)$ for thin $BSCO$ films, which was 5 times that expected for a conventional superconductor at the lowest temperature. The observed dependencies of $H_{c2}(T)$ are remarkably different from that predicted with the canonical Ginzburg-Landau theory, $H_{c2} \sim T_c - T$. The unusual temperature dependence of H_{c2} of a 'low T_c ' overdoped $Tl_2Ba_2CuO_{6+\delta}$ can be quantitatively described by the formula for the BEC critical field, derived in section 7.7 ,

$$H^*(T) = \text{ constant } \times \left(\frac{1 - 2n_L(\tau)/x}{\tau\,[1 - 2n_L(1)/x]} - \sqrt{\tau} \right)^{3/2} \tag{8.20}$$

Here $\tau = T/T_c$ with T_c the experimental critical temperature, x is the chemical polaron density determined in $Tl_2Ba_2CuO_{6+\delta}$ by the excess oxygen content $\delta, x = 2\delta$, and $n_L(\tau)$ is the number of localized bipolarons. $x/2 - n_L$ should be very small. In fact, at zero temperature the condition $2n_L(0)/x = 1$ is satisfied because each bipolaron is localised on the excess oxygen ion. In the 'single well-single particle' approximation
the number of localised bipolarons is determined by

$$n_L(\tau) = \int_{-\infty}^{0} d\epsilon \frac{N_L(\epsilon)}{\exp(\epsilon/T) + 1} \tag{8.21}$$

where $N_L(\epsilon)$ is the density of localised states.

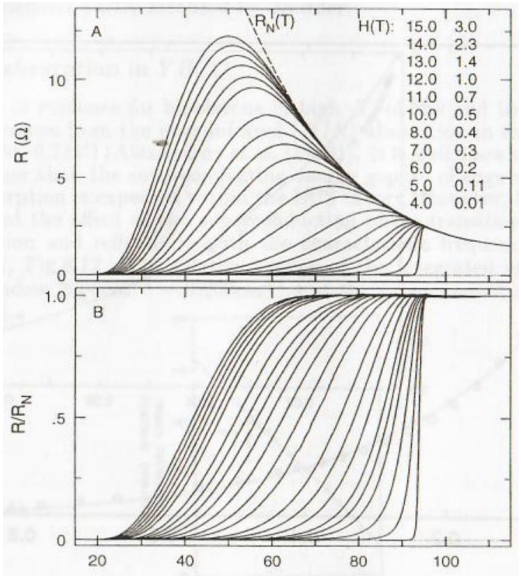

Fig.8.14. C-axis resistivity of single -crystal $Bi_2Sr_2CaCu_2O_8$ in a magnetic field (A) normalised with respect to the normal state resistivity (B).

The positive curvature of $H^*(T)$ on the temperature scale of the order of T_c does not depend on the particular shape of $N_L(\epsilon)$. However, at mK temperatures shallow potential wells are important. Therefore the low-temperature behaviour of $H^*(T)$ is sensitive to the shape of $N_L(\epsilon)$ just below the mobility edge. One can model

$$N_L(\epsilon) = 0.5 n_L(0) \left[\frac{e^{\epsilon/\gamma}}{\gamma} + \delta\left(\epsilon + E_0\right) \right] \tag{8.22}$$

to imitate both the discrete levels with the energy E_0 and the exponential shallow tail due to the randomness of the impurity potential. Then one can quantitatively describe the experimental curve $H_{c2}(T)$ with Eq.(8.20) and $\gamma/T_c = 0.13$ and $E_0/T_c = 0.3$ for three decades of temperature, Fig.8.13. This equation was also applied by Osofsky et al (1993, 1994) to describe H_{c2}(T) of $Bi_2Sr_2CuO_y$ with an excellent agreement for the critical temperature.

However, in the highest T_c cuprates the in-plane superconducting transition is known to display pronounced broadening in a magnetic field, with the top of the
transition having a much weaker field dependence than in the region near the bottom. This together with the high values of H_{c2} have made an experimental determination of H_{c2} very difficult in materials with $T_c > 60K$, with the consequence that widely varying values of $H_{c2}(0)$ have been estimated based on different models. The out-of-plane resistive transition shows a different behaviour in a magnetic field. An increasingly pronounced maximum (peak) developes below T_c and shifts to lower temperature rather than broadened with increasing field. By the use of the out-of-plane resistivity of BSCCO-2212 crystals measured in the field up to $15T(H\|c)$ Alexandrov et al (1995) proposed a procedure for extrapolating the values of the resistive upper critical field $H_{c2}(T)$ which is independent of the background normal resistance. The typical out-of-plane resistive transition in a magnetic field up to $15T$ is shown in Fig.8.14 ($H\|c$). No significant c -axis magnetoresistance at temperatures well above the peak is observed. Therefore $R_N(T)$ is independent of the field and can be represented by a single function obtained by extrapolating the $R(T)$ curves from temperatures well above the transition, Fig.8.14A. After dividing the $R(T)$ curves taken at different fields by $R_N(T)$, the resultant curves (Fig.8.14B)

show a nearly parallel shift of the transition, particularly at high fields. Not surprisingly $H^*(T)$ obtained for different R/R_N values has a similar shape. To determine $H_{c2}(T)$ one can extrapolate $H^*(T)$ up to $R \longrightarrow R_N$. The extrapolated $H_{c2}(T)$ is shown in Fig.8.15 as the upper limit of $H^*(T)$. The uncertainty in determining $H_{c2}(T)$ due to fluctuations as $R(T)$ approaches $R_N(T)$ near the top of the transition are represented by different experimental points for the same temperature. As a result the measured $H_{c2}(T)$ does not follow the conventional model, which predicts a zero or positive curvature very close to T_c and negative at lower temperatures. Just the opposite behaviour is observed, which we believe is related to a very small coherence volume in high- T_c oxides as discussed above. The temperature dependence of $H_{c2}(T)$ is that of the CBG critical field (solid line).

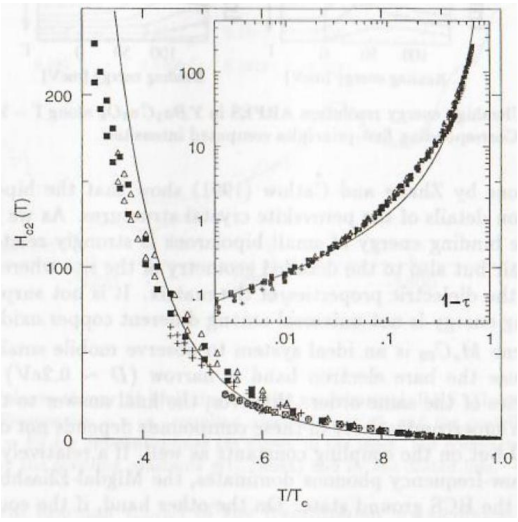

Fig.8.15. Resistive upper critical field of high- T_{c} BSCCO - 2212 single crystals.

5.9.13 8.6 Polaronic ARPES in high- T_c oxides and fullerene

Small- polaron features of the energy spectrum and the formation of bipolarons can be verified by the angle resolved photoemission spectra (ARPES) as discussed in section 4.12. We believe that the high resolution ARPES (Gofron et al (1994)) shows such features, Fig.8.16. The extremely flat anisotropic bands have been measured in several copper high- T_c oxides which display at least an order of magnitude less dispersion than the first-principles band structure methodology can provide (Fig.8.16b). This flatness is due to the polaron narrowing of the band, and the anisotropy is due to the remarkable difference of p_x overlaps in x and y direction, respectively. If bipolarons are formed the spectral weight is shifted down by half of the bipolaron binding energy with respect to the chemical potential. This could provide an explanation why the flat band observed with $ARPES$ in $YBa_2Cu_4O_8$ does not cross the Fermi level. It lies approximately 20 meV below the chemical potential which means that the bipolaron binding energy is about $\Delta \simeq 40$meV in this material.

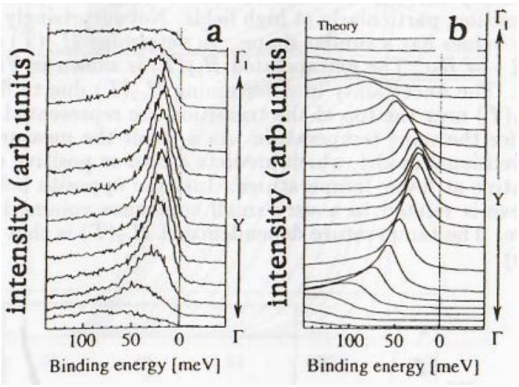

Fig.8.16. (a) Ultrahigh energy resolution ARPES in $\mathrm{YBa}*{2}* \mathrm{Cu}{4} \mathrm{O}_{8}$ along $\Gamma - Y$ direction of the Brillouin zone. (b) Corresponding first-principles computed intensities.

The calculations by Zhang and Catlow (1991) show that the bipolaron binding energy depends on details of the perovskite crystal structures. As we have discussed in Chapter 2 the binding energy of small bipolarons is strongly related not only to the size of the pair but also to the detailed geometry of the site where the polaron is situated and to the dielectric properties of the matrix. It is not surprising that the bipolaron binding energy is not universal among different copper oxides.

Doped fullerene M_xC_{60} is an ideal system to observe mobile small polarons and bipolarons because the bare electron band is narrow ($D \sim 0.2$eV) and there are phonon frequencies of the same order. However, the final answer to the question on the nature of the superconductivity in these compounds depends not only on the adiabatic ratio ω/D but on the coupling constants as well. If a relatively weak coupling ($\lambda \leq 0.5$) with low-frequency phonons dominates, the Migdal-Eliashberg theory can be applied with the BCS ground state. On the other hand, if the coupling is strong or high-frequency phonons are involved, our bipolaron theory should be applied. The photoemission spectroscopy of a molecule C_{60}^{-}(Gunnarsson et al (1995)) allows us to estimate the relative contribution of different phonon modes to the electron-phonon interaction (Alexandrov et al (1995b)). The Hamiltonian at hand, describing three degenerate t_{1u} electron states coupled with phonons, is diagonalised with respect to the coupling with the A_{g2}-vibration mode using the canonical Lang-Firsov displacement transformation $\exp(S)$ with the following result

$$\tilde{H} = -E_p^{A_{g2}} \sum_{m=1}^{3} \psi_m^{\dagger}\psi_m + \sum_{\nu=1}^{8} g^{\nu}\omega_{\nu} \sum_{n,m=1}^{3} \psi_n^{\dagger} M_{nm}^{\nu} \psi_m + \sum_{\nu}^{8}\sum_{\mu=1}^{5} \omega_{\nu} n_{\nu,\mu} \tag{8.23}$$

where $E_p^{A_{g2}} = \left(g^{A_{g2}}\right)^2 \omega_{A_{g2}}$ is the polaron shift due to the A_{g2} mode, $\hat{M}^{\nu}$ is the Hermitian dimensionless coupling matrix (of order of unity) for the five-fold degenerate H_g modes, and $n_{\nu,\mu}$ are the phonon occupation numbers for H_g modes.

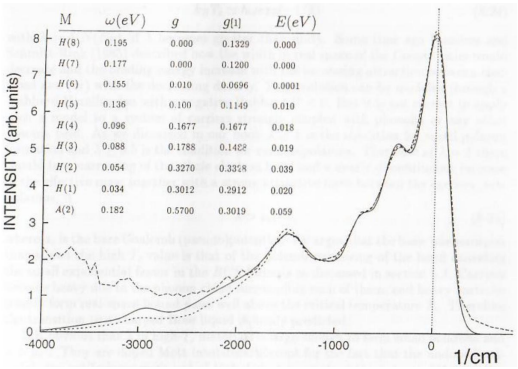

Fig.8.17. Polaron theory fit (full line) to the experimental PES (Gunnarsson et al (1995)) (dashed line). Frequencies \$\omega=\omega_{\nu}\$, coupling constants $g = g^{\nu}$, and the contribution to the ground state energy $E = E_p^{\nu}$ for different modes are shown in the inset. For comparison the variational fit is represented by the coupling constants g[1], (inset) and by the dotted line.

The spectral function $I_{pol}(\omega)$ of the Hamiltonian is calculated by the numerical diagonalisation in truncated Hilbert space for the H_g modes and integrated with the Gaussian instrumental resolution function of width $\sim$ 41meV as described in section 4.12. Thus one can fit the PES in a wide energy region as shown in Fig.8.17 with
g^{ν} being the fitting parameters. Due to an exact treatment of $A_g(2)$ mode the highenergy part of PES including the maximum at *ca*.3000 cm^{-1} is better represented compared with the variational analysis by Gunnarsson et al. The coupling with high frequency phonons $\omega_{\nu} \geq 0.096$eV dominates in the electron-phonon interaction as one can see in the inset of Fig.8.17, where the coupling to the $A_g(2)$ high-frequency mode turns out to be most important. This fact as well as the observation of the phononsided bands in PES by itself suggest that the nonadiabatic small polaron theory of this book rather than the adiabatic Migdal-Eliashberg approach should be applied to M_xC_{60}.

5.10 Conclusion

In this book we have put forward a multi-polaron theory of low-mobility solids. We believe that this theory is the only possibility for a description of what happens to the BCS model for superconductivity, in which

$$k_BT_c \simeq \hbar\omega \exp(-1/\lambda) \tag{8.24}$$

with $\lambda = VN(E_F)$, if λ becomes greater than unity. Some time ago Noziéres and Schmitt-Rink (1985) described how the width in real space of the Cooper pairs would decrease and the binding energy increase with the increasing attraction between electrons and (or) with the decreasing density. This evolution can be modeled through a Hubbard Hamiltonian with a negative Hubbard $U < 0$. But it is not correct to apply such a model to a system of carriers strongly coupled with phonons or any other bosonic field. As we discussed in our book $\lambda \geq 1$ is the condition for small polaron formation and $\lambda \geq 0.5$ is the condition for small bipolarons. Therefore at $\lambda \sim 1$ there should be a narrowing of the whole electron band and a nearly discontinuous increase in the effective mass together with a strong attractive force between the carriers, now polarons, if

$$\lambda > \mu_c \tag{8.25}$$

where μ_c is the bare Coulomb (pseudo)potential. We argue that the basic phenomenon that allows the high T_c value is that of the polaron narrowing of the band canceling the small exponential factor in the BCS formula as discussed in section 5.3. Carriers become heavy due to the phonon cloud surrounding each of them, and heavy particles readily form real-space bound pairs well above the critical temperature T_c. Therefore the transition to a charged Bose liquid is firmly predicted.

Is it obvious that λ in high- T_c materials is large enough to form small polarons and $\lambda > \mu_c$? They are doped Mott insulators. Except for the fact that the undoped materials are antiferromagnets and of high dielectric constant the nature of the carriers will be similar to that in $Si:B$: holes tunneling in a narrow band. The strong correlations will further decrease the bandwidth and therefore increase the bare $N(E)$ in a rigid lattice - just the condition for large λ. This conclusion is perfectly confirmed by the numerical calculations within the Holstein $t-J$ model, as discussed in section 5.5. One can argue that the Coulomb repulsion is not suppressed in narrow bands because there is no retardation contrary to the wide-band BCS superconductors. But it is well established for some simple metals that $\lambda > \mu_c$ even without retardation and the static dielectric constant $\epsilon(q,0)$ is negative for finite q. Many models with a pure 'electronic' mechanism of pairing have been discussed in the literature during the last decade. To the best of our knowledge none of them has explained how to
overcome the direct Coulomb repulsion by the exchange Coulomb attraction. This is quite unlikely at the small distance of the order of two lattice constants, which is the characteristic size of pairs in high- T_c oxides. In contrast, the question does not arise for the electron-phonon interaction. The Coulomb repulsion in ionic solids is screened by polar optical phonons and the deformation potential rather easily makes $\lambda > \mu_c$.

We take the point of view that the carriers in a doped Mott insulator are small bipolarons surrounded by the spin and lattice polarised region. Both spin and lattice polarisation contribute to the high effective mass $m^{**} > 10m_e$, but only the latter to the isotope effect. In general, bosons and unbound electrons (or holes) can coexist, but trapping of bosons in a random field explains alone the metal-semiconductor duality of overdoped copper oxides.

According to the Fermi liquid (FL) scenario high- T_c superconductors are metals with a large Fermi surface of copper electrons. Within this scenario the pronounced deviation from the canonical FL behavior are due to the Fermi surface anisotropy and a large damping. We believe that the existence of the Mott parent insulators suggests just the opposite scenario according to which high- T_c superconductors are doped semiconductors with hole carriers bound into small bipolarons. All thermodynamic and kinetic properties favor this model.

Some direct evidence that these materials contain a charged $2e$ Bose liquid would be highly desirable. We have discussed the thermal conductivity; the contribution from the carriers given by the Wiedemann-Franz ratio depends strongly on the elementary charge as $\sim (e^*)^{-2}$ and should be significantly suppressed in case of $e^* = 2e$ compared with the Fermi-liquid contribution. The evidence for $e^* = 2e$ is strong, but perhaps not entirely convincing because one has to subtract the much larger phonon contribution to the heat transport. Stronger evidence comes from the measurements by Dewing and Salje (1992) of the temperature dependent infrared absorption band, centered at $\sim 0.5 - 0.7$eV as discussed in section 8.5.3. The intensities of absorption and transmission show a pronounced change of the slope of the temperature dependence at $T = T_c$, which is unusual at frequencies as high as 20 times of an estimated BCS gap. We have explained this observation assuming that below T_c a macroscopic proportion of singlets are condensed into the state with zero total momentum and hence with zero dipole moment. Possibly the most striking evidence for the charged Bose-liquid in high- T_c oxides comes from the unusual temperature dependence of the upper critical field H_{c2} as discussed in section 8.5.4. The direct experiment could be the classical Aharonov-Bohm interference above T_c in a mesoscopic oxide with low T_c at low temperatures where the inelastic mean free path is

large.

In using this model, we have to realise that the insulating properties of a Mott insulator do not depend on the ordering of the spins; they persist above the Neel temperature, and arise because the on-site Coulomb repulsion is larger than the polaron bandwidth. From the observation by Morris and co-workers (Zhao et al (1994)) of the oxygen isotope effect on the Néel temperature in La_2CuO_4 we know that the polaron band narrowing takes place also in the Mott insulators.

The problem of low-mobility conductors became a challenging problem about half a century ago, when the low mobility was observed in transition-metal oxides. The explanation was found with polarons. With the discovery of high- T_c superconductors this problem received renewed attention. We believe that bipolarons are the explanation.

Part V
Old, Fundamental Theories

Part VI
Special Effects: Useful, Selected Articles

Part VII
Experiments: Main Articles

6 Application of the polaron-transport theory to $\sigma(\omega)$ in $Tl_2Ba_2Ca_{1-x}Gd_xCu_2O_8$, $YBa_2Cu_3O_{7-8}$, and $La_{2-x}Sr_xCuO_4$ by D. Mihailovic, Foster, Voss, Heeger

Abstract

We analyze the frequency-dependent photoinduced infrared conductivity, $\sigma_P(\omega)$, obtained from photoinduced absorption measurements of the insulators $Tl_2Ba_2Ca_{0.98}Gd_{0.02}Cu_2O_8$, $YBa_2Cu_3O_{6.3}$, and La_2CuO_4 in terms of $\sigma_{PT}(\omega)$ calculated from nonadiabatic polaron-transport theory. The calculated $\sigma_{PT}(\omega)$ is in good agreement with the experimental $\sigma_P(\omega)$ in the midinfrared. We also compare $\sigma_P(\omega)$ with the infrared conductivity, $\sigma(\omega)$, of the high- T_c superconductors $Tl_2Ba_2CaCu_2O_8$, $YBa_2Cu_3O_7$, and $La_{1.85}Sr_{0.15}CuO_4$. The similar spectral shape and systematic trends in both $\sigma_P(\omega)$ and $\sigma(\omega)$ indicate that the carriers in the concentrated (metallic) regime retain much of the character of the carriers in the dilute (photoexcited) regime. Together, these results imply that in the superconducting cuprates and in their "parent" insulators, the carriers are polarons dressed with a phonon polarization cloud.

6.0.1 I. INTRODUCTION

An extensive body of infrared reflectance data has established that the normal-state frequency-dependent conductivity $\sigma(\omega)$ of the high-temperature superconductors, $Tl_2Ba_2CaCu_2O_8$, $YBa_2Cu_3O_7$, and $La_{1.85}Sr_{0.15}CuO_4$ consists of a narrow, temperature-dependent, Drude-like peak centered at zero frequency, and a broad, temperature-independent excitation in the midinfrared, the so-called "mid-ir" feature. [1–5] The systematic appearance of the mid-ir feature in $\sigma(\omega)$ and the direct correlation of its intensity with doping has been established experimentally for many perovskites (including Ba_{1-x} Pb_xBiO_3, $La_{2-x}Sr_xNiO_4$, $SrTiO_3$, and $BaTiO_3$) .[6–9] In the cuprate perovskites, similar correlations exist between the mid-ir peak and high-temperature superconductivity at moderate doping levels (less than $\approx$ 0.5 holes /Cu).[1] Further doping into a metallic phase reduces the intensity of the mid-ir feature [10] as well as T_c.[11,12] This close correspondence of the mid-ir intensity with T_c in cuprate perovskites suggests that the origin of $\sigma(\omega)$ in the mid-ir warrants further investigation, particularly in relation to the mechanism for high-temperature superconductivity.

The mid-ir feature in high- T_c superconductors has been interpreted by many groups. In the case of $YBa_2Cu_3O_{7-\delta}$, it has been attributed to a direct electronic transition distinct from the Drude-like free carrier contribution at low frequency, [2] to a contribution from free holes, but with an ω-dependent scattering rate arising from either a polaron shakeoff of dressed carriers (which are renormalized by strong interactions with phonons, spin waves, etc.), [2,4] or to an intrinsic ω dependence of the scattering mechanism. [3,13]

In systems which have large electronic bandwidth, carrier transport can be accurately described by adiabatic processes in which the crystal lattice is assumed to be static with respect to carrier motion (i.e., the Drude model, Fermi liquid theory, etc.). In narrower band systems, carrier motion becomes nonadiabatic. When the sound velocity becomes comparable to the Fermi velocity, as has been shown to be the case in the cuprates, [14] carrier motion is intimately linked to lattice vibrations. In doped titanates, for example, $BaTiO_3$ and

$SrTiO_3$, the origin of mid-ir features in $\sigma(\omega)$ and their relationship to transport mechanisms has been a subject of study for many years. [9,15–20] Both adiabatic and nonadiabatic mechanisms have been proposed for modeling the transport properties. The application of polaron transport theory (PTT), in which carriers move nonadiabatically with respect to the lattice, eventually proved successful as a model of carrier transport in these materials. [9,15–20]

In nonadiabatic PTT, carriers interact with both optical and acoustic phonons; the acoustic phonons determine the temperature-dependent contribution to $\sigma(\omega)$ near zero frequency [16] and the optical phonons give rise to a broad temperature-independent "shakeoff" peak in $\sigma(\omega)$ in the midinfrared for temperatures $T < T_D$, where T_D is the Debye temperature. [15,19,20] In addition to successfully describing the shape of the mid-ir peak in $\sigma(\omega)$ upon doping, [17,18] the model also correctly predicted the dc transport properties [16,18] of the doped titanates.

In this paper, we apply PTT as a model of the frequency-dependent transport process experimentally observed as the mid-ir features in $\sigma(\omega)$ in the high- T_c cuprates, restricting ourselves to carrier interactions with optical phonons. [15,17] The calculated $\sigma_{\mathrm{PT}}(\omega)$ is fit to the photoinduced infrared conductivity, $\sigma_P(\omega)$, obtained from photoinduced absorption (PIA) measurements of the insulating precursor materials, [21–24] where the carrier concentration is in the dilute limit and carrier-carrier interactions are thus assumed to be negligible. These spectra are compared to the infrared conductivity $\sigma(\omega)$ obtained from Kramers-Kronig analysis of reflectivity mea-
surements in the doped, metallic (superconducting) materials. The similar spectral shape and consistent trend toward lower energy of the mid-ir peak in both $\sigma_p(\omega)$ and $\sigma(\omega)$ indicate that carriers in the concentrated (metallic) regime retain much of the character of carriers in the dilute (photoexcited) regime. We conclude that the mid-ir absorption in $Tl_2Ba_2CaCu_2O_8$, $YBa_2Cu_3O_{7-\delta}$, and La_2CuO_4 can be assigned to nonadiabatic polaron (or possibly bipolaron) transport and suggest that the differences between $\sigma_P(\omega)$ and $\sigma(\omega)$ can be attributed to the onset of carrier-carrier interactions in the concentrated regime. Since we cannot make any experimental distinction between polaron or bipolaron transport, we refer to the carriers simply as polarons.

6.0.2 II. CALCULATION OF $\sigma(\omega)$ AND COMPARISON WITH EXPERIMENTAL RESULTS

The theoretical treatment of polaron transport is based on Holstein's molecular crystal Hamiltonian; [25]$\sigma_{\mathrm{PT}}(\omega)$ is calculated [15,16,19] in both the low-temperature ($T \to 0$) and high-temperature limit ($k_BT > \omega_D/2$), where ω_D is the Debye frequency and k_B is Boltzmann's constant. The $\sigma_{\mathrm{PT}}(\omega)$ spectrum reflects the shakeoff of the optical phonon cloud (the localized distortion) from the polaron as a result of nonadiabatic transport from site to site, with the peak [19] in the spectrum corresponding approximately to $2E_b$, where E_b is the polaron binding energy. Whereas the original calculation was done by Reik [15,17] in the limit of strong coupling, [i.e., with $(2E_b/k_BT)\,(a/r)^3 \gg 1$, where k_B is Boltzmann's constant, a is the lattice constant, and r is the polaron radius], the theory has been extended by Emin [19] to the weak-coupling regime to include large polarons where the range of the polaron extends beyond one unit cell.

In PTT, the polarons are considered as noninteracting particles [15–20] in the dilute limit. We can probe the transport of such isolated carriers by measurements of $\sigma_P(\omega)$, and we can probe the transport of carriers in the concentrated regime from measurements of $\sigma(\omega)$. However, we expect departures from the theoretically calculated $\sigma_{\mathrm{PT}}(\omega)$ in a system with a high density of carriers exhibiting collective phenomena (e.g., superconductivity), as is the case in the high- T_c cuprates where $\sigma(\omega)$ is the response of the carriers at a density in the range of $0.1 - 0.5$ per unit cell.

In the PIA technique, $\sigma_P(\omega)$ is derived from $(-\Delta T/T)$ of the insulating precursor com-

pounds of the same materials, where T is the transmission, and ΔT is the change in transmission upon photoexcitation with weak laser light ($\cong 40$ mW/cm^2). In the insulator limit, where $\epsilon_1 \gg \epsilon_2$, the photoinduced infrared conductivity $\sigma_P(\omega)$ is related to $-\Delta T/T$ by

$$\sigma_P(\omega) = (nc/4\pi d)(-\Delta T/T)$$

where $n = \sqrt{\epsilon_1}$ is the refractive index, d is the absorption length, and c is the speed of light. The response of the system in the dilute limit, $\sigma_P(\omega)$, should correspond closely to the idealized theoretical model. Thus we compare $\sigma_P(\omega)$ with the predictions of PTT. We fit $\sigma_{\rm PT}(\omega)$ to the mid-ir $\sigma_P(\omega)$ in $Tl_2Ba_2Ca_{0.98}Gd_{0.02}Cu_2O_8$, [23] $YBa_2Cu_3O_{6.3}$, [22] and La_2CuO_4.[21] This approach is justified because of the observation of infrared active vibrational features in the PIA (which imply the existence of localized lattice distortions) and because the experimentally determined effective masses in the cuprates [21–24] (see Table I) are similar to the titanates ($3 < m^*/m_e < 30$) (Refs. 9 and 26) and thus suggest polaron formation.

The frequency-dependent conductivity $\sigma_{\rm PT}(\omega, T \to 0)$ in the low-temperature limit is given by [15,17]

$$\sigma_{\mathbf{PT}}(\omega, T \to 0) = \frac{\sqrt{2\pi} t^2 e^2 N}{\hbar^3 \omega_0^2} e^{-\eta} \left(\frac{\omega_0}{\omega}\right)^{(\omega/\omega_0 + 2/3)} e^{(\omega/\omega_0)} \eta^{\omega/\omega_0} \tag{1}$$

where η is the number of phonons in the polaron polarization cloud, ω_0 is an averaged phonon frequency, t is the electronic resonance overlap integral, $\hbar$ is Planck's constant, and N is the number density of carriers of charge e; η and ω_0 are parameters describing the electron-phonon interaction and are related to the electron-phonon coupling constant $\alpha_j(\mathbf{q})$ through the relations

$$\omega_0 = \frac{\sum_{j,q} \alpha_j(\mathbf{q}) \sin^2\left(\frac{1}{2}q\right) \omega_j^2(\mathbf{q})}{\sum_{j,q} \alpha_j(\mathbf{q}) \sin^2\left(\frac{1}{2}q\right) \omega_j(\mathbf{q})} \tag{2}$$

and

$$\eta = \frac{1}{\omega_0} \sum_{j,q} 2\alpha_j(\mathbf{q}) \sin^2\left(\frac{1}{2}q\right) \omega_j(\mathbf{q}) \tag{3}$$

with the sum over the wave vector $\mathbf{q}$ of the j th optical phonon branch. The characteristic frequency ω_0 represents an averaged phonon frequency involved in the carrier hopping, weighted by the electron-phonon interaction $\alpha_j(\mathbf{q})$. If the phonon dispersion is not too large, formula (3) can be approximated by the more familiar form, [17]

$$\eta \approx \sum_{j,q} 2\alpha_j(\mathbf{q}) \sin^2\left(\frac{1}{2}q\right) \tag{4}$$

which represents a weighted average of $\alpha_j(\mathbf{q})$ over the Brillouin zone. The two parameters η and ω_0 essentially determine the shape of the spectrum, and the prefactor is a constant proportional to the square of t.

The dashed curves in Fig. 1 show the calculated $\sigma_{\rm PT}(\omega)$ [Eq. (1)] using the parameters η and ω_0 listed in Table I. The fits to $\sigma_P(\omega)$ for $Tl_2Ba_2CaCu_2O_8$ and $YBa_2Cu_3O_{7-\delta}$ [Figs. 1(a) and 1(b)] are excellent over the entire frequency range. The value of $\omega_0 = 200$ cm^{-1} is

consistent with calculated values of $\alpha_j(\mathbf{q})$ obtained recently from a linearized-augmented-plane-wave calculation [27] for $YBa_2Cu_3O_{7-\delta}$ as well as with experimental evidence for strong coupling of the low-frequency modes from infrared spectroscopy. [28] In addition to the polaron

TABLE I. Effective masses and parameters describing the electron-phonon interaction.

	m^*/m_e	η	ω_0 (cm^{-1})
$La_{2-x}Sr_xCuO_4$	23	10	450
$YBa_2Cu_3O_7$	13	7	200
$Tl_2Ba_2CaCu_2O_8$	11	5.6	200

shakeoff, we observe structure from photoinduced localized phonon modes in all three systems; for $Tl_2Ba_2CaCu_2O_8$ and $YBa_2Cu_3O_{7-\delta}$, they [21–24] distort the low-frequency edge of the peak in $\sigma_P(\omega)$. These vibrational modes are not described by Eqs. (1)-(3) (which are valid only above $\omega > \omega_D/2$) and will therefore be discussed elsewhere. In La_2CuO_4, the fit is good for $\omega > 3000$ cm^{-1}. The deviations at lower frequency possibly arise from the fact that the La_2CuO_4 PIA experiments [21] were carried out before highest quality materials were available.

In agreement with polaron theory, the values of η and ω_0 obtained from the theoretical fits for the three systems scale with the polaron effective masses obtained from the PIA data [24] (see Table I) reflecting a trend in $\alpha_j(\mathbf{q})$. In addition, as η and ω_0 (and the effective mass) decrease, T_c of the system increases. We have previously shown [24] that T_c is inversely proportional to m^* for the cuprates. This behavior is consistent with theories of bipolaronic super-

conductivity which predict $k_BT_c \cong \hbar^2 n^{2/3} m^*$ (Ref. 29), where n is the number of bipolarons of effective mass m^*.

In Fig. 2, we compare the frequency-dependent conductivity $\sigma(\omega)$, obtained from reflectivity measurements of $Tl_2Ba_2CaCu_2O_8$ thin films [4] ($T_c = 100$ K) , $YBa_2Cu_3O_7$ single crystals [5] ($T_c = 90$ K), and $La_{2-x}Sr_xCuO_4$ ceramic samples [30] ($T_c = 35$ K), with the photoinduced infrared conductivity $\sigma_P(\omega)$. The similar spectral shape and the consistent trend of the mid-ir peak toward lower energy in both $\sigma_P(\omega)$ and $\sigma(\omega)$ indicate that carriers in the concentrated (metallic) regime retain much of the character of carriers in the dilute (photoexcited) regime.

6.0.3 III. DISCUSSION

A number of qualitative observations follow from the comparison of $\sigma(\omega)$ and $\sigma_P(\omega)$:
(i) In all perovskites exhibiting superconductivity, the peak energy in both $\sigma(\omega)$ and $\sigma_P(\omega)$ shifts toward lower energy as T_c of the material increases; from $\cong$ 1.2eV (12000 cm^{-1}) in Ba_{1-x} Pb_xBiO_3(Refs. 6 and 31) to $\simeq$ 0.5eV (4000 cm^{-1}) in $La_{2-x}Sr_xCuO_4$ (Refs. 1, 21, and 30) to 0.13eV (1300 cm^{-1}) in $YBa_2Cu_3O_7$(Refs. 1-3, 5, and 22) and to 0.09eV (950 cm^{-1}) in $Tl_2Ba_2CaCu_2O_8$ (Refs. 4 and
23) (see Table II).
(ii) The concurrent shift in energy of both $\sigma(\omega)$ and $\sigma_P(\omega)$ from system to system implies that both are intrinsic features of the frequency-dependent conductivity and that the origin of the mid-ir feature is the same in both the dilute and concentrated limits.
(iii) The primary difference between $\sigma_P(\omega)$ (the dilute limit) and $\sigma(\omega)$ (the concentrated limit) is the broadening of the mid-ir peak which we expect to occur as the carrier concentration increases to a level at which the exclusion principle and polaron-polaron interactions become important.

The differences between the experimental spectra obtained in the concentrated and the dilute limits (Fig. 2) imply that polaron-transport theory ceases to provide an accurate description of $\sigma(\omega)$ in the concentrated limit and emphasizes the need for generalization of the PTT to the concentrated regime appropriate to the metallic phases of the high- T_c cuprates.

In a given cuprate system, the energy of the mid-ir peak shifts only slightly to higher energy with increased carrier concentration. However, the intensity of the mid-ir peak significantly

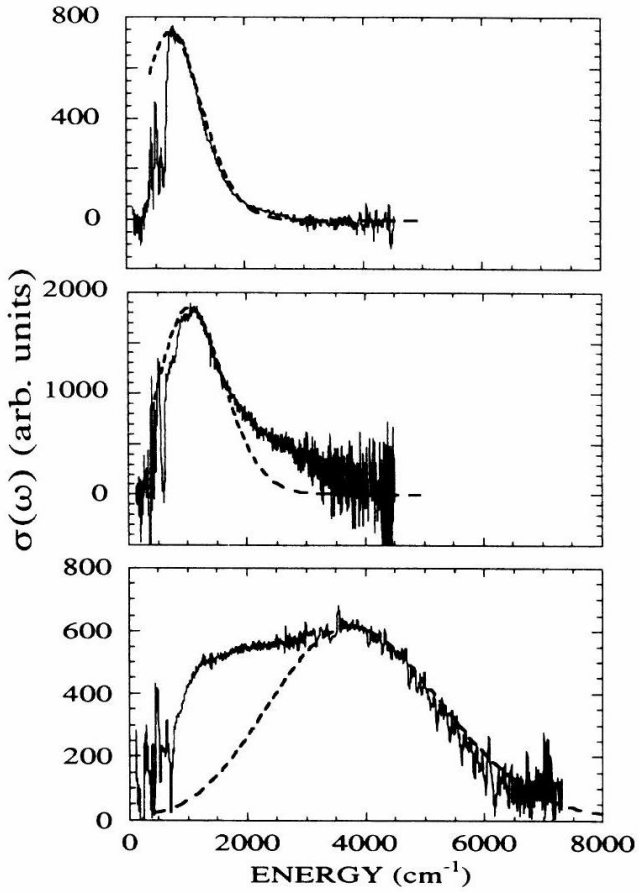

FIG. 1. The photoinduced infrared conductivity $\sigma_{P (\omega)$ (solid lines) in the insulator precursors for $Tl_2Ba_2CaCu_2O_8$ (top), $YBa_2Cu_3O_7$ (middle), and $La_{2-x}Sr_xCuO_3$ (bottom) compared with fits to polaron-transport theory $\sigma_{PT}(\omega)$ as calculated using Eq. (1) (dashed lines).}

increases until the maximum T_c is reached at approximately $0.12 - 0.25$ holes /Cu.[1,11,30] A similar dependence of $\sigma(\omega)$ and T_c with doping concentration is seen in the titanates and bismuthates. [6,8,9] Recent data on $La_{2-x}Sr_xCuO_4$ show that upon further doping into the metallic region $(x > 0.2), T_c$ decreases [10,12] concurrent with a reduction of the intensity of the mid-ir feature. Table II compares the energy ($\approx 2E_b$) of the mid-ir peak and T_c for some cuprate, titanate, and bismuthate superconductors.

In the present analysis, we have not explicitly considered the effect of spin-wave "shakeoff" resulting from coupling of carriers to spin excitations (rather than phonons) as a source of $\sigma(\omega)$ in the mid-ir. The similarity of the line shapes of the $\sigma(\omega)$ spectra and the two-magnon spectra observed in Raman scattering of $Tl_2Ba_2CaCu_2O_8$, [32] $YBa_2Cu_3O_{7-\delta}$, [33] and La_2CuO_4 (Ref. 34) suggest that spin-polaron shakeoff might provide a contribution. A strong spin-lattice interaction has recently been suggested by the temperature dependence of the two-magnon relaxation [35] via coupling to the lattice as inferred from Raman scattering experiments. However, since the electron-phonon interaction arises from the spatial dependence of the transfer integral t, it is expected to be larger than the spin-phonon interaction which originates in the spatial dependence of $d \cong t^2/4U$, where d is the magnetic coupling and U is the on-site Coulomb interaction strength. [36] Thus, any contribution to $\sigma(\omega)$ arising from magnon shakeoff should be significantly weaker

than the direct contribution to $\sigma(\omega)$ arising from electron-phonon coupling.

We have not discussed in detail the low-frequency, temperature-dependent part of the $\sigma(\omega)$

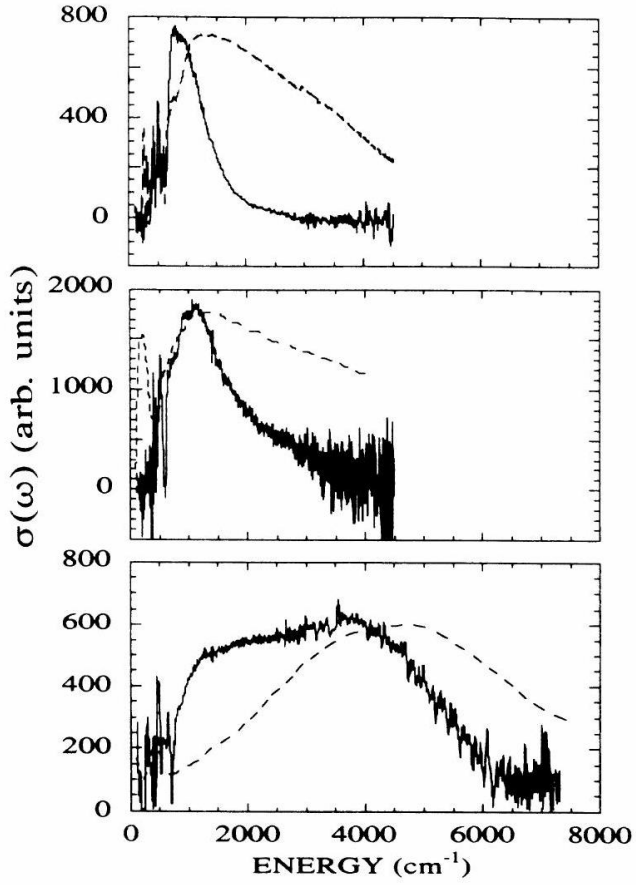

FIG. 2. The infrared conductivity $\sigma(\omega)$ (dashed lines) for $\mathrm{Tl
{2} *mathrm{Ba}*{2} \mathrm{CaCu}*{2}* *mathrm{O}*{8}$ (top), $YBa_2Cu_3O_7$ (middle), and $La_{2-x}Sr_xCuO_4$ (bottom) compared with the photoinduced infrared conductivity $\sigma_P(\omega)$ (solid lines) in their respective insulator precursors.}

spectra, [1–5] which has been attributed to free carriers scattering in the weak-coupling limit of a quasimetallic system. In the context of polaron transport theory, these free carriers are dressed polarons with dc transport lifetime (and mean free path) limited by acoustic mode scattering for $k_BT < \hbar\omega_D$ and by a combination of acoustic and optical-mode scattering at higher temperatures.

6.0.4 IV. CONCLUSION

We conclude that the photoinduced infrared conductivity of dilute carriers photoinjected into $Tl_2Ba_2CaCu_2O_8$, $YBa_2Cu_3O_{7-\delta}$, and La_2CuO_4 is well described by nonadiabatic polaron hopping (polarontransport theory). The similar spectral shape and systematic trends in both $\sigma_P(\omega)$ and $\sigma(\omega)$ indicate that carriers in the concentrated (metallic) regime retain much of the character of carriers in the dilute (photoexcited) regime implying that the charge carriers in the normal state of high- T_c cuprates are polarons or bipolarons. This is in a general sense consistent with the evidence of ferroelectric distortions (doping-induced distortions correlated from cell to cell) in the high T_c cuprates. [37] Furthermore, the absence of a shift [2,4] in the mid-ir feature in $\sigma(\omega)$ at the superconducting transition suggests that if bipolaronic superconductivity is present in the cuprates, bipolarons are formed above T_c.

[1] For a review, see T. Timusk and D. B. Tanner, in Physical Properties of High Temperature Superconductors I, edited by Donald M. Ginsberg (World Scientific, Singapore, 1989), p.

TABLE II. Critical temperatures and values of the mid-ir peak position in superconducting perovskites.

	T_c(K)	Mid-ir peak (eV)
$SrTiO_3$	0.3[8]	> 1[8]
Ba_{1-x} Pb_xBiO_3	13[6]	1.2[6]
La_2CuO_4	34	0.5
$YBa_2Cu_3O_7$	93	0.13
$Tl_2Ba_2CaCu_2O_8$	110	0.09

339.
[2] K. Kamaras, S. L. Herr, C. D. Porter, N. Tache, D. B. Tanner, S. Etemad, T. Venkatesen, E. Chase, A. Inam, X. D. Wu, M. S. Hegde, and B. Dutta, Phys. Rev. Lett. 64, 84 (1990).
[3] R. T. Collins, Z. Schlesinger, F. Holtsberg, and C. Feild, Phys.
Rev. Lett. 63, 422 (1989); Z. Schlesinger, R. T. Collins, F. Holtsberg, C. Feild, S. H. Blanton, U. Welp, G. W. Crabtree, Y. Fang, and J. Z. Liu (unpublished).
[4] C. M. Foster, K. F. Voss, T. W. Hagler, D. Mihailovic, A. J. Heeger, M. M. Eddy, W. L. Olsen, and E. J. Smith, Solid State Commun. (to be published).
[5] G. A. Thomas, J. Orenstein, D. H. Rapkine, M. Capizzi, A. J. Millis, R. N. Bhatt, L. F. Schneemeyer, and J. V. Waszczak, Phys. Rev. Lett. 61, 1313 (1988).
[6] S. Tajima, S. Uchida, A. Masaki, H. Takagi, K. Kitazawa, S. Tanaka, and A. Katsui, Phys. Rev. B 32, 6302 (1985); S. Tajima, S. Uchida, A. Masaki, H. Takagi, K. Kitazawa, S. Tanaka, and S. Sugai, ibid. 35, 696 (1987).
[7] Xiang-Xin Bi, P. C. Eklund, E. McRae, Ji-Guang Zhang, P. Metcalf, J. Spalek, and J. M. Honig, Phys. Rev. B 42, 4756 (1990).
[8] J. F. Schooley, H. P. R. Frederikse, W. R. Hosler, and E. R. Pfeiffer, Phys. Rev. 159, 301 (1967).
[9] E. V. Bursian, Ya. G. Girshberg, and E. N. Starov, Phys. Status Solidi B 46, 529 (1971).
[10] J. Orenstein, G. A. Thomas, D. H. Rapkine, C. G. Bethea, B. F. Levine, B. Batlogg, R. J. Cava, D. W. Johnson, Jr., and E. A. Rietman, Phys. Rev. B 36, 8892 (1987); S. L. Herr et al., in High Temperature Superconducting Materials: Preparation, Properties and Processing, edited by William Hatfield and J. J. Miller (Marcel Dekker, New York, 1988), p. 275.
[11] J. B. Torrance, Y. Tokura, A. I. Nazzal, A. Bezinge, T. C. Haung, and S. S. P. Parkin, Phys. Rev. Lett. 61, 1127 (1988).
[12] K. Sreedhar and P. Ganguly, Phys. Rev. B 41, 371 (1990).
[13] J. Ruvalds and A. Virosztek, Phys. Rev. B 42, 399 (1990); (unpublished).
[14] V. Z. Kresin and S. A. Wolf, Phys. Rev. B 41, 4278 (1990); W. Pickett, Rev. Mod. Phys. 61, 433 (1989); J. Fink, N. Nucker, H. Romberg, and J. C. Fuggle, J. Res. Dev. (to be published); M. Lang, T. Lechner, S. Riegel, F. Steglich, G. Weber, T. J. Kim, G. Luthi, B. Wolf, H. Rietschel, and M. Wilhelm, Z. Phys. B 69, 459 (1988).
[15] H. G. Reik and D. Heese, J. Phys. Chem. Solids 28, 581 (1967).
[16] H. G. Reik, Solid State Commun. 1, 67 (1963).
[17] H. G. Reik, Z. Phys. 203, 346 (1967).
[18] E. V. Bursian, Ya. G. Girshberg, and E. N. Starov, Fiz. Tverd. Tela (Leningrad) 14, 1019 (1972) [Sov. Phys. Solid State 14, 872 (1972)].
[19] D. Emin, Adv. Phys. 24, 305 (1975).
[20] M. Klinger, Phys. Lett. 7, 102 (1963).
[21] Y. H. Kim, A. J. Heeger, L. Acedo, G. Stucky, and F. Wudl, Phys. Rev. B 36, 7252 (1987).
[22] Y. H. Kim, C. H. Foster, A. J. Heeger, S. Cox, and G. Stucky, Phys. Rev. B 38, 6478

(1988); C. Taliani, R. Zamboni, G. Ruani, F. C. Matacotta, and K. I. Pokhodnya, Solid State Commun. 66, 487 (1988).
[23] C. M. Foster, A. J. Heeger, G. Stucky, and N. Herron, Solid State Commun. 71, 945 (1989).
[24] C. M. Foster, A. J. Heeger, Y. H. Kim, G. Stucky, and N. Herron, Synth. Met. 33, 171 (1989).
[25] T. Holstein, Ann. Phys. (N.Y.) 8, 343 (1959).
[26] H. G. Reik and D. Heese, Phys. Status Solidi 24, 281 (1967); also see Lines and Glass, Principles and Applications of Ferroelectrics and Related Materials (Clarendon, Oxford, England, 1977), and references therein.
[27] I. Batistic, A. R. Bishop, R. L. Martin, and Z. Tešanovic, Phys. Rev. B 40, 6896 (1989); R. E. Cohen, W. E. Pickett, and H. Krakauer, Phys. Rev. Lett. 64, 2575 (1990).
[28] L. Genzel, A. Wittlin, M. Bauer, M. Cardona, E. Schonherr, and A. Simon, Phys. Rev. B 40, 2170 (1989).
[29] D. Emin and M. S. Hillery, Phys. Rev. B 39, 6575 (1989); D. Emin, Ferroelectrics (to be published); A. S. Alexandrov, J. Ranninger, and S. Robaszkiewcz, Phys. Rev. B 33, 4526 (1986).
[30] S. L. Herr, K. Kamaras, C. D. Porter, M. G. Doss, D. B. Tanner, D. A. Bonn, J. E. Greedan, C. V. Stager, and T. Timusk, Phys. Rev. B 36, 733 (1987).
[31] C. Taliani, A. J. Pal, G. Ruani, and R. Zamboni, in Proceedings of the International Conference on Superconductors, Bangalore, India, 1990 [Bull. Mater. Sci. (to be published)].
[32] P. E. Sulewski, P. A. Fleury, K. B. Lyons, S-W. Cheong, and Z. Fisk, Phys. Rev. B 41, 225 (1990).
[33] K. B. Lyons, P. A. Fleury, L. F. Schneemeyer, and J. V. Waszczak, Phys. Rev. Lett. 60, 732 (1988).
[34] K. F. McCarty, E. L. Venturini, D. S. Ginley, B. Morosin, and J. F. Kwak, Physica C 159, 603 (1989).
[35] P. Knoll, C. Thomsem, M. Cardona, and P. Murugaraj, Phys. Rev. B 42, 4842 (1990).
[36] F. C. Zhang and T. M. Rice, Phys. Rev. B 37, 3759 (1988).
[37] D. Mihailovic and A. J. Heeger, Solid State Commun. 75, 319 (1990).

Bibliography

References

6.1 Bibliography from Most Useful Articles

References from Alexandrov, Mott

Abrikosov A A 1957 Zh.Eksp.Teor.Fiz. 1442.

Adamowski J 1989 Phys.Rev. B39, 3649-3652.

Alexandrov A S 1983 Zh.Fiz.Khim. 57, 273 (Russ.J.Phys.Chem.57, 167(1983));
1992a Phys.Rev. B46, 14932-35;
1992b Phys.Rev. B46, 2838-44;
1992c J.Low Temp. Phys. 87, 721-29;
1993 Phys.Rev B48, 10571-74;
1995 unpublished.

Alexandrov A S and Beere W H 1995 Phys.Rev. B51, 5887-91.

Alexandrov A S, Bratkovsky A M, and Mott N F 1994 Phys.Rev.Lett. 72, 1734-37.

Alexandrov A S, Bratkovsky A M, Mott N F and Salje E K H 1993 Physica C215, 359-70.

Alexandrov A S and Kabanov V V 1986 Fiz.Tverd.Tela (Leningrad) 28, 1129-35.

Alexandrov A S, Kabanov V V and Ranninger J 1995b unpublished.

Alexandrov A S, Kabanov V V and Ray D K 1994a Phys.Rev. B49, 9915-23; 1994b Physica C224, 247-55.

Alexandrov A S and Kornilovitch P E 1993 Z.Phys. B91, 47-50.

Alexandrov A S and Mazur E A 1989 Zh.Eksp.Teor.Fiz. 96, 1773-82.

Alexandrov A S and Mott N F 1993 Phys.Rev.Lett. 71, 1075-78; 1994 'High Temperature Superconductors and Other Superfluids',
Taylor & Francis;
ibid, Rep.Prog.Phys. 57, 1197-1290.

Alexandrov A S and Ranninger J 1981a Phys.Rev. B23, 1796-801;
1981b Phys.Rev. B24, 1164-69;
1992a Solid St.Commun.81, 403-406;
1992b Phys.Rev. B45, 13109-12.

Alexandrov A S, Ranninger J and Robaszkiewicz S 1986 Phys.Rev. B33, 4526-42;

Alexandrov A S, Samarchenko D A and Traven S V 1987 Zh. Eksp. Teor. Fiz. 93, 1007-19 (1987 Sov.Phys.JETP 66, 567).

Alexandrov A S, Zavaritsky V N, Liang W Y, and and Nevsky P L 1995 unpublished.

Allan N L and Mackrodt W C 1990 J.Chem.Soc., Faraday Trans. 86, 1227.

Allcock G R 1962 in 'Polarons and Excitons', eds. Kuper C G and Whitfield G D 45-70.

Anderson P W 1975 Phys.Rev.Lett. 34, 953-56;

Appel J 1968 in Solid State Physics, eds. Seitz F, Turnbull D and Ehrenreich H, Academic Press 21.

Aubry S 1995 in 'Polarons and Bipolarons in High- T_c Superconductors and Related Materials', eds. Salje E K H, Alexandrov A S and Liang W Y 271-308.

Austin I G and Mott N F 1969 Adv.Phys. 18, 41-102

Bardeen J, Cooper L N, and Schrieffer J R 1957 Phys.Rev. 108, 1175-1204.

Bassani F, Geddo M, Iadonisi G, and Ninno D 1991 Phys.Rev. B43, 5296-306.

Batlogg B, Hwang H Y, Takagi H, Cava R J, Kao H L and Kwo J 1995 unpublished.

Bednorz J G and Muller K A 1986 Z.Phys. B64, 189-93; 1988 Angew.Chem.Int.Ed.Engl. 27, 735-43.

Bishop R F 1974 J.Low Temp.Phys. 15, 601-35.
Bishop A R and Salkola M I 1995 in 'Polarons and Bipolarons in High- T_c Superconductors and Related Materials', eds. Salje E K H, Alexandrov A S and Liang W Y 353-366.

Bogoliubov N N 1947 J.Phys.USSR 11, 23-32;
1950 Ukr.Mat.Zh. 2 3;
1958 Zh.Eksp.Teor.Fiz. 34, 58, 73.
Bogoliubov Jr N N 1994 in 'Superconductivity and Strongly Correlated Electron Systems' eds. Noce C, Romano A and Scarpetta G, World Scientific 107-123.

Bogomolov V N, Kudinov E K and Firsov Yu A 1967 Fiz.Tverd.Tela (Leningrad) 9, 3175.
Bogomolov V N, Kudinov E K, Pavlov S T, and Sochawa L S 1968 Sov.Phys.Solid State 10, 2043.

Bornemann H J, Morris D E and Liu H B 1991a Physica C182, 132-36.
Bornemann H J, Morris D E, Liu H B, Sinha A P, Narwankar P
and Chandrachood M 1991b Physica C185-189, 1359-60.
Böttger H and Bryksin V V 1985 'Hopping Conduction in Solids', Academie-Verlag Berlin.

Brueckner K A 1967 Phys.Rev. 156, 204.
Bryksin V V and Gol'tsev A V 1988 Fiz.Tverd.Tela 30,1476-86 (1988 Sov.Phys.Solid State 30, 851-56).
Bryksin V V and Voloshin V S 1984 Fiz.Tverd.Tela (Leningrad) 26, 2357-65 (1984 Sov.Phys.Solid State 26, 1429-34).
Calvani P, Capizzi M, Lupi S, Maselli P, Paolone A, Roy P, Cheong S-W, Sadowski W, and Walker E 1994 Solid State Commun. 91, 113-16;
Calvani P, Lupi S, Roy P, Capizzi M, , Maselli P, Paolone A, Sadowski W, and Cheong S-W 1995 in 'Polarons and Bipolarons in High- T_c Superconductors and Related Materials', eds. Salje E K H, Alexandrov A S and Liang W Y 133-45.
Calvani P, Capizzi M, Lupi S, Maselli P, Paolone A, Roy P 1995 unpublished.
Catlow C R A 1989 J.Chem.Soc., Faraday Trans.2, 85, 335.
Chakraverty B K 1981 J.Physique 42, 1351-56.
Chen C Y, Branlund E C, Bae C-S, Yang K, Kastner M A, Cassanho A, and Birgeneau R J 1995 Phys.Rev. B51, 3671-77.
Cohen M H, Economou E N and Soukoulis C M Phys.Rev. B 29, 4496-99.
Cooper L N 1957 Phys.Rev. 104, 1189.
Crawford M K, Farneth W E, McCarron E M III, Harlow R L and Moudden A H 1990 Science 250, 1309-18.
Dagotto E 1994 Rev.Mod.Phys. 66, 763.
De Raedt H and Lagendijk Ad 1983 Phys.Rev. B27, 6097-109.
Devreese J T (ed) 1972 Polarons in Ionic Crystals and Polar Semiconductors, North-Holland (Amsterdam).
Devreese J T and Peeters (eds) 1984 Polarons and Excitons in Polar Semiconductors and Ionic Crystals, Plenum Press, New York.
Dewing H L and Salje E K H 1992 Supercond.Sci.Technol.5, 50-53.
Dolgov O V, Kirzhnits D A and Maximov E G 1981 Rev.Mod.Phys. 53, 81.
Eagles D M 1963 Phys.Rev. 130, 1381-1400; 1966 Phys.Rev. 145, 645-66;
1969 Phys. Rev. 186, 456-63.

Eliashberg G M 1960 Zh.Eksp.Teor.Fiz. 38, 966-76; 39, 1437-41
(1960 Sov.Phys.JETP 11, 696-702; 12, 1000-1002).
Emin D 1970 Phys.Rev.Lett. 25, 1751-54;
1971 Ann.Phys.(N.Y.) 64, 336.
1973 Adv.Phys. 22, 57;
1993 Phys.Rev. 48, 13691;

1995 in 'Polarons and Bipolarons in High- T_c Superconductors
and Related Materials', eds. Salje E K H, Alexandrov A S and Liang W Y 80-109.
Emin D and Holstein T 1969 Ann.Phys.N.Y. 53, 439-520.
Falk J P, Levy A, Kastner M A, and Birgeneau R J 1993 Phys.Rev. B48, 4043-48.
Fehske H, Röder H, Wellein G and Mistriotis A 1995 Phys.Rev. B51 16582-593.
Feinman R P 1955 Phys.Rev. 97660.
Feinman R P, Hellwarth R W, Iddings C K and Platzmann P M 1962 Phys.Rev. 127, 1004-17.
Fetter A L 1971 Ann.Phys.(N.Y.) 64,1.
Firsov Yu A (ed) 1975 Polarons, Nauka (Moscow).
Fisher A J, Hayes W and Wallace D S 1989 J. Phys.: Condens. Matter 15567-93.
Fisher R A, Kim S, Lacy S E, Phillips N E, Morris D E, Markelz
A G, Wei J Y T and Ginley D S 1988 Phys.Rev. B38, 11942-45.
Foldy L L 1961 Phys.Rev. 124, 649-51.
Franck J P et al. 1991 Physica C185-189, 1379-80.
Friedman L 1964 Phys.Rev. A 135, 233-46; 1995 in 'Polarons and Bipolarons in High- T_c Superconductors and Related Materials', eds. Salje E K H, Alexandrov A S and Liang W Y 180-87.
Friedman L and Holstein T 1963 Ann.Phys.(N.Y.) 21, 494.
Fröhlich H 1950 Phys.Rev. 79, 845;
1954 Adv.Phys. 3, 325-61;
Fröhlich H, Pelzer H an Zienau S 1950 Phil. Mag. 41221.
Geilikman B T 1975 Usp.Fiz.Nauk 115, 403-26 (1975 Sov.Phys.-Usp. 18, 190-202).
Gerlach B and Lowen H 1991 Rev. Mod. Phys. 63, 63-90.
Göbel U, Alexandrov A S and Capellmann H 1994 Z.Phys. B96, 47-52.
Gofron K, Campuzano J C, Abrikosov A A, Lindroos M, Bansil A, Ding H, Koelling D, and Dabrowski B 1994 Phys.Rev.Lett. 73, 3302-05.
Gogolin A A 1982 Phys.Status Solidi B109, 95-108.
Gold A 1991 Z.Phys. B83, 429.
Gor'kov L P 1958 Zh.Eksp.Teor. Fiz. 34, 735-39 (1958 Soviet Phys.JETP 7, 505-08).
Gunnarsson O, Handschuh H, Bechthold P S, Kessler B, Ganteför G, and Eberhardt W 1995 Phys.Rev.Lett. 74, 1875-78.
Gurari M 1953 Phil.Mag. 44329.
Harrison W A 1989 'Electronic Structure and the Properties of Solids', Dover Pub. (NY).
Hohenberg P and Kohn W 1964 Phys.Rev. B136, 864-72.
Hines D F and Frankel N 1979 Phys.Rev. B20, 972-83.
Hiramoto H and Toyozawa Y 1985 J.Phys.Soc.Jpn. 54, 245-59.
Hirsch J E and Fradkin E 1983 Phys.Rev. 27, 1680.
Holstein T 1959 Ann.Phys. 8, 325-42; ibid p. 343-89.
Holstein T and Friedman L 1968 Phys.Rev. 165, 1019-31.
Hore S R and Frankel N E 1975 Phys.Rev. B12, 2619-28; 1976 ibid 14, 1952-62.
Hwang H Y, Batlogg B, Takagi H, Kao H L, Kwo J, Cava R J, Krajewski J J, and Peck Jr W F 1994 Phys.Rev.Lett. 72, 2636-39.
Inderhees S E, Salamon M B, Goldenfeld N, Rice J P, Pazol B G and Ginzberg D M 1988 Phys.Rev.Lett. 60, 1178-81.
Junod A, Eckert D, Triscone G, Lee V Y and Muller J 1989 Physica C159, 215-25.
Kabanov V V and Mashtakov O Yu 1993 Phys.Rev. B47 6060-64.
Khomskii D 1995 in 'Polarons and Bipolarons in High- T_c Superconductors and Related Materials', eds. Salje E K H, Alexandrov A S and Liang W Y 375-84.
Kim Y H, Foster C M, Heeger A J, Cos S and Stucky G 1988 Phys.Rev. B38, 6478-82.
Klein B M, Boyer L L, Papaconstantopoulos D A 1978 Phys.Rev. B18, 6411-38.

Klinger M I 1961 Izv.Acad.Nauk SSSR, ser.Fiz. 25, 342-45; 1963 Phys.Letters 7, 102;
1979 Problems of electron (polaron) transport theory in semiconductors, Oxford: Pergamon Press.

Kochetov E A, Kuleshov S P, Mateev V A, and Smondyrev M A 1977 Teor.Mat.Fiz. 30, 183.

Kongeter A and Wagner M 1990 J.Chem.Phys. 92, 4003-11.
Kubo R 1957 J.Phys.Soc.Japan 12, 570.
Kubo K and Takada S 1983 J.Phys.Soc.Japan 52, 2108-17.
Kudinov E K, Mirlin D N and Firsov Yu A 1969 Fiz.Tverd.Tela (Leningrad) 11, 2789.
Lakkis S, Schlenker C, Chakraverty B K and Buder R 1976 Phys.Rev. B14, 1429-40.

Landau L D 1933 Phys.Z.Sowjetunion 3, 664.
Landau L D and Lifshitz E M 1977 'Quantum Mechanics - Non relativistic theory', third English edition, Pergamon Press.
Lang I G and Firsov Yu A 1962 Zh.Eksp.Teor.Fiz. 43, 1843-60 (1963 Sov.Phys.JETP 16, 1301-12).

Lee D K and Feenberg E 1965 Phys.Rev. 137, A731.
Lee T-D and Pines D 1952 Phys.Rev. 88960.
Lee T-D, Low F and Pines D 1953 Phys.Rev. 90297.
Loram J W, Mirza K A, Liang W Y and Osborne J 1988 Physica C162 - 164, 498-99.
Loram J W, Cooper J R, Wheatley J M, Mirza K A and Liu R S 1992 Phil. Mag. B65, 1405-17.

Mackenzie A P, Julian S R, Lonzarich G G, Carrington A, Hughes S D, Liu R S and Sinclair D C 1993 Phys.Rev.Lett. 71, 1238-41.
Marsiglio F 1995 Physica C 244, 21-34.
Matsubara T 1955 Prog.Theor.Phys. 14, 351-78.
McMillan W J 1968 Phys.Rev. B167, 331-44.
Migdal A B 1958 Zh.Eksp.Teor.Fiz. 34, 1438-46 (1958 Sov.Phys. JETP 7, 996-1001).
Mihailovic D, Foster C M, Voss K and Heeger A J 1990 Phys.Rev. B42, 7989-93.
Morel P and Anderson P W 1962 Phys.Rev. 125, 1263-71.
Mott N F 1990 Adv.Phys. 39, 55-81;
1993 Physica C205, 191-205;
1995 unpublished
Mott N F and Davis E A 1979 Electronic processes in non-crystalline materials, 2nd edn. Oxford University Press, Oxford.

Mott N F and Gurney R W 1940 Electronic Processes in Ionic Crystals, Oxford: Clarendon Press.
Mukhomorov V K 1982 Fiz.Tekh.Poluprovodn. 16, 1095-96 (1982 Sov.Phys.Semicond. 16, 700-701).
Nagaev E L 1979 Physics of Magnetic Semiconductors (Moscow) Mir.
Nambu Y 1960 Phys.Rev. 117, 648-63.
Nasu K 1985 J.Phys.Soc.Japan 54, 1933-43;
1991 in 'Electronic Conduction in Oxides', eds. Tsuda N, Nasu K, Yanase A, and Siratori K, Springer-Verlag, p. 81.
Nozieres, P. and Schmitt-Rink, J. J. 1985 Low Temp.Phys. 59, 195-211.
Osofsky M S et al. 1993 Phys.Rev.Lett. 71, 2315-18; 1994 ibid 72, 3292.

Overend N, Howson M A and Lawrie I D 1994 Phys.Rev.Lett. 72, 3238-41.

Peierls R E 1933 Z.Phys. 80, 763-91;
1955 in Quantum Theory of Solids (Oxford University Press, London).
Pekar S I 1946 Zh. Eksp. Teor. Fiz. 16, 335-339; 1951 (Russ.original Gostekhizdat), Research in Electron Theory of Crystals, US AEC Report AEC-tr- 5575 (1963).
Pines D 1961 The Many-Body Problem, Benjamin/Cummings, Reading, Massachusetts.

Ranninger J and Thibblin U 1992 Phys.Rev. B45, 773.
Rashba E I 1957 Opt.Spectr. 2, 75; 1985 in Excitons ed. by Rashba E I and Struge D M, Nauka (Moscow).
Robaszkiewicz S, Micnas R and Chao K A 1981 Phys.Rev. B23, 1447-58; ibid 24, 1579-82.
Reik H G 1963 Solid State Commun. 1, 67-71.
Salamon M B, Inderhees S E, Rice J P and Ginsberg D M 1990 Physica A168, 283.
Salje E K H 1995 in 'Polarons and Bipolarons in High- T_c Superconductors and Related Materials', eds. Salje E K H, Alexandrov A S and Liang W Y 110-31.
Scalapino D J 1969 in Superconductivity 1, ed. Parks R D, Marcel Deccer, 449-560.
Schafroth M R 1955 Phys.Rev. 100, 463-75
Schnelle W, Braun E, Broicher H, Dömel R, Ruppel S, Braunisch
W, Harnischmacher J and Wohlleben D 1990 Physica C168, 465-74.
Schultz T D 1962 in 'Polarons and Excitons', eds. Kuper C G and Whitfield G D 71-121.
Sewell G L 1958 Phil.Mag. 3, 1361-80.
Shluger A L and Stoneham A M 1993 J. Phys.: Condens. Matter 5, 3049-86.
Staunton J B 1994 Rep.Prog.Phys. 57, 1289-1344.
Street R A and Mott N F 1975 Phys.Rev.Lett. 35, 1293-96.
Suprun S G and Moizhes B Ya 1982 Fiz.Tverd.Tela (Leningrad) 24, 1571-73.
Takada Y Phys.Rev. B26 1223-32.
Taliani C, Pal A J, Ruani G, Zamboni R, Wei X and Vardini Z V 1990 Electronic Properties of HT_cSC and Related Compounds, Springer Series of Solid State Science (Springer-Verlag, Berlin) 99, 280.
Tjablikov S V 1952 Zh.Eksp.Teor.Fiz. 23, 381.
Tolmachev V V 1958 in Bogoliubov N N, Tolmachev V V and Shirkov D V 'A New Method in the Theory of Superconductivity', Academy of Science (Moscow) (1959 Consultant Bereau, New York).
Toyozawa Y 1961 Prog.Theor.Phys. 26, 29-44; 1990 Rev. Solid State Sci. 4133.
Uemura Y J 1995 in 'Polarons and Bipolarons in High- T_c Superconductors and Related Materials', eds. Salje E K H, Alexandrov A S and Liang W Y 453-59.
Verbist G, Peeters F M and Devreese J T 1991 Phys.Rev. B43, 2712-20.
Vinetskii V L and Giterman M Sh 1957 Zh. Eksp. Teor. Fiz. 33, 730 (1958 Sov.Phys. - JETP 6 560).
Vinetskii V L and Pashitskii E A 1983 Fiz. Tverd. Tela (Leningrad) 25, 1744-47 (1983 Sov.Phys.Solid State 25, 1005-06).
Von Molnar S and Methfessel S 1967 J. Appl. Phys. 38, 959.
Woo C-W and Ma S 1967 Phys.Rev. 159, 176-83.
Yagil Y, Zhang M, Baudenbacher F, and Salje E K H 1995 Phys.Rev. B, to be published.
Yamashita J and Kurosawa T 1958 J. Phys.Chem.Solids 5, 34.
Zhang X and Catlow C R A 1991 J.Mater.Chem. 1, 233-38.
Zhao G, K.K. Singh and D.E. Morris 1994 Phys.Rev. B50, 4112.
Zheng H 1988 Solid State Commun. 65, 731.
Zheng H, Feinberg D and Avignon M 1989 Phys.Rev. B39, 9405-22.

6.2 Bibliography from Old, Fundamental Articles

6.3 Bibliography from Articles about Special Models and Effects

6.4 Bibliography from articles about main experiments